



**ScuDo**  
Scuola di Dottorato ~ Doctoral School  
WHAT YOU ARE, TAKES YOU FAR

Doctoral Dissertation  
Doctoral Program in Mechanical Engineering (29<sup>th</sup> Cycle)

# **A new constitutive equation to predict the nonlinear behavior of short fiber reinforced composite materials**

By

**Hadi Mehdipour**

\*\*\*\*\*

**Supervisor:**

Prof. Giovanni Belingardi

**Doctoral Examination Committee:**

Prof. Ahmed Elmarakbi, University of Sunderland  
Prof. Ermias G. Koricho, Southern Georgia University  
Prof. Sayed A. Nassar, Oakland University  
Prof. Davide S. Paolino, Politecnico di Torino  
Prof. Andrea Bernasconi, Politecnico di Milano

Politecnico di Torino  
2017

## Declaration

I hereby declare that, the contents and organization of this dissertation constitute my own original work and does not compromise in any way the rights of third parties, including those relating to the security of personal data.

Hadi Mehdipour

2017

\* This dissertation is presented in partial fulfillment of the requirements for **Ph.D. degree** in the Graduate School of Politecnico di Torino (ScuDo).

*I would like to dedicate this thesis to my loving parents*

## **Acknowledgment**

My sincerest gratitude first and foremost, goes to my advisor, Professor Giovanni Belingardi, for giving me the opportunity of joining to his group and having the companionship of a great personality as well as a prominent academic feature. I will never be thankful enough for all the supports I have received from him and it cannot be gathered in some words. I am most indebted to my tutor, Dr. Enrico Mangino, for helping me in Centro Ricerca Fiat (CRF) and for his excellent technical guidance, encouragement, and academic advice. I would also like to acknowledge Dr. Andrea Pipino for his time, valuable advice and feedback. My special thank goes to Professor Pedro Camanho from the university of Porto whose deep knowledge about composite materials and numerical methods as well as his time devoted to me during my stay in Portugal. Their unsurpassed knowledge in their respective fields made it possible for this thesis to be completed.

I also appreciate the knowledge and time investment made by my friends Dr. Ali Moshrefzadeh from Politecnico di Torino and Mr. Amit Sharma from MSC software. Their technical guidance played a major role with regard to the numerical solutions of this thesis. The friendly and cheerful nature of the entire CRF group; Luca Belforte, Enea de Meo, Igor Manetti, Antonio Veca, made this research work possible. I am very grateful for the group's assistance and guidance at the initial stages of the component fabrication process, experimental and numerical testing. Special thanks to Davide Gabellone and for his valuable experimental results as inputs in the numerical modeling.

My especial thanks go to my two beautiful sisters Farzaneh and Maryam, and also my lovely dad and mom because of their supports and kindness.

## **Abstract**

Organic sheets and short fiber-reinforced composite materials as well as the components made of their combination, i.e., hybrid components, play a significant role in the automotive industry. Producing conventional thermoset-based composite materials have difficulties such as their improper automatic production procedure, major scrap rate, and high production price. The new generation of thermoplastic-based composites show advantages over thermoset-based composites such as their volume production capability, lower production prices, formability, and recyclability. Therefore, the thermoplastics seem to be a proper replacement for the conventional thermosets. Organic sheets made of glass fibers with a thermoplastic matrix and usually delivered as an unfinished production to exert final procedure such as thermoforming or over injection to achieve the final component. In addition to organic sheets, short fiber reinforced thermoplastics are increasingly used in automotive industry, mostly using mold flow process, which offers a high design freedom and faster volume production procedure. Combining short fiber reinforced composite materials and organic sheets reaches the hybrid components which show excellent mechanical performance in comparison to their remarkably lower weight.

This research begins with the production of the hybrid composite component which is supposed to be used for the load-bearing parts in the light vehicles. The production procedure, as well as the constituents decompositions, are explained. Even though the hybrid components are made by two different technologies, i.e., back-injected and compression molding, but since our main objective is to simulate the injected elements, then the compression molding procedure will be skipped in the numerical simulations. In the next step, the 3-point bending experiments are performed on the hybrid component in both direction and different loading rates. The configuration of the test is explained in detail. The components demonstrate different response under different loading rates and various boundary conditions which is widely discussed in this work.

According to the experimental results, the hybrid component under 3-point bending test does not show a high degree of nonlinearity before damage. Therefore, to simulate the back-injected hybrid component under bending, we introduce a linear elastic model including a damage model. The proposed model is described and a rate-sensitive damage model, as well as the integration schemes, are introduced for either of the implicit and explicit solvers.

The torsion test is prepared for the back-injected-made hybrid component which from the very beginning demonstrates a high degree of nonlinearity. The nonlinear behavior of the component is related to its elasto-plastic response, and it is our main concern in the current research. The short fiber-reinforced composites can be considered as transversely-isotropic materials. Thus, to catch the plasticity induced nonlinearity, we introduce an elastic-plastic model and the post-plasticity damage model. The model is founded on the representation theory of the basic invariants of the anisotropic materials. The associated constitutive equations for transversely isotropic materials are proposed. This work comprises the representation of the general constitutive equations, an introduction to the representation theory and the elastic constitutive equations for transversely isotropic materials. Since we deal with the non-metallic materials, then the elasto-plastic model must be non-associated which requires a potential function be defined besides of a yield function. These requirements, as well as the proper invariants for the transversely isotropic materials, are discussed and introduced.

Having defined the basic requirements of an elasto-plasticity model, we introduce the elasto-plasticity model. Since the numerical integration scheme requires a general definition of the model, then it is formulated in a general continuum mechanics fashion. Also, to deal with the rate-dependent behavior of the hybrid component under bending, a simple model is introduced. A Continuum Damage Model (CDM) is proposed for the post elasticity damage phenomenon. A damage model for degradation of the transversely isotropic material after reaching the saturation stress is developed based on the CDM concept. The so-called non-local damage model is described as well. The numerical implementation and the integration schemes are discussed which include the description of the backward Euler and the explicit integration algorithms.

In the last step, the numerical and experimental results are given and discussed. The bending test for the hybrid components are performed under quasi-static and the velocity of 127 mm/sec loading conditions. Other than ambient condition, the quasi-static bending experiment is performed for the components preheated by 90 degree Celsius, and the results are available. The numerical results for the quasi-static and dynamic 3-point bending are given, respectively. The elasto-plasticity plus the damage after plasticity models' numerical results are presented and validated by the results taken from [1] for the basic tensile and compression test results of PA6GF60. The numerical and experimental results for the back-injected-made hybrid component under torsion are presented.

# Contents

1	Introduction.....	1
1.1	Motivation.....	1
1.1.1	Industrial and economic-oriented comparison between polymers and traditional materials .....	3
1.1.2	What is thermoplastics, reinforced thermoplastics, and hybrid components? ..	4
1.1.3	Thermoplastics mechanical properties .....	4
1.1.4	Methods of improving mechanical properties of thermoplastics .....	8
1.1.5	Reinforced plastics .....	8
1.2	Introducing the case study .....	11
1.2.1	Manufacturing in detail .....	11
1.3	Literature review .....	14
1.3.1	Fiber length measurement .....	15
1.3.2	Fiber orientation in SFRPs .....	15
1.3.3	Macromechanical approach.....	17
1.3.4	Damage.....	17
1.4	Framework and objectives .....	20
2	Invariants theory for transversely isotropic materials.....	23
2.1	Constitutive equations in a general view .....	23
2.1.1	Structural tensor for short fiber reinforced thermoplastics.....	26
2.2	Physical and mathematical concept of space isotropy .....	29
2.3	Isotropic functions .....	31
2.4	Representation for polynomial scalar and tensor functions.....	31
2.4.1	Representation for anisotropic scalar- and tensor-valued functions.....	32
2.5	Elasticity .....	33
2.5.1	Transversely isotropic elasticity .....	36
2.5.2	Scalar- and tensor-valued isotropic functions for transversely isotropic materials	36

2.5.3	Kinematic constraints .....	44
3	Transversely isotropic yield function and plastic flow potential .....	48
3.1	Foundation of plasticity theory .....	48
3.2	Invariants of transversely isotropic symmetry group.....	50
3.2.1	Formulation of yield surface for short fiber reinforced thermoplastics.....	57
3.2.2	Yield function's parameter determination.....	58
3.2.3	Plastic flow potential function for short fiber reinforced thermoplastics .....	61
4	Elasto-plasticity model.....	64
4.1	Elasto-plasticity continuum .....	64
4.2	Generalized elasto-plasticity model.....	70
4.3	Rate-dependent material behaviour .....	72
4.4	Damage .....	74
4.4.1	Elastic damage.....	74
4.4.1	Elasto-plastic damage modelling.....	81
4.5	Numerical methods .....	86
4.5.1	Backward Euler integration algorithm .....	87
4.5.2	Explicit subroutine (VUMAT) for CDM.....	101
5	Short fiber reinforced thermoplastics simulation.....	104
5.1	Hybrid component response under 3-point bending test .....	104
5.2	Simulation of the back-injected manufactured hybrid component under quasi-static bending at ambient conditions.....	114
5.3	Rate-dependent simulation of the back-injected manufactured hybrid .....	117
5.4	Elasto-plasticity results .....	119
5.5	Elasto-plastic simulation of the main component under torsion.....	134
6	Summery and future works.....	137
6.1	Conclusion .....	137
6.2	Future work.....	138
	References .....	139
8	Appendix.....	150
8.1	Appendix1.....	150

8.1.1	Elasto-plasticity with damage UMAT subroutine .....	150
8.2	Appendix.2.....	193
8.3	Appendix.3.....	208
8.4	Appendix.4.....	209
Figure 1-1	schematic representation of individual molecules in thermoplastic matrixes [3] .	4
Figure 1-2	typical behavior of thermoplastic matrix under uniaxial tension [3] .....	5
Figure 1-3.	The component called PROVETTONE .....	11
Figure 1-4	Hybrid component: cross-section and upper view [6].....	12
Figure 1-5	The injection gates positions .....	13
Figure 1-6	Short fiber orientation in injected constituent; picture (a) shows the material orientation at the injection gate area and picture (b) at one of the randomly selected zones which both taken from damaged zones [6].....	13
Figure 1-7	Short fiber orientation in injected constituent; pictures (a) and (b) show glass fibers distribution and orientation on the surface of two randomly chosen areas [6].....	14
Figure 1-8	skin-core-skin pattern [25] .....	17
Figure 2-1	Difference between the principal directions of the input agency and the response of an anisotropic material [56].....	24
Figure 2-2	Polar coordinate system definition for a single cylindrical fiber .....	27
Figure 2-3	The illustration of a single ellipsoidal fiber and the corresponding eigenvectors and eigenvalues.....	29
Figure 2-4	Principal of the isotropy of space [56] .....	30
Figure 2-5	uniaxial loading-unloading stress-strain curves [71].....	33
Figure 2-6	A typical substructure of a short fiber reinforced composite and transversely isotropic materials. The direction $\mathbf{e}_3$ indicates the isotopy plane normal .....	36

Figure 3-1 Schematic isotropic hardening including primary(blue) and subsequent yield surfaces [85].....	58
Figure 3-2 Schematic curve of yield strength versus equivalent strain .....	61
Figure 3-3 schematic description of associated and non-associated flow rules.....	62
Figure 4-1 schematic elastic, plastic and damage response of the material [1] .....	64
Figure 4-2 Linear Damage evolution law .....	75
Figure 4-3 Schematic elato-plastic damage in the equivalent displacement-stress state .....	83
Figure 4-4 Schematic return algorithm [86].....	95
Figure 4-5 The iterative procedure to calculate the disturbed stress components .....	98
Figure 4-6 implicit user-defined subroutine (UMAT ) algorithm.....	100
Figure 4-7 Explicit user-defined subroutine (VUMAT ) algorithm.....	103
Figure 5-1 Bending tests; (a) Case1 (b) Case2[6] .....	105
Figure 5-2 Bending test configuration; (a) test starting point (b) ending point [6].....	105
Figure 5-3 The 3-point bending; component type is Compression Molding (CM); The test is conducted in the ambient temperature (AM); Boundary condition: case1 .....	106
Figure 5-4 The 3-point bending; component type is Back-Injected (BI); The test is conducted in the ambient temperature (AM); Boundary condition: case1 .....	106
Figure 5-5 Comparison between the responses of the hybrid components manufactured by the back-injected and compression molding; temperature: Ambient (AM); Case1 .....	107
Figure 5-6 The 3-point bending; component type is Back-Injected (BI); The test is conducted in the ambient temperature (AM); Boundary condition: case2 .....	108
Figure 5-7 The 3-point bending; component type is Compression Molding (CM); The test is conducted in the ambient temperature (AM); Boundary condition: case2 .....	109
Figure 5-8 Comparison between the responses of the hybrid components manufactured by the back-injected and compression molding; temperature: Ambient(AM); Case2 .....	110

Figure 5-9 The 3-point bending; component type is Compression Molding (CM); The test is conducted on the component preheated by 90 Degree Celsius (90Deg); Boundary condition: case1.....	111
Figure 5-10 The 3-point bending; component type is Back-Injected (BI); The test is conducted on the component preheated by 90 Degree Celsius (90Deg); Boundary condition: case1.....	111
Figure 5-11 Comparison between the responses of the hybrid components manufactured by the Back-Injected (BI) and Compression Molding (CM); temperature: 90 Degree Celsius (90Deg); Case1 .....	112
Figure 5-12 Comparison between the responses of the hybrid components manufactured by the Compression Molding (CM); temperature: Ambient (AM); Case1& 2 .....	113
Figure 5-13 Comparison between the responses of the hybrid components manufactured by the Back-Injected (BI); temperature: Ambient (AM); Case1& 2 .....	113
Figure 5-14 Isometric view of the injected part of the hybrid component. The dimensions are in centimeters.....	115
Figure 5-15 The distinguished parts of the internal part in terms of the fiber distribution and determination of the structural tensors.....	115
Figure 5-16 Quasi static bending experimental and numerical results for Case1 and back-injection technology [6] .....	116
Figure 5-17 Quasi static bending experimental and numerical results for Case2 and back-injection technology [6] .....	116
Figure 5-18 Quasi static bending experimental and numerical results for Case1 with compression molding technology .....	117
Figure 5-19 The comparison between the Back-Injected component under loading condition Case1 at the ambient conditions subjected to the quasi-static and 127 mm/sec loading.....	118
Figure 5-20 The comparison between the Compression Molding (CM) made component under loading condition Case1 at the ambient conditions subjected to the quasi-static and 127 mm/sec loading .....	119
Figure 5-21 The comparison between the numerical and experimental results for the BI made component under 3-point bending test with 127 mm/sec puncher velocity [6].....	119

Figure 5-22 the variation of the stiffness matrix components with respect to the fiber distribution function.....	120
Figure 5-23 variations of the invariant <b>I1</b> versus $\sigma_{11}$ under longitudinal tension .....	122
Figure 5-24 variations of the invariant <b>I2</b> versus $\sigma_{11}$ under longitudinal tension .....	122
Figure 5-25 variations of the invariant <b>I3</b> versus $\sigma_{11}$ under longitudinal tension .....	123
Figure 5-26 variations of the invariant <b>I4</b> versus $\sigma_{11}$ under longitudinal tension .....	124
Figure 5-27 hardening parameter $\alpha_1$ vs $\sigma_1$ .....	124
Figure 5-28 hardening parameter $\alpha_3$ vs $\sigma_1$ .....	125
Figure 5-29 hardening parameter $\alpha_4$ vs $\sigma_1$ .....	125
Figure 5-30 one element analysis ( $\sigma_1$ vs $\epsilon_1$ ) of a short fiber reinforced thermoplastic under loading condition 1 (see Table 3-1) with different fiber distribution ( <b>a11</b> ).....	126
Figure 5-31 one element analysis ( $\sigma_1$ vs $\epsilon_1$ ) of a short fiber reinforced thermoplastic under loading condition 1 (see Table 3-1) with different fiber distribution ( <b>a11</b> ).....	127
Figure 5-32 one element analysis ( $\sigma_2$ vs $\epsilon_2$ ) of a short fiber reinforced thermoplastic under loading condition 1 (see Table 3-1) with different fiber distribution ( <b>a11</b> ).....	128
Figure 5-33 2D-orientation tensor components according to the CT scan results taken from Ref [1] .....	129
Figure 5-34 tests specimens geometries (a) tension based on ASTM D3039; (b) compression based on ASTM D695 –10 .....	130
Figure 5-35 FEM models for the tensile test; (a) one eighth of the real specimen with boundary conditions. The red and yellow parts represent the core and the skin, respectively. (b) the complete FEM model after applying the symmetries. ....	131
Figure 5-36 one element analysis ( $\sigma_1$ vs $\epsilon_1$ ) of PA6GF60 under loading condition 1 (see Table 3-1) using inter-extrapolation method .....	131
Figure 5-37 one element analysis ( $\sigma_2$ vs $\epsilon_2$ ) of PA6GF60 under loading condition 2 (see Table 3-1) using inter-extrapolation method .....	132
Figure 5-38 plasticity and damage progression status .....	133

Figure 5-39 displacement versus force; the experimental and the numerical results for the longitudinal direction .....	134
Figure 5-40 displacement versus force; the experimental and the numerical results for the transverse direction .....	134
Figure 5-41 torsion test configuration; (a) with component (b) without component.....	135
Figure 5-42 main model in ABAQUS; blue area are injected, and the red one is made of the thermoplastic fabric shell.....	136
Figure 5-43 numerical and experimental results for the component under torsion .....	136
Figure 5-44 different damage modes under torsion .....	136

Table 1-1 Growth of consumption rate of the conventional and plastic materials [2].....	3
Table 1-2 Mechanical properties of plastic and non-plastic materials [4].....	6
Table 1-3 Various industrial application for thermoplastics.....	9
Table 2-1 Irreducible representations for transversely isotropic functions with one and two arguments [73].....	38
Table 3-1 loading conditions.....	52
Table 3-2 The values of basic invariants under different loading conditions.....	54
Table 3-3 the combined invariants based on the basic invariants.....	56
Table 3-4 The introduced yield criterion's parameters.....	60
Table 4-1 Elasto-plasticity constitutive equation's overview [1].....	69
Table 4-2 Failure criterion for the internal part of the case study; $\sigma_{ij}$ are effective stress tensor components, $X_T$ $X_C$ , $Y_T$ and $Y_C$ are strengths of material. $X$ and $Y$ denote two perpendicular directions of the material. While $T$ and $C$ denote tension and compression, respectively. $S_{12}$ and $S_{21}$ are longitudinal and transverse shear strengths [6].....	77
Table 4-3 Failure criterion for the internal constituent of the hybrid component; $\sigma_{ij}$ are effective stress components, $X_T$ $X_C$ , $Y_T$ and $Y_C$ are strengths of material. $X$ and $Y$ denote warp and woof directions, respectively. While $T$ and $C$ denote tension and compression, respectively [6]. .....	77
Table 4-4 Equivalent values of displacements and stresses for different damage modes of fabric; the symbol indicates Macaulay operator which is defined as $x = 12x + x$ ; $\forall x \in R$ .....	79
Table 4-5 Equivalent values of displacements and stresses for different damage modes of internal constituent; the symbol indicates Macaulay operator which is defined as $x = 12x + x$ ; $\forall x \in R$ .....	80
Table 4-6 Scaling factors for different damage modes [46] .....	81
Table 4-7 Damage parameters definition.....	85

Table 4-8 Failure criteria for different damage modes for non-local elasto-plastic damage method.....	86
Table 4-9 Overview of the plasticity algorithm [1] .....	93
Table 5-1 material properties of molded and injected constituents of the hybrid component; all modules of elasticity presented in GPa and strengths in MPa[6] .....	114
Table 5-2 the mechanical properties of PA6GF60.....	132





# Chapter 1

## 1 Introduction

### 1.1 Motivation

Nowadays for both technical and economic concerns use of plastic materials in industries are inevitable, but the following issues must be considered:

1. The environmental issues including the energy consumption to manufacture a certain volume of a component, recyclability, etc.
2. The costs
3. The manufacturability
4. The functionalities
5. The characteristics such as specific weight, strength, and stiffness to weight, etc.

Organic sheets and short fiber reinforced composite materials, in addition to the components made of their combination, so-called hybrid components, are having a major role in the automotive industry. Producing conventional thermoset-based composite materials have difficulties such as their non-proper automatic production procedure, major scrap rate, besides high production price. Considering the benefits of the new generation of thermoplastic-based composite materials including their volume production capability, lower production prices, formability, and recyclability, seems to be a proper replacement for the conventional ones.

Organic sheets made of glass fibers with a thermoplastic matrix and usually delivered as an unfinished production to exert final procedure such as thermoforming or over injection to achieve a final component. In addition to organic sheets, short fiber reinforced thermoplastics are increasingly used in automotive industry, mostly using mold flow process, which offers a high design freedom and faster volume production procedure. Combining short fiber reinforced composite materials and organic sheets reaches the hybrid components which show excellent mechanical performance in comparison to their extremely lower weight.

In this study, a hybrid component made of an organic sheet as an open section reinforced by a back injection of short fiber glass is investigated. The 3-point bending with different velocities and quasi-static torsion test have been conducted. Other than whole hybrid component, the organic sheet and short fiber have been experimented separately such as size effect phenomenon of the open-hole organic sheet.

To manufacture the hybrid component the organic sheet is heated by certain temperature applying infrared radiation; then it is formed to the favorite shape and consummated by the injection of the reinforcing short fiber-thermoplastic on the open section organic sheet.

Besides the advantages of using thermoplastics, there are several disadvantages of them, especially for low price thermoplastics such as Polyamides (PA), which should be noted here such as their low-temperature resistance and humidity sensitivity which can extremely affect their application.

To have an acceptable design, a proper mechanical behavior prediction is needed. These responses might include the elastic behavior, the failure strength and also sensitivity to load rate. An acceptable prediction of the material response depends on an appropriate definition of their constitutive equations which must relate the strain states to the stress states. Considering the short fiber reinforced thermoplastic directional and completely nonlinear behavior defining the constitutive equations might be totally different from the conventional metallic materials.

Comparing to the conventional materials such as steels, the thermoplastics have a higher strength to weight ratio, but lower stiffness to weight ratio which leads them to the buckling phenomenon so that their design is more affected by stiffness than by strength.

Considering thermoplastics three significant advantages including higher toughness, formability, low specific gravities, low energy demand for manufacturing, low fabrication cost and their capability to be manufactured by an automated production procedure comparing to thermosets, this research has been dedicated to investigate on their mechanical behavior including plastic and damage behavior under quasi-static and high rate velocities.

### 1.1.1 Industrial and economic-oriented comparison between polymers and traditional materials

Based on the data are available in [2] the annual consumption of plastics is about a sixth of the consumption of steel and six times of aluminum in term of weight, and slightly higher than steel, roughly 1.4 times of the consumption of steel, but 15 times of the consumption of aluminum in term of volume. In term of equal rigidity, the consumption of plastics is about 1% of steel and almost half of aluminum. Another concern is the annual growth rate of their consumption which, considering the years at Table 1-1, over the past 35 five years the average growth of plastics and steel were 5.1% and 1%, respectively. These growth rates had been confirmed in 15 years from 1985 to 2000 for both steel and plastics (Table 1-1). Other than plastics and steel, polymer composites show about two times of consumption rate growth, while aluminum indicates a smaller amount of increase comparing to the other material, but steel.

Table 1-1 Growth of consumption rate of the conventional and plastic materials [2]

Normalized on 100 for the reference year 1985

Year	Plastics	Polymer composites	Aluminium	Steel
1985	100	100	100	100
1990	135	150	112	107
1995	179	160	118	104
2000	216	190	141	115
2005(prediction)	265	200	165	130

### 1.1.2 What is thermoplastics, reinforced thermoplastics, and hybrid components?

Thermoplastics chemically made of a simple structure of independent macromolecules which heating simply makes them melted, formed, re-shaped, welded and cooling causes their solidifications. Since heating and cooling process can be repeated several times without causing severe damages, thermoplastic can be reproduced, reshaped and recycled times and times in the manufacturing process [2]. Adding compatible additives or fillers, short, long, or continuous fibers, can improve thermoplastics properties, for instance, their durability, thermal and UV resistance, ultimate strengths, the module of elasticity and etc.

### 1.1.3 Thermoplastics mechanical properties

Despite thermosets, there are no crosslinks between individual molecules in thermoplastics, which means they are not chemically joined to each other Figure 1-1 which means the weak intermolecular forces such as Van der Waals and hydrogen bonds. Under the heating process, the weak intermolecular bonds in thermoplastics allow them to be reconfigured, sub-structurally, and reshaped, at the continuum level, if the temperature is beyond its glass point. This heating and cooling process in thermoplastic can be accomplished as many times as desired [3].

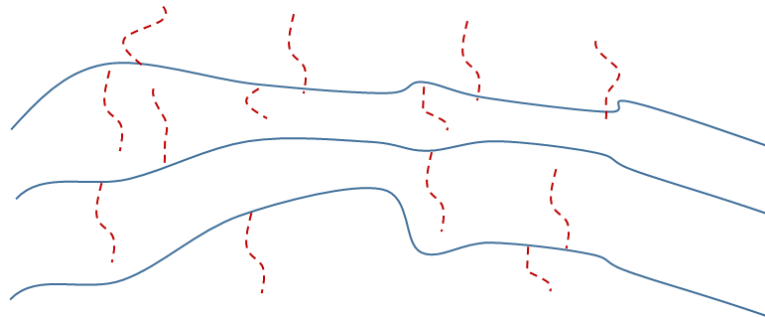


**Figure 1-1 schematic representation of individual molecules in thermoplastic matrixes [3]**

Coming back to the mechanical level, the typical response of thermoplastic matrix in a simple unidirectional test can be found in Figure 1-2. The mechanical response of thermoplastics can be interpreted according to the individual

molecules relative movements against each other. In the elastic zone, the whole deformation is reversible, and it means that removing the load, the entire movement of the substructure will go back to the original place, which is illustrated in the orange line.

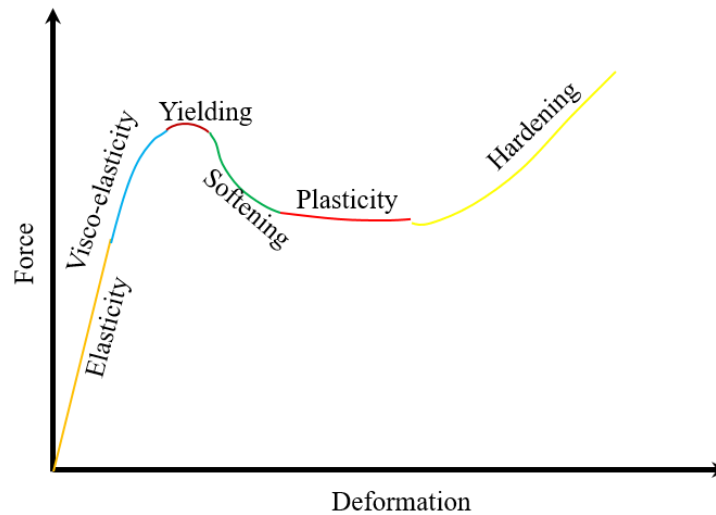


**Figure 1-2 typical behavior of thermoplastic matrix under uniaxial tension [3]**

If the loading is kept continued, then the thermoplastic will arrive at the next level of elasticity, but removing the load, the material will need some time to restore its initial position. This nonlinear elasticity is shown in blue line in Figure 1-2 typical behavior of thermoplastic matrix under uniaxial tension [3] and macro-mechanically called nonlinear viscoelasticity. Continuing loading procedure, after nonlinear viscoelasticity, the material will change the phase and the substructure, the molecular chains, is started to be reshaped, and yielding will occur. From this point, part of the deformation is irreversible, and unloading will not cause a complete restore of the deformation. As mentioned by [1] there is no an exact point on the displacement-force or stress-strain curves to be pointed out as a yield point, and the yield initiation can be considered as a region. While the yielding is initiated, the cross-links are gradually broken, and the molecular chains are inclined towards loading direction. This phenomenon, which called softening, yields a considerable reduction in the amount of the stress that the material demands for the continuation of the yielding process and in the meantime it will experience the necking phenomenon (green line in Figure 1-2 typical behavior of thermoplastic matrix under uniaxial tension [3]). After necking the plastic deformation will occur just in the necking zone. Hardening will be the next

phenomenon, and it can be explained by the complete reorientation of the molecular substructure of the thermoplastics so that the majority of the individual molecules are fully stretched and inclined towards loading direction, and there is no more re-orientation. Plasticity and hardening in thermoplastic materials can happen in both compression and tension and will differ from each other even the direction of loading might strongly affect the results. In the other word, thermoplastic materials are pressure dependent, and the yielding component is governed by dominant stress state. The reason relies on the fact that the individual molecules illustrate different deformation mechanism under different loading condition so that undergoing tension, as mentioned before, are reoriented and aligned with the loading direction, but under compression the are compacted which leads different hardening and plastic behaviors. Another phenomenon which can be observed in the thermoplastics is the change in the volumetric plastics strains, unlike metals which in classical plasticity it is supposed to be zero, in both tension and compression and which can be observed in the change of the Poisson ratio. The contractility can be observed while the thermoplastic is subjected to the compression and dilatancy occurs under tension.

For load-bearing application both strength to weight and stiffness to weight, ratios must be considered. Since the thermoplastics have a higher strength to weight ratio than steel and aluminum, but lower stiffness to weight ratio (Table 1-2), their design is more influenced by the stiffness than the strengths [4].

Table 1-2 Mechanical properties of plastic and non-plastic materials [4]

Material	Specific gravity ( gr/cm <sup>3</sup> )	Modulus(GN/m <sup>2</sup> )	Specific modulus(MN m/kg)	Strength (MN/m <sup>2</sup> )	Specific strength (kN/m kg)
Aluminium	2.7	71	26	80	30
Brass (70Cu/30Zn)	8.5	100	12	550	65

Mild steel	7.86	210	27	460	59
Polyamide 66	1.14	3	2.6	80	70
Polycarbonate	1.24	2.3	1.9	60	48
Polyamide 66/30% glass	1.38	8	5.8	160	116

Some general advantages and disadvantages of thermoplastics are listed below [2]:

Advantages:

- Heating allows thermoplastics to be welded or shaped by thermoforming process
- Not having the chemical reaction of crosslinking, the processing cycles are very short
- Having just physical transformation, the manufacturing process is easy to monitor
- Reversible softening and melting allows recycling
- If the dried semi-perfectly before manufacturing process, then gas or water vapor release might be negligible

Disadvantages:

- Rising the temperature decrease thermoplastics stiffness significantly and this is the result of the absence of the chemical links between macromolecules
- The creep behavior is not as good as thermosets due to the same reason
- Few thermoplastics are available to be used in the liquid state

Also thermoplastics main families are classified here [2]

- Engineering thermoplastics: PA, PC, PMMA, POM, PPE, PET, PBT
- Engineering thermoplastics with slightly more specific performances: PSU, PEI, PPS
- High technology performances: ETFE, PEEK

- High-tech thermoplastics with less consumption than the previous type: LCP, PTFE, PFA, FEP, PI
- Ordinary applications: PE, PP, PVC, PS

For more information about the different phenomenon can be observed in the thermoplastics, such as crazing and shear band formation and their characteristics and their behaviors in detail see [2, 5]. Hereafter, we will discuss the particle reinforced thermoplastics specifically and their mechanical behaviors and the methods of improving mechanical properties of the thermoplastics.

#### **1.1.4 Methods of improving mechanical properties of thermoplastics**

There are several mechanical and chemical methods to improve thermoplastics behavior for specific performances [4]. Here the main approaches are listed, and those details are not discussed, but additives or fillers:

- Molecular architecture manipulation
- Copolymerization; if the mixing of polymers is accomplished in the chemical rather than a mechanical level
- Crystallinity; to reach higher temperature resistant and stiffer plastics
- Crosslinking; one of the cheapest method to improve thermoplastics' stiffness
- Reinforcement;

Here in this study will focus on the reinforcement category and the polymers which are reinforced by adding additives.

#### **1.1.5 Reinforced plastics**

Adding some particles such as ceramics, metallic or polymeric fibers into the resins results in a reinforced composite material. The new combination is easily achieved, and generally, the outcome might be cheaper than the plastic matrix itself with great advantages comparing to the basic constituents. In the other words, since the fibers are dramatically brittle and might not carry load alone, they are added to the matrix which is, in term of the thermoplastics, more ductile and might transfer the load so that it can be said that the reinforced composite inherited the high level of stiffness and the strength from the fillers and good shock and environmental resistance of the resin. As a material with an acceptable range of creep, strength, and stiffness, the fiber reinforced composites might

compete with the well-known traditional materials in various applications, such as vehicle and aerospace industries [4]. Since this research is dedicated to the automotive industry, introducing some example about the application of the thermoplastic in this industry might be helpful to have a primary idea that how widely they spread in this specific field ( to see more examples one can refer to [2]).

Table 1-3 Various industrial application for thermoplastics

Application	Type of thermoplastic
Air and water filter elements	PA
Airbag cover	PEBA
Airbag covers, steering wheels...	COPE
Bobbins for electronically controlled automatic transmissions for trucks, solenoid coils in control modules for five-speed automatic truck transmissions: aromatic	PA
Air intake manifolds for top-of-the-range cars	PPA
Airbag canister	PA
Engine covers	PA
Engine covers are generally made out of glass-reinforced polyamide PA	PA
Bearing retainers in engine compartments, gears, pivots... Aromatic PA	PA
Airbag covers, armrests, upholster	TPO
Airbag covers, armrests, upholster	TPS

Airbrake hose and tubing	PEBA
Airbrake tubing	COPE
Apparel and automotive mats and carpets: Sorona® biopolymer	Bioplastics
Automobile parts: BIOFRONT (stereocomplex PLA)	Bioplastics
Automotive parts and other products: Sorona® EP	Bioplastics

However, the strengthening procedure depends on the filler's type which might be categorized according to their geometries. The particle type additives have no long dimensions, and since they cannot resist against an initial crack growth, except for the rubber-like substance, and consequently are not able to improve the fracture toughness of brittle matrixes, therefore they might not be used in such a matrix. The introduced exception particulate filler offers a high level of toughening for brittle matrixes, and it is a typical way to improve thermoplastics behavior for impact condition where the toughness plays a significant role. As an example of this type of thermoplastics, we can mention high-impact polystyrene and ABS. Also, a particulate reinforced improves the stiffness of the matrix, but might not improve, always, strengthen. The reason might be related to the level of load sharing with the matrix, which for particulate fillers is lesser extent than fibrously reinforces. Another important point about the hard particle reinforces is a localized stress concentration which will be occurred when they are incorporated into the brittle matrixes and will reduce the impact strength of the composite. Generally speaking, the particulate additives might improve the following aspects of a matrix:

- High-temperature performance
- Reduction in frictions
- wear resistance
- Machinability
- Shrinkage reduction

Since the particle reinforcers sometimes just are added to the matrixes to reduce the cost, and in this case, they cannot be considered as the reinforcement which is not the case of this work.

## 1.2 Introducing the case study

The primary object of this study is dedicated to a hybrid composite part which is manufactured by FCA and combined a thermoformed organic sheet and a reinforcer internal part made of a back injection process. Here, we will introduce the main component which forms the backbone of the current study in the sense that we are supposed to introduce a material model to numerically simulate the component under different loading conditions. Since, the approach, to simulate the component, has been chosen is macromechanical-based. Therefore, we will not deeply discuss the substructure of the constituent of the component and just will give a concise description of them and also the manufacturing process. The main component made of two different composites including a thermoformed open section organic composite sheet and injected reinforcer. The thermoforming and the injection processes are accomplished simultaneously when the organic sheet is heated by an infrared and molded, the particle glass fiber reinforced polyamide is injected over the molded organic sheet. Then applying the cooling to the mold, after a certain span of time the component can be removed.

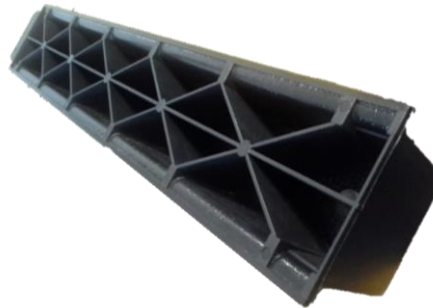


**Figure 1-3. The component called PROVETTONE**

### 1.2.1 Manufacturing in detail

In this section, we describe the manufacturing process of the main hybrid component (the case study) as well as the compositions of the constituents. The molded part is made of an organo-sheet which consists of a thermoplastic (Polyamide 66) as a matrix and 63% plain weave glass fiber as reinforcement. Injected part is made of the combination of Polyamide 66 as its matrix and 30% of short glass fiber as reinforcement.

The manufacturing process begins with forming of the organo-sheet which must be heated up to 300°C. Afterwards, it is inserted into the mold and mold is

closed. In order to achieve a more uniform heat distribution all over the sheet, this process is performed by infrared technology. Molding process does not take more than 4 seconds. After completion of organo-sheet shaping process, the injection process is performed with two distinct phases, without extracting the part from the mold. The melted short fiber composite is injected over the molded sheet at 320°C temperature within 3 seconds. Then, to compensate the volume reduction during the cooling phase, injection process must be continued which the so-called packing phase. The volume reduction is the result of mold cooling, at the mean temperature of 70°C and it approximately equals 5% of total injected material volume. The packing phase takes about 10 seconds and then the final cooling phase, which lasts 60 seconds, is started. After cooling phase, by which the mean temperature of the injected material is reduced to about 90°C, the final product is ejected in 3 seconds. It should be noted that a mean temperature of 90°C seems to be quite enough to prevent the final shape of the component from distortion and deformation after ejection. The whole production process is continuous because during the cooling phase of the process there is enough time to refill the injector with short fiber composite granules and melting them [6]. The final shape of the hybrid component is illustrated in Figure 1-3 and its cross-section in Figure 1-4.

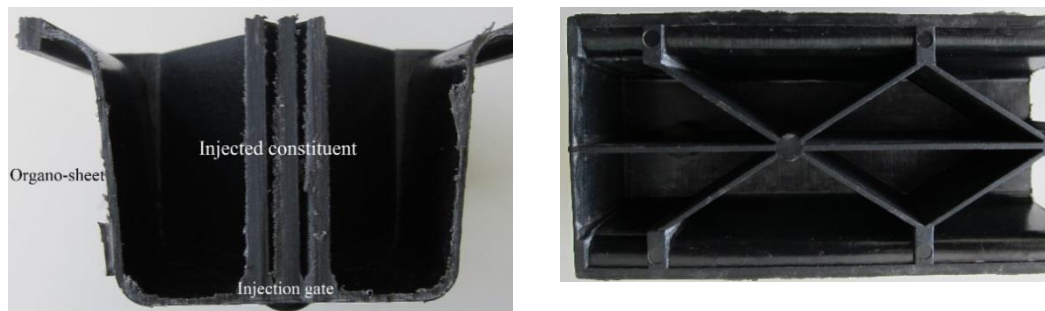


**Figure 1-4 Hybrid component: cross-section and upper view [6]**

The injection gates are indicated in Figure 1-5 in order to show the flow directions which strongly affect the substructure of the internal constituent substructures. The knowledge about the flow directions can help to make a reasonable decision about the structural tensor (see sections 1.3.2 and 2.1.1 in order to have a clear idea about the structural tensor functions in the simulation process and their application).

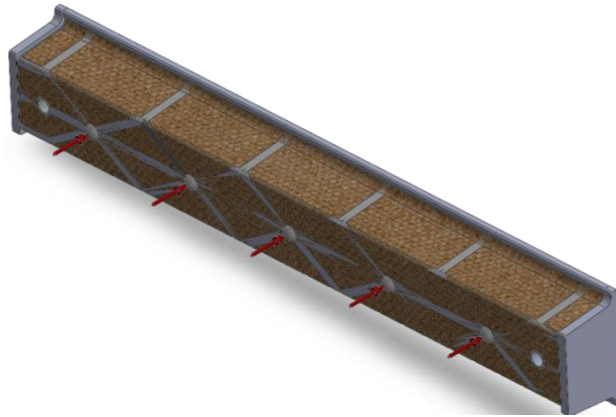


**Figure 1-5 The injection gates positions**

The Figure 1-6 shows the distributions of the short glass fibers in the two area near the injection gates, and clearly, we can observe the accumulation of the fibers. In Figure 1-6 the red arrow shows the injection direction.

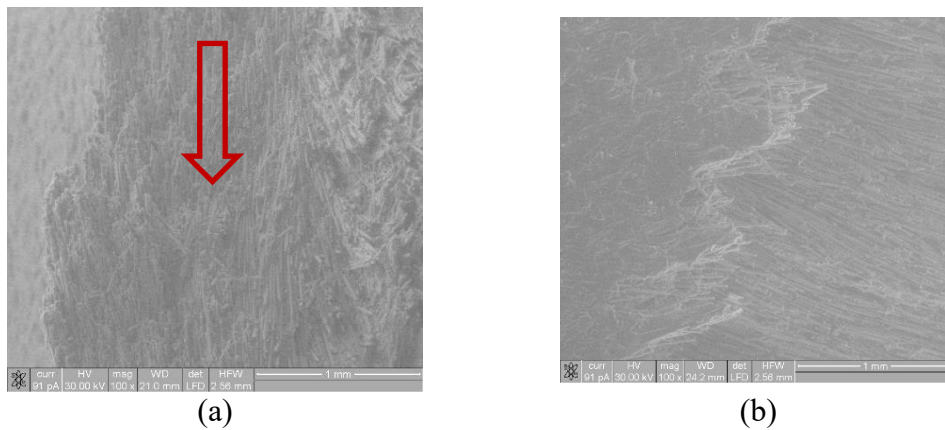


**Figure 1-6 Short fiber orientation in injected constituent; picture (a) shows the material orientation at the injection gate area and picture (b) at one of the randomly selected zones which both taken from damaged zones [6]**

Figure 1-7 clearly shows the distribution of the fibers in the ribs is random. Comparing two figures (Figure 1-6 and Figure 1-7) signifies that the fiber orientation patterns are completely different in the zones near the gates and those located far from the direct flow stream.

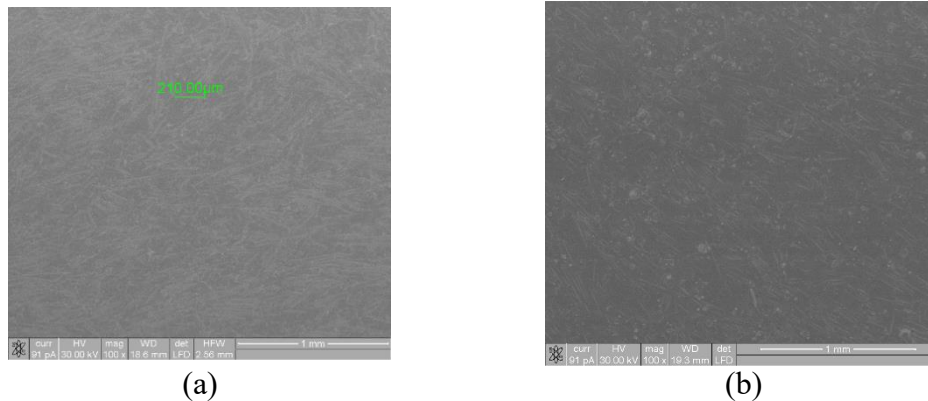


**Figure 1-7 Short fiber orientation in injected constituent; pictures (a) and (b) show glass fibers distribution and orientation on the surface of two randomly chosen areas [6]**

### 1.3 Literature review

In this section, we briefly present the literature of the current work and especially will focus on the major parameter which will affect the performance of short fiber reinforced thermoplastics (SFRTs) and post plasticity damage concept.

A Short Fiber Reinforced Polymer is employed for a type of composite materials which the polymer matrix dominate the fibers which are relatively short with variable length, imperfectly aligned and randomly distributed. The fibers are mostly glass, as it is used in the current work, carbon, graphite, and natural fibers. Major parameters which affect the SFRT's mechanical properties include fibers and matrix's individual properties, fiber-matrix interface characteristics, fibers' aspect ratio, the volume fraction of the fillers and the orientation and length distribution. [7]. Knowing that one of the major advantages of the SFRT's over the long fiber reinforced plastics is the injectability and therefore, the mechanical behavior of a SFRT will not be fully predictable, unless having complete data of the orientation and accumulation of the short fibers in the matrix and the interconnection between individual filler and the dominant resin. According to the major effective factors on the mechanical properties of the SFRPs, the research from the mechanical point of view have been reclined towards the following categories:

- Measurement of the fiber length distribution (FLD)
- Detection of the fiber orientation distribution (FOD)

- Predicting the final production SFRP's effective properties, considering the constituents characterizations (Micromechanical or multiscale approach); a most conventional model in this category is the so-called mixture rule.
- Predicting the SFRP's behavior by introducing a constitutive equation for entire media, considering the entire media as a specific anisotropic material and incorporating the major effective parameters into the governing equations (Macromechanical approach)

A short introduction is presented here for the first category, but we will skip the multiscale and micromechanical approaches as they are not in this research scope, but we will mostly focus on the second and further on the fourth category as the backbone of the current study found by these two categories.

### 1.3.1 Fiber length measurement

Mechanical properties of a SFRT, including their stiffness, yield strength, and the energy release rates, severely depend on the Fiber's Lengths Distribution (FLD). This concept might be practically achieved by burning off a SFRT specimen whom the matrix will almost disappear, and the fibers will last. This method is accomplished by many researchers due to the simplicity [8]. Number of investigations can be found in the composites' micromechanics literature, so that tried to define this phenomenon at the micromechanical level using a probability function [9-11], but according to the author's knowledge they have the same effect as fiber weight or volume fractions and probably because of this, even in the micromechanics approach, has not become as popular as the volume fraction or weight fraction concepts. Macroscopically, the FOD might be a representative of a material symmetry, but it seems the FLD does not represent any special mechanical aspect.

### 1.3.2 Fiber orientation in SFRPs

SFRPs conventionally are fabricated using injection molding, and due to their advantages, broad studies have been done by many researchers on different aspects of this composites, for example, see( [12-18]). Fibers orientations in SFRPs is one of the interesting parts of this class which has persuaded many researchers to perform experiments and propose many theories to detect this phenomenon, express the SFRPs' anisotropy and predict the mechanical behaviors. Such a strong influence of the fiber orientation distribution on the

forming of the material properties of SFRPs, demands a broad investigation in this matter and many researchers have been done. For instance [19-23] demonstrated that the distributions of the fibers, due to the injection process, is quite complex and not only vary from point to point along the SFRP molding but also through the thickness. From the micromechanical point of view the SFRPs are supposed to act as orthotropic materials due to the misalignment, but instead, a Representative Volume Element (RVE) also can be considered as a transversely isotropic material if someone ignores the misalignment. This can be extended to the macromechanical scale and if the fibers are aligned in a certain direction, for example, mold flow direction, then again it can be considered as a transversely isotropic material [1]. This study is accomplished in the framework of the latter assumption. However, the orientation of the short fibers in a SFRP is strongly influenced by processing conditions and mold geometry and hence the specimen geometry itself[7]. The so-called skin-core-skin is typical through the thickness pattern of FODs for the large injection molded, which the two skins contain the flow direction oriented fibers and instead, the core includes the fibers that aligned mostly in the transversely with respect to the flow direction [7, 19, 22, 24-26]. On the contrary, the small specimens with narrower cross sections do not follow this pattern, and presumably, the core part is eliminated from the pattern so that the fibers prefer to be aligned with the mold flow direction [7, 27-29].

Either non-destructive and destructive techniques might be used to capture the FODs. In the destructive method, a piece is cut off from the sample's section using microtome, and the fibers' elliptical footprints are analysed using an image analyzing software[30]. Despite its main drawback of uncertainty, especially due to the difficulties of extracting the volume properties from the information of area measurement, it is still used widely just because of the simplicity and low cost [19, 30]. The limitation might be overcome using a technique called successive sectioning which instead of physical sectioning employs confocal scanning laser microscopy to focus successive sections parallel to each other [30, 31]. On the other hand, conventional non-destructive technique is conducted using X-ray to capture a projection of the fibers as an image. Therefore, it cannot obtain a 3-D-form FOD, and the given data remain 2-D, but to overcome this problem a technique named computed micro-tomography, which uses a rotating X-ray sources, is employed[32].

### 1.3.3 Macromechanical approach

Introducing a constitutive equation for a material will be possible if its behavior under different kind of loading and boundary conditions are observed and are quantitated conducting the proper experiments. Generally, the quantity which is intended to be measured is deformation under certain field such as external or body forces, the temperature gradient, magnetic field and etc. from all the possible field, here, it is focused on the external forces, therefore the required constitutive equation must define relation between force and displacement or alternatively stress versus strain [33]. However, to obtain the knowledge about SFRPs' mechanical responses, they have been broadly experimented by many researchers and for many motivations. For example, an experimental study has been conducted to improve the knowledge about the failure mechanisms of injection molding polyamide reinforced by the inclusions of either glass and carbon fibers [15]. They recognized that the thermoplastic matrix failure mechanism occurs in a brittle fashion, even though the unfilled matrix behaves in a ductile way, and the total failure of the SFRP was referred to the progression of the cracks in the matrix at the end of fibers, but beyond any interpretation of failure mechanisms, they have obtained a nonlinear behavior for SFRPs.

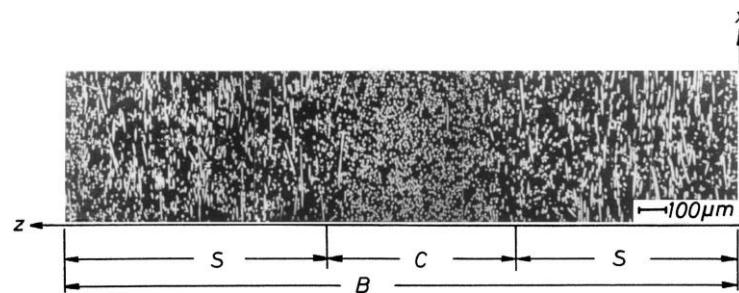


Figure 1-8 skin-core-skin pattern [25]

### 1.3.4 Damage

Among the several methods to model fracture and damage in solid mechanics, continuum damage mechanics (CDM) approaches have become more popular due to the convenience of their implementation in general purpose finite element software [34]. First successful application of the softening theory was in concrete structures to model the global load redistribution as a result of the development of the damage zone, without the need for complex modelling of detailed progressive damage mechanisms [35-37]. Continuum Damage Mechanics (CDM) approach

deals with material damage based on stiffness component degradation[38]. Also, CDM method which incorporates damage in the material response functions might be introduced as a set of internal vector field variables [39]. To define a damage model based on CDM approach, a constitutive model including damage variables must be presented. Generally, a constitutive model relates stresses to strains components using a fourth order stiffness tensor. To incorporate damage variables in constitutive equations, a reasonable way is redefining the stiffness tensor by implementing damage variables. The redefined stiffness tensor called degraded stiffness tensor. To achieve a physical base damage model and extract the constitutive equations, thermodynamic laws are considered which needs to define Helmholtz free energy [40]. To detect a specific damage mode activation a failure criterion, which represent the damaged surface in stress or strain space, must be defined. The damage envelope might be in a separated form such as Hashin-Rotem criterion for unidirectional composite plies[41]. In this type of failure criterion for each mode of damage, in longitudinal and transverse direction and under compression and tension, damage surfaces defined by different formulas. Later, Puck and Schurman based on Hashin and Rotem's hypothesis formulated another separated form of failure criterion which deals with inter-fiber failures and has a capability of detection of crack direction [42]. Even though based on World Wide Failure Exercise (WWFE) [43] Puck's failure theory showed the best agreement with experimental results, but there are some non-physically based parameters in this theory which make its application hard for users. To overcome this difficulty, Davila and Camanho developed a failure criterion based on Hashin and Puck theories, where no nonphysical parameters are needed[44]. Formerly, Chang and Chang suggested a separated form of failure criterion for notched laminated composites with consideration of material nonlinearity [45]. In addition to the separated type of failure criteria, one can implement an integrated type in CDM which are mostly the generalized form of Hill's criterion for orthotropic materials [46].

To deal with a progressive damage modeling, in addition to a failure criterion, a damage propagation law must be defined to govern the growth of existing damage. Lemaitre et al. formulated an anisotropic damage law in the framework of equivalent strain which the evolution of damage variables governed by plastic strains [47]. Maimi et al. suggested a general exponential form of damage law which used to represent the cohesive response of all the failure modes of the ply, except for the longitudinal tension damage [48]. For simulation of delamination in composite materials, Camanho and Davila proposed a new decohesion element

with the mix-mode capability and for applying the softening law, they used a displacement-based damage parameter to track the damage state of interface [49].

Finding a proper failure criterion to active the initial damage, and a constitutive equation to govern stress-strain relation before and after damage, and also defining sufficient numbers of damage variables, are just the beginning of damage problem modelling difficulties. Mesh sensitivity and convergence come out during the numerical solution of damage problem which severely affects the results. Lapczyk and Hurtado proposed an orthotropic damage model for pre and post damage in brittle laminated composites [50]. In this model LaRC04 failure criterion which proposed by Davila and Camanho [44] is used to predict the onset of damage. In LarC04 is same as Hashin's failure criterion, but stresses replaced by effective stress components. Also for damage evolution, they generalized Camanho and Davila method for delamination [49] and used specified fracture energy. Also to alleviate mesh dependency in numerical implementation they used crack band model which had been already proposed by Bazant and Oh[37] and to overcome convergence difficulties by following the Duvaut and Lions regularization method [51], instead of direct use of damage variables, a set of regularized form of damage variables are utilized .

On the other hand, mechanical properties of reinforced polymeric composite materials including unidirectional, short fiber and woven reinforcement are drastically rate-dependent [52]. In unidirectional composite materials, the module of elasticity in fiber direction is not rate-dependent as much as material tensile strengths at fiber direction [53]. Also, it has been shown that the module of elasticity and material strength in transverse directions are rate-dependent[54]. Also, it has been shown that woven fabric composites with a different pattern, laminated sequence and material are rate dependent [55, 56].

Considering the manufacturing process, see the section 1.2.1, the internal part made of short fiber composite material, it might be assumed that the constituent is governed entirely by the matrix and the open section is made of a fabric composite which is supposed to be dominated by fibers. Since from the beginning the main concern was about the bending response of the hybrid component. Therefore, the plastic response of the material was a lateral concern due to the fact that in 3-point bending the component response might be assumed. For the pointed out the reason, at the first step we assume the damage is initiated right after the elastic response of the material ends for both internal and external part of the cases study. To predict damage initiation of the internal part, the second part of

Hashin-Rotem's which is dealing with matrix damage initiation has been chosen. For the external part by considering the same reason, maximum stress theory is chosen which is dealing with fibers damage failure. Based on two failure criteria two different kinds of damage propagation models have been developed and implemented in ABAQUS using subroutines so-called VUMAT. Also, since the components have been shown rate dependent behavior, another model is suggested and developed to dealing with this kind of behavior and implemented in another VUMAT to investigate the rate-dependent behavior of the component. It should be noted that this rate dependency is just assigned to the internal part which is entirely dominated by the matrix. The model is developed assuming that plastic strain in these composite material is negligible, and also strain and stress are evenly distributed through an element. CDM approach has been followed to correlate damage variables determined using Lapczyk-Hurtado's model[50] and their effects upon stiffness matrix and consequently stress-strain relationship. The rate-dependent response is incorporated into modules of elasticity and strength of reinforcing constituent, using a logarithmic function and following Daniel and Wei et al.'s works [57, 58]. Also, mesh dependency problem has been alleviated following Lapczyk-Hurtado's model which strains are replaced by characteristic length and displacements of damage variables. Convergence problem has been solved following Duvaut and Lions regularization method [51] which instead of direct use of damage variables, a set of the regularized form of damage variables are utilized. In the next section, elasto-damage response of the material will be discussed and formulated for the 2-D case.

In the recent decades, CDM approaches for damage simulation in composite structures have received notable attention. For example, the NASA/Boeing-lead programme for Advanced Technology Composite Aircraft Structure (ATCAS) in collaboration with the University of British Columbia provided the first comprehensive experimental and strain-softening based modelling framework to simulate damage and failure in laminated composites[59-64].

## 1.4 Framework and objectives

This research begins with the production of the hybrid composite component which is supposed to be used in load-bearing part of the light vehicles. The production procedure as well as the constituents decompositions are explained in section 1.2. Due to confidentiality reasons, some of the information including the duration of each process and some of the precise temperatures are not given. Even though the hybrid components are made by two different technologies, i.e., back-

injected and compression molding, but since our main object is to simulate the injected components, then the compression molding procedure will be skipped in the numerical simulations.

In the next step, the 3-point bending experiments are performed on the hybrid component in both direction and different loading rates. The configuration of the test is explained in section 5.1 with details. The component demonstrates different response under different loading rates and different boundary conditions which is widely discussed in chapter 5 and more specifically in section 5.1.

According to the experimental results, the hybrid component under 3-point bending test does not show a high degree of nonlinearity before damage. Therefore, to simulate the back-injected hybrid component under bending, we introduce a linear elastic model including a damage model. The introduced model is described in section 4.4.1 as well as a rate-sensitive damage model which can be found in section 4.3. The model's integration scheme is broadly discussed in section 4.5 for either of the implicit and explicit solvers.

Also, the torsion test is prepared for the back-injected-made hybrid component which from the very beginning demonstrates a high degree of nonlinearity (see section 5.5). The nonlinear behavior of the component is related to its elasto-plastic response, and it is our main concern in the current research. The short fiber-reinforced composites can be considered as transversely-isotropic materials. Thus, to catch the plasticity induced nonlinearity, we introduce an elastic-plastic model and the post plasticity damage model. The entire models are founded on the representation theory of the basic invariants of the anisotropic materials. The associated constitutive equations for transversely isotropic materials are introduced in chapter 2. The chapter comprises the representation of the general constitutive equations (see section 2.1), an introduction to the representation theory in section 2.4 and the elastic constitutive equations for transversely isotropic materials in section 2.5. Since we deal with the non-metallic materials, then the elasto-plastic model must be non-associated which requires a potential function be defined besides of a yield function. These requirements as well as the proper invariants for the transversely isotropic materials are discussed and introduced in chapter 3.

Having defined the basic requirements of an elasto-plasticity model in chapters 2 and 3, we introduce the elasto-plasticity model in chapter 4. Since the numerical integration scheme requires a general definition of the model, then it is

formulated in a general continuum mechanics fashion in section 4.2. Also, to deal with the rate-dependent behavior of the hybrid component under bending, a simple model is introduced in section 4.3. A Continuum Damage Model (CDM) is introduced in section 4.4.1 for the post elasticity damage phenomenon. A damage model for degradation of the transversely isotropic material after reaching the saturation stress is developed based on the CDM concept in section 4.4.1.1. The so-called non-local damage model is described in section **Error! Reference source not found.** as well. The numerical implementation and the integration schemes are discussed in section 4.5 which includes the description of the backward Euler and the explicit integration algorithms in subsection 4.5.1 and 4.5.2, respectively.

In the last step, the numerical and experimental results are given and discussed in chapter 5. The bending test for the hybrid components are performed under quasi-static and the velocity of 127 mm/sec loading conditions. Other than ambient condition, the quasi-static bending experiment is performed for the components preheated by 90 degree Celsius and the results are available in section 5.1. The numerical results for the quasi-static and dynamic 3-point bending are given in sections 5.2 and 5.3, respectively. The elasto-plasticity plus the damage after plasticity models' numerical results are presented in section 5.4 and validated by the results taken from [1] for the basic tensile and compression test results of PA6GF60. The numerical and experimental results for the back-injected-made hybrid component under torsion are presented in section 5.5.

## Chapter2

# 2 Invariants theory for transversely isotropic materials

In the ongoing chapter, the invariant theory and its application to establish coordinate-free constitutive equations are addressed. The major portion of the basic formulations are grounded on the outstanding works of [65] on the application of tensor functions in solid mechanics, and also [66] which is dedicated to the continuum theory of short fiber-reinforced material. Besides these classical textbooks, the framework of this chapter follows the structure of [1]'s dissertation which categorized the invariant theory and its application for anisotropic materials in an admirable way.

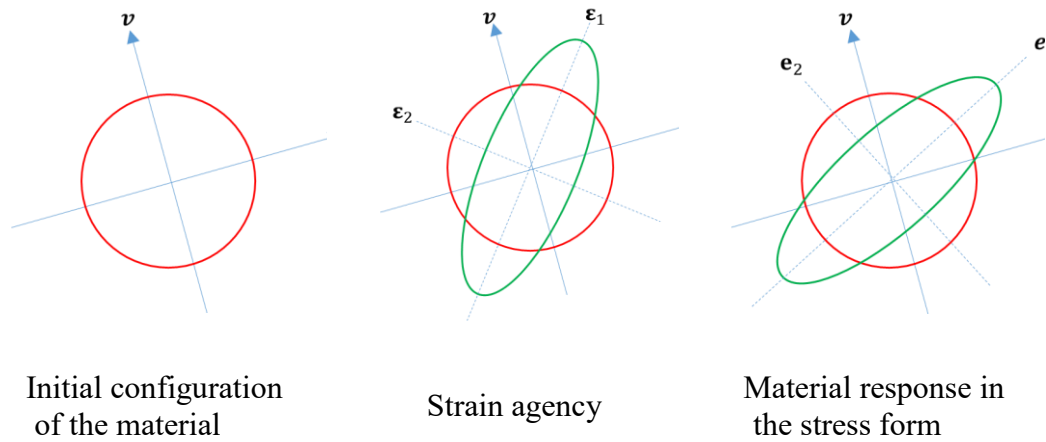
### 2.1 Constitutive equations in a general view

In the Newtonian world, the cause and effect rule is confirmed so that any events might have a cause and the event and causes might be related using an equation or number of equations which called constitutive equations. In solid mechanics, which the main concern is to find the relation between displacement and force, and consequently their tensorial representatives namely strain and stress tensors, respectively, the constitutive equation might be presented in the general form of:

$$\sigma = \widehat{\sigma}(\varepsilon, a_i) \quad (2-1)$$

The agent  $a_i$  called the structural tensor and represents the symmetries of the material either locally or globally. It means the material could be considered as a continuum which for instance is symmetric with respect to the x-direction, or the symmetry might be locally observed, and the entire continuum cannot be addressed as a material having a unique symmetry. The reinforced composites with randomly distributed short fiber might be an excellent example of the latter argument and in this case the agent  $a_i$  is a function of position [66]. Since the

main topic of this research is about the so-called anisotropic materials, especially transversely isotropic materials, let's define the anisotropy and the transversely isotropic phenomena. Materials called anisotropic if their behaviors vary from direction to another one, in other words these materials behave direction-dependently. since the main concern in solid mechanic is a stress-strain relationship, then material anisotropy also means that the principal strains and stresses do not coincide (see Figure 2-1), on the contrary, a material called isotropic if its principal stresses and strains for an arbitrary deformation filed coincide.



In general:  $(\varepsilon_1, \varepsilon_2) \neq (e_1, e_2)$

**Figure 2-1 Difference between the principal directions of the input agency and the response of an anisotropic material [65]**

Mathematically, isotropic material means that applying an arbitrary rotation on the constitutive equation of equation (2-1) causes no change in the results

$$\sigma = \hat{\sigma}(\varepsilon, a_i) = \hat{\sigma}(\varepsilon, Q(a \otimes a)_i Q^T) \quad \forall Q \in O(V) \quad (2-2)$$

The symbol  $\otimes$  implies the dyadic product and the index  $i$  is intentionally bolded just to signify that the outcome of the term  $a \otimes a$  is the structural tensor. The determination and importance of the structural tensor is discussed in section 2.1.1. The mathematical meaning of the orthogonal transformation tensor could be explained as

$$Qu \cdot Qv = u \cdot v \quad (2-3)$$

Which means that the orthogonal transformation tensor is orthogonal if it can preserve the inner product of the vector basis of a set of vectors, regarding that  $u, v \in V$  and  $Q \in L(V)$ .

Before going through the rest of the subject let's have a distinct definition of orthogonal transformation groups which might help to have a clear understanding of the symmetry groups in terms of orthotropic or transversely isotropic symmetry and so on. The orthogonal transformation in three-dimensional space includes rotations and reflections. A rotation  $\theta$  about an axis which defined by a unit vector  $\hat{v}_1$  with the components  $v_i^{(1)}$  might be characterized employing the following matrix; note that  $\hat{M}_\theta = M_{ij}^{(\theta)}$ :

$$M_{ij}^{(\theta)} = \delta_{ij} \cos(\theta) + e_{ijk} v_k^{(1)} \sin(\theta) + (1 - \cos(\theta)) v_i^{(1)} v_j^{(1)} \quad (2-4)$$

Which

$$e_{ijk} = \begin{cases} 1 & \text{if } ijk = 123, 231, 312; \\ -1 & \text{if } ijk = 132, 321, 213; \\ 0 & \end{cases} \quad (2-5)$$

If  $\hat{v}_1$  coincides with the basic Cartesian space vector  $\hat{e}_1$ , then the following matrix represents an orthogonal transformation in the rectangular Cartesian space  $Ox_1x_2x_3$ :

$$\hat{M}_\theta = \begin{bmatrix} 1 & 0 & 0 \\ 0 & \cos(\theta) & \sin(\theta) \\ 0 & -\sin(\theta) & \cos(\theta) \end{bmatrix} \quad (2-6)$$

And the reflection for an example in the plane with the normal  $\hat{v}_1$  can be characterized such as:

$$R_{ij}^{(1)} = \delta_{ij} - 2v_i^{(1)} v_j^{(1)} \quad (2-7)$$

Defining  $\hat{R}_1 = R_{ij}^{(1)}$ , Again for the particular case of the coincidence between  $\hat{v}_1$  and  $\hat{e}_1$ , the following reflection transformation matrix is valid:

$$\hat{R}_1 = \begin{bmatrix} -1 & 0 & 0 \\ 0 & 1 & 0 \\ 0 & 0 & 1 \end{bmatrix} \quad (2-8)$$

To whom looks for more details about the orthogonal symmetry concept and its application in invariant theory in anisotropic material might refer to [67]. However, some features of the orthogonal transformation tensors are needed in this research and listed below

$$\begin{aligned}
 Q^T &= Q^{-1} \\
 Q^2 &= 1 \\
 |\det(Q)| &= 1 \\
 |Q \cdot v| &= |v| \\
 \theta(Q \cdot u, Q \cdot v) &= \theta(u, v)
 \end{aligned} \tag{2-9}$$

The two latter properties even prove that the orthogonal transformation can reserve the norm and the angle between two vectors [65].

### 2.1.1 Structural tensor for short fiber reinforced thermoplastics

Structural tensors or internal variables or tensorial internal variables in conjunction with the so-called representation theorems are used in order to provide macromechanical explicit formulation to predict the rotation of the initial symmetry groups under any type of loading which leads the change in the primary symmetry groups such as off-axis tensile loading [68-71]. The short fiber reinforced composites mechanical responses are dominated by the fibers distribution pattern[72]. We presented the fiber orientation and distribution literature in the section 1.3.2 and do not intend to reiterate it. Since our intention is to simulate the nonlinear behavior of the SFRPs which are assumed to be transversely isotropic materials, then we just present a concise description of the sub-structural origin of the structural tensor. But the general meaning and mathematical concept of the structural tensor will be discussed in section 2.2. Following [72] we assume that the fibers as rigid cylinders which are uniform in length and diameter. The distribution of fiber orientation can be prescribed with a probability distribution function  $\psi$ . The number of the fibers per unit is also assumed to be constant. Then according to [72] we might construct the probability distribution function  $\psi$  in the polar coordinate system which is illustrated at Figure 2-2. Having mentioned assumptions, the orientation of a single fiber is determined using just a pair of angles  $(\theta, \phi)$  in the polar coordinate system. The orientation state can be described by a probability distribution function,  $\psi(\theta, \phi)$ . The definition of the function is so that it is supposed to determine the probability of existence of a fiber in the spans of  $[\theta_1, \theta_1 + d\theta]$  and  $[\phi_1, \phi_1 + d\phi]$  [1, 72]:

$$P(\theta_1 \leq \theta \leq \theta_1 + d\theta, \phi_1 \leq \phi \leq \phi_1 + d\phi) = \psi(\theta_1, \phi_1) \sin \theta_1 d\theta d\phi \quad (2-10)$$

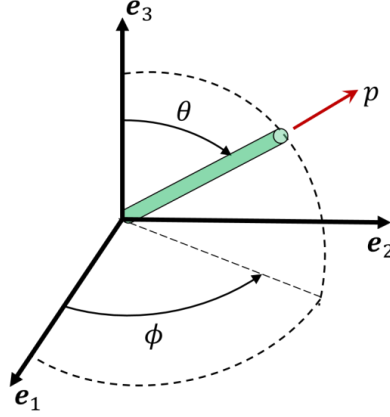


**Figure 2-2 Polar coordinate system definition for a single cylindrical fiber**

An alternative way to prescribe a probability distribution function as  $\psi(p)$  where  $p$  might be written in a vector shape:

$$p = \begin{bmatrix} \sin \theta \cos \phi \\ \sin \theta \sin \phi \\ \cos \theta \end{bmatrix} \quad (2-11)$$

Since the length of the fiber is fixed, then the components of the vector  $p$  are interrelated, and the following relationship can be written:

$$p_i p_i = 1 \quad (2-12)$$

The set of all possible directions of  $p$  corresponds to the unit sphere, and the integration over the surface of the sphere is:

$$\oint dp = \int_{\phi=0}^{2\pi} \int_{\theta=0}^{\pi} \sin \theta d\theta d\phi \quad (2-13)$$

the function  $\psi$  is symmetric and periodic, therefore:

$$\psi(\theta, \phi) = \psi(\pi - \theta, \pi - \phi) \quad (2-14)$$

or

$$\psi(p) = \psi(-p) \quad (2-15)$$

Also, the function  $\psi$  must be normalized which means that its integration over the unit surface must be equal to one [72]:

$$\oint \psi(\mathbf{p}) d\mathbf{p} = \int_{\phi=0}^{2\pi} \int_{\theta=0}^{\pi} \psi(\theta, \phi) \sin \theta d\theta d\phi = 1 \quad (2-16)$$

Here we do not intend to discuss the continuity condition which describes the change in  $\psi$  over time while fibers are changing the orientation under flow conditions. Therefore, the orientation distribution function is a function of two variables describe the orientation of a single fiber ( $\theta$  and  $\phi$  or the  $p_i$ 's) as well as its position within a physical structure [72]. According to [1, 72] the numerical calculation of the probability distribution function (2-16) is expensive and cumbersome. Also, one set of the function can be constructed based on the dyadic multiplication of the vector  $\mathbf{p}$ , and since the distribution function is even then only the even-order tensors are admissible, and all odd-order tensors are zero. Therefore, the fiber orientation tensor can be defined using a second order tensor as suggested by [72] as follows:

$$\mathbf{A} = a_{ij} = \oint \psi(\mathbf{p}) p_i p_j d\mathbf{p} \quad (2-17)$$

Which is an integral over all  $\mathbf{p}$  weighted by  $\psi(\mathbf{p})$ . As it is pointed out by [72], there is an infinite number of even-order tensors which can be used to describe the fiber orientations, but we limit our discussion to the second-order one. The second-order tensor in a discrete way, where it is intended to be written for a finite number ( $n$ ) of fibers, can be written as:

$$a_{ij} = \frac{1}{n} \sum_{k=1}^n a_{ij}^k = \frac{1}{n} \left( \sum_{k=1}^n p_i^k p_j^k \right) = \begin{bmatrix} a_{11} & a_{12} & a_{13} \\ a_{21} & a_{22} & a_{23} \\ a_{31} & a_{32} & a_{33} \end{bmatrix} \quad (2-18)$$

This tensor has the capability of defining the orientation of a single fiber in a given point of the continuum. The orientation tensor is symmetric, and the diagonal components can hold the values between 0 and 1. Also, due to the normalization condition, the summation of the diagonal components becomes one ( $a_{11} + a_{22} + a_{33} = 1$ ). Hence, the orientation tensor has five independent components which can fully describes the distribution and orientation of the fibers at one point in the space [1]. The off-diagonal components of the orientation tensor represent the amount of the fiber misalignments from the principal directions, and they are zero if the fiber aligns with the principal directions [73].

Commonly the structural tensor is applied using its eigenvalues which can be derived solving the characteristic equation. The eigenvectors are the representatives of the principal directions of the fiber orientation, and the

corresponding eigenvalues represent the statistical distribution of the fibers. Therefore, it would be better to define the structural tensor (2-18) with the corresponding eigenvalues and eigenvectors[73]:

$$a_{ij} \Rightarrow \begin{bmatrix} \lambda_1 & 0 & 0 \\ 0 & \lambda_2 & 0 \\ 0 & 0 & \lambda_3 \end{bmatrix} \cdot [e_1, e_2, e_3] \quad (2-19)$$

To have a visual perspective of the eigenvectors and eigenvalues for a single fiber, an ellipsoidal fiber is represented in the Eigen-space and can be seen in Figure 2-3.

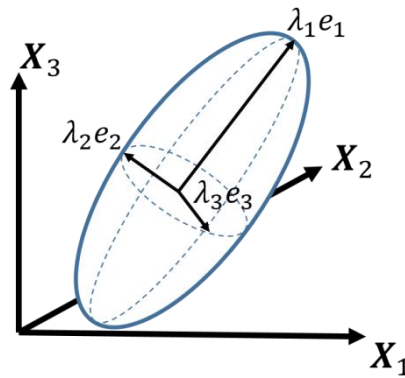


**Figure 2-3 The illustration of a single ellipsoidal fiber and the corresponding eigenvectors and eigenvalues.**

The first eigenvector represents the direction in which the fibers are mostly aligned, and the corresponding eigenvalue shows the probability in the direction which the fibers are aligned [73].

## 2.2 Physical and mathematical concept of space isotropy

The physical meaning of isotropy of space is that applying an arbitrary transformation  $Q$  of the orthogonal group  $O$  on both the agency, here is strain, and the material, read the material intrinsic property  $A = a \otimes a$ , causes in the same transformation of the material response. A straightforward explanation for this phenomena might be that the orientation of the space does not affect the constitutive equation of its own [65] which can be found in Figure 2-4.

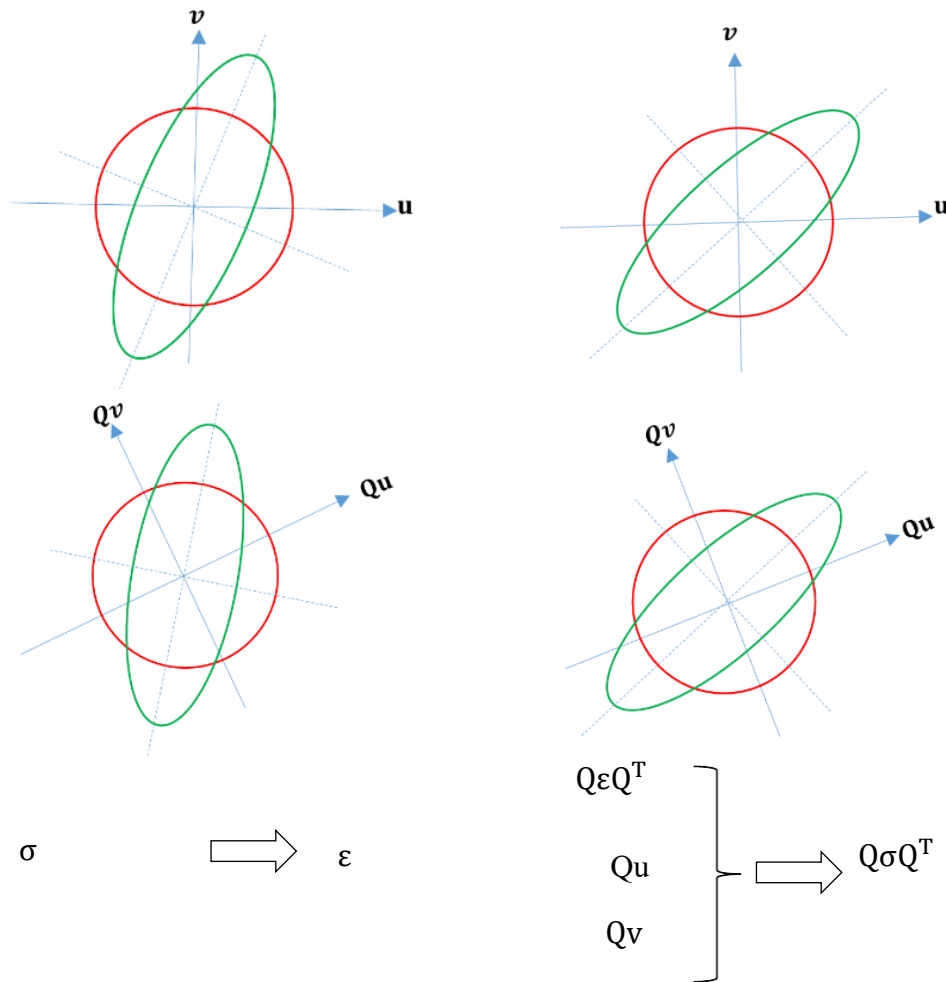


Figure 2-4 Principal of the isotropy of space [65]

Considering the physical meaning of the isotropy space concept and regarding the results have been achieved by that, which the transformation of the body, which is represented by the structural tensor, and transformation of the agency, read strain, causes the same transformation of the response (stress) reaches:

$$\forall Q \in O: \sigma(Q\epsilon Q^T, QAQ^T) = Q\sigma(\epsilon, A)Q^T \quad (2-20)$$

Then the function stress which can be any material response might be called Therefore, the constitutive function, which here is the stress function, but in general can be any material response, is isotropic with respect to the central agencies strain and structural tensor  $\mathbf{A}$  [65].

## 2.3 Isotropic functions

If  $\phi$ ,  $h$  and  $S$  are the scalar-valued, vector-valued and tensor-valued functions which are defined on the space  $\mathbb{R} \times V \times \mathcal{L}(V)$  and  $\mathbb{R}$  is the real number field,  $V$  represents a vector space and  $\mathcal{L}(V)$  shows a space made of the second-order tensors on  $V$ , then the following function shall be scalar, vector or tensor-valued isotropic functions [1]:

$$\begin{aligned} \phi(s, Qv, QAQ^T) &= \phi(s, v, A) & \forall Q \in O(V) \\ h(s, Qv, QAQ^T) &= Qh(s, v, A) & \text{Where } s \in \mathbb{R}, v \in V, A \in \\ & & L(V) \\ S(s, Qv, QAQ^T) &= QS(s, v, A)Q^T \end{aligned} \quad (2-21)$$

## 2.4 Representation for polynomial scalar and tensor functions

To start with the representation theory it is necessary to assume that the function  $\phi$  and the components are polynomials in a reference frame of the function  $S$ . Thus, the values  $A$  and  $S$  are polynomial invariants under the introduced orthogonal group [65]. The representation problem for the scalar valued function  $\phi$  is to calculate a basic set of polynomial scalar invariants ( $I_1, I_2, \dots, I_n$ ) such that an arbitrary polynomial scalar invariant of the same arguments can be explained as a polynomial in the basic invariants. The mentioned set of invariants called “integrity basis” for the considered list of arguments such as those can be found in the equation (2-21). One of the important concepts in the representative problem is the term so-called “irreducible integrity basis” which demonstrates that none of its subsets constitutes a compete for representation of itself [65].

The problem of representation for the tensor-valued function  $S$  is to find a generating set of tensors, so that the symmetric second-order tensors which are invariant under the group  $O$ , thus the represented tensor might be determined as a linear combination of the generating set’s arguments. The same concept is applicable for the vectors, so that under the representation problem, following relations might be written:

$$\begin{aligned} \phi &= \phi_s(\gamma_s) \\ h &= \sum_{u_a \in \gamma_v} \phi_a(\gamma_s) u_a \end{aligned} \quad (2-22)$$

$$S = \sum_{u_a \in Y_t} \phi_b(Y_s) T_b$$

Which  $Y_s, Y_v$  and  $Y_t$  are sets of scalar, vector and tensor invariants, respectively, while  $\phi_s, \phi_a$  and  $\phi_b$  are arbitrary polynomial functions of the invariants of the integrity basis of  $Y_s$  [65]. It is shown that representation for polynomial cases establishes a complete representation for non-polynomial cases as well [65, 74, 75]. Then, the coefficient  $\phi_x$  might be non-polynomial, but for the non-polynomial cases, the representations might not be “irreducible” in general [76, 77]. It should be noted that  $Y_s$  is called the basic invariants, while  $Y_v$  and  $Y_t$  are generating sets for isotropic vector and tensor functions, respectively [1]. Another point which should be noted here is the definition of so-called “irreducible” concept which means that the basic invariants elements, functionally, are not related to each other and also the generating set’s elements are linearly independent concerning isotropic functions. If a set of basic invariants or a generating set are irreducible, it is called functional basis. However, for the fundamental works on the integrity basis and the generating tensor concepts one can refer to [33, 65-67, 78].

Here we present the integrity bases for the scalar function  $\phi$  which in the following sections is typically appeared with the symbol  $f$  which are established by [79] and generating sets for tensor function  $S$  are presented which are established in [76].

#### 2.4.1 Representation for anisotropic scalar- and tensor-valued functions

If an anisotropic material possesses a specific symmetry group which might be defined in the form of a symmetric line or plane or a specific direction, then those symmetric groups could be defined using some unit vectors  $m = (m_1, \dots, m_a)$  or a set of tensors  $M = (M_1, \dots, M_a)$  such as following group which we assume the characterizes of the material are preserved:

$$\mathcal{G} = \{Q \in O, Qm = m, QMQ^T = M\} \quad (2-23)$$

Having defined the anisotropic symmetry group  $\mathcal{G}$ , let's define the so-called “isotropization theorem”[1] which explains that if  $f(v, A)$  be a scalar-, vector- or tensor-valued function and  $\mathcal{G}$  is the group which is defined above, then the

function  $f$  is invariant in this specific group if and only if it can be written in the following form:

$$f(v, A) = \hat{f}(v, A, m, M) \quad (2-24)$$

The function  $\hat{f}$  in  $\mathcal{O}$ . The latter equation illustrates that the anisotropic invariants might be transformed to the isotropic ones if the arguments are extended by adding the structural tensors which are invariants to the transformation of the material symmetries.

## 2.5 Elasticity

Elastic behavior characterized by two conditions:

1. The mechanical response of the material (stress) is a unique function of the strain
2. Removing the complete loading causes its return to the primary state (its natural shape without loading)

The elastic behavior might be linear or nonlinear which is illustrated in the figure below.

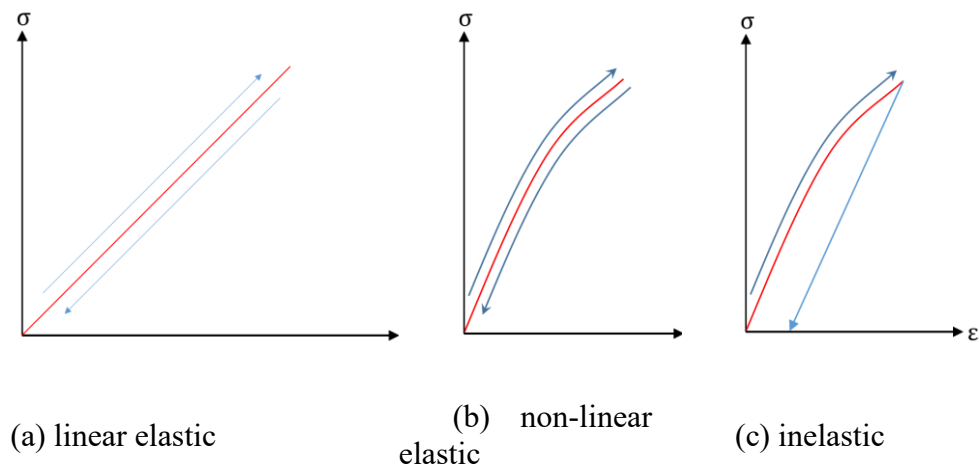


**Figure 2-5 uniaxial loading-unloading stress-strain curves [80]**

Symbolically, the most general constitutive equation for elastic behavior might be written in the following form [80]:

$$\sigma = G(\epsilon) \quad (2-25)$$

Where  $G$  is a symmetric tensor-valued function and  $\varepsilon$  might be any of strain tensors which can be found in the literature, but in the present text, it is assumed that the stress is a linear function of strain in relation (2-25). Besides, it is assumed that, in the deformed material, the displacement gradients are small, compare to unity. Thus, the Lagrangian and Eulerian description of the material can be considered as the same concept. Considering the assumptions, the infinitesimal strain tensor might be:

$$\varepsilon_{ij} = \frac{1}{2} \left( \frac{\partial u_i}{\partial x_j} + \frac{\partial u_j}{\partial x_i} \right) = \frac{1}{2} \left( \frac{\partial u_i}{\partial x_j} + \frac{\partial u_j}{\partial x_i} \right) = \frac{1}{2} (u_{i,j} + u_{j,i}) \quad (2-26)$$

Where  $u$  is the displacement field and the  $X_{...}$  represents the material labels in its Lagrangian format, while  $x_{...}$  illustrates the material's deformed configuration and called the Eulerian description of deformation. The Later equation in its rate form can be found in the equation (2-73) as well as brief descriptions of Lagrangian and Eulerian approaches are presented in section 2.5.3. considering the above assumptions, the general constitutive equation for elastic material can be written as:

$$\sigma_{ij} = C_{ijkl} \varepsilon_{kl} \text{ or } \sigma = C : \varepsilon \quad (2-27)$$

This equation called "Hook's law". The elastic tensor coefficients, in general, has  $3^4 = 81$  components which due to the symmetry of the stress and strain tensors drops to 36 distinct coefficients by the following descriptions:

$$C_{ijkl} = C_{jikl} = C_{ijlk} \quad (2-28)$$

Also for certain purposes is convenient to write the fourth-order coefficient tensor in a matrix form using two subscript and stress and strain tensors by one subscript which called "Voigt notation" as follows:

$$\sigma_{\alpha} = C_{\alpha\beta} \varepsilon_{\beta} \quad (2-29)$$

The Voigt notations have to be written in the following pattern:

$$\begin{aligned} \sigma_{11} &= \sigma_1 & \sigma_{22} &= \sigma_2 & \sigma_{33} &= \sigma_3 \\ \sigma_{12} &= \sigma_{21} = \sigma_4 & \sigma_{13} &= \sigma_{31} = \sigma_5 & \sigma_{23} &= \sigma_{32} = \sigma_6 \end{aligned} \quad (2-30)$$

And for the strain component:

$$\begin{aligned} \varepsilon_{11} &= \varepsilon_1 & \varepsilon_{22} &= \varepsilon_2 & \varepsilon_{33} &= \varepsilon_3 \\ 2\varepsilon_{12} &= 2\varepsilon_{21} = \varepsilon_4 & 2\varepsilon_{13} &= 2\varepsilon_{31} = \varepsilon_5 & 2\varepsilon_{23} &= 2\varepsilon_{32} = \varepsilon_6 \end{aligned} \quad (2-31)$$

Combining the equations to (2-29) to (2-31) the matrix form of Hook's law can be written as follows:

$$\begin{bmatrix} \sigma_{11} \\ \sigma_{22} \\ \sigma_{33} \\ \sigma_{12} \\ \sigma_{13} \\ \sigma_{23} \end{bmatrix} = \begin{bmatrix} C_{11} & C_{12} & C_{13} & C_{14} & C_{15} & C_{16} \\ C_{21} & C_{22} & C_{23} & C_{24} & C_{25} & C_{26} \\ C_{31} & C_{32} & C_{33} & C_{34} & C_{35} & C_{36} \\ C_{41} & C_{42} & C_{43} & C_{44} & C_{45} & C_{46} \\ C_{51} & C_{52} & C_{53} & C_{54} & C_{55} & C_{56} \\ C_{61} & C_{62} & C_{63} & C_{64} & C_{65} & C_{66} \end{bmatrix} \begin{bmatrix} \varepsilon_{11} \\ \varepsilon_{22} \\ \varepsilon_{33} \\ \varepsilon_{12} \\ \varepsilon_{13} \\ \varepsilon_{23} \end{bmatrix} \quad (2-32)$$

Since this text is addressed to the elastic and inelastic mechanical response of transversely isotropic material, thus the material symmetry group including three mutually perpendicular planes in the Cartesian configuration as well as one of the main directions, here  $e_3$ , causes the reduction of the number of material constants to five and the general equation (2-41) might be rewritten as:

$$\begin{bmatrix} \sigma_{11} \\ \sigma_{22} \\ \sigma_{33} \\ \sigma_{12} \\ \sigma_{13} \\ \sigma_{23} \end{bmatrix} = \begin{bmatrix} C_{11} & C_{12} & C_{13} & 0 & 0 & 0 \\ & C_{22} & C_{23} & 0 & 0 & 0 \\ & & C_{33} & 0 & 0 & 0 \\ & & & C_{44} & 0 & 0 \\ & \text{Symmetric} & & & C_{44} & 0 \\ & & & & & \frac{1}{2}(C_{11} - C_{12}) \end{bmatrix} \begin{bmatrix} \varepsilon_{11} \\ \varepsilon_{22} \\ \varepsilon_{33} \\ \varepsilon_{12} \\ \varepsilon_{13} \\ \varepsilon_{23} \end{bmatrix} \quad (2-33)$$

The material stiffness tensor for the transversely isotropic material is presented in the next sub-section which is based on invariant theory, hyperelasticity assumption for the material response and free strain energy function.

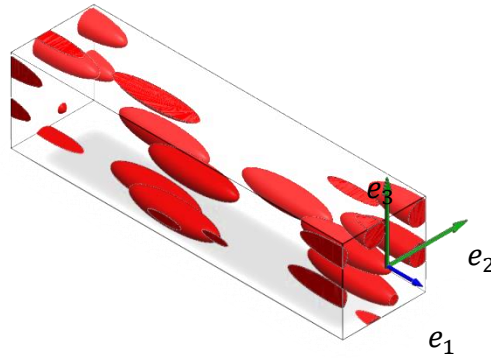


**Figure 2-6 A typical substructure of a short fiber reinforced composite and transversely isotropic materials. The direction  $e_3$  indicates the isotropy plane normal**

### 2.5.1 Transversely isotropic elasticity

In this section, following the representation approach, the elastic response of materials with transversely isotropic symmetries are presented. For complementary information about the elastic response of the materials with different symmetry groups and by using the representation theory, one can refer to [33, 65, 66].

### 2.5.2 Scalar- and tensor-valued isotropic functions for transversely isotropic materials

According to the representation theory and considering equation (2-22) construction of a constitutive equation for an anisotropic material needs its relevant arguments' generators and integrity bases to be defined. Since the topic is addressed to transversely isotropic materials and the relevant symmetry group, then here we focus on the irreducible representations, read generators and integrity bases. Since the vector invariants and their integrity bases and generators do not play a role in the current research activity, then only scalar- and tensor-valued function are intended to be constructed based on the representation theory. Let's start with the definition of the transversely isotropic material. Material is transversely isotropic if we could find a privileged direction  $a$  which the material is symmetric about this axis. The constitutive equations for transversely isotropic materials are invariant under rotation about the preferred direction  $a$  under the orthogonal rotation tensor (2-6) [67].

A transversely isotropic material is symmetric with respect to the preferred direction  $\mathbf{a}$  which is the normal of the isotropy plane. Then the constitutive equation restriction becomes the invariance of the equations under rotation about the direction  $\mathbf{a}$ . The symmetry transformation group can be easily defined based on the orthogonal rotation tensor and reflection tensor which might be a particular case of the rotation about the preferred direction  $\mathbf{a}$  such as follows:

$$\mathfrak{g}_{12} = \{Q \in \widehat{M}_\theta \text{ which } 0 < \theta < 2\pi, \widehat{R}_1, \pm I\} \quad (2-34)$$

Which  $I$  is the identity tensor. According to the hexagonal symmetry group in (2-25) which proposed by [81], the relative structural tensor reads:

$$A = \mathbf{a} \otimes \mathbf{a} \quad (2-35)$$

In fact, this structural tensor is one of the possibilities for the transversely isotropic symmetry, and also the introduced symmetry group in (2-25) is one of the five options which is given in [81], but the other four are a subgroup of this symmetry group. This new argument, e.g., structural tensor, which represents the symmetry of the material has to be invariant under an arbitrary rotation in (2-25), thus:

$$QAQ^T = A \quad \forall Q \in \mathfrak{g}_{12} \quad (2-36)$$

Then, we have a new argument as well as the strain tensor  $\boldsymbol{\varepsilon}$ . Therefore, there are two arguments to construct the invariant scalar- and tensor-valued functions to explain the transversely isotropic material response so that the general representation of transverse isotropy reads:

$$\begin{aligned} \Phi &= \widehat{\Phi}(\boldsymbol{\varepsilon}, A) \\ \sigma &= \widehat{\sigma}(\boldsymbol{\varepsilon}, A) \end{aligned} \quad (2-37)$$

Where  $\widehat{\Phi}$  is an isotropic scalar-valued function and  $\widehat{\sigma}$  is an isotropic tensor-valued function which both functions are isotropic with respect to two strain tensor and structural tensor arguments. Comparing the relations (2-22) and (2-28) illustrates that the main procedure to convert this two general equation to two specific equations which might characterize the transversely isotropic material behaviors in linear and nonlinear states is to find the sets of generators and integrity basis under symmetric group of  $\mathfrak{g}_{12}$ . The irreducible sets of generators and integrity bases for isotropic functions with respect to the entire arguments including the structural tensor can be found in Table 2-1. Note that the generators and the integrity bases are transversely isotropic with respect to the agents, but are

generators or integrity of isotropic functions if structural tensor is taken into account.

Table 2-1 Irreducible representations for transversely isotropic functions with one and two arguments [82]

Variables	Generators for polynomial functions	Integrity bases
	1, A	-
D	D, AD + DA, D <sup>2</sup> , AD <sup>2</sup> + D <sup>2</sup> A	trD, trD <sup>2</sup> , trD <sup>3</sup> , trAD, trAD <sup>2</sup>
D <sub>1</sub> , D <sub>2</sub>	AD <sub>1</sub> D <sub>2</sub> + D <sub>1</sub> D <sub>2</sub> A, AD <sub>2</sub> D <sub>1</sub> + D <sub>1</sub> D <sub>2</sub> A, AD <sub>1</sub> <sup>2</sup> D <sub>2</sub> + D <sub>2</sub> D <sub>1</sub> <sup>2</sup> A, AD <sub>1</sub> D <sub>2</sub> <sup>2</sup> + D <sub>2</sub> <sup>2</sup> D <sub>1</sub> A	trD <sub>1</sub> D <sub>2</sub> , trAD <sub>1</sub> D <sub>2</sub> , trD <sub>1</sub> <sup>2</sup> D <sub>2</sub> , trD <sub>1</sub> D <sub>2</sub> <sup>2</sup> , trD <sub>1</sub> <sup>2</sup> D <sub>2</sub> <sup>2</sup> , trAD <sub>1</sub> <sup>2</sup> D <sub>2</sub> , trAD <sub>1</sub> D <sub>2</sub> <sup>2</sup>

If the strain tensor is considered as the main variable and assuming a linear dependency of the material response, read the stress tensor, to the strain tensor, then the cubic term trD<sup>3</sup> must be dropped from the integrity bases and the new set of integrity bases might be written as:

$$\Upsilon_s: \text{tr}\varepsilon, \text{tr}\varepsilon^2, \text{tr}A\varepsilon, \text{tr}A\varepsilon^2 \quad (2-38)$$

This set represents the reduced integrity bases and incorporating it into the equation (2-37) gives:

$$\Phi = \hat{\Phi}(\text{tr}\varepsilon, \text{tr}\varepsilon^2, \text{tr}A\varepsilon, \text{tr}A\varepsilon^2) \quad (2-39)$$

Before constructing the tensor-valued isotropic function of transversely isotropic materials, it should be noted that the second order identity matrix and the structural tensor itself are involved in all generator sets with any number of variables. Again considering a linear response of the material, the set of generators is reduced to:

$$\Upsilon_t: 1, A, \varepsilon, A\varepsilon + \varepsilon A \quad (2-40)$$

Where 1 represents the second order identity tensor. Thus, the tensor-valued isotropic function might be constructed such as following:

$$\sigma = \hat{\sigma}(1, A, \varepsilon, A\varepsilon + \varepsilon A) \quad (2-41)$$

Incorporating the equation (2-41) into the (2-22) the second order tensor-valued isotropic function can be written in the below format:

$$\sigma = \widehat{\sigma}(\varepsilon, A) = \sum_{u_a \in Y_t} \phi_b(Y_s) T_b = \alpha_1 1 + \alpha_2 A + \alpha_3 \varepsilon + \alpha_4 (A\varepsilon + \varepsilon A) \quad (2-42)$$

Where the coefficients of  $\alpha$  as mentioned before are the polynomials employing the introduced integrity bases elements. To determine the coefficient, it is necessary to apply the material restrictions and also taking into account the primary assumptions such as the linearity. The presumption of linear behavior of the material leads that the coefficient  $\alpha_3$  and  $\alpha_4$  must be constant and the  $\alpha_1$  and  $\alpha_2$  have to have a linearly dependent relation with the strain tensor with respect to the linear arguments of the given integrity bases in (2-29) which reads:

$$\begin{aligned} \alpha_1 &= \alpha_{11} + \alpha_{12} \text{tr} \varepsilon + \alpha_{13} \text{tr} A \varepsilon \\ \alpha_2 &= \alpha_{21} + \alpha_{22} \text{tr} \varepsilon + \alpha_{23} \text{tr} A \varepsilon \\ \alpha_3 &= \alpha_{31} \\ \alpha_4 &= \alpha_{41} \end{aligned} \quad (2-43)$$

One the very natural restriction which can be applied to the equation set (2-43) in the free stress field for the understored continuum which means  $\varepsilon = 0$  causes  $\sigma = 0$  which lead to  $\alpha_{11} = \alpha_{21} = 0$  and furthermore applying on the equation (2-42) leads [1]:

$$\sigma = \widehat{\sigma}(\varepsilon = 0, A) = \alpha_1 1 + \alpha_2 A \stackrel{*}{=} 0 \quad (2-44)$$

Inserting (2-43) into (2-44) and considering that the constants became zero by applying the assumptions yields to:

$$\sigma = (\alpha_{12} \text{tr} \varepsilon + \alpha_{13} \text{tr} A \varepsilon) 1 + (\alpha_{22} \text{tr} \varepsilon + \alpha_{23} \text{tr} A \varepsilon) A + \alpha_{31} \varepsilon + \alpha_{41} (A \varepsilon + \varepsilon A) \quad (2-45)$$

By now the transversely isotropic material elastic constitutive equation has six constants to be defined which according to the relation (2-35) five constants left independent. To achieve a complete set of independent material constants for transversely isotropic material its strain energy in the framework of a scalar-valued function might be defined:

$$\Psi = \widehat{\Psi}(\text{tr} \varepsilon, \text{tr} \varepsilon^2, \text{tr} A \varepsilon, \text{tr} A \varepsilon^2) \quad (2-46)$$

And it is known from the classic elasticity theories, which by assuming hyperelastic behavior for the material under an infinitesimal deformation, the first order partial derivative of the strain energy with respect to the strain tensor  $\varepsilon$  shall define the mechanical response of the material  $\sigma$ . Therefore, it can be written:

$$\sigma = \frac{\partial \Psi}{\partial \varepsilon} \quad (2-47)$$

assuming linear elasticity lead to the assumption of the free energy function  $\hat{\Psi}$  which is quadratic in terms of strains [1]. Again the derivative of this free energy ( $\Psi$ ), (2-37), with respect to the strain tensor  $\varepsilon$  can give the material response to stress:

$$\begin{aligned} \sigma &= \frac{\partial \Psi}{\partial \varepsilon} = \frac{\partial \Psi}{\partial \text{tr} \varepsilon} \frac{\partial \text{tr} \varepsilon}{\partial \varepsilon} + \frac{\partial \Psi}{\partial \text{tr} \varepsilon^2} \frac{\partial \text{tr} \varepsilon^2}{\partial \varepsilon} + \frac{\partial \Psi}{\partial \text{tr} A \varepsilon} \frac{\partial \text{tr} A \varepsilon}{\partial \varepsilon} \\ &\quad + \frac{\partial \Psi}{\partial \text{tr} A \varepsilon^2} \frac{\partial \text{tr} A \varepsilon^2}{\partial \varepsilon} \\ &= \frac{\partial \Psi}{\partial \text{tr} \varepsilon} 1 + \frac{\partial \Psi}{\partial \text{tr} \varepsilon^2} A + \frac{\partial \Psi}{\partial \text{tr} A \varepsilon} 2\varepsilon + \frac{\partial \Psi}{\partial \text{tr} A \varepsilon^2} (A\varepsilon + \varepsilon A) \end{aligned} \quad (2-48)$$

Then the comparison between the coefficients of two equation of (2-36) and (2-48) yields:

$$\begin{aligned} \frac{\partial \Psi}{\partial \text{tr} \varepsilon} &= \alpha_{12} \text{tr} \varepsilon + \alpha_{13} \text{tr} A \varepsilon \\ \frac{\partial \Psi}{\partial \text{tr} \varepsilon^2} &= \alpha_{22} \text{tr} \varepsilon + \alpha_{23} \text{tr} A \varepsilon \\ \frac{\partial \Psi}{\partial \text{tr} A \varepsilon} &= \frac{1}{2} \alpha_{31} \\ \frac{\partial \Psi}{\partial \text{tr} A \varepsilon^2} &= \alpha_{41} \end{aligned} \quad (2-49)$$

and since the function  $\Psi$  has to satisfy the integrability condition then:

$$\frac{\partial}{\partial \text{tr} \varepsilon} \left( \frac{\partial \Psi}{\partial \text{tr} A \varepsilon} \right) = \frac{\partial}{\partial \text{tr} A \varepsilon} \left( \frac{\partial \Psi}{\partial \text{tr} \varepsilon} \right) \quad (2-50)$$

And the last relation results in the following conditions:

$$\alpha_{13} = \alpha_{22} \quad (2-51)$$

Hence, just five independent material constants remained to describe transversely isotropic material mechanical response subjected to infinitesimal and linear deformations. Integration of the partial derivative of the stress function gives free energy function and conventionally for any common material symmetry the specific notations are used for introducing the constants [83]. However, the free energy for transversely isotropic material with symbolic notation might be written in the following form :

$$\begin{aligned}\hat{\Psi}(\varepsilon, A) = & \frac{1}{2}\lambda(\text{tr}\varepsilon)^2 + \mu_T\text{tr}(\varepsilon)^2 + \alpha(a\varepsilon a)\text{tr}\varepsilon + 2(\mu_L - \mu_T)(a\varepsilon^2 a) \\ & + \frac{1}{2}\beta(a\varepsilon a)^2\end{aligned}\quad (2-52)$$

where all constants  $\lambda$ ,  $\mu_T$ ,  $\alpha$ ,  $\mu_L$  and  $\beta$  are the transversely isotropic elastic constants. In the present text if an index notation of a formula could assist its clarification it will be used. For the same reason the index notation of the free energy equation (2-52) is rewritten:

$$\begin{aligned}\hat{\Psi}(\varepsilon, A) = & \frac{1}{2}\lambda(\varepsilon_{ii})^2 + \mu_T\varepsilon_{ij}\varepsilon_{ij} + \alpha a_i\varepsilon_{ij}a_j\varepsilon_{kk} \\ & + 2(\mu_L - \mu_T)a_i\varepsilon_{ij}\varepsilon_{jk}a_k + \frac{1}{2}\beta(a_i\varepsilon_{ij}a_j)^2\end{aligned}\quad (2-53)$$

Accordingly, if the hyperelasticity condition is assumed to be preserved, then the equation (2-38) can be used, and the stress tensor can be derived by taking the first partial derivative of the elastic free energy density function with respect to the strain tensor:

$$\begin{aligned}\sigma = \partial_\varepsilon \hat{\Psi}(\varepsilon, A) = & \lambda(\text{tr}\varepsilon)1 + 2\mu_T\varepsilon + \alpha(a\varepsilon a1 + \text{tr}\varepsilon A) + 2(\mu_L \\ & - \mu_T)(A\varepsilon - \varepsilon A) + \beta(a\varepsilon a)A\end{aligned}\quad (2-54)$$

Although, care must be taken that the dot product of two second-order tensor is given without “.” Symbol, therefore, the term  $A\varepsilon = A \cdot \varepsilon = A_{im}\varepsilon_{mj}$ . Consequently, the second partial derivative of the elastic free energy function with respect to the strain tensor gives the fourth-order material's stiffness tensor:

$$\begin{aligned}C = \partial_{\varepsilon\varepsilon}^2 \hat{\Psi}(\varepsilon, A) \\ = \lambda 1 \otimes 1 + 2\mu_T \mathbb{I} + \alpha(A \otimes 1 + 1 \otimes A) + 2(\mu_L - \mu_T)\mathbb{I}_A + \beta A \\ \otimes A\end{aligned}\quad (2-55)$$

The hollow symbols illustrate fourth-order tensors and their equivalent matrix form in VOIGT notation. The stiffness tensor can be written in index notation as follows:

$$\begin{aligned}C_{ijkl} = & \lambda\delta_{ij}\delta_{kl} + 2\mu_T I_{ijkl} + \alpha(a_i a_j \delta_{kl} + \delta_{ij} a_k a_l) \\ & + 2(\mu_L - \mu_T)(I_A)_{ijkl} + \beta a_i a_j a_k a_l\end{aligned}\quad (2-56)$$

Where

$$I_{ijkl} = \frac{1}{2}(\delta_{ik}\delta_{jl} + \delta_{il}\delta_{jk})\quad (2-57)$$

And

$$(I_A)_{ijkl} = A_{im}I_{jmkl} + A_{jm}I_{mikl} \quad (2-58)$$

Where  $1 = \delta_{ij}$  defines the Kronecker delta so that

$$\delta_{ij} = \begin{cases} 1 & \text{for } i = j \\ 0 & \text{for } i \neq j \end{cases} \quad (2-59)$$

If  $e_1 = [1,0,0]$  considered as the material's privileged direction (see Figure 2-6) then the material's stiffness matrix in the Voigt notation reads:

$$C = \begin{bmatrix} \lambda + 2\alpha + \beta + 4\mu_L - 2\mu_T & \lambda + \alpha & \lambda + \alpha & 0 & 0 & 0 \\ & \lambda + 2\mu_T & \lambda & 0 & 0 & 0 \\ & & \lambda + 2\mu_T & 0 & 0 & 0 \\ & & & \mu_L & 0 & 0 \\ & \text{Sym} & & & \mu_L & 0 \\ & & & & & \mu_T \end{bmatrix} \quad (2-60)$$

The important matter after the construction of the stiffness tensor is the limits of elasticity constants which means that the constants cannot hold the arbitrary values. The product of a stress and corresponding strain shows work done by the stress. Hence, to avoid the creation of energy the sum of the work done by all stresses must be positive. The later condition provides a “thermodynamic constraint” on the material's elastic constants[84, 85]. Assuming the free energy potential  $\Psi$  and the complimentary free energy  $\tilde{\Psi}$  by the following definition:

$$\begin{aligned} \Psi &= \frac{1}{2} \varepsilon : C : \varepsilon \\ \tilde{\Psi} &= \frac{1}{2} \sigma : C^{-1} : \sigma \end{aligned} \quad (2-61)$$

where  $C^{-1}$  is the elasticity compliance tensor which for the convenience consider it is written in the Voigt notation as well as the other arguments including stress and strain tensors. Since both free energies carry the positive values and both right hands of the equations in (2-61) includes the quadratic terms of strain and stress tensors' components, then the elasticity tensor  $C$  and the elastic compliance tensor must be positive definite for arbitrary strains and stresses, respectively[1]. A symmetric tensor called “positive/negative definite” matrix if all its eigenvalues are positive/negative [80]. Such a tensor contains special features such that its diagonal entities, which has by definition the real numbers, as well as its determinant, must be positive [86, 87]. It might be convenient using the engineering constants instead of the tensor-oriented constants so that the

compliance elastic constants tensor in Voigt notation which is appeared in equation (2-61) can be translated to:

$$C^{-1} = \begin{bmatrix} \frac{1}{E_{11}} & -\frac{\nu_{12}}{E_{22}} & -\frac{\nu_{12}}{E_{22}} & 0 & 0 & 0 \\ -\frac{\nu_{21}}{E_{11}} & \frac{1}{E_{22}} & -\frac{\nu_{23}}{E_{22}} & 0 & 0 & 0 \\ -\frac{\nu_{21}}{E_{11}} & -\frac{\nu_{23}}{E_{22}} & \frac{1}{E_{22}} & 0 & 0 & 0 \\ 0 & 0 & 0 & \frac{1}{G_{12}} & 0 & 0 \\ 0 & 0 & 0 & 0 & \frac{1}{G_{12}} & 0 \\ 0 & 0 & 0 & 0 & 0 & \frac{1}{G_{23}} \end{bmatrix} \quad (2-62)$$

Considering the symmetry of the matrix leads:

$$-\frac{\nu_{21}}{E_{11}} = -\frac{\nu_{12}}{E_{22}} \quad \rightsquigarrow \quad \nu_{21} = \frac{E_{11}}{E_{22}} \nu_{12} \quad (2-63)$$

$$C^{-1}(4,4) = 2(C^{-1}(3,3) - C^{-1}(2,3)) \quad \rightsquigarrow \quad G_{23} = \frac{E_{33}}{2(1+\nu_{23})}$$

According to the positive definite of compliance matrix yields:

$$C^{-1}(1,1), C^{-1}(3,3), C^{-1}(4,4), C^{-1}(6,6) > 0 \quad (2-64)$$

Therefore

$$E_{11}, E_{22}, G_{12} \text{ and } G_{23} > 0 \quad (2-65)$$

must be regarded. Inversion of the compliance matrix gives the elasticity constants matrix:

$$C = \begin{bmatrix} \frac{1-\nu_{23}^2}{\text{Det}} E_{11} & \frac{\nu_{21}+\nu_{21}\nu_{23}}{\text{Det}} E_{22} & \frac{\nu_{21}+\nu_{21}\nu_{23}}{\text{Det}} E_{22} & 0 & 0 & 0 \\ \frac{\nu_{12}+\nu_{12}\nu_{23}}{\text{Det}} E_{11} & \frac{1-\nu_{12}\nu_{21}}{\text{Det}} E_{22} & \frac{\nu_{23}+\nu_{12}\nu_{21}}{\text{Det}} E_{11} & 0 & 0 & 0 \\ \frac{\nu_{12}+\nu_{12}\nu_{23}}{\text{Det}} E_{11} & \frac{\nu_{23}+\nu_{12}\nu_{21}}{\text{Det}} E_{22} & \frac{1-\nu_{12}\nu_{21}}{\text{Det}} E_{22} & 0 & 0 & 0 \\ 0 & 0 & 0 & G_{12} & 0 & 0 \\ 0 & 0 & 0 & 0 & G_{12} & 0 \\ 0 & 0 & 0 & 0 & 0 & G_{23} \end{bmatrix} \quad (2-66)$$

where  $\text{Det} = 1 - 2\nu_{12}\nu_{21}(1 + \nu_{23}) - \nu_{23}^2$ . Since the compliance matrix is needed as well must be considered positive infinite, therefore the diagonal must be positive:

$$\begin{aligned}
C(1,1) > 0 & \rightsquigarrow 1 - \nu_{23}^2 > 0 \rightsquigarrow |\nu_{23}| < 1 \\
C(3,3) > 0 & \rightsquigarrow 1 - \nu_{12}\nu_{21} > 0 \rightsquigarrow |\nu_{12}| < \sqrt{\frac{E_{22}}{E_{11}}} \text{ and } |\nu_{21}| < \sqrt{\frac{E_{11}}{E_{22}}}
\end{aligned} \quad (2-67)$$

At the same time the term Det must be greater than zero which results:

$$|\nu_{12}| < \sqrt{\frac{(1-\nu_{23})E_{22}}{2E_{11}}} \text{ and } \nu_{23} < 1 - 2\nu_{12}^2 \frac{E_{11}}{E_{22}} \quad (2-68)$$

The restrictions must be taken into account, especially, for the coding procedure to be implemented into the Finite Element solver and have to be applied putting the “exit/break conditions”.

However, elastic response of different symmetry groups such as isotropic, transversely isotropic, orthotropic and monoclinic materials are well established so far, and they can be found in many textbooks [33, 66, 85, 88, 89]. In the next section, we talk about the kinematic constraints and their effects on the mechanical response of the transversely isotropic material and this concise introduction of kinematic constraints may explain the necessity of the current research.

### 2.5.3 Kinematic constraints

Here we describe two common kinematic constraints which in many branches of continuum mechanics can be found. The first and most important one might be “incompressibility” which means that the material’s volume remains constant subjected to a specific range of deformations. Another example of the kinematic constraints is “inextensibility” condition in a specified direction. Clearly, in some particular type of fiber reinforced composites, such as unidirectional composites, the material shows a significant level of resistance to extension in a specific direction. Evidently, the high level of resistance to an extension is defined comparing the deformation of the material in other directions such as transverse direction or shear condition. This approximation might leads a proper analysis with a reduction in the level of complexity of the problem[83].

To have a concise explanation of the effect of the kinematic constraints on the constitutive equations the two mentioned kinematic constraints are considered. let’s suppose the primary configuration system is a fixed Cartesian one, and a material point  $\mathbf{P}$  introduces a representative position of the material in its free state, and the current deformation might be:

$$x_0^p = x(X_0, t = 0) \Rightarrow x_i^p = x_i(X_R, t = \tau) \quad (2-69)$$

For readability, consider  $x_i^p = x_i$ , therefore the deformation can be described by the dependency of  $x$  on  $X$  and time. The deformation gradient in its notation form reads:

$$F_{iR} = \frac{\partial x_i}{\partial X_R} \quad (2-70)$$

The finite strain tensors  $C$  and  $\hat{B}$ , consequently, are employed, where

$$C = F^T F \text{ and } \hat{B} = F F^T \quad (2-71)$$

And the infinitesimal strain tensor can be defined such as following:

$$\boldsymbol{\varepsilon} = \frac{1}{2} (F + F^T) - 1 \quad (2-72)$$

All symbols in bold letters illustrate second-order tensors unless otherwise stated. The rate of deformation might be introduced as the symmetric part of spatial velocity gradient:

$$D_{ij} = \frac{1}{2} \left( \frac{\partial v_i}{\partial x_j} + \frac{\partial v_j}{\partial x_i} \right) \quad (2-73)$$

Having defined the deformation gradient and finite strain tensors, the incompressibility condition for all possible deformations might read:

$$\det F = 1, \text{ or } \det C = 1, \text{ or } \det F = 1 \quad (2-74)$$

Considering each of the circumstances causes the following constraint for incompressible materials under infinitesimal deformation condition:

$$\text{tr} \boldsymbol{\varepsilon} = 0 \text{ infinitesimal deformation; } \text{tr} D = 0 \text{ finite deformation} \quad (2-75)$$

The large deformations are not the main concern of the study. Thus, the strain tensor  $\boldsymbol{\varepsilon}$  is taken into account instead of the deformation rate tensor  $\mathbf{D}$ .

The inextensibility constraints might be achieved by introducing the unit vector for the preferred direction in the un-deformed (reference) configuration  $\mathbf{a}_0$  and  $\mathbf{a}$  in a deformed configuration which might be related considering the deformation gradient tensor  $F$  and a scalar-valued stretch of the line element( $\lambda$ ):

$$\lambda \mathbf{a} = F \mathbf{a}_0 \text{ or } \lambda a_i = a_R^{(0)} F_{iR} \quad (2-76)$$

Inserting the definition of the deformation gradient from equation (2-70) into (2-76) the following relation can be constructed:

$$\lambda^2 = a_R^{(0)} a_S^{(0)} \frac{\partial x_i}{\partial X_R} \frac{\partial x_i}{\partial X_S} = a. C. a \quad (2-77)$$

If the material is inextensible in the preferred direction, then  $\lambda = 1$  and, therefore, the following relation might be written:

$$a. C. a = 1 \quad (2-78)$$

And for infinitesimal deformation it might be read:

$$a. \varepsilon. a = 1 \quad (2-79)$$

Having determined two kinematic constraints now their effect, which is to produce a reaction stress, on the mechanical response of the material might be investigated. Thus a stress state (T) can be divided into two distinct portions of reaction and extra-stresses, so that

$$T = S + R \quad (2-80)$$

Where for an incompressible material the reaction can be an arbitrary hydrostatic stress[83]:

$$R = -p1 \quad (2-81)$$

$p$  is a scalar and define the magnitude of the hydrostatic pressure. The reaction portion of the total stress can be defined as the projection of the total stress on to the preferred direction  $a$ :

$$R = T_a a \otimes a \quad (2-82)$$

Then, applying the yield stress condition, the unknown values of  $p$  and reaction stress tensor  $T_a$  might be determined[1, 65]. The reaction pressure  $p$  and  $T_a$  are arbitrary values in the sense that they are determined based on the equilibrium or momentum equations and the boundary conditions and not the given constitutive equation. It can be easily seen that a material with incompressible constraint requires that  $\text{tr}S = 0$  and with inextensible constraints in the privileged direction  $a$  needs that  $a.S.a = 0$ , and consequently, the remainder of the extra-stress to be determined requires the constitutive equation. The entire later arguments about the kinematic constraint concept and its effect on the mechanical response of the material prove that by increasing the number of kinematic constraints, the constitutive equation itself becomes less significant.

Probably the rigid body motion could help to have a better understanding of the latter expression which the constitutive equation has no role in the determination of the stresses since the total stress is an indeterminate reaction stress[83]. Thus, such presumptions which cause the kinematic constraints and decrease the level of involvement of the relevant constitutive equation in governing the mechanical response of the material have to be avoided as much as possible. It might be even useful to examine the effect of the mentioned constraints on the free energy function.

3. If the material is incompressible, then  $\text{tr}\varepsilon = 0$  and free energy can be explained such as:

$$\hat{\Psi}(\varepsilon, A) = \mu_T \text{tr}(\varepsilon)^2 + 2(\mu_L - \mu_T)(a\varepsilon^2 a) + \frac{1}{2}\beta(a\varepsilon a)^2 \quad (2-83)$$

And as it can be seen here, incompressible transversely isotropic material elastic behavior can be described using just 3 independent constants  $\mu_T$ ,  $\mu_L$  and  $\beta$ .

4. If the material is inextensible in the preferred direction  $a$ , then the assumption leads  $a\varepsilon a = 0$ , and consequently free energy function reads:

$$\hat{\Psi}(\varepsilon, A) = \frac{1}{2}\lambda(\text{tr}\varepsilon)^2 + \mu_T \text{tr}(\varepsilon)^2 + 2(\mu_L - \mu_T)(a\varepsilon^2 a) \quad (2-84)$$

Then, having three independent constants  $\lambda$ ,  $\mu_T$  and  $\mu_L$ , one can completely characterize the elastic response of inextensible transversely isotropic materials.

5. Having both constraints of incompressibility and inextensibility in the fiber direction, the elastic response of the transversely isotropic material reaches:

$$\hat{\Psi}(\varepsilon, A) = \mu_T \text{tr}(\varepsilon)^2 + 2(\mu_L - \mu_T)(a\varepsilon^2 a) \quad (2-85)$$

The above formulation can be interpreted such that the transversely isotropic material with both incompressibility in fiber direction and incompressibility constraints can be specified only by material's shear moduli  $\mu_T$  and  $\mu_L$

## Chapter 3

# 3 Transversely isotropic yield function and plastic flow potential

The key point of introducing a yield function in the theory of plasticity for the anisotropic material is to transform the anisotropic function into the isotropy space. As the basic rules of the invariant theory are introduced in section 2.2, by following the rules in the framework of invariant theory, this main object might be achieved. Assume that there is a scalar-valued function, for instance the strain energy function or yield function, which are anisotropic with respect to the strain or the stress arguments, respectively. The invariant theory states that adding an internal variable, which the material inherited its anisotropy and symmetry groups from it, an isotropic function might be constructed. In other words, the embedded internal variable undertakes the local coordinate systems role in the isotropic function. The details of plastic yield criterion and the potential function based on the invariant theory can be found in [33, 65, 66].

### 3.1 Foundation of plasticity theory

Assume that a non-fragile material is subjected to a certain stress state and the combination of the stress components grow, gradually. For any type of ductile material, a material which the yield and rupture points are different, there is a certain value when the combination of the stress tensor elements surpasses, the material behavior begins to be different than this specific critical point. The term “different” may be interpreted from different point of views so that one can say that the material stiffness matrix changes or the entire strain energy is not recoverable anymore or the material’s behavior is not independent of the strain and it means that the material’s response depends on the history of strain and so on. All the definition may be true, and a relationship may define this critical point called “yield criterion”. The Von Mises yield criterion is one of the initial yield function and probably the most famous one which is presented for the isotropic

materials. The Von Mises and in general any yield criterion for isotropic materials have some the following restrictions[90]:

- Yielding is practically unaffected by the hydrostatic stress
- Yield criterion is a function of the invariants of the deviatoric stress tensor
- The so-called Bauschinger is neglected

Considering the second restriction, it is quite reasonable to present the deviatoric stress tensor invariants:

$$\sigma'^3 - J_2 \sigma' - J_3 = 0 \quad (3-1)$$

Which its first invariant is  $J_1 = \sigma'_{ii} = 0$ . since we are not looking for the formulation of isotropic material yield criterion, then in this part the formulas are selected according to their relevance to the topic. Thus, the invariant  $J_3$  is skipped, but the second invariant can be written as:

$$J_2 = \frac{1}{6} [(\sigma_{11} - \sigma_{22})^2 + (\sigma_{22} - \sigma_{33})^2 + (\sigma_{33} - \sigma_{11})^2] + \sigma_{12}^2 + \sigma_{13}^2 + \sigma_{23}^2 \quad (3-2)$$

Von Mises suggested that yielding occurs when  $J_2$  reaches a certain value in the following form:

$$f(\sigma) = J_2 - k^2 \quad (3-3)$$

so that the yield locus is a circle of radius  $\sqrt{2}k$ . More detail about Von Mises yield criterion and other criteria for isotropic material can be found in[90]. As it can be easily recognized by equation (3-3) that any change over the indices does not affect the yield function.

For isotropic materials the isotropic yield function can be established just based on the stress components and there is no need for a complementary agent such as the structural tensor. Unlike the isotropic materials, for anisotropic materials the similar isotropic function may not be constructed by a single argument (stress tensor) and the internal variables which identifies the symmetry of the material must be added to the stress tensor to build up the respective isotropic function. This argument is established, theoretically, in the section 2.5.2 and is discussed with the relevant invariants for transversely isotropic materials in detail.

### 3.2 Invariants of transversely isotropic symmetry group

As it is mentioned earlier the construction of a scalar-valued isotropic function for an anisotropic material needs the material's intrinsic internal variables; here, it may be the material's symmetry, to be added to the basic arguments which are needed to be considered for isotropic materials. According to the Von Mises yield criterion which is an isotropic yield function in equation (3-3) the yield function for isotropic materials might be introduced in its general form as:

$$f = f(\sigma) \leq 0 \quad (3-4)$$

To introduce a transversely isotropic yield function which is a scalar-valued isotropic function, the transversely isotropic symmetry group argument must be added to the set of arguments. The transversely isotropic symmetry might be represented by the structural tensor  $A = a \otimes a$  is shown in equation (2-35) and means a dyadic product of the preferred direction by itself, and the general isotropic yield function might be introduced as:

$$f = f(\sigma, A) \leq 0 \quad (3-5)$$

where the stress tensor itself, due to applying the isotropic hardening rule, depends on the scalar-valued argument of equivalent plastic strain  $\bar{\epsilon}^p$ . According to the equation (2-22) which represents the basic theorem of the representation theory, the next step is to find the integrity bases for the arguments  $\sigma$  and  $A$ . The integrity bases are available for two arguments including an arbitrary second-order tensor  $\mathbf{D}$  and the structural tensor  $\mathbf{A}$  in Table 2-1 so that the associated integrity bases might reads[1, 65]:

$$\text{tr}[\sigma], \text{tr}[\sigma^2], \text{tr}[\sigma^3], \text{tr}[A\sigma] \text{ and } \text{tr}[A\sigma^2] \quad (3-6)$$

According to [1], having defined the integrity bases, the relevant yield function might be constructed without violating the basic principles of the representation theory is established in [33, 65, 66, 79]. The deviatoric stress might be substituted with the stress tensor itself in the integrity bases introduced in(3-6) and may build up a new set of integrity bases without undermining the basis of representation theory [1]:

$$\text{tr}[\sigma'^2], \text{tr}[\sigma'^3], \text{tr}[A\sigma'] \text{ and } \text{tr}[A\sigma'^2] \quad (3-7)$$

The term  $\text{tr}[\sigma']$  is dropped just because of the deviatoric stress tensor definition[1]:

$$\sigma' = \sigma - \frac{1}{3}\text{tr}(\sigma)1 \quad (3-8)$$

Which mean that  $\text{tr}[\sigma'] = 0$ . Each linear independent combination of the given invariants in the equations (3-6) and (3-7) represent equivalent invariant bases [1]. This result might be achieved directly from the equation (2-22) which says that any linear and independent combination of the integrity bases might be a new scalar-valued function which here can be interpreted as a new invariant. However, adding  $\text{tr}[\sigma]$  to the equations (3-7) might represent an equivalent invariant set to the basis(3-6) [1].

Some of the invariants which are built using this method contain interesting properties such as

- Decoupling of the stress states; and
- Consideration of a specific physical meaning

Decoupling the stress states causes to connect a certain loading condition, which generally appears in the mechanical tests such as tensile, shear and compression, to its associated mathematical expression which appears in the constitutive equations. Since according to the first line of equation (2-22), there are undetermined parameters in the scalar-valued isotropic function, then having decoupled stress states might ease their identification procedure. In other words, instead of dealing with a system of equations it might be possible to address separated equations.

Since the primary objective of the current research is to formulate the non-linear behavior of short fiber reinforced composite thermoplastics, in terms of plastic deformation as well as elastic and elasto-plastic damage, then the primary assumptions must be carefully chosen. As it is shown earlier in the section 2.5.3, the kinematic constraints as the primary assumptions, significantly affect the functionality of the constitutive equations. Thus, since it is known that the short fiber reinforced thermoplastics drastically extends even in the direction of that the major alignment of the fibers can be observed and show non-linear response under tension and compression, it would be acceptable if the “inextensibility” assumption disregarded from the very beginning[1]. Through this effort to establish the constitutive equation the framework is considered to be the invariant theory. However, disregarding the inextensibility presumption raises some difficulty so that the division of the total stress into two distinct “reaction response” and “extra stress”, according to the equation (2-80), would be pointless

due to the fact that to determine the scalar-valued part of both extra stress ( $p$ ) and reaction stress ( $T_a$ ) it must be two linearly independent equations. These two equations as mentioned in [1, 65] raise from the following stress-oriented assumptions:

- Yielding is independent of the hydrostatic pressure
- Yielding is independent of the projection of the stress tensor onto the preferred direction  $\mathbf{a}$  (inextensibility conditions)

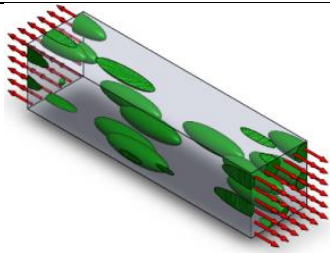
And a strain oriented presumption:

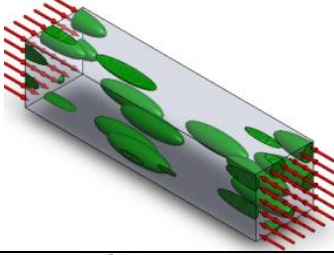
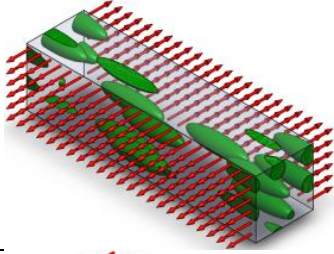
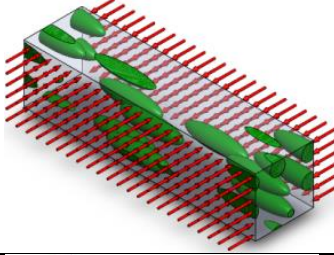
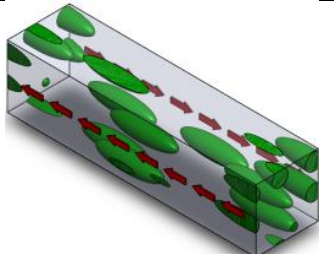
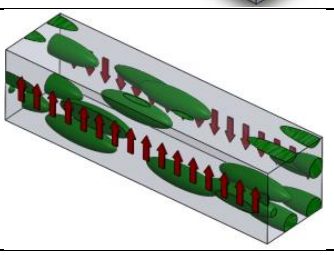
Yielding occurs without volumetric plastic strain (incompressibility)

Employing the deviatoric stress instead of the stress itself automatically satisfies the first stress-oriented condition and the strain-oriented assumption can be achieved using a proper flow rule. The second stress-oriented presumption is valid for the unidirectional composite materials, but short fiber reinforced composites.

To introduce a proper invariant set to construct an appropriate yield criterion in the framework of the invariant theory which, especially, meets the decoupling condition, it might be useful, to begin with the simple loading conditions and see each of the primary invariants of equations (3-6) and (3-7)'s response. The motive to start with the simple experiments pattern is that their unknown parameter identification procedure, finally, must be accomplished under the simple loading conditions. To avoid repeating the different loading condition in the text we prefer to assign a number to each as are illustrated in Table 3-1.

Table 3-1 loading conditions

No.	Loading conditions	Visual expression	Associated stress tensor
1	Tension the preferred direction		$\sigma = \begin{bmatrix} Y_{1T} & 0 & 0 \\ 0 & 0 & 0 \\ 0 & 0 & 0 \end{bmatrix}$

2	Compression the preferred direction		$\sigma = \begin{bmatrix} Y_{1C} & 0 & 0 \\ 0 & 0 & 0 \\ 0 & 0 & 0 \end{bmatrix}$
3	Tension perpendicular to the preferred direction		$\sigma = \begin{bmatrix} 0 & 0 & 0 \\ 0 & Y_{2T} & 0 \\ 0 & 0 & 0 \end{bmatrix}$
4	Compression perpendicular to the preferred direction		$\sigma = \begin{bmatrix} 0 & 0 & 0 \\ 0 & Y_{2C} & 0 \\ 0 & 0 & 0 \end{bmatrix}$
5	In-plane shear		$\sigma = \begin{bmatrix} 0 & Y_{IP} & 0 \\ Y_{IP} & 0 & 0 \\ 0 & 0 & 0 \end{bmatrix}$
6	Transverse shear		$\sigma = \begin{bmatrix} 0 & 0 & 0 \\ 0 & 0 & Y_{TR} \\ 0 & Y_{TR} & 0 \end{bmatrix}$

And accordingly the value of each basic invariant of equations(3-6) and (3-7) under the various simple loading of Table 3-1 is determined and can be found in Table 3-2. From parameter identification point of view the Table 3-2 reveals valuable data, for an instance in this matter (parameter identification) there is no difference between  $\text{tr}[\sigma^2]$  and  $\text{tr}[\sigma'^2]$  where both invariants have values for all loading conditions, and we intend to call those: “passive invariants” which means that they do not manifest a specific physical condition. So in this matter, we recognize three “neutral invariant” including  $\text{tr}[\sigma^2]$ ,  $\text{tr}[\sigma'^2]$  and  $\text{tr}[A\sigma'^2]$  and in

the matter of decoupling there, is no difference between them and each of them might be replaced by another. On the other hand, there are some basic invariants which do not show any specific physical or loading conditions which we call “semi-active”, for example,  $\text{tr}[A\sigma^2]$  which is the projection of the tensor  $\sigma^2 = \sigma_{im}\sigma_{mj}$  onto the preferred direction  $a = [1,0,0]$ . Since the latter invariant is not involved in transverse direction loadings and also transverse shear while it manages the loading in the longitudinal direction as well as in-plane shear, then its role in the introduction of the combined invariants is quite unique. In fact, the manifestation of the in-plane shear without the transverse shear may cause shear decoupling by subtraction between the “semi-active” invariant and one of the “passives”. This is the method which introduced by [65] and even used by [1], but using the total stress which is the combination of the reaction stress and extra stress as in equation (2-80).

Table 3-2 The values of basic invariants under different loading conditions

Loading condition	$\text{tr}[\sigma^2]$	$\text{tr}[\sigma'^2]$	$\text{tr}[A\sigma]$	$\text{tr}[A\sigma']$	$\text{tr}[A\sigma^2]$	$\text{tr}[\sigma]$	$\text{tr}[A\sigma'^2]$
1	$Y_{1T}^2$	$(2/3)Y_{1T}^2$	$Y_{1T}$	$(2/3)Y_{1T}$	$Y_{1T}^2$	$Y_{1T}$	$(4/9)Y_{1T}^2$
2	$Y_{1C}^2$	$(2/3)Y_{1C}^2$	$-Y_{1C}$	$(2/3)Y_{1C}$	$Y_{1C}^2$	$-Y_{1C}$	$(4/9)Y_{1C}^2$
3	$Y_{2T}^2$	$(2/3)Y_{2T}^2$	0	$(1/3)Y_{2T}$	0	$Y_{2T}$	$(1/9)Y_{2T}^2$
4	$Y_{2C}^2$	$(2/3)Y_{2C}^2$	0	$(1/3)Y_{2C}$	0	$-Y_{2C}$	$(1/9)Y_{2C}^2$
5	$2Y_{IP}^2$	$2Y_{IP}^2$	0	0	$Y_{IP}^2$	0	$Y_{IP}^2$
6	$2Y_{TR}^2$	$2Y_{TR}^2$	0	0	0	0	$Y_{TR}^2$

Here, to introduce the combined decoupling invariants, we start with the following invariants:

$$I_1 = \frac{1}{2} \text{tr}[\sigma^2] - \text{tr}[A\sigma^2] \quad (3-9)$$

Which is the combination of the passive and semi-active basic invariants and results in a complete decoupling of the in-plane and transverse shear. The invariant  $I_1$  is activated by transverse shear, but under transverse shear becomes zero. According to Table 3-2, within the basic invariants other than passive invariants and  $\text{tr}[A\sigma^2]$  the shear components are not involved in the basic invariants under simple loading conditions. Thus, to have the in-plane shear be activated the only possible option is  $\text{tr}[A\sigma^2]$  itself, otherwise any subtraction with any of the passive basic invariant causes loss of in-plane shear involvement. Therefore, the second invariant may be introduced as:

$$I_2 = \text{tr}[A\sigma^2] \quad (3-10)$$

According to Each invariant responses to different loadings are given in Table 3-3.

Table 3-3 the invariant  $I_2$  is the only activated one, thus by introducing two first invariants the in-plane and transverse shear are decoupled. Therefore, in the parameter identification process, they are two separated equations instead of a system of equations.

Having decoupled two different shear states, now it is essential to choose and combine the basic invariants, according to the Table 3-2, so that other loading situations are decoupled as much as possible. Some of the basic invariants might be called “active” in the sense that they carry physical meaning in some certain loading conditions. For example,  $\text{tr}[A\sigma]$ , as it represents the projection of the total stress tensor onto the preferred direction  $a$ , is active just under tension and compression in the longitudinal direction. Therefore it seems to be a perfect choice for the next invariant:

$$I_3 = \text{tr}[A\sigma] \quad (3-11)$$

Now we probably could search for the last invariant to describe the tensile and compression in the transverse direction. Considering the Table 3-2 the following combination may provide the requested invariant with the mentioned features:

$$I_4 = \text{tr}[\sigma] - \text{tr}[A\sigma] \quad (3-12)$$

Each invariant responses to different loadings are given in Table 3-3.

Table 3-3 the combined invariants based on the basic invariants

Loading condition	$I_1$	$I_2$	$I_3$	$I_4$
1	$-(1/2)Y_{1T}^2$	$Y_{1T}^2$	$Y_{1T}$	0
2	$-(1/2)Y_{1C}^2$	$Y_{1C}^2$	$-Y_{1C}$	0
3	$(1/2)Y_{2T}^2$	0	0	$Y_{2T}$
4	$(1/2)Y_{2C}^2$	0	0	$-Y_{2C}$
5	0	$Y_{IP}^2$	0	0
6	$Y_{TR}^2$	0	0	0

It is more convenient to gather all the invariants from equation (3-9) to (3-12) in one set:

$$\begin{aligned}
 I_1 &= \frac{1}{2} \text{tr}[\sigma^2] - \text{tr}[A\sigma^2] \\
 I_2 &= \text{tr}[A\sigma^2] \\
 I_3 &= \text{tr}[A\sigma] \\
 I_4 &= \text{tr}[\sigma] - \text{tr}[A\sigma]
 \end{aligned} \tag{3-13}$$

The required set of invariants are provided to construct the yield criterion and also the potential function. As pointed out and applied by [1] just the linear and quadratic terms are picked from the basic invariants of the equations (3-6) and (3-7) and the cubic invariants are discarded. The reason as , again, notified in the same reference is to avoid the complication of integration algorithm due to the fact that the derivative of the cubic term with respect to the stress tensor would not be constant so that the integration algorithm introduced by [1] cannot be employed anymore. The next section is devoted to the formulation of the yield and potential function using invariant theory by considering the introduced set of invariants in (3-13).

### 3.2.1 Formulation of yield surface for short fiber reinforced thermoplastics

Having introduced the required set of invariants in the equation (3-13) which are decoupled and also considering the equations (2-22) and (3-5) the following yield criterion can be represented:

$$f = \hat{f}(\sigma, \bar{\varepsilon}_p, A) = \alpha_1 I_1 + \alpha_2 I_2 + \alpha_3 I_3 + \alpha_{32} I_3^2 + \alpha_4 I_4 + \alpha_{42} I_4^2 - 1 \quad (3-14)$$

Where the coefficients  $\alpha_{nm}$  are not constants and may carry the hardening of the material under plastic flow. The coefficients are functions of the equivalent plastic strain  $\bar{\varepsilon}^p$ :

$$\alpha_{nm} = \hat{\alpha}_{nm}(\bar{\varepsilon}^p) \quad (3-15)$$

The definition of the equivalent plastic strain is given in equation (4-5). The hardening rule can be isotropic, kinematic, combined hardening and isotropic or even distortional. in the next chapter while we introduce the non-associated plastic theory the different kind of strain hardenings are discussed. For now, since we intend to choose the simplest version of the strain hardening rule, e.g., isotropic hardening, then let's have a geometrical definition of the isotropic hardening (see Figure 3-1) in the stress state which the yield envelope itself is defined in. for a material with isotropic hardening, the yield locus is expanded while the material is under plastic deformation[90]. For the sake of clarification, it should be noted that the kinematic hardening in the short fiber reinforced thermoplastics is studied and observed, but the data are available for some specific materials, and there are not a complete set of data to be used in the constitutive equation [91-93]. Thus, the isotropic rule is chosen and applied to the introduced non-linear constitutive equation.

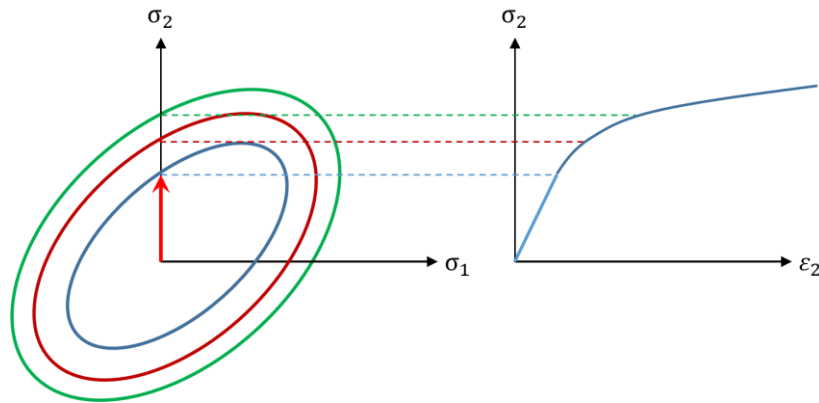


**Figure 3-1 Schematic isotropic hardening including primary(blue) and subsequent yield surfaces [94]**

Each of the invariants in the yield surface as explained in the previous section governs one of the major yielding modes. Considering the equation (3-13), and since we do not employ the stress tensor division into two parts of reaction and extra stresses (see equation (2-80)), then one specific invariant does not characterize a specific loading condition alone, in general, except for transverse and in-plane shear loadings which characterized by  $I_1$  and  $I_2$ , respectively. According to Table 3-3, the least involvement of the combined invariants is related to the loading conditions 5 and 6 (transverse and in-plane shears) while for three of them including  $I_1$ ,  $I_2$  and  $I_3$  participate in loading conditions 1 and 2, i.e., tensile and compression in the longitudinal direction, respectively. For the loading conditions 3 and 4, i.e., tension and compression in transverse direction, respectively, only two of the invariants including  $I_1$  and  $I_4$  are active. Evidently, the maximum participation is related to the first invariant ( $I_1$ ) which involves in 5 out of six loading conditions and the least is related to  $I_3$  and  $I_4$  which are categorized as “active invariants”. In the results and discussions sections, they will be discussed widely with numbers and in details for the short fiber reinforced polyamide PA6GF60.

### 3.2.2 Yield function’s parameter determination

In this section, we determine the hardening parameters of the introduced yield criterion in equation (3-14) according to the simple loading conditions illustrated in Table 3-1. According to Table 3-3, and considering the involvement degree of the invariant in the yield function under each loading condition, we start with transverse shear and substituting the associated invariants values into the yield function (3-14) reads:

$$\alpha_1 Y_{TR}^2 - 1 = 0 \quad (3-16)$$

And directly the parameter  $\alpha_1$  can be extracted:

$$\alpha_1 = 1/Y_{TR}^2 \quad (3-17)$$

Accordingly, for the in-plane stress, the yield stress is:

$$\alpha_2 Y_{IP}^2 - 1 = 0 \quad (3-18)$$

Which leads:

$$\alpha_2 = 1/Y_{IP}^2 \quad (3-19)$$

Substitution of the invariants of the longitudinal tension and compression from Each invariant responses to different loadings are given in Table 3-3.

Table 3-3 into the yield function (3-14) causes the following linear system of equation:

$$\begin{cases} -(1/2)Y_{1T}^2\alpha_1 + Y_{1T}^2\alpha_2 + Y_{1T}\alpha_3 + Y_{1T}^2\alpha_{32} = 1 \\ -(1/2)Y_{1C}^2\alpha_1 + Y_{1C}^2\alpha_2 - Y_{1C}\alpha_3 + Y_{1C}^2\alpha_{32} = 1 \end{cases} \quad (3-20)$$

Simultaneously solving the two equations results:

$$\alpha_{32} = \frac{\frac{1}{Y_{1C}} + \frac{1}{Y_{1T}} + \left(\frac{1}{2}\alpha_1 - \alpha_2\right)(Y_{1T} + Y_{1C})}{Y_{1T} + Y_{1C}} \quad (3-21)$$

$$\alpha_3 = \frac{1}{Y_{1T}} + Y_{1T}\left(\frac{1}{2}\alpha_1 - \alpha_2 - \alpha_{32}\right)$$

Following the same procedure for the transverse direction and by substituting the associated invariants from the Each invariant responses to different loadings are given in Table 3-3.

Table 3-3 into the yield criterion results in:

$$\begin{cases} -(1/2)Y_{2T}^2\alpha_1 + Y_{2T}\alpha_4 + Y_{2T}^2\alpha_{42} = 1 \\ -(1/2)Y_{2C}^2\alpha_1 - Y_{2C}\alpha_4 + Y_{2C}^2\alpha_{42} = 1 \end{cases} \quad (3-22)$$

And, consequently, solving the system of the equation gives:

$$\alpha_{42} = \frac{\frac{1}{Y_{2C}} + \frac{1}{Y_{2T}} - \frac{1}{2}\alpha_1(Y_{2T} + Y_{2C})}{Y_{2T} + Y_{2C}} \quad (3-23)$$

$$\alpha_4 = \frac{1}{Y_{2T}} - Y_{2T}\left(\frac{1}{2}\alpha_1 + \alpha_{42}\right)$$

By now the entire hardening parameters  $\alpha_{nm}$  of the yield criterion are known. For the sake of convenience, we gather all the determined parameters in Table 3-4.

Table 3-4 The introduced yield criterion's parameters

Stress state	Parameter
Transverse shear No.6	$\alpha_1 = 1/Y_{TR}^2$
In-plane shear No.5	$\alpha_2 = 1/Y_{IP}^2$
Longitudinal tension and compression No.s 1,2	$\alpha_{32} = \frac{\frac{1}{Y_{1C}} + \frac{1}{Y_{1T}} + \left(\frac{1}{2} \alpha_1 - \alpha_2\right) (Y_{1T} + Y_{1C})}{Y_{1T} + Y_{1C}}$
	$\alpha_3 = \frac{1}{Y_{1T}} + Y_{1T} \left(\frac{1}{2} \alpha_1 - \alpha_2 - \alpha_{32}\right)$
Transverse tension and compression No.s 1,2	$\alpha_{42} = \frac{\frac{1}{Y_{2C}} + \frac{1}{Y_{2T}} - \frac{1}{2} \alpha_1 (Y_{2T} + Y_{2C})}{Y_{2T} + Y_{2C}}$
	$\alpha_4 = \frac{1}{Y_{2T}} - Y_{2T} \left(\frac{1}{2} \alpha_1 + \alpha_{42}\right)$

The identified parameters of the introduced yield functions can evolve regarding their relationship with the different modes yield strengths. It means that each of the yield strengths including  $Y_{1T}$ ,  $Y_{1C}$ ,  $Y_{2T}$ ,  $Y_{2C}$ ,  $Y_{TR}$ ,  $Y_{IP}$  evolves according to its special  $Y(\bar{\epsilon}^p)$  versus  $\bar{\epsilon}^p$  curves which obtain from the associated experiments (see Figure 3-2 ). These data are available from the relevant test such as uniaxial tensile test, but if not, for example, due to technical difficulties, they have to be prescribed using hardening rule which the part of the process, in this case, is based on admissible guesses which have to be accomplished carefully and by considering all consequences. However, it must be taken into account that this hardening curves must be prepared as an input for the finite element analysis either as a tabulated data which the provided code must be able to look up in the given data and find the proper strength for a certain equivalent strain or such an isotropic hardening formula where the only variable is the equivalent strain, and the relevant function is the associated yield strength.

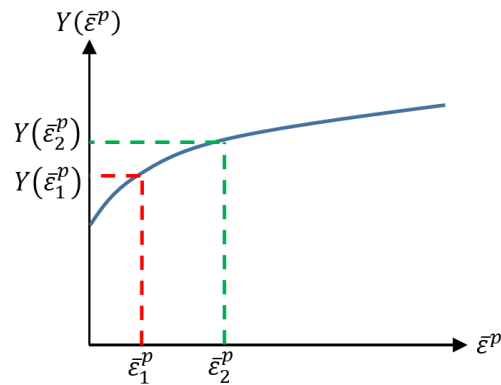


**Figure 3-2 Schematic curve of yield strength versus equivalent strain**

Having obtained the current yield strengths, the yield function parameters can be updated via given formula in Table 3-4.

### 3.2.3 Plastic flow potential function for short fiber reinforced thermoplastics

According to the fact that beyond the yield point the linear relation between stress and strain is not valid anymore and the component of the stiffness matrix shrink so that for a given strain increment the stress tensor components increases less comparing to the same inelastic region. However, in the plastic region, the relation between stress and strain is not straightforward such as the elastic response and might be calculated by adding some phenomenon such as plastic flow rule which requires a scalar-valued function to be defined. This phenomenon is described and formulated in the next chapter in elasto-plasticity constitutive equations. But what important is in this section to find the plastic flow rule's corresponding potential function. To deal with the plastic flow potential function in the plasticity theory, there are two different approaches:

- Associated flow rule
- Non-associated flow rule

In associated flow rule the flow potential function and the yield function are the same and as the plastic strain tensor direction is defined by the gradient of the flow potential function (see equation (4-20)), then the direction of the yield function expansion in the stress state is normal to the yield envelope (see Figure 3-3).

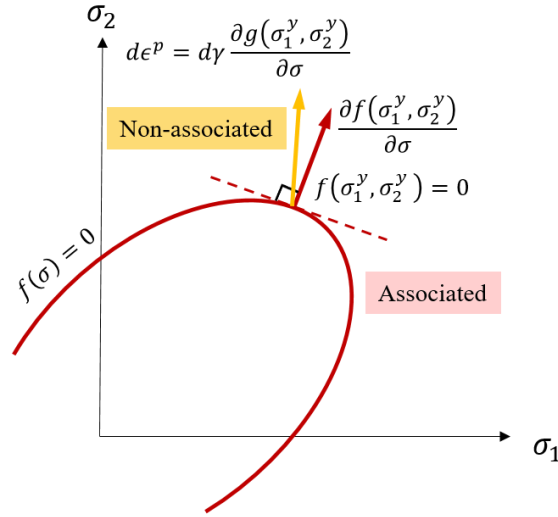


**Figure 3-3 schematic description of associated and non-associated flow rules**

Associated flow rule and associated plasticity, in general, fails to describe the non-metallic materials plastic behaviors [95]. The reason for the failure is due to that an accurate prediction of the plastic Poisson coefficient and also the volumetric plastic strains cannot be obtained using the associated flow rule[1]. The solution is to define an independent flow potential function which allows controlling the plastic strain independent from the yield criterion. However, two main concepts dominate the representation of the flow potential functions:

- The experimental observation
- Expected application of the model
- The algorithm applied to the numerical solution

Taking into account these points we introduce the following potential flow function, and later the issues will be discussed:

$$g = \hat{g}(\sigma, A) = \beta_1 I_1 + \beta_2 I_2 + \beta_{32} I_3^2 + \beta_{42} I_4^2 - 1 \quad (3-24)$$

According to the invariant set in equation (3-13), the introduced potential function is a quadratic function with respect to the stress tensor due to that the invariants  $I_1$  and  $I_2$  are linear with respect to the stress tensor while the other two  $I_3$  and  $I_4$  are quadratic. The reason why only the quadratic terms are incorporated into the flow potential function returns to the selection of the numerical algorithm which is discussed in section 4.2. If the exact representation of the volumetric plastic strain is required, then the introduced flow potential function's coefficients must be able to evolve unless they might be constants and hold the initial values

of the yield criterion's coefficient ( $\alpha_{mn}$  at  $t = 0$  and  $\bar{\epsilon}^p = 0$ ). Also, the particular application and the degree of freedom strongly affect the dilatation so that for example in the uniaxial tensile due to that the material can freely deform in the lateral directions. Thus, the plastic potential function's parameters are not that much sensitive and consequently the plastic Poisson ratios. Besides, the short fiber reinforced thermoplastic PA6GF60 does not exhibit dilatation which the assumption of constant parameters for the flow potential function might be admissible [1].

# Chapter 5

## 4 Elasto-plasticity model

In the current section, we intend to describe the non-associated elasto-plasticity constitutive equation based on the introduced yield function and flow potential function. The corresponding formulas, based on the introduced yield and flow potential functions, are derived specifically for the introduced model in section 4.1 and generalized version in section 4.2. the generalized configuration of the elsto-plastic constitutive equation is more conveniently can be implemented into the numerical solution. The model is incorporated into either implicit or explicit finite element method which is described in the last section of this chapter.

### 4.1 Elasto-plasticity continuum

The elastic constitutive equation for the transversely isotropic material is established in the section 2.5.1. Assuming the infinitesimal and hyperplastic deformation the elastic constitutive equation in the rate form can be written as follow:

$$\dot{\sigma} = \mathbb{C} : \dot{\varepsilon}^e \quad (4-1)$$

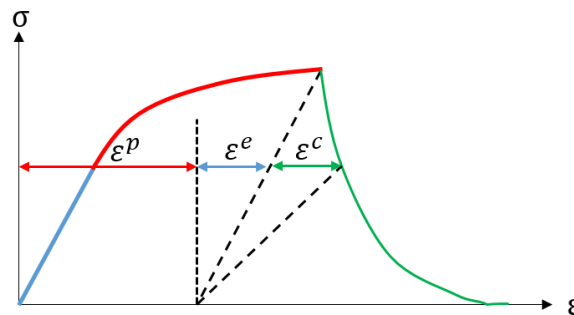


Figure 4-1 schematic elastic, plastic and damage response of the material [1]

Using the rate form of the constitutive equation can provide a possibility to incorporate the plastic response into the material response where reads:

$$\dot{\boldsymbol{\varepsilon}} = \dot{\boldsymbol{\varepsilon}}^e + \dot{\boldsymbol{\varepsilon}}^p \quad (4-2)$$

Then, substituting the elastic portion of the strain tensor rate from the equation (4-2) into the equation (4-1) reads:

$$\dot{\boldsymbol{\sigma}} = \mathbb{C} : \dot{\boldsymbol{\varepsilon}}^e = \mathbb{C} : (\dot{\boldsymbol{\varepsilon}} - \dot{\boldsymbol{\varepsilon}}^p) \quad (4-3)$$

According to the above general elasto-plastic constitutive equation, the only unknown argument is the plastic strain portion which has to be defined. According to non-associated elasto-plasticity flow rule which has been chosen for the short fiber reinforced material (see section 3.2.3), it is necessary to use the introduced flow potential function's (equation (3-24) ) gradient to define the direction of plastic flow:

$$\mathbf{n}_g = \partial_{\boldsymbol{\sigma}} g(\boldsymbol{\sigma}, A) \quad (4-4)$$

where  $\mathbf{n}_g$  is the vector which is normal to the potential flow function ,which does not have any physical meaning, in the stress space. Accordingly, the plastic strain rate can be defined multiplying the plastic flow direction ( $\mathbf{n}_g$ ) by a scalar value ( $\gamma$ ) as follows:

$$\dot{\boldsymbol{\varepsilon}}^p = \gamma \mathbf{n}_g \quad (4-5)$$

where  $\gamma$  called the “consistency parameter”. The consistency parameter is the key ingredient of the plasticity theory which beyond the elastic region guarantees the presence of the stress state on the yield function [95]. This parameter can be achieved by applying the consistency condition ( $\dot{f} = 0$ ) on the introduced yield function (equation (3-14)):

$$\dot{f} = \frac{\partial f}{\partial \boldsymbol{\sigma}} : \dot{\boldsymbol{\sigma}} + \frac{\partial f}{\partial \bar{\boldsymbol{\varepsilon}}^p} \dot{\bar{\boldsymbol{\varepsilon}}^p} = 0 \quad (4-6)$$

Since the structural tensor does not depend on the history of the strain, or loading, then it does not appear in the consistency condition. According to the equation (4-6), to complete the elasto-plastic theory, the gradient of the yield function as well as the derivative of the yield function with respect to the equivalent plastic strain are required. Therefore, first of all, a definition of the equivalent plastic strain is needed which normally performed using the plastic strain itself definition such as follows:

$$\dot{\bar{\epsilon}}^p = \sqrt{\frac{2}{3}} \|\dot{\epsilon}^p\| = \sqrt{\frac{2}{3}} \gamma \|\mathbf{n}_g\| \quad (4-7)$$

where the consistency parameter holds a positive value. Having defined the equivalent plastic strain, the different derivatives of the consistency condition ( equation (4-6) ) can be determined. The first term in the right hand of the consistency equation is the gradient of the yield function and can be derived by taking the derivative of the equation (3-14) with respect to the stress tensor:

$$\mathbf{n}_f = \frac{\partial f}{\partial \boldsymbol{\sigma}} = \partial_{I_i} f \partial_{\sigma} I_i \quad (4-8)$$

Where

$$\begin{aligned} \frac{\partial I_1}{\partial \boldsymbol{\sigma}} &= \boldsymbol{\sigma} - A\boldsymbol{\sigma} - \boldsymbol{\sigma}A \\ \frac{\partial I_2}{\partial \boldsymbol{\sigma}} &= A\boldsymbol{\sigma} + \boldsymbol{\sigma}A \\ \frac{\partial I_3}{\partial \boldsymbol{\sigma}} &= A \\ \frac{\partial I_4}{\partial \boldsymbol{\sigma}} &= 1 - A \end{aligned} \quad (4-9)$$

Inserting the derivatives of the invariants with respect to the stress tensor in equation (4-8) reads:

$$\begin{aligned} \mathbf{n}_f &= \frac{\partial f}{\partial \boldsymbol{\sigma}} \\ &= \alpha_1(\boldsymbol{\sigma} - A\boldsymbol{\sigma} - \boldsymbol{\sigma}A) + \alpha_2(A\boldsymbol{\sigma} + \boldsymbol{\sigma}A) + \alpha_3 A + 2\alpha_{32} \text{tr}[A\boldsymbol{\sigma}]A \\ &\quad + \alpha_4(1 - A) + 2\alpha_{42}(\text{tr}[\boldsymbol{\sigma}] - \text{tr}[A\boldsymbol{\sigma}])(1 - A) \end{aligned} \quad (4-10)$$

Having determined the gradient of the yield function based on the primary arguments stress and structural tensors as well as the hardening parameters, the next step would be the determination of the derivative of the yield function with respect to the equivalent plastic strain. Assuming that the plastic strain history is carried by the hardening parameters (equation (3-14)), the following equation shall be valid:

$$\begin{aligned} \frac{\partial f}{\partial \bar{\epsilon}^p} &= \frac{\partial f}{\partial \alpha_i} \frac{\partial \alpha_i}{\partial \bar{\epsilon}^p} = I_1 \frac{\partial \alpha_1}{\partial \bar{\epsilon}^p} + I_2 \frac{\partial \alpha_2}{\partial \bar{\epsilon}^p} + I_3 \frac{\partial \alpha_3}{\partial \bar{\epsilon}^p} + I_3^2 \frac{\partial \alpha_{32}}{\partial \bar{\epsilon}^p} + I_4 \frac{\partial \alpha_4}{\partial \bar{\epsilon}^p} \\ &\quad + I_4^2 \frac{\partial \alpha_{42}}{\partial \bar{\epsilon}^p} \end{aligned} \quad (4-11)$$

where considering the Table 3-4, the hardening parameters can be achieved by the following equation:

$$\begin{aligned}\frac{\partial \alpha_1}{\partial \bar{\epsilon}^p} &= \frac{\partial \alpha_1}{\partial Y_{TR}} \frac{\partial Y_{TR}}{\partial \bar{\epsilon}^p} = -\frac{2}{Y_{TR}^3} \frac{\partial Y_{TR}}{\partial \bar{\epsilon}^p} \\ \frac{\partial \alpha_2}{\partial \bar{\epsilon}^p} &= \frac{\partial \alpha_2}{\partial Y_{IP}} \frac{\partial Y_{IP}}{\partial \bar{\epsilon}^p} = -\frac{2}{Y_{IP}^3} \frac{\partial Y_{IP}}{\partial \bar{\epsilon}^p}\end{aligned}\quad (4-12)$$

Deriving the rest of the hardening coefficients derivative with respect to the equivalent plastic strain needs some assumptions for readability concern then let's assume:

$$\begin{aligned}NU\alpha_{32} &= \frac{1}{Y_{1C}} + \frac{1}{Y_{1T}} + \left(\frac{1}{2} \alpha_1 - \alpha_2\right) (Y_{1T} + Y_{1C}) \\ DN\alpha_{32} &= Y_{1T} + Y_{1C}\end{aligned}\quad (4-13)$$

NU is the abbreviation of “numerator” and DN points to “denominator” of the associated hardening parameter and then the derivative of the  $\alpha_{32}$  with respect to the equivalent plastic strain reads:

$$\begin{aligned}\frac{\partial \alpha_{32}}{\partial \bar{\epsilon}^p} &= \left[ \left( -\frac{1}{Y_{1T}^2} + \frac{\alpha_1}{2} - \alpha_2 \right) DN\alpha_{32} - NU\alpha_{32} \right] \frac{1}{DN\alpha_{32}^2} \frac{\partial Y_{1T}}{\partial \bar{\epsilon}^p} \\ &\quad + \left[ \left( -\frac{1}{Y_{1C}^2} + \frac{\alpha_1}{2} - \alpha_2 \right) DN\alpha_{32} \right. \\ &\quad \left. - NU\alpha_{32} \right] \frac{1}{DN\alpha_{32}^2} \frac{\partial Y_{1C}}{\partial \bar{\epsilon}^p} + \frac{1}{2} \frac{\partial \alpha_1}{\partial \bar{\epsilon}^p} - \frac{\partial \alpha_2}{\partial \bar{\epsilon}^p}\end{aligned}\quad (4-14)$$

Having determined the  $\frac{\partial \alpha_{32}}{\partial \bar{\epsilon}^p}$  the derivative of the  $\alpha_3$  with respect to the equivalent strain can be determined:

$$\begin{aligned}\frac{\partial \alpha_3}{\partial \bar{\epsilon}^p} &= \left( -\frac{1}{Y_{1T}^2} + \frac{\alpha_1}{2} - \alpha_2 - \alpha_{32} \right) \frac{\partial Y_{1T}}{\partial \bar{\epsilon}^p} \\ &\quad + Y_{1T} \left( \frac{1}{2} \frac{\partial \alpha_1}{\partial \bar{\epsilon}^p} - \frac{\partial \alpha_2}{\partial \bar{\epsilon}^p} - \frac{\partial \alpha_{32}}{\partial \bar{\epsilon}^p} \right)\end{aligned}\quad (4-15)$$

To calculate the derivative of the last hardening parameter with respect to the equivalent plastic strain and again for the readability reason we define its associated denominator and numerator as below:

$$\begin{aligned}NU\alpha_{42} &= \frac{1}{Y_{2C}} + \frac{1}{Y_{2T}} - \frac{1}{2} \alpha_1 (Y_{2T} + Y_{2C}) \\ DN\alpha_{42} &= Y_{2T} + Y_{2C}\end{aligned}\quad (4-16)$$

Consequently, it can be written:

$$\begin{aligned} \frac{\partial \alpha_{42}}{\partial \bar{\epsilon}^p} = & \left[ - \left( \frac{1}{Y_{2T}^2} + \frac{\alpha_1}{2} \right) DN\alpha_{42} - NU\alpha_{42} \right] \frac{1}{DN\alpha_{42}^2} \frac{\partial Y_{2T}}{\partial \bar{\epsilon}^p} \\ & - \left[ \left( \frac{1}{Y_{2C}^2} + \frac{\alpha_1}{2} \right) DN\alpha_{32} + NU\alpha_{32} \right] \frac{1}{DN\alpha_{42}^2} \frac{\partial Y_{2C}}{\partial \bar{\epsilon}^p} \\ & - \frac{1}{2} \frac{\partial \alpha_1}{\partial \bar{\epsilon}^p} \end{aligned} \quad (4-17)$$

And

$$\frac{\partial \alpha_4}{\partial \bar{\epsilon}^p} = - \left( \frac{1}{Y_{2T}^2} + \frac{\alpha_1}{2} + \alpha_{42} \right) \frac{\partial Y_{2T}}{\partial \bar{\epsilon}^p} - Y_{2T} \left( \frac{1}{2} \frac{\partial \alpha_1}{\partial \bar{\epsilon}^p} + \frac{\partial \alpha_{42}}{\partial \bar{\epsilon}^p} \right) \quad (4-18)$$

Having determined all the parameters of the consistency condition based on the primary arguments, now the consistency parameter can be achieved by inserting the equivalent plastic strain definition from the equation (4-7) into the consistency condition relation (equation (4-6)):

$$\dot{f} = n_f : \mathbf{C} : (\dot{\epsilon} - \gamma n_g) + \frac{\partial f}{\partial \bar{\epsilon}^p} \sqrt{\frac{1}{2}} \|n_g\| \gamma = 0 \quad (4-19)$$

The final stage to have the consistency parameter fully defined is to determine the gradient of the flow potential function which appears in the consistency parameter's denominator. Considering the flow potential function definition in the equation and its gradient definition in the equation (4-4) it can be written:

$$n_g = \frac{\partial g}{\partial \sigma} = \partial_{I_i} g \partial_{\sigma} I_i \quad (4-20)$$

Inserting the derivatives of the invariants with respect to the stress tensor from the equation (4-9) into the above equation gives the gradient of the flow potential function's gradient in the stress state:

$$\begin{aligned} n_g = \frac{\partial g}{\partial \sigma} = & \alpha_1 (\sigma - A\sigma - \sigma A) + \alpha_2 (A\sigma + \sigma A) + 2\alpha_{32} \text{tr}[A\sigma]A \\ & + 2\alpha_{42} (\text{tr}[\sigma] - \text{tr}[A\sigma])(1 - A) \end{aligned} \quad (4-21)$$

Therefore the consistency parameter can be derived:

$$\gamma = \frac{n_f : \mathbf{C} : \dot{\epsilon}}{n_f : \mathbf{C} : n_g - \frac{\partial f}{\partial \bar{\epsilon}^p} \sqrt{\frac{1}{2}} \|n_g\|} \quad (4-22)$$

According to the one-dimensional schematic stress-strain curve which is depicted in the Figure 4-1 it can be deduced that the current version of the material's stiffness shall be less than the virgin one, i.e., the material's current constant one of  $s$  are kind of degraded or softened comparing to the original one. It is not intended to undermine the hardening concept while we are talking about the current stress status on the yield surface while we are not talking about the unloading condition. The current material tangent must be defined, since it will be needed for the implicit finite element method which is one of our main concern in this research. However, to have the elasto-plastic continuum tangent or the current tangent, the elasticity constitutive equation must be reshaped and rewritten so that the elastic constitutive equation be converted to elasto-plastic one. This can be accomplished by incorporating the consistency parameter from the equation (4-22) into the plastic strain tensor definition which is given in the equation (4-5) such as follows:

$$\dot{\sigma} = \mathbb{C} : \left( \dot{\varepsilon} - \frac{n_f : \mathbb{C} : \dot{\varepsilon}}{n_f : \mathbb{C} : n_g - \frac{\partial f}{\partial \bar{\varepsilon}^p} \sqrt{\frac{1}{2}} \|n_g\|} n_g \right) \quad (4-23)$$

By reordering the equation as below

$$\dot{\sigma} = \left( \mathbb{C} - \frac{\mathbb{C} : n_f \otimes n_g : \mathbb{C}}{n_f : \mathbb{C}_e : n_g - \frac{\partial f}{\partial \bar{\varepsilon}^p} \sqrt{\frac{1}{2}} \|n_g\|} \right) : \dot{\varepsilon} \quad (4-24)$$

One can say the elasto-plastic continuum tangent might be:

$$\mathbb{C}^{ep} = \frac{\partial \sigma}{\partial \varepsilon} = \mathbb{C} - \frac{\mathbb{C} : n_f \otimes n_g : \mathbb{C}}{n_f : \mathbb{C}_e : n_g - \frac{\partial f}{\partial \bar{\varepsilon}^p} \frac{1}{2} \|n_g\|} \quad (4-25)$$

A brief version of the elasto-plasticity constitutive equation is presented in the table:

Table 4-1 Elasto-plasticity constitutive equation's overview [1]

Order	Explanation	Formula
1	kinematic	$\dot{\varepsilon} = \dot{\varepsilon}^e + \dot{\varepsilon}^p$

2	Elastic constitutive equation	$\dot{\sigma} = \mathbf{C} : \dot{\varepsilon}^e$
3	Yield function	$f = \hat{f}(\sigma, \bar{\varepsilon}_p, A) \leq 0$
4	Plastic potential function	$g = \hat{g}(\sigma) = 0$
5	Plastic strain tensor	$f = \hat{f}(\sigma, \bar{\varepsilon}_p, A)$
6	Consistency condition	$\dot{f} = 0$
7	Consistency parameter	$\gamma = \frac{n_f : \mathbf{C} : \dot{\varepsilon}}{n_f : \mathbf{C} : n_g - \frac{\partial f}{\partial \bar{\varepsilon}_p} \sqrt{\frac{1}{2}} \ n_g\ }$
8	Elastic-plastic continuum tangent	$\mathbf{C}^{ep} = \frac{\partial \sigma}{\partial \varepsilon} = \mathbf{C} - \frac{\mathbf{C} : n_f \otimes n_g : \mathbf{C}}{n_f : \mathbf{C}_e : n_g - \frac{\partial f}{\partial \bar{\varepsilon}_p} \frac{1}{2} n_g}$

## 4.2 Generalized elasto-plasticity model

The generalized elasto-plasticity constitutive equation, especially, serves as the base for the construction of the numerical solution and makes the implementation more convenient. Since the isotropic yield function in equation (3-14) includes both first order and quadratic terms of the stress tensors, therefore it can be written as follows:

$$f(\sigma, \bar{\varepsilon}^p) = \frac{1}{2} \sigma : \mathbf{K} : \sigma + L : \sigma - 1 \quad (4-26)$$

$\mathbf{K}$  and  $L$  describe the fourth- and second-order tensors, respectively. It is quite clear that the fourth-order tensor  $\mathbf{K}$  can be attained by taking the second derivative of the “anisotropic yield function” in equation (4-26) with respect to the stress tensor:

$$\partial_\sigma f(\sigma, \bar{\varepsilon}^p) = \mathbf{K} : \sigma + L \quad (4-27)$$

$$\partial_{\sigma\sigma}f(\sigma, \bar{\varepsilon}^p) = \frac{\partial^2 f(\sigma, \bar{\varepsilon}^p)}{\partial \sigma^2} = \mathbb{K}$$

The fourth-order tensor  $\mathbb{K}$  and the second order tensor  $L$  both depend on two arguments of equivalent plastic strain  $\bar{\varepsilon}^p$  and the structural tensor  $A$  so that

$$\begin{aligned} \mathbb{K} &= \hat{\mathbb{K}}(\bar{\varepsilon}^p, A) \\ L &= \hat{L}(\bar{\varepsilon}^p, A) \end{aligned} \quad (4-28)$$

And these two tensor can be determined according to the introduced yield function of the equation (3-14) and taking its second derivative with respect to the stress tensor which gives:

$$\begin{aligned} \mathbb{K} := \frac{\partial^2 f}{\partial \sigma^2} &= \alpha_1(\mathbb{I} - A \cdot \mathbb{I} - \mathbb{I} \cdot A) + \alpha_2(A \cdot \mathbb{I} + \mathbb{I} \cdot A) + 2\alpha_{32}A \otimes A \\ &\quad + 2\alpha_{42}(1 - A) \otimes (1 - A) \end{aligned} \quad (4-29)$$

where  $\mathbb{I}_{ijkl} = \frac{\partial \sigma_{ij}}{\partial \sigma_{kl}} = \delta_{ik}\delta_{jl}$ . Comparing the equations (4-10) and (4-29), simultaneously, to the equation (4-27), gives the second order tensor :

$$L = \alpha_3 A + \alpha_4 (1 - A) \quad (4-30)$$

It is evident that the linear part of the yield criterion only depends on the hardening parameters which means it depends upon the equivalent plastic strain  $\bar{\varepsilon}^p$  and the structural tensor. Having defined the general version of the yield criterion, now it is time to redefine the flow potential function in a general form. Regarding that, the introduced flow potential function is only composed of the quadratic stresses (see the equation (3-24)), its generalized version can be characterized in the following form:

$$g(\sigma) = \frac{1}{2} \sigma : \mathbb{M} : \sigma - 1 \quad (4-31)$$

which means that the fourth-order tensor  $\mathbb{M}$  might be determined by taking the second derivative of the flow potential function (equation (3-24))

$$\partial_{\sigma\sigma}g(\sigma) = \mathbb{M} \quad (4-32)$$

Thus, having the first derivative of the flow potential function in equation (4-21) by taking its derivative with respect to the stress tensor the fourth-order tensor  $\mathbb{M}$  can be formulated such as follows:

$$\mathbf{M} = \beta_1 \mathbf{I} - \mathbf{A} \cdot \mathbf{I} - \mathbf{I} \cdot \mathbf{A} + \beta_2 \mathbf{A} \cdot \mathbf{I} + \mathbf{I} \cdot \mathbf{A} + 2\beta_{32} \mathbf{A} \otimes \mathbf{A} + 2\beta_{42} \mathbf{1} - \mathbf{A} \otimes \mathbf{1} - \mathbf{A} \quad (4-33)$$

The only difference between two fourth-order tensors  $\mathbf{K}$  and  $\mathbf{M}$  is that the later one does not depend on the loading history and the equivalent plastic strain since the flow potential function parameters are not evolutionary. It must be kept in mind that the reason for the generalization is that the numerical treatment might be more convenient. According to the algorithm which is presented in [1] in the next section, the numerical approach for the introduced constitutive equation is described.

### 4.3 Rate-dependent material behaviour

In this section, we introduce a simple rate dependent model to deal with the rate sensitivity of the component under bending (see the rate dependent results in section 5.3). According to [96, 97] and [53, 98] strain rate affects material properties of glass-reinforced composite materials including module of elasticity, strengths and toughness energies. In this study following Daniel's and later Wei et al. works [58, 99] , and for keeping the numerical implementation of the models simple, the effects of strain-rate have been applied on modules of elasticity and strengths of the material and rate dependent toughness energies are ignored. Following equations[6]:

$$\begin{aligned} E_{11} &= E_{11,qs} \left[ m_f^{E_{11}} \log \left( \frac{|\dot{\epsilon}_{11}|}{\dot{\epsilon}_{11,qs}} \right) + 1 \right]^2 \\ E_{22} &= E_{22,qs} \left[ m_f^{E_{22}} \log \left( \frac{|\dot{\epsilon}_{22}|}{\dot{\epsilon}_{22,qs}} \right) + 1 \right]^2 \\ G_{12} &= G_{12,qs} \left[ m_f^{G_{12}} \log \left( \frac{|\dot{\epsilon}_{12}|}{\dot{\epsilon}_{12,qs}} \right) + 1 \right]^2 \end{aligned} \quad (4-34)$$

The abbreviation of "qs" mentions to the amount of a specific value of a material constant under quasi-static condition.  $\dot{\epsilon}_{11,qs}$ ,  $\dot{\epsilon}_{22,qs}$  and  $\dot{\epsilon}_{12,qs}$  are reference values of strain rates in longitudinal normal, transverse normal and in-plane shear statuses. As Wei et al. [58] to assure the stability of the damage propagation model, it is assumed that all strain-rate dependence material properties have a uniform type of governing equations. Therefore, for rate dependent strengths can be written as follows[6]:

$$\begin{aligned}
X_T &= X_T^{qs} \left[ m_f^{X_T} \log \left( \frac{|\dot{\epsilon}_{11}|}{\dot{\epsilon}_{11,qs}} \right) + 1 \right]^2 \\
X_C &= X_C^{qs} \left[ m_f^{X_C} \log \left( \frac{|\dot{\epsilon}_{11}|}{\dot{\epsilon}_{11,qs}} \right) + 1 \right]^2 \\
Y_T &= Y_T^{qs} \left[ m_f^{Y_T} \log \left( \frac{|\dot{\epsilon}_{22}|}{\dot{\epsilon}_{22,qs}} \right) + 1 \right]^2 \\
Y_C &= Y_C^{qs} \left[ m_f^{Y_C} \log \left( \frac{|\dot{\epsilon}_{22}|}{\dot{\epsilon}_{22,qs}} \right) + 1 \right]^2 \\
S_{12} &= S_{12}^{qs} \left[ m_f^{S_{12}} \log \left( \frac{|\dot{\epsilon}_{12}|}{\dot{\epsilon}_{12,qs}} \right) + 1 \right]^2
\end{aligned} \tag{4-35}$$

The constants  $m_f$  and all which shown by “qs” indices could vary even case by case, but here it is assumed that these constants become equals for all the cases. For an instance, here in this study for calculation of  $X_T, X_C, Y_T$  and etc. the same value of  $m_f$  are considered. To determine the constant of  $m_f$  for each different condition, one has to perform different sorts of basic material property characterization tests with some various loading speeds to compare that specific material constant to its quasi-static condition. Then by data fitting procedure with each set of experimental result, the related rate-dependency constant will be determined. In this study, the above mentioned rate-dependent material properties have been applied in the subroutines, but since the rate dependency experiments just have been performed for the whole component and have not conducted for constituents of the beam, then in order to determine the constant of  $m_f$  the following equations have been suggested for this specific boundary conditions[6]:

$$E_{eq.}^{dy.Bend.} = E_{eq.}^{QS.Bend.} \left[ m_{eq.}^{Moduli} \log \left( \frac{V_{dynamic}}{V_{qs}} \right) + 1 \right]^2 \tag{4-36}$$

$E_{eq.}^{dy.Bend.}$  and  $E_{eq.}^{QS.Bend.}$  indicate the equivalent stiffness of the beam subjected to 3-point bending (Case1) under dynamic and quasi – static loadings, respectively. In

this study, the approximate slope of the force-displacement graphs of quasi-static and loading velocity of 127 mm/sec has been considered as  $E_{eq}^{QS.Bend.}$  and  $E_{eq}^{dy.Bend.}$ , respectively.  $m_{eq}^{Moduli}$  shows an effective coefficient of  $m$  for dealing with the total stiffness of the beam under this particular boundary and loading conditions, and  $V_{dynamic}$  and  $V_{qs}$  indicate puncher velocity for dynamic and quasi-static cases, respectively. A similar formula is suggested to determine the rate-dependent strength of the component as follows [6]:

$$X_{eq}^{dy.} = X_{eq}^{QS.Bend.} \left[ m_{eq}^{Strength} \log \left( \frac{V_{dynamic}}{V_{qs}} \right) + 1 \right]^2 \quad (4-37)$$

$X_{eq}^{dy.Bend.}$  and  $X_{eq}^{QS.Bend.}$  indicate the equivalent strengths of the internal constituent material without considering material direction, for dynamic and quasi-static loadings, respectively.  $m_{eq}^{Strength}$  demonstrates an effective coefficient of  $m$  to shift the results of material strength under quasi-static loading to dynamic level. In this study, since the Eq. (12) which suggests a direct proportionality of quasi-static and dynamic strengths of the material, then the maximum forces of force-displacement graphs have been considered as representatives of the material strengths.

## 4.4 Damage

In this section, both elastic and elasto-plastic damages concepts are discussed, separately, but exploiting the same idea. First of all, the corresponding literature of the composite materials' damage is reviewed, then the relevant formulation, which is used in the present text, are discussed in detail. The major portion of the literature review belongs to the work which is published in [6].

### 4.4.1 Elastic damage

The component, i.e., the case study, showed a minimum level of non-linearity under 3-point bending test, which could be neglected. Therefore, we began with the elastic-response of the material, and the material degradation occurs right after the elastic response.

#### 4.4.1.1 Elastic damage based on Continuum Damage Mechanics (CDM)

The elastic damage constitutive equations in the current study are built upon the Continuum Damage Mechanics (CDM) principals, so that employs the

damage variables to degrade the material stiffness matrix components as proposed by Matzenmiller et al. [38]. The damage initiation is detected based on Hashin and Rothem [41] failure criterion. It is well known that the Hashin and Rothem failure criterion has been developed for unidirectional reinforced laminates which are assumed, in general, as the transversely isotropic materials. Damage propagation is applied based Lapczyk-Hurtado's model which damage propagation is governed by energy release rates, and strains are replaced by characteristic length  $L_c$ , and associated displacements to alleviate mesh sensitivity problem[50].

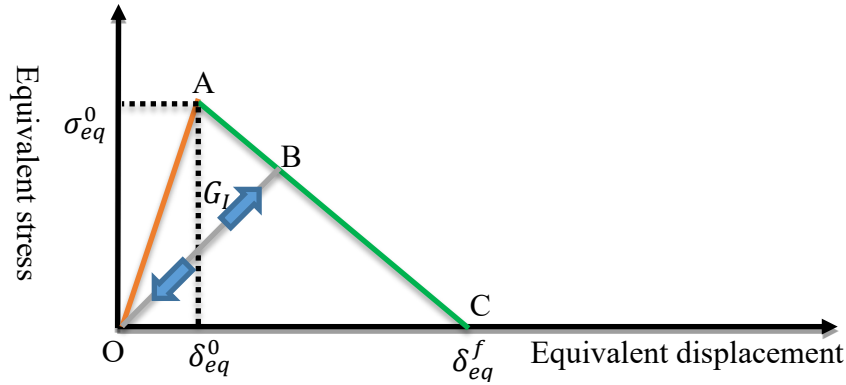


Figure 4-2 Linear Damage evolution law

The constitutive equation for the transversely isotropic material under certain assumptions, such as infinitesimal deformation and hyperelasticity, are presented for the 3D stress states in the equation (2-29) and the corresponding stiffness matrix in the equation (2-66). Since the modelling of the complex hybrid component as our case study in a 3D form is not numerically efficient, then we define the 2D stiffness matrix for the transversely isotropic materials. Thus, rewriting the transversely isotropic stiffness matrix for the planar stress state reaches:

$$C = \begin{bmatrix} \frac{E_{11}}{1 - \nu_{12}\nu_{21}} & \frac{\nu_{21}E_{11}}{1 - \nu_{12}\nu_{21}} & 0 \\ \frac{\nu_{12}E_{22}}{1 - \nu_{12}\nu_{21}} & \frac{E_{22}}{1 - \nu_{12}\nu_{21}} & 0 \\ 0 & 0 & G_{12} \end{bmatrix} \quad (4-38)$$

It should be noted that the restriction between longitudinal and transverse Poisson ration ( $v_{21} = \frac{E_{11}}{E_{22}}v_{12}$ , also see the section 2.5.1) is still satisfied with the short fiber reinforced thermoplastics while they are independent of each other in the case of fabric thermoplastic based sheet. Inserting the different modes damage variables into the original undamaged stiffness matrix (4-38) shall represent the degraded stiffness matrix in the following shape:

$$C^D = \frac{1}{\Xi} \begin{bmatrix} (1 - d_f) \frac{E_{11}}{1 - v_{12}v_{21}} & (1 - d_f)(1 - d_m) \frac{v_{21}E_{11}}{1 - v_{12}v_{21}} & 0 \\ (1 - d_f)(1 - d_m) \frac{v_{12}E_{22}}{1 - v_{12}v_{21}} & (1 - d_m) \frac{E_{22}}{1 - v_{12}v_{21}} & 0 \\ 0 & 0 & (1 - d_s)G_{12} \end{bmatrix} \quad (4-39)$$

where  $\Xi = 1 - (1 - d_f^t)(1 - d_f^c)(1 - d_m^t)(1 - d_m^c)v_{12}v_{21}$ ,  $d_s = 1 - (1 - d_f^t)(1 - d_f^c)(1 - d_m^t)(1 - d_m^c)$ .  $d_f$  and  $d_m$  indicate the material degradation in longitudinal and transverse direction, but we call them  $f$  and  $m$  while representing the fiber and matrix, respectively. The reason why we show longitudinal direction by  $f$  and the transverse direction by  $m$  lay in the tradition of the composite material when the most dominant composite types were unidirectional whose fiber direction is longitudinal, and the transverse direction is governed by the matrix [6].

Damage initiation must be defined in one of the stress or strain state called failure criterion. Variety of failure criteria for composite materials have been proposed over the years. Some of them are more considered in real applications such as Maximum stress, Maximum strain, Hashin-Rotem, Chang-Chang, Puck and LaRC [41, 42, 44, 45]. But, as Hinton et al. mentioned in the conclusive evaluation of the results obtained with the World-Wide Failure Exercise (WWFE) [43], despite recent improvements of failure criteria for composite material, still the majority of researchers insist in using classic form such as Maximum stress or Maximum strain theory, Tsai-Wu and Hashin-Rotem criteria. In this paper, Hashin-Rotem criterion is used, by considering that the stress space is an effective one. This criterion has a separated type which presents a separated criterion for each mode of failure including matrix and fiber failure in tension and compression and it is illustrated at Table 4-2 for the short fiber reinforced thermoplastics [6].

Table 4-2 Failure criterion for the internal part of the case study;  $\sigma_{ij}$  are effective stress tensor components,  $X_T$ ,  $X_C$ ,  $Y_T$  and  $Y_C$  are strengths of material. X and Y denote two perpendicular directions of the material. While T and C denote tension and compression, respectively.  $S_{12}$  and  $S_{21}$  are longitudinal and transverse shear strengths [6].

Failure mode	2-D Hashin-Rotem (for matrix)
Tensile Matrix in X direction ( $\sigma_{11} \geq 0$ )	$F_{XT}^H = \left(\frac{\sigma_{11}}{X_T}\right)^2 + \left(\frac{\sigma_{12}}{S_{12}}\right)^2 = 1$
Compressive Matrix in X direction ( $\sigma_{11} < 0$ )	$F_{XC}^H = \left(\frac{\sigma_{11}}{2S_{21}}\right)^2 + \left[\left(\frac{X_C}{2S_{21}}\right)^2 - 1\right] \frac{\sigma_{11}}{ X_C } + \left(\frac{\sigma_{12}}{S_{12}}\right)^2 = 1$
Tensile Matrix in Y direction ( $\sigma_{22} \geq 0$ )	$F_{YT}^H = \left(\frac{\sigma_{22}}{Y_T}\right)^2 + \left(\frac{\sigma_{12}}{S_{12}}\right)^2 = 1$
Compressive Matrix in Y direction ( $\sigma_{22} < 0$ )	$F_{YC}^H = \left(\frac{\sigma_{22}}{2S_{21}}\right)^2 + \left[\left(\frac{Y_C}{2S_{21}}\right)^2 - 1\right] \frac{\sigma_{22}}{ Y_C } + \left(\frac{\sigma_{12}}{S_{12}}\right)^2 = 1$

The failure criterions for the fabric in different damage mechanisms are considered much more straightforward than those for short fiber reinforced thermoplastics. The corresponding damage initiation criterion is listed in Table 4-3.

Table 4-3 Failure criterion for the internal constituent of the hybrid component;  $\sigma_{ij}$  are effective stress components,  $X_T$ ,  $X_C$ ,  $Y_T$  and  $Y_C$  are strengths of material. X and Y denote warp and woof directions, respectively. While T and C denote tension and compression, respectively [6].

Failure mode	Maximum stress theory
Tensile in warp Direction ( $\sigma_{11} \geq 0$ )	$F_{XT}^{MS} = \left(\frac{\sigma_{11}}{X_T}\right)^2 = 1$
Compressive in warp Direction ( $\sigma_{11} < 0$ )	$F_{XC}^{MS} = \left(\frac{\sigma_{11}}{X_C}\right)^2 = 1$
Tensile in woof Direction ( $\sigma_{22} \geq 0$ )	$F_{YT}^{MS} = \left(\frac{\sigma_{22}}{Y_T}\right)^2 = 1$
Compressive in woof Direction ( $\sigma_{22} < 0$ )	$F_{YC}^{MS} = \left(\frac{\sigma_{22}}{Y_C}\right)^2 = 1$

#### 4.4.1.2 Damage evolution law

Once damage initiation criterion is satisfied in any of the damage modes, damage evolution law is activated, and any further loading will be caused degradation of stiffness matrix. The propagation of damaged governed by damage evolutions law which is based on damage variables varying between zero and one. Zero amount of damage variables indicates the virgin status of material, while the amount of one notes a fully damaged material point. There are two different approaches to represent a damage law to control damage evolution: ply-discount method and damage laws based on energy release rates. Ply-discount method is the simplest one and degrades material just is taken a value zero or one which zero one shows virgin material and value of one indicates again fully damaged the material. But, from a numerical point of view using the value of one for the thoroughly damaged material point is not reasonable because sometimes leads to a stiffness matrix with an entire zero row or columns. So, to implement a ply-discount method to capture damage evolution instead of the value of one, one has to set a value such as 0.99 to avoid numerical instability. The second one is founded on energy release rate concept and leads a gradual degradation of material properties. This gradual release of energy could be governed by any equation, providing passes through points A and B and becomes strictly descending according to Figure 4-2. A strain-softening equation can have physical meaning or can be proposed considering a non-physical data fitting methods. Mainly this strain-softening equation is chosen linear as presented in [50, 100, 101] or could be exponential such as proposed in [102, 103]. In this study the linear damage law proposed in [50] which is governed by energy release rates, equivalent displacements and characteristic lengths of associated elements.

Based on damage model proposed by Lapczyk-Hurtado which also used in this paper for a specific damage mode, a linear strain-softening leads [58]:

$$G_{I,C} = \frac{1}{2} \sigma_{I,eq}^0 \delta_{I,eq}^f \quad (4-40)$$

Which  $\sigma_{I,eq}^0$  is maximum achievable equivalent stress before damage initiation and  $\delta_{I,eq}^f$  is maximum equivalent displacement when the material point is failed, while index  $I$  indicate a specific damage mode. For an element which is subjected to damage and the damage can be total or partial, before damage the slope of equivalent stress-equivalent displacement is  $E/L_c$  (the segment line of OA in

Figure 4-2), and after damage will be  $(E/L_c)(1 - d)$  (the segment line of OB in

Figure 4-2). Referring to the

Figure 4-2, the area of the  $OAB$  triangle represents the amount of energy that has been released during damage process while the area of the  $OBC$  triangle represents the remaining deformation energy that can be released until the material is completely damaged[6].

Table 4-4 Equivalent values of displacements and stresses for different damage modes of fabric; the symbol  $\langle \cdot \rangle$  indicates Macaulay operator which is defined as

$$\langle x \rangle = \frac{1}{2}(x + |x|); \forall x \in \mathbb{R}$$

Equivalent stresses and displacements for fabric outer shell		
Failure mode	$\delta_{eq}$	$\sigma_{eq}$
Tensile in warp Direction ( $\sigma_{11} \geq 0$ )	$L_c \langle \varepsilon_{11} \rangle$	$\frac{L_c \langle \sigma_{11} \rangle \langle \varepsilon_{11} \rangle}{\delta_{eq}^{xt}}$
Compressive in warp Direction ( $\sigma_{11} < 0$ )	$L_c \langle -\varepsilon_{11} \rangle$	$\frac{(L_c \langle -\sigma_{11} \rangle \langle -\varepsilon_{11} \rangle)}{\delta_{eq}^{xc}}$
Tensile in woof Direction ( $\sigma_{22} \geq 0$ )	$L_c \langle \varepsilon_{22} \rangle$	$\frac{L_c \langle \sigma_{22} \rangle \langle \varepsilon_{22} \rangle}{\delta_{eq}^{yt}}$
Compressive in woof Direction ( $\sigma_{22} < 0$ )	$L_c \langle -\varepsilon_{22} \rangle$	$\frac{L_c \langle -\sigma_{22} \rangle \langle -\varepsilon_{22} \rangle}{\delta_{eq}^{yc}}$

In this model, two main variables are equivalent displacement, and equivalent stresses calculated regards to the equations presented in Table 4-4. The characteristic length is related to the element geometry and formulation; it can be calculated by means of many different methods [37, 50]. The calculation of the characteristic length ( $L_c$ ) is left to ABAQUS's default which assumed to be equal to the length of a line across the element for a first-order element and half of that length for a second-order element. If one intends to apply a user-defined formula to calculate the characteristic length, it would be possible by coding in a

subroutine called VUCHARLENGTH. The damage for any of damage modes are calculated as follows:

$$d_I = \frac{\delta_{I,eq}^f (\delta_{eq} - \delta_{I,eq}^0)}{\delta_{eq} (\delta_{I,eq}^f - \delta_{I,eq}^0)}; \quad \delta_{I,eq}^0 \leq \delta_{eq} \leq \delta_{I,eq}^f \quad (4-41)$$

Which  $I$  indicate different modes of damage. while  $\delta_{I,eq}^0$  and  $\delta_{I,eq}^f$  describe equivalent displacement for  $d_I = 0$  (i.e. no damage) and  $d_I = 1$ , (i.e., material complete failure), respectively. Equation (4-41) is a function which varies between zero and one in accordance with the  $\delta_{eq}$  interval of variation. According to the fact that the damage is irreversible, the function (4-41) must be strictly increasing in its domain. The value of  $\delta_{I,eq}^f$  can be calculated based on the critical energy release rate concept as follows:

$$\delta_{I,eq}^f = \varepsilon_{eq}^f L_c = \frac{2G_{I,c}}{\sigma_{I,eq}^0} \quad (4-42)$$

where  $\sigma_{I,eq}^0$  is the equivalent stress value at the damage initiation state as mentioned before. Considering the Hashin-Rothem failure criterion, Table 4-5 summarizes the relationships to achieve equivalent stress and displacement in the different modes of damage.

Table 4-5 Equivalent values of displacements and stresses for different damage modes of internal constituent; the symbol  $\langle \cdot \rangle$  indicates Macaulay operator which

is defined as  $\langle x \rangle = \frac{1}{2}(x + |x|)$ ;  $\forall x \in \mathbb{R}$

<b>Equivalent stresses and displacements for internal part</b>		
<b>Failure mode</b>	$\delta_{eq}$	$\sigma_{eq}$
Tensile Matrix in X direction ( $\sigma_{11} \geq 0$ )	$L_c \sqrt{\langle \varepsilon_{11} \rangle^2 + \varepsilon_{12}^2}$	$\frac{L_c (\langle \sigma_{11} \rangle \langle \varepsilon_{11} \rangle + \sigma_{12} \varepsilon_{12})}{\delta_{eq}^{Xt}}$
Compressive Matrix in X direction ( $\sigma_{11} < 0$ )	$L_c \langle -\varepsilon_{11} \rangle$	$\frac{(L_c \langle -\sigma_{11} \rangle \langle -\varepsilon_{11} \rangle)}{\delta_{eq}^{Xc}}$
Tensile Matrix in Y direction ( $\sigma_{22} \geq 0$ )	$L_c \sqrt{\langle \varepsilon_{22} \rangle^2 + \varepsilon_{12}^2}$	$\frac{L_c (\langle \sigma_{22} \rangle \langle \varepsilon_{22} \rangle + \sigma_{12} \varepsilon_{12})}{\delta_{eq}^{Yt}}$
Compressive Matrix in Y direction ( $\sigma_{22} < 0$ )	$L_c \sqrt{\langle -\varepsilon_{22} \rangle^2 + \varepsilon_{12}^2}$	$\frac{L_c (\langle -\sigma_{22} \rangle \langle -\varepsilon_{22} \rangle + \sigma_{12} \varepsilon_{12})}{\delta_{eq}^{Yc}}$

Equivalent values of stress and displacement at the damage initiation point might be calculated as follows:

$$\begin{aligned}\delta_{I,eq}^0 &= \delta_{I,eq} f_I^{SC} \\ \sigma_{I,eq}^0 &= \sigma_{I,eq} f_I^{SC}\end{aligned}\quad (4-43)$$

where the scaling factors  $f_I^{SC}$  are adequately presented for different modes of damage in Table 4-6.

Table 4-6 Scaling factors for different damage modes [50]

Failure mode	Scaling Factors (for fabric outer shell)
Tensile Matrix in X direction ( $\sigma_{11} \geq 0$ )	$1/\sqrt{F_{XT}^{MS.or.H}}$
Compressive Matrix in X direction ( $\sigma_{11} < 0$ )	$1/\sqrt{F_{XC}^{MS.or.H}}$
Tensile Matrix in Y direction ( $\sigma_{22} \geq 0$ )	$1/\sqrt{F_{YT}^{MS.or.H}}$
Compressive Matrix in Y direction ( $\sigma_{22} < 0$ )	$1/\sqrt{F_{YC}^{MS.or.H}}$

Having defined the damage variables for each mode the degraded stiffness matrix can be constructed as mentioned in the equation (4-39) and replacing the original stiffness matrix by the degraded in the equation (4-1) reads:

$$\sigma = C^D : \varepsilon \quad (4-44)$$

Which implies the degradation of the stress array components.

#### 4.4.1 Elasto-plastic damage modelling

Short fiber reinforced thermoplastics under a certain amount of displacement begin to yield, plastically, and continuing the loading the plasticity will be saturated, and under a certain amount of deformation the damage begins and progress until the material is ruptured (see the Figure 4-1 ). Since the material has been already experienced the maximum stress state and the damage initiation might not be detected accurately based on a stress-based failure criterion. Thus, mostly the damage variables are introduced according to the maximum experienced strain in a specific failure mode, and the scalar-valued damage variables are defined to degrade the stress tensor components [104, 105]. According to the continuum damage mechanic (CDM) approach and following [50], as well as using equivalent displacements and characteristic lengths, an

elasto-plastic damage method is presented. For the elasto-plastic damage phenomenon, the original stiffness matrix components degradation can be accomplished as the elastic damage approach (see section 4.4.1.1). In addition to the later approach, the nonlocal damage method which is introduced by [104] is common while applying the damage by degrading the maximum stress vector, i.e., the saturated stress array's components. Even though, the nonlocal damage approach is rather straightforward than the degradation of the stiffness matrix components in the elasto-plasticity damage concept, but, however looking at the schematic equivalent displacement-stress diagram (Figure 4-3) we recognize that the elasto-plastic damage phenomenon might be treated as the damaging phenomenon exactly as introduced for the brittle materials which is discussed earlier in the section 4.4.1.1.

#### 4.4.1.1 Elasto-Plastic Continuum Damage Mechanics (EPCDM)

We start with the second method, using the CDM method for the elasto-plasticity damage, and in this method the calculation of the equivalent plastic deformation ( $\delta_{I,eq}^P$ ) plays the central mode. This value is approximate and not the exact for two reasons:

- In the CDM method, the damage variables are needed to be defined in the equivalent one-dimensional equivalent deformation-equivalent deformation state.
- The stress state in the saturation point is determined, approximately, according to the nonlinear plasticity solution.

These two reasons cause the discontinuity problem in the two-dimensional function in the saturation point. It means that the stress which is produced in the saturation point by using the CDM method, sometimes, might not be equal to the stress in the very point calculated by the plasticity numerical algorithm. The stress can be determined by CDM method by replaying the corresponding strain in the equation (4-44) and reaches:

$$\sigma = C^D : \varepsilon^{eff}. \quad (4-45)$$

where  $\varepsilon^P$  is the corresponding plastic strain for  $\delta_{I,eq}^P$  (see the Figure 4-3 ) and its determination is a critical point. The effective strain can be defined as follows

$$\varepsilon^{eff.} = \frac{\delta_{I,eq}^{sat.}}{\delta_{I,eq}^0} (\varepsilon - \varepsilon^P) \quad (4-46)$$

As mentioned before the plastic strain which can be easily achieved within the nonlinear numerical computation of the plasticity is not precise just because of the approximated nature of the numerical solution. Thus, the corresponding stress might exceed from the saturation point (the D point in Figure 4-3). To be sure that the stresses do not go beyond the saturation point, a correction factor is added to the equation (4-46) as  $\delta_{I,eq}^{sat}/\delta_{I,eq}^0$ .

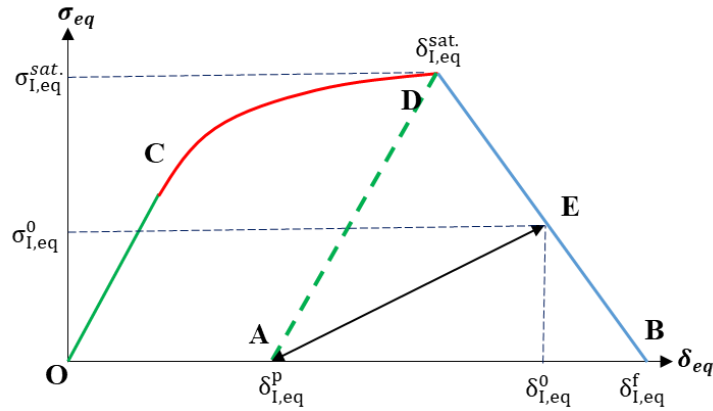


**Figure 4-3 Schematic elasto-plastic damage in the equivalent displacement-stress state**

Since the manifestation of the damage is along with the dissipation of the fracture energy of the corresponding damage mode; then a rational damage law might be written using these terms as presented by [49] for modeling the interlaminar delamination using cohesive element, then generalized by [50]. Also, if the corresponding constitutive equations are written in the stress-strain form, as is typically in continuum mechanics, leading to strain localization, a mesh dependency problem will be appeared [50]. To obviate this problem, the so-called crack band model proposed by [106] is considered as a proper solution and utilized by [50]. To define the damage variables, the CDM approach can be applied by shifting the origin of the equivalent displacement axis from O to A (see the Figure 4-3). Having done this, the equation (4-40) can be rewritten for the Elasto-Plastic Continuum Damage Mechanics (EPCDM) as follows:

$$G_{I,C} = \frac{1}{2} \sigma_{I,eq}^0 (\delta_{I,eq}^f - \delta_{I,eq}^p) \quad (4-47)$$

Such as [50]'s assumption to preserve the value of energy release rate for a particular mode of damage, the value of the final equivalent displacement  $\delta_{I,eq}^0$  and the values of the initial equivalent stress  $\sigma_{I,eq}^0$  and displacement  $\delta_{I,eq}^p$  are

not kept fix. Dividing the corresponding strain by the characteristic length of the elements the corresponding equivalent displacements are achieved. The amount of maximum plastic strain for a certain type of damage ( $\delta_{I,eq}^p$ ) is also a characteristic of the material and assumed to set to the corresponding maximum plastic strain of the relevant damage mode. Since the values of the initial equivalent stress and displacements are still unknowns; then the following formulation might be used to calculate these parameters [50]:

$$\sigma_{I,eq}^0 = f_I^{SC} \sigma_{I,eq} \quad (4-48)$$

where the  $f_I^{SC}$  is the scaling factor which can be found in the The corresponding equivalent values can be found in Table 4-7.

#### 4.4.1.2 Non-local elasto-plastic damage

Non-local damage approach as discussed in the section 4.4.1.1 degrades the saturated plastic stress (see the Figure 4-3). Since the non-local damage approach demands the damage variables to be defined, then the damage initiation and progression law must be established. The stress degradation can be written in the following mode:

$$\sigma^D = \sigma(1 - d_I^{nl}) \quad (4-52)$$

The damage variable for each mode is different than those introduced in the equation (4-49) and we define them according to the work has accomplished by [107-109] and numerically developed and implemented into ABAQUS (see [110]).

Table 4-7. The damage variables can be reproduced for EPCDM as CDM by the replacement of  $\delta_{I,eq}^0$  with  $\delta_{I,eq}^0 - \delta_{I,eq}^p$  such as follows:

$$d_I = \frac{(\delta_{I,eq}^f - \delta_{I,eq}^p)(\delta_{I,eq} - \delta_{I,eq}^0)}{(\delta_{I,eq} - \delta_{I,eq}^p)(\delta_{I,eq}^f - \delta_{I,eq}^0)} \quad (4-49)$$

where

$$\delta_{I,eq}^f = (\varepsilon_{eq}^f - \varepsilon_{eq}^p)L_c = \frac{2G_{I,C}}{\sigma_{I,eq}^0} \quad (4-50)$$

And finally

$$\delta_{I,eq}^0 = f_I^{SC} \delta_{I,eq} \quad (4-51)$$

The corresponding equivalent values can be found in Table 4-7.

#### 4.4.1.3 Non-local elasto-plastic damage

Non-local damage approach as discussed in the section 4.4.1.1 degrades the saturated plastic stress (see the Figure 4-3). Since the non-local damage approach demands the damage variables to be defined, then the damage initiation and progression law must be established. The stress degradation can be written in the following mode:

$$\sigma^D = \sigma(1 - d_i^{nl}) \quad (4-52)$$

The damage variable for each mode is different than those introduced in the equation (4-49) and we define them according to the work has accomplished by [107-109] and numerically developed and implemented into ABAQUS (see [110]).

Table 4-7 Damage parameters definition

Loading condition	Initial crack criterion	Scaling Factor	$\delta_{eq}$	$\sigma_{eq}$
1	$\varepsilon_{11} \geq \varepsilon_{1T}^p$	$\left(\frac{\varepsilon_{1T}^p}{\varepsilon_{11}}\right)^n$	$L_c \langle \varepsilon_{11} - \varepsilon_{1T}^p \rangle$	$\langle \sigma_{11} \rangle$
2	$\varepsilon_{11} \geq \varepsilon_{1C}^p$	$\left(\frac{\varepsilon_{1C}^p}{\varepsilon_{11}}\right)^n$	$L_c \langle -(\varepsilon_{11} - \varepsilon_{1C}^p) \rangle$	$\langle -\sigma_{11} \rangle$
3	$\varepsilon_{22} \geq \varepsilon_{2T}^p$	$\left(\frac{\varepsilon_{2T}^p}{\varepsilon_{22}}\right)^n$	$L_c \langle \varepsilon_{22} - \varepsilon_{2T}^p \rangle$	$\langle \sigma_{22} \rangle$
4	$\varepsilon_{22} \geq \varepsilon_{2C}^p$	$\left(\frac{\varepsilon_{2C}^p}{\varepsilon_{22}}\right)^n$	$L_c \langle -(\varepsilon_{22} - \varepsilon_{2C}^p) \rangle$	$\langle -\sigma_{22} \rangle$

The CDM method, which is introduced in the later references, is redeveloped to be applied on the non-local method. The damage initiation in the fiber direction,  $a = [1,0,0]$ , is identified by the strain-based failure criterion proposed by [107] as in Table 4-8. Consequently, the damage variables can be determined according to the failure criterion in Table 4-8 for the damage progression in the fiber direction, i.e.,  $a = [1,0,0]$  direction, as follows:

$$d_f^{nl} = 1 - \frac{\varepsilon_1^{sat,t}}{f_{f.}} e^{(-C_{11} \varepsilon_1^{sat,t} (f_{f.} - \varepsilon_1^{sat,t}) L_c / G_f)} \quad (4-53)$$

where according to the loading status, the compression or tension condition can be selected from the Table 4-8 and incorporated into the damage propagation equation (4-53) and the next one for the propagation of the damage in the transverse direction which reads:

$$d_m^{nl} = 1 - \frac{\varepsilon_2^{sat,t}}{f_{m,.}} e^{(-C_{22}\varepsilon_2^{sat,t}(f_{m,.} - \varepsilon_2^{sat,t})L^c/G_m)} \quad (4-54)$$

The characteristic length  $L^c$  and the energy release rate  $G_m$  concepts are introduced earlier in the section 4.4.1.2.

Table 4-8 Failure criteria for different damage modes for non-local elasto-plastic damage method

Failure mode	Failure criterion
$(\sigma_{11} \geq 0)$	$f_{f,t} = \sqrt{\frac{\varepsilon_1^{sat,t}}{\varepsilon_1^{sat,c}} \varepsilon_1^2 + \left( \varepsilon_1^{sat,t} - \frac{(\varepsilon_1^{sat,t})^2}{\varepsilon_1^{sat,c}} \right) \varepsilon_1} > \varepsilon_1^{sat,t}$
$(\sigma_{11} < 0)$	$f_{f,c} = \sqrt{\frac{\varepsilon_1^{sat,c}}{\varepsilon_1^{sat,t}} \varepsilon_1^2 + \left( \varepsilon_1^{sat,c} - \frac{(\varepsilon_1^{sat,c})^2}{\varepsilon_1^{sat,t}} \right) \varepsilon_1} > \varepsilon_1^{sat,c}$
$(\sigma_{22} \geq 0)$	$f_{m,t} = \sqrt{\frac{\varepsilon_2^{sat,t}}{\varepsilon_2^{sat,c}} \varepsilon_2^2 + \left( \varepsilon_2^{sat,t} - \frac{(\varepsilon_2^{sat,t})^2}{\varepsilon_2^{sat,c}} \right) \varepsilon_2} + \frac{\varepsilon_2^{sat,t}}{\varepsilon_4^{sat}} \varepsilon_4^2 > \varepsilon_2^{sat,t}$
$(\sigma_{22} < 0)$	$f_{m,c} = \sqrt{\frac{\varepsilon_2^{sat,c}}{\varepsilon_2^{sat,t}} \varepsilon_2^2 + \left( \varepsilon_2^{sat,c} - \frac{(\varepsilon_2^{sat,c})^2}{\varepsilon_2^{sat,t}} \right) \varepsilon_2} + \frac{\varepsilon_2^{sat,c}}{\varepsilon_4^{sat}} \varepsilon_4^2 > \varepsilon_2^{sat,c}$

Since the non-local approach degrades the stress array components instead of the stiffness matrix components, then it has a significant advantage over the EPCDM method, in the sense that it is more convenient to be applied in the numerical coding, while it implies less physical meaning. According to [1] using the non-local damage fashion assists the reduction of mesh dependency in elasto-plasticity damage simulation.

## 4.5 Numerical methods

According to the introduced elasto-plasticity model it can be quickly realized that there is no an explicit solution for the presented constitutive equations due to that fact that the model is completed by the consistency parameter calculation, but the consistency parameter itself requires the gradient of the yield surface to be

determined while the gradient itself needs the hardening parameter themselves become identified and they themselves depend on the hardening parameters which are the functions of the equivalent plastic strain which is the function of the consistency parameter. This is a loop, and in this cases, the systems of the equations require a numerical solution which begins with a guess and the entire procedure is based on the try and error idea. In fact, the core equation must be solved is the consistency condition and in the plasticity theory, we try to find its root to guarantee that the stress state will be on the progressive yield surface beyond the primary yield surface. However, to solve the numerical problem and at the same time to implement the constitutive equation into the finite element solver, a proper numerical method must be chosen as well as a proper solver. In the current research to use Finite Element Method (FEM) the commercial FEM called “ABAQUS” is chosen which has both explicit and implicit FEM solver. Since the implicit method is an unconditionally stable method, then it is chosen as a benchmark, but also the model is solved using the explicit solver. However, both implicit and explicit methods are discussed in the next section in detail. An integration scheme must be chosen for the numerical plasticity, and here we follow the [111]’work such as [105].

#### 4.5.1 Backward Euler integration algorithm

The generalized elasto-plastic model in section 4.2 has to be reformulated to be prepared to be implemented into the FEM model. Following [1, 105]’s works, we begin with the elastic strain definition in equation (4-5) and rewiring it a discrete fashion in the time interval  $\Delta t = t_{n+1} - t_n$  :

$$\varepsilon_{n+1}^p = \varepsilon_n^p + \Delta t \dot{\varepsilon}_{n+1}^p = \varepsilon_n^p + \Delta \gamma_{n+1} (n_g)_{n+1} \quad (4-55)$$

Since the algorithm, conceptually, is based on try and error numerical method, then the first guess or trial does have a significant effect on the convergence issue. Since in a FEM we are numerically looking for the response of the material using a specific constitutive equation, then in a try and error concept, the element which might be used is the response argument (stress tensor). The most reasonable trial for the stress tensor in the plastic zone might be the stress calculated by the elastic constitutive equation (4-1) using the concept of the decomposition of the total strain to two elastic and plastic portion presented in equation (4-2) where the current step’s total strain, which is of course known as the input, minus the previous step’s plastic strain gives the elastic portion of the strain. According to the later explanation, it can be written:

$$\varepsilon_{n+1}^p = \varepsilon_n^p + \Delta t \dot{\varepsilon}_{n+1}^p = \varepsilon_n^p + \Delta \gamma_{n+1} (\mathbf{n}_g)_{n+1} \quad (4-56)$$

The elastic trial step can be attained considering the assumption of the additive strain (see equation (4-2)) and Hook's law (equation (4-1)) such as follows:

$$\begin{aligned} \varepsilon_{n+1}^{\text{tr}} &:= \varepsilon_{n+1} - \varepsilon_n^p = \varepsilon_{n+1}^e + (\varepsilon_{n+1}^p - \varepsilon_n^p) \\ &= \mathbf{C}^{-1} : \sigma_{n+1} + (\mathbf{n}_g)_{n+1} \Delta \gamma_{n+1} \end{aligned} \quad (4-57)$$

Then associated trial stress can be achieved:

$$\sigma_{n+1}^{\text{tr}} = \mathbf{C} : \varepsilon_{n+1}^{\text{tr}} = \sigma_{n+1} + \Delta \gamma_{n+1} \mathbf{C} : (\mathbf{n}_g)_{n+1} \quad (4-58)$$

Besides, considering the equation (4-32) the gradient of the flow potential function can be determined as follows based on the fourth-order tensor  $\mathbf{M}$  :

$$\mathbf{n}_g = \mathbf{M} : \sigma \quad (4-59)$$

Inserting equation (4-57) into the equation (4-58) yields:

$$\sigma_{n+1}^{\text{tr}} = \sigma_{n+1} + \Delta \gamma_{n+1} \mathbf{C} : \mathbf{M} : \sigma_{n+1} = (\mathbf{I} + \Delta \gamma_{n+1} \mathbf{C} : \mathbf{M}) : \sigma_{n+1} \quad (4-60)$$

This equation is derived based on the most basic arguments of the plasticity constitutive equation including the fourth order identity tensor  $\mathbf{I}$ , the original stiffness tensor  $\mathbf{C}$ , the fourth-order tensor  $\mathbf{M}$ . the latter fourth-order tensor  $\mathbf{M}$  is independent of the plastic history and in the scalar consistency parameter which is the only link between equation (4-60) and the plasticity constitutive equation. Since we are looking for the updated stress then reordering equation (4-60) gives the current stress tensor beyond the yielding point:

$$\begin{aligned} \sigma_{n+1} &= (\mathbf{I} + \Delta \gamma_{n+1} \mathbf{C} : \mathbf{M})^{-1} : \sigma_{n+1}^{\text{tr}} = \mathbf{F} : \sigma_{n+1}^{\text{tr}} \\ \mathbf{F} &= \mathbf{I} + \Delta \gamma_{n+1} \mathbf{C} : \mathbf{M}^{-1} \end{aligned} \quad (4-61)$$

Which means that the current stress in the plastic zone just depends on one updatable variable of the consistency parameter and the other arguments including the trial stress itself are constant in the local try and error procedure. Nevertheless, and having determined the trial strain and stress and the other engaged arguments, it seems the only parameter left undetermined is the consistency parameter and as it is discussed in the previous section, it can be achieved by applying the consistency condition which means the stress state must remain on the growing yield surface. Rewriting the general anisotropic yield function in a discrete method so that it can be employed in a numerical method, reaches:

$$f_{n+1}^{(k)} \equiv \frac{1}{2} \sigma_{n+1}^{(k)} : \mathbb{K}^{(k)} : \sigma_{n+1}^{(k)} + L^{(k)} : \sigma_{n+1}^{(k)} - 1 = 0 \quad (4-62)$$

Where the yield function only depends on the consistency parameter and  $k$  represents the local iteration. Since the aim is to satisfy the consistency condition and determine the consistency parameter, then a numerical solution such as Newton-Raphson can be employed to approximately satisfy the equation (4-62). The Newton-Raphson method needs a residual function to be defined such as follows:

$$R|_{n+1}^{(k)} = f_{n+1} \left( \sigma_{n+1}^{(k)} \left( \Delta\gamma_{n+1}^{(k)} \right) \right) \equiv 0 \quad (4-63)$$

The linear approximation of the residual function based on Taylor series reads:

$$f_{n+1}^{(k+1)} = f_{n+1}^{(k)} + \frac{\partial f_{n+1}^{(k)}}{\partial \Delta\gamma_{n+1}^{(k)}} \left( \Delta\gamma_{n+1}^{(k+1)} - \Delta\gamma_{n+1}^{(k)} \right) \approx 0 \quad (4-64)$$

Therefore, the consistency parameter at the end of the iteration can be determined, approximately, based on the current consistency parameter, the current value of the yield function and the current derivative of the yield function with respect to the current consistency parameter:

$$\Delta\gamma_{n+1}^{(k+1)} = \Delta\gamma_{n+1}^{(k)} - \frac{f_{n+1}^{(k)}}{\frac{\partial f_{n+1}^{(k)}}{\partial \Delta\gamma_{n+1}^{(k)}}} \quad (4-65)$$

The term left undetermined is  $\frac{\partial f_{n+1}^{(k)}}{\partial \Delta\gamma_{n+1}^{(k)}}$  which can be obtained using the chain rule such as follows:

$$\begin{aligned} \frac{\partial f_{n+1}}{\partial \Delta\gamma_{n+1}} &= \frac{\partial f_{n+1}}{\partial \sigma_{n+1}} : \frac{\partial \sigma_{n+1}}{\partial \Delta\gamma_{n+1}} + \frac{\partial f_{n+1}}{\partial \mathbb{K}_{n+1}} \dots \frac{\partial \mathbb{K}_{n+1}}{\partial \Delta\gamma_{n+1}} \\ &\quad + \frac{\partial f_{n+1}}{\partial L_{n+1}} : \frac{\partial L_{n+1}}{\partial \Delta\gamma_{n+1}} \end{aligned} \quad (4-66)$$

For the readability, the local iteration counter ( $k$ ) is eliminated from the equations. The equation (4-49) contains five undetermined terms which have to be characterized. However, we begin with the derivative of the stress tensor with respect to the current consistency parameter. According to [1], since the trial stress remain unchanged in a local iteration procedure, then its derivative with

respect to the current consistency parameter must be zero ( $\partial_{\Delta\gamma_{n+1}} \sigma_{n+1}^{\text{tr}} = 0$ ), therefore inserting this circumstance into the equation (4-43) gives :

$$\frac{\partial \sigma_{n+1}}{\partial \Delta\gamma_{n+1}} = -\mathbf{F}_{n+1} : (\mathbf{C} : \mathbf{M}) : \sigma_{n+1} \quad (4-67)$$

Which the result is a second order tensor. According to the general definition of the yield function (see equation (4-26)), the derivative of the yield function with respect to the fourth-order tensor  $\mathbf{K}$  might be obtained without any difficulty:

$$\frac{\partial f_{n+1}}{\partial \mathbf{K}_{n+1}} = \sigma_{n+1} \otimes \sigma_{n+1} \quad (4-68)$$

The second order tensor L can be achieved as easy as its fellow:

$$\frac{\partial f_{n+1}}{\partial L_{n+1}} = \sigma_{n+1} \quad (4-69)$$

Again using the chain rule, the derivative of the fourth-order tensor  $\mathbf{K}$  with respect to the consistency parameter might be achieved:

$$\begin{aligned} \frac{\partial \mathbf{K}_{n+1}}{\partial \bar{\epsilon}_{n+1}^p} &= \frac{\partial \mathbf{K}_{n+1}}{\partial \alpha_i^{n+1}} \frac{\partial \alpha_i^{n+1}}{\partial \bar{\epsilon}_{n+1}^p} \\ &= (\mathbf{I} - \mathbf{A} \cdot \mathbf{I} - \mathbf{I} \cdot \mathbf{A}) \frac{\partial \alpha_1^{n+1}}{\partial \bar{\epsilon}_{n+1}^p} + (\mathbf{A} \cdot \mathbf{I} + \mathbf{I} \cdot \mathbf{A}) \frac{\partial \alpha_2^{n+1}}{\partial \bar{\epsilon}_{n+1}^p} \\ &\quad + 2\mathbf{A} \otimes \mathbf{A} \frac{\partial \alpha_{32}^{n+1}}{\partial \bar{\epsilon}_{n+1}^p} + 2(1 - \mathbf{A}) \otimes (1 - \mathbf{A}) \frac{\partial \alpha_{42}^{n+1}}{\partial \bar{\epsilon}_{n+1}^p} \end{aligned} \quad (4-70)$$

where the derivatives of the hardening parameters with respect to the equivalent plastic strains are available in the equations (3-12), (4-14), (4-17) and (4-18). The same procedure can be accomplished to determine the derivative of the second order tensor with respect to the equivalent plastic strain

$$\frac{\partial L_{n+1}}{\partial \bar{\epsilon}_{n+1}^p} = \frac{\partial L_{n+1}}{\partial \alpha_i^{n+1}} \frac{\partial \alpha_i^{n+1}}{\partial \bar{\epsilon}_{n+1}^p} = \mathbf{A} \frac{\partial \alpha_3^{n+1}}{\partial \bar{\epsilon}_{n+1}^p} + (1 - \mathbf{A}) \frac{\partial \alpha_4^{n+1}}{\partial \bar{\epsilon}_{n+1}^p} \quad (4-71)$$

where the derivative of the hardening parameters with respect to the equivalent plastic strain can be found in the equations (4-15) and (4-18). Having determined the last term of the equation (4-49), the consistency parameter can be updated (see equation (4-65)) through the local iteration and accordingly the stress tensor can be updated via equation (4-44).

#### 4.5.1.1 Implicit solver requirements

Here we discuss very briefly the implicit solver, especially implicit solver of ABAQUS, and its requirements, but it is not intended to be in detail. However, for more details, one can refer to the ABAQUS documentations which are available online [110]. Let's begin with the basic discretized FEM equilibrium which is applicable for both explicit and implicit FEM solvers under certain circumstances:

$$P^N - I^N = M^{NM}\ddot{u}^M \quad (4-72)$$

where  $P^N$  is the external force vector and  $I^N$  represents the internal force vector which is created by the stress tensor in the elements and  $M^{NM}\ddot{u}^M$  characterizes the force vector owing to the material inertia. Also,  $M^{NM}$  is the mass matrix and  $\ddot{u}^M$  describes the acceleration vector. The internal forces can be obtained by:

$$I^N = \int_V \beta^N : \sigma dV \quad (4-73)$$

where  $V$  is the current volume of the model and  $\beta$  is defined as the transformation of the strain rate-displacement rate:

$$\dot{\epsilon} = \beta^N \dot{u}^N \quad (4-74)$$

Having defined the elements of the basic FEM equilibrium, now it is possible to describe the major difference between two approaches. In dynamic equilibrium the d'Alembert forces (the right hand side of the equation (4-72)) is significant while the static equilibrium implies that the d'Alembert forces vary gradually, or are constants, over time which yields:

$$M^{NM}\ddot{u}^M \approx 0 \quad (4-75)$$

If the analysis (simulation) can be carried out in few time increments, then the implicit solution is effective. ABAQUS/Standard employs Newton's method to solve the static equilibrium. An approximate solution of the equation (4-72) at iteration ( $i$ ), i.e.  $u_i^N$ , can be represented by the Taylor expansion as follows:

$$P^N - I^N + \left( \frac{\partial P^N}{\partial u^M} - \frac{\partial I^N}{\partial u^M} \right) c^M + \dots = 0 \quad (4-76)$$

which it can be written as:

$$P^N - I^N = K^{NM}c^M \quad (4-77)$$

where

$$K^{NM} = \frac{\partial I^N}{\partial u^M} - \frac{\partial P^N}{\partial u^M} \quad (4-78)$$

And it is called the tangent stiffness or Jacobian Matrix and  $c^N$  is the correction to the solution at the degree of freedom  $N$ . At the end, the incremental displacements are updated as follows:

$$\Delta u_{(i+1)}^N = \Delta u_{(i)}^N + c_{(i)}^N \quad (4-79)$$

The system of equation is iterated until it gets converged [110].

#### 4.5.1.2 Algorithmic tangent

However, the intention to solve the FEM problem with ABAQUS/Standard solver which uses the implicit method requires the Jacobian matrix to be defined at Gauss-point level. In the stress-strain level, the Jacobian is the derivative of the stress with respect to the stress. In the computational elasto-plasticity the numerical tangent is called algorithmic consistent tangent operator since it must be consistent with the time integration [1, 105]. Since the theoretical Jacobian matrix, or material tangent, which appears in the equation (4-25) is not consistent with the time integration and the consistency parameter is an infinitesimal and not finite number. It is shown that if the time step tends to zero number, then the algorithmic tangent tends to the material tangent [1, 112]. However, as it is required by the implicit solver the algorithmic consistent elasto-plastic tangent

$$\mathbb{C}^{\text{ep\_alg}} = \frac{d\sigma_{n+1}}{d\varepsilon_{n+1}} \quad (4-80)$$

In order to determine the algorithmic tangent in the equation (4-80), we refer to the equations (4-40) and (4-43) where it can be easily shown that an infinitesimal increment of the total stress reads:

$$\begin{aligned} \sigma_{n+1}^{\text{tr}} &= \mathbb{C} : (\varepsilon_{n+1} - \varepsilon_n^p) = \mathbb{F}_{n+1}^{-1} : \sigma_{n+1} \\ d\sigma_{n+1}^{\text{tr}} &= \mathbb{C} : d\varepsilon_{n+1} = d\mathbb{F}_{n+1}^{-1} : \sigma_{n+1} + \mathbb{F}_{n+1}^{-1} : d\sigma_{n+1} \\ &= d\Delta\gamma_{n+1} \mathbb{C} : \mathbb{M} : \sigma_{n+1} + \mathbb{F}_{n+1}^{-1} : d\sigma_{n+1} \\ d\sigma_{n+1} &= \mathbb{F}_{n+1} : [\mathbb{C} : d\varepsilon_{n+1} - d\Delta\gamma_{n+1} \mathbb{C} : \mathbb{M} : \sigma_{n+1}] \end{aligned} \quad (4-81)$$

And if the equation (4-80) is rearranged as follows:

$$d\sigma_{n+1} = \mathbb{C}^{\text{ep\_alg}} : d\varepsilon_{n+1} \quad (4-82)$$

And it means if we could find a link between the consistency parameter differential which appear in (4-81), then it would be possible to rearrange the

equation so that the algorithmic tangent might come out, automatically. If the consistency condition is applied to the equation (4-46), then its differential form reaches:

$$df_{n+1} = \frac{\partial f}{\partial \sigma_{n+1}} : d\sigma_{n+1} + \frac{\partial f}{\partial \Delta\gamma_{n+1}} d\Delta\gamma_{n+1} \equiv 0 \quad (4-83)$$

Inserting  $d\sigma_{n+1}$  from the equation (4-81) into the equation (4-83) gives:

$$d\Delta\gamma_{n+1} = \frac{\frac{\partial f}{\partial \sigma_{n+1}} : \mathbf{F}_{n+1} : \mathbf{C} : d\varepsilon_{n+1}}{\frac{\partial f}{\partial \sigma_{n+1}} : \mathbf{F}_{n+1} : \mathbf{C} : \mathbf{M} : \sigma_{n+1} - \frac{\partial f_{n+1}}{\partial \Delta\gamma_{n+1}}} \quad (4-84)$$

Substitution of the term  $\frac{\partial f}{\partial \sigma_{n+1}}$  by its general form from the equation (4-27) and inserting the result into the equation (4-81) yields:

$$\begin{aligned} d\sigma_{n+1} \\ = \mathbf{F}_{n+1} : \left[ \mathbf{C} \right. \\ \left. - \frac{\mathbf{C} : \mathbf{M} : \sigma_{n+1} \otimes (\mathbf{K}_{n+1} : \sigma_{n+1} + L_{n+1}) : \mathbf{F}_{n+1} : \mathbf{C}}{(\mathbf{K}_{n+1} : \sigma_{n+1} + L_{n+1}) : \mathbf{F}_{n+1} : \mathbf{C} : \mathbf{M} : \sigma_{n+1} + \frac{\partial f_{n+1}}{\partial \Delta\gamma_{n+1}}} \right] : d\varepsilon_{n+1} \end{aligned} \quad (4-85)$$

And subsequently, the comparison between the equations (4-82) and (4-85), gives the algorithmic tangent such as follows:

$$\mathbf{C}^{\text{ep\_alg}} = \mathbf{F}_{n+1} : \left[ \mathbf{C} - \frac{\mathbf{C} : \mathbf{M} : \sigma_{n+1} \otimes (\mathbf{K}_{n+1} : \sigma_{n+1} + L_{n+1}) : \mathbf{F}_{n+1} : \mathbf{C}}{(\mathbf{K}_{n+1} : \sigma_{n+1} + L_{n+1}) : \mathbf{F}_{n+1} : \mathbf{C} : \mathbf{M} : \sigma_{n+1} + \frac{\partial f_{n+1}}{\partial \Delta\gamma_{n+1}}} \right] \quad (4-86)$$

Since all engaged terms are characterized, therefore the elasto-plastic algorithmic tangent is determined, and as it is shown in [1], it would be equal to the continuum tangent (see equation (4-25)) if the time step inclines to zero. The integration scheme for the local-plasticity is presented in the following table, but the complete elasto-plasticity implicit algorithm is presented in the next section.

Table 4-9 Overview of the plasticity algorithm [1]

Order	Explanation	Formula
1	Inputs for the local plastic corrector at Gauss point level	Total strain of the current step ( $\varepsilon_{n+1}$ ), the plastic strain tensor and the equivalent plastic strain from the previous step $\varepsilon_n^p, \bar{\varepsilon}_n^p$
2	Elastic predictor	Initial guesses including the trial strain tensor $\varepsilon_{n+1}^{tr} := \varepsilon_{n+1} - \varepsilon_n^p$ and trial stress tensor $\sigma_{n+1}^{tr} = \mathbf{C} : \varepsilon_{n+1}^{tr}$
3	Local loop to correct the initial guess based on the plasticity algorithm. In this stage, we set the local loop counter k to zero (k=0) and the associated inputs to start the local numerical procedure to correct the initially guessed stress and the equivalent plastic strain $\sigma_{n+1}^{(k=0)} = \sigma_{n+1}^{tr}$ , $(\bar{\varepsilon}_{n+1}^p)^{(k=0)} = \bar{\varepsilon}_n^p$ and the consistency parameter is set to zero $(\Delta\gamma_{n+1})^{(k=0)} = 0$	
3.1	The first step is to determine the $\mathbf{F}$ tensor using the initial guesses. Obviously, the consistency parameter is the only variable.	$\mathbf{F}_{n+1}^{(k)} = \mathbf{I} + \Delta\gamma_{n+1}^{(k)} \Delta\gamma_{n+1} \mathbf{C} : \mathbf{M}^{-1}$
3.2	Then, the stress can be updated.	$\sigma_{n+1}^{(k)} = \mathbf{F}_{n+1}^{(k)} : \sigma_{n+1}^{tr}$
3.3	The hardening parameters must be updated using the look-up procedure or using the associated formula	$(\bar{\varepsilon}_{n+1}^p)^{(k=0)} \Rightarrow Y_{(\dots)}(\bar{\varepsilon}_{n+1}^p) \text{ can be calculated from } Y_{(\dots)} - \bar{\varepsilon}_{n+1}^p \text{ curves} \\ \Rightarrow \text{hardening parameters } \alpha_{(\dots)} \text{ (see Table 3-4)}$
3.4	Calculate the yield function ( $f_{n+1}^{(k)}$ ) value	From the equation (4-62)
3.5	Define a tolerance value to leave the local	if $f_{n+1}^{(k)} \leq \text{TOL}$ . goto (4)

	loop	
3.6	Update the consistency parameter from equation (4-65)	$\Delta\gamma_{n+1}^{(k+1)} = \Delta\gamma_{n+1}^{(k)} - \frac{f_{n+1}^{(k)}}{\frac{\partial f_{n+1}^{(k)}}{\partial \Delta\gamma_{n+1}^{(k)}}}$
3.7	Update the equivalent plastic strain	$(\bar{\epsilon}_{n+1}^p)^{(k+1)} = (\bar{\epsilon}_{n+1}^p)^{(k)} - \frac{f_{n+1}^{(k)}}{\frac{\partial f_{n+1}^{(k)}}{\partial \Delta\gamma_{n+1}^{(k)}}} \ \mathbf{M} : \sigma_{n+1}^{(k)}\ $
4	Update the internal variables	$\sigma_{n+1} = \sigma_{n+1}^{(k)}, \quad \bar{\epsilon}_{n+1}^p = (\bar{\epsilon}_{n+1}^p)^{(k)} \text{ and}$ $\epsilon_{n+1}^p = \epsilon_n^p + \Delta\gamma_{n+1}^{(k)} \mathbf{M} : \sigma_{n+1}^{(k)}$
5	Calculate the algorithmic tangent	The algorithmic tangent can be determined using the equation (4-86)

It should be noted that the entire plasticity model’s philosophy is constructed on the return algorithm and the schematic idea is illustrated in 2D stress space in Figure 4-4.

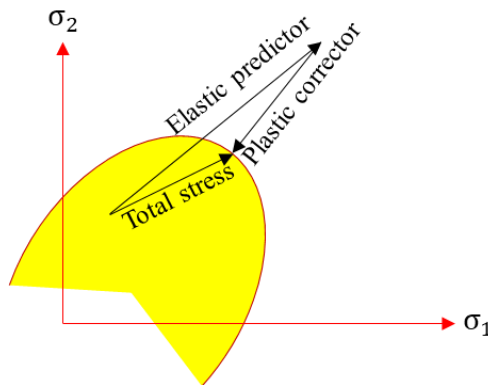


Figure 4-4 Schematic return algorithm [95]

### 4.5.1.3 Implementation into ABAQUS (UMAT)

For verification of the introduced model, it has to be incorporated into a FEM solver which might be implicit or explicit. ABAQUS/Standard, which uses the Euler backward (implicit method) to deal with the FEM analysis (see section 4.5.1), is more efficient for solving smooth nonlinear (e.g., quasi-static elasto-plasticity) problems than explicit fashion. However, under certain circumstances such as complicated contacts or some convergence problem or even material complexities, where for example we need to delete the element from the computational calculation, ABAQUS/Explicit has some advantages over the ABAQUS/Implicit solver. In the current research the introduced model is coded in both fashion, but as mentioned before, the benchmark code is the one is programmed for ABAQUS/Implicit. ABAQUS/Implicit allows the user to define and implement her/his own material model in the form of a subroutine called UMAT into the software in the Gauss-point level. The subroutine is allowed to be written in FORTRAN, C and C++, but since the most available examples in the ABAQUS document are related to FORTRAN, then both implicit and explicit subroutines are written in FORTRAN environment. Here we intend to explain some important features of the UMAT subroutine, but for the details, one can refer to [110].

User subroutine UMAT:

- Is used to define the material behavior in the constitutive equation form
- And called in each of the integration points
- Must update the stress tensor (STRESS(NTENS)) at the end of the increment; NTENS is the size of the stress or strain component array
- Must provide the Jacobian matrix (DDSDDE(NTENS,NTENS))

ABAQUS uses the stress tensor as in the Voigt notation such as defined in the equation (2-30). An overview of the user-defined UMAT flowchart is presented in Figure 4-6. ABAQUS itself, based on the boundary conditions, the material elastic constants, the associated time-step and etc., generates the initial strain increments components DSTRAN and sets the STRESS components to zero at the beginning of the simulation when the total time is equal to zero (TIME(2)=0). These values are accumulated type and are updated during the FEM-analysis procedure while the associated Jacobian matrix components at the beginning of each time step are set to be zero and are not accumulated type. This latter explanation seems to be

quite proper since the nature of the Jacobian matrix is instantaneous so that  $DDSDDE(i,j)$  describes the change in the  $i^{\text{th}}$  component of the stress at the end of the time increment caused by the infinitesimal perturbation of the  $j^{\text{th}}$  component of the strain increment array. It must be beared in mind that almost always the accuracy of the definition of the Jacobian matrix is the most crucial factor in the implicit FEM-analysis convergence. But, its definition does not affect the accuracy of the results; i.e., once the problem is converged then the results achieved by any definition of the Jacobian matrix will be the same. Nevertheless, the Jacobian matrix, as the derivative of the stress with respect to the strain, might be achieved numerically as well as the presented exact solutions. In this research, we use the forward difference differential scheme in order to obtain the Jacobian matrix as explained in [1], but to obtain higher convergence rate, the exact solution is considered, unless otherwise stated.

Since the Jacobin matrix itself describes a system of ordinary differential equations, then it can be solved by a so-called perturbation method. Assume we have a stress function which each of the components just depends on the variation of the strain components. Also, we consider that we are in the plasticity zone due to the fact that our aim is to calculate the Jacobian matrix and in the elastic area the Jacobian is equal to the stiffness matrix. It can be casted into the index notation:

$$DDSDDE(i,j) = \frac{\Delta\sigma(i)}{\Delta\varepsilon(j)} \quad (4-87)$$

We know the stress array can be updated according to the locally defined iterative plasticity algorithm presented in Table 4-9, then the stress component are known, and it is evident that to build the Jacobian matrix we need to determine the variation of each of the stress components under perturbation of one of the strain components. As an example, assume that we add up a specific disturbance value  $\varepsilon^{\text{pert}}$  to the second component of the strain vector. The entire components of the stress vector are affected by the disturbance of the second component of the strain vector which can be presented as follows:

$$\varepsilon_2^{\text{pert.}} = \begin{bmatrix} \varepsilon_1 \\ \varepsilon_2 + \varepsilon^{\text{pert}} \\ \varepsilon_3 \\ \varepsilon_4 \\ \varepsilon_5 \\ \varepsilon_6 \end{bmatrix} \quad (4-88)$$

where the perturbed strain tensor is constructed, and the disturbed stress can be calculated. Since, there are six disturbed strain arrays, for the 3D problem, then there will be six corresponding stress vectors, therefore, for the convenience, we may construct the disturbed stress matrix such as follows:

$$\sigma_{ij}^{\text{pert.}} = \begin{bmatrix} \sigma_{11}^{\text{pert.}} & \sigma_{12}^{\text{pert.}} & \sigma_{13}^{\text{pert.}} & \sigma_{14}^{\text{pert.}} & \sigma_{15}^{\text{pert.}} & \sigma_{16}^{\text{pert.}} \\ \sigma_{21}^{\text{pert.}} & \sigma_{22}^{\text{pert.}} & \sigma_{23}^{\text{pert.}} & \sigma_{24}^{\text{pert.}} & \sigma_{25}^{\text{pert.}} & \sigma_{26}^{\text{pert.}} \\ \sigma_{23}^{\text{pert.}} & \sigma_{32}^{\text{pert.}} & \sigma_{33}^{\text{pert.}} & \sigma_{34}^{\text{pert.}} & \sigma_{35}^{\text{pert.}} & \sigma_{36}^{\text{pert.}} \\ \sigma_{24}^{\text{pert.}} & \sigma_{42}^{\text{pert.}} & \sigma_{43}^{\text{pert.}} & \sigma_{44}^{\text{pert.}} & \sigma_{45}^{\text{pert.}} & \sigma_{46}^{\text{pert.}} \\ \sigma_{25}^{\text{pert.}} & \sigma_{52}^{\text{pert.}} & \sigma_{53}^{\text{pert.}} & \sigma_{54}^{\text{pert.}} & \sigma_{55}^{\text{pert.}} & \sigma_{56}^{\text{pert.}} \\ \sigma_{26}^{\text{pert.}} & \sigma_{62}^{\text{pert.}} & \sigma_{63}^{\text{pert.}} & \sigma_{64}^{\text{pert.}} & \sigma_{65}^{\text{pert.}} & \sigma_{66}^{\text{pert.}} \end{bmatrix} \quad (4-89)$$

Where the first column belongs to the stress vector cause by the disturbance of the first component of the strain component, the second column is the result of the disturbance of the second component of the strain vector and so on. The entire procedure is illustrated in Figure 4-5.

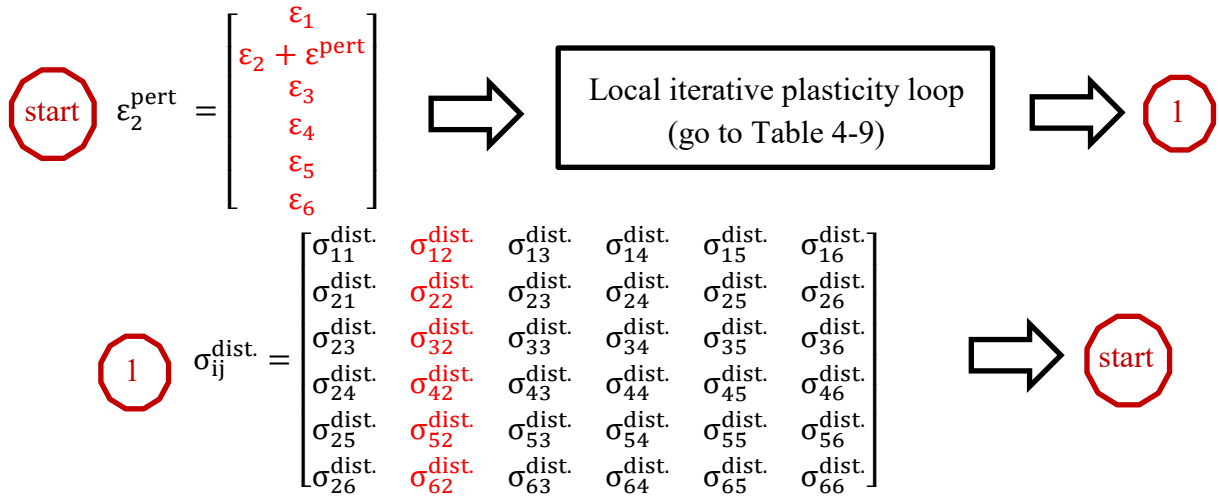


Figure 4-5 The iterative procedure to calculate the disturbed stress components

When the disturbed stress matrix is constructed, then the following formula gives the corresponding Jacobian matrix as follows:

$$\text{DDSDDE}(i, j) = \frac{\sigma_{ij}^{\text{dist.}} - \sigma_i^{\text{undist.}}}{\varepsilon_j^{\text{pert.}}} \quad (4-90)$$

A corresponding developed subroutine based on the perturbation method is given in Appendix.2 with this explanation that the fourth-order tensor  $\mathbb{M}$  which

has to be determined by the equation (4-32), is calculated using the flow potential function which introduced by [105] and can be easily replaced by the introduced  $\mathbf{M}$  in Appendix 1.

Having determined the initial elastic stress vector, where the stress tensor is converted to the Voigt form, and also the Jacobian matrix in the elastic zone, the user-defined subroutine checks if the plasticity, according to the corresponding yield function (equation (4-26)), occurs. If yes, the stress in the plastic state and according to the return backward Euler algorithm (see Table 4-9) can be determined and again the associated elasto-plastic Jacobian is determined. Having determined the stress and the Jacobian matrix the subroutine checks the damage. If the damage happens, even in one of the modes, then the subroutine will bypass the plasticity portion and jump from the elasticity governing constitutive equations to the damage. However, for each of the scenarios, the stress array, and the Jacobian matrix must be determined at the end of the increment and passed back to the ABAQUS implicit solver. Other than stress array and the Jacobian matrix which are mandatory to pass into the ABAQUS implicit solver, there are several variables which are accumulative and must be determined at the end of the current increment to be used at the beginning of the next increment as the old version of the accumulative variables which the provided solution-dependent variables used in the form of the array STATEV(NSTATV). The NSTATV indicated the number of the solution-dependent variables which has to be specified in the input file such as follows:

```
*Material, name=DEFINE THE MATERIAL NAME
*Depvar
  NSTATV,
```

The number of the solution dependent variables defined in the Depvar must be equal or “more than” the STATEVs. It is important to be noted that since the Jacobian matrix is asymmetric, then to define the steps it is necessary to choose asymmetric solver such as follows:

```
*Step, name=..., nlgeom=YES, extrapolation=NO, inc=..., solver=ITERATIVE,
unsymm=YES
```

Otherwise ABAQUS/Standard will use the symmetric part of the Jacobian matrix which calculated by taking one half the sum of the matrix and its transpose [110].

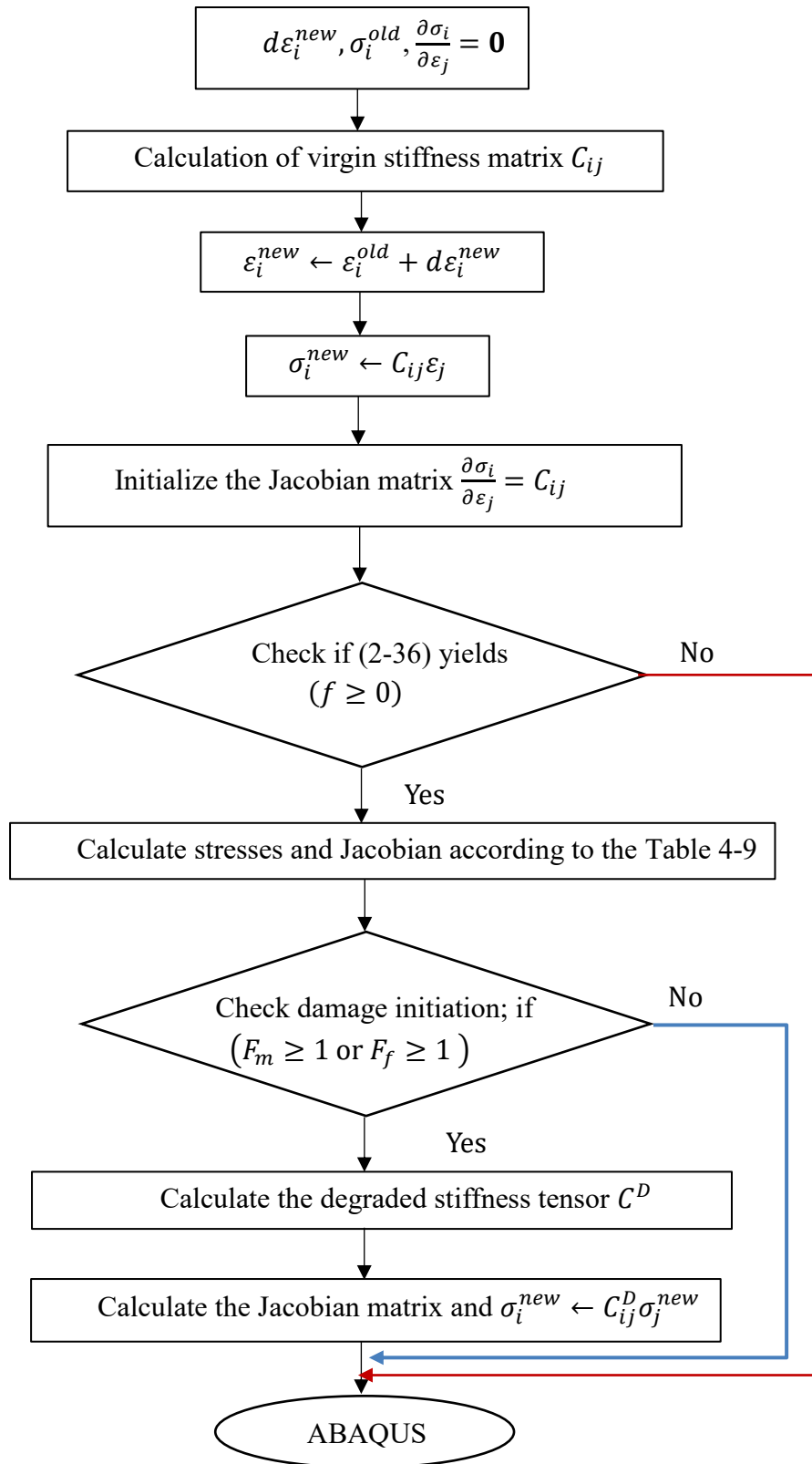


Figure 4-6 implicit user-defined subroutine (UMAT) algorithm

### 4.5.2 Explicit subroutine (VUMAT) for CDM

Hereafter, we introduce the numerical procedure for the Continuum Damage Mechanics (CDM), e.g., elastic-damage, in an explicit fashion. The explicit method for the hybrid component is preferred due to the geometrical complexity of the case study as well as the self-contact issue. The introduced model in section 4.4.1 is coded in both implicit and explicit manners, but the implicit one is just applied on the simple geometries. Here, we do not intend to reiterate the ABAQUS subroutine explanation which is explained earlier in the previous section 4.5.1.3, but instead, we focus on some general differences between UMAT and VUMAT subroutines. The equilibrium equation for the explicit solver is the same as introduced in the equation (4-72) while the mass matrix  $M^{NM}$  is not zero anymore. Contrasted with the unconditional stability of the implicit method, the explicit solver (Forward Euler integration method) has a stability limit as follows:

$$|\Delta \epsilon| < \Delta \epsilon_{\text{stab.}} \quad (4-91)$$

And it implies that the increment of the displacement and the time increment must be controlled [110]. In an explicitly written subroutine the Jacobian matrix is not needed to be updated, and it is the most important advantage of using VUMAT over UMAT (see also sections 4.5.1.1, 4.5.1.2 and 4.5.1.3) and the stress array is the only basic variable which must be updated in the Gaussian level as well as the Solution Dependent Variables (SDVs). The general VUMAT flowchart for the elastic damage model, presented in section 4.4.1.1, is illustrated in Figure 4-7. The strain, strain increment, old stress and old SDVs arrays are given at the beginning of the increment which have to be updated at the Gaussian level and then the updated values are passed in the ABAQUS' explicit solver to be used at the beginning of the next increment as the old values. Since the entire procedure for the subroutine writing is discussed in section 4.5.1.3, then, to avoid repetition, we just mention some specific aspects of writing the VUMAT subroutines. Other than Jacobian matrix issue which is not needed to be defined in VUMAT, there is two major difference between VUMAT and UMAT subroutines:

- In VUMAT the variables must be defined as VAR(nblock, dimension) while they are characterized as VAR(nblock, dimension) which the dimension indicates the size of the variable. If the variable is not an array, e.g., the variable is a scalar, then the dimension must be omitted. The nblock is a variable which is defined according to the

- element type and signifies the number of material points to be processed in the call to VUMAT [110, 113].
- Initial calculations and checks must be accomplished. In the data check phase of the analysis Abaqus/Explicit calls user subroutine VUMAT with a set of fictitious strains and a totalTime and stepTime both equal to 0.0. This is done as a check on the initial elastic constitutive relation and to calculate the equivalent initial material properties, based upon which the initial elastic wave speeds are computed[113]. The way to define the initial calculation is sometimes misunderstood and ,for the clarification, the piece of code of the VUMAT ,which characterizes the initial calculation, is given in Appendix.3.

Since the case study is made of two different material, then it might be helpful if we introduce the way that more than one user-defined material can be implemented in VUMAT or UMAT as mentioned in ABAQUA manual [113] which is presented in Appendix.4. For further details about the writing, VUMAT see ABAQUA manual [113]. However, once the UMAT code is prepared, it can be easily converted to the VUMAT type by considering the points mentioned earlier.

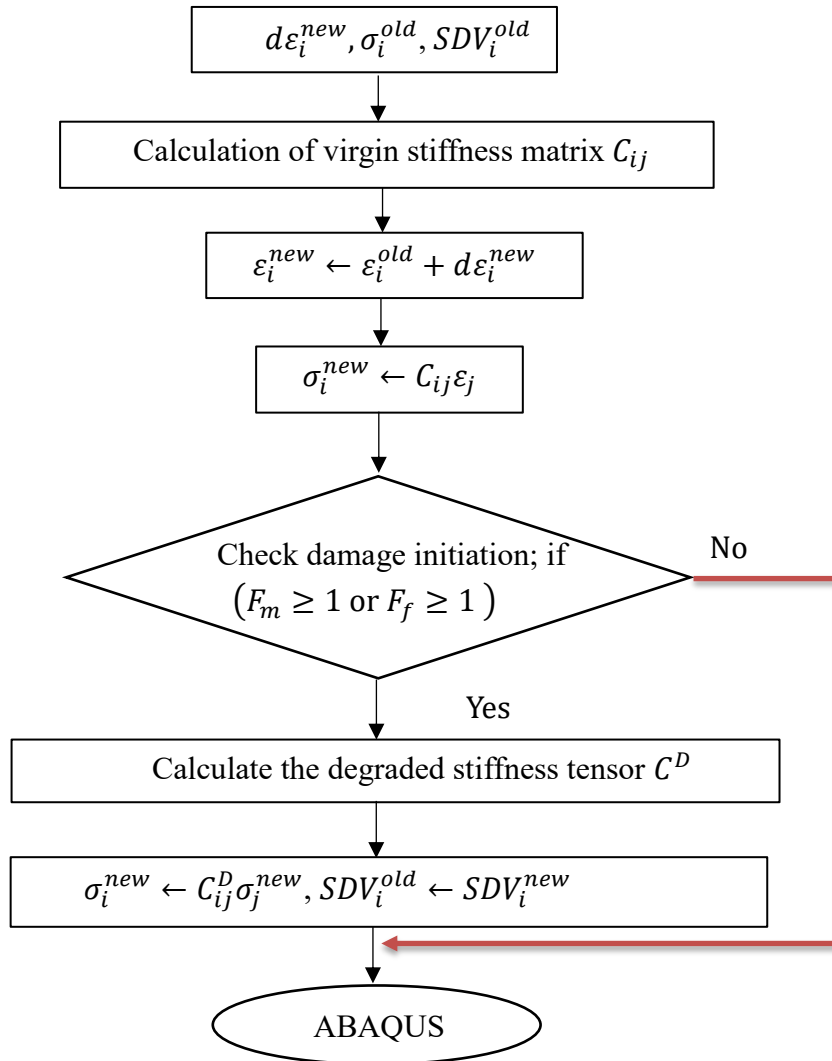


Figure 4-7 Explicit user-defined subroutine (VUMAT ) algorithm

## Chapter 6

# 5 Short fiber reinforced thermoplastics simulation

In this chapter, the numerical simulations of the short fiber reinforced thermoplastics, which have been carried out using the introduced transversely isotropic model in chapter 4, are addressed. This is the model introduced for the nonlinear behavior of the short fiber reinforced thermoplastics, but also here in this section, we deal with the elastic-damage presented in section 4.4.1 as well as elasto-plastic damage model which introduced in section 4.4.1.1. The models are applied on a single element plus with a model with the same size, but with refine meshes. The hybrid component, which was the primary motive of this study, is simulated by both elastic damage and elasto-plastic damage models. In this chapter we will represent the computational and experimental results according to the time sequences, but hierarchically. It means, instead of presenting the results according to their mathematical and physical importance and positions, we prefer to characterize them based on their time of occurrence from the beginning of the project by now. The representation approach might show why and how we began from the linear damage model and, in the end, it is ended up the presentation of the new non-linear plasticity include damage model. Hence, in the first section, we open the discussion with the quasi static 3-points bending and continue the test by changing the loading rate. To simulate the rate dependent behavior of the hybrid component, in the beginning, it was more convenient to apply the rate effect on the material constants, explicitly.

### 5.1 Hybrid component response under 3-point bending test

The hybrid component is made by two different technologies:

- Back injection molding

- Compression molding

The 3-point bending test is carried out in two different sides as illustrated in Figure 5-1 and for the simplicity, we call them case1 and 2 to avoid repetition.

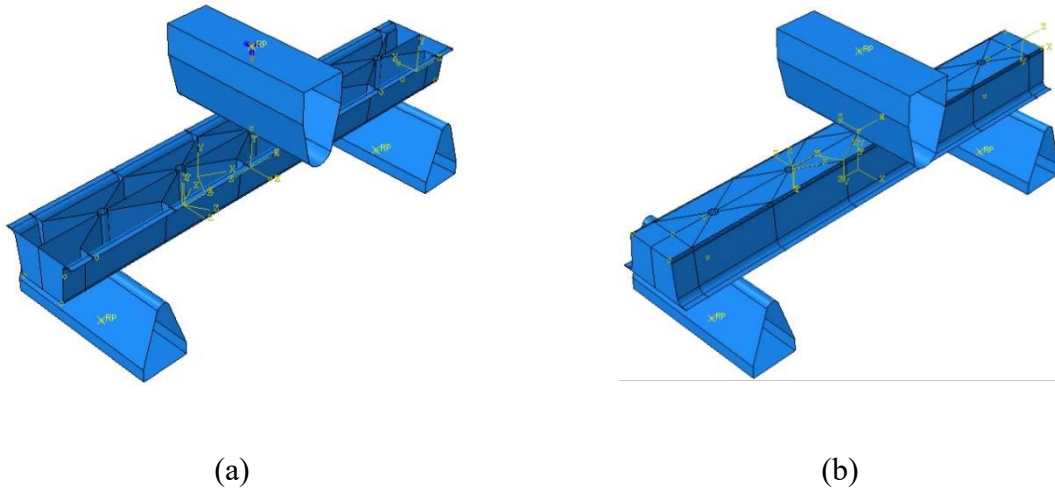


**Figure 5-1 Bending tests; (a) Case1 (b) Case2[6]**

The configuration of the 3-point bending test for the Case1 is illustrated in Figure 5-2 at the beginning and end of the experiment. The span (distance between two supports; e.g.  $\overline{A_1A_2}$ ) is 338 mm, and it is constant during all the tests.



**Figure 5-2 Bending test configuration; (a) test starting point (b) ending point [6]**

The 3-point bending test is conducted for both categories, but since our main interest is about injected molding short fiber reinforced thermoplastics, then we focus on these experiments. However, the results for two differently manufactured hybrid components are illustrated to compare the responses. The experimental results of the bending test for three different components, which is shown by C1,

C2 and C3, are illustrated in Figure 5-3. As expressed in Figure 5-3, the components manufacture by compression molding technique in the ambient temperature and the tests are carried out under quasi-static conditions. The results for the components one and two are most similar, therefore, they will be considered as the representatives of the component with the mentioned features and under loading and boundary conditions in Figure 5-3. The representative results are compared to the representative results of the components manufactured by injection molding process which are illustrated in Figure 5-4.

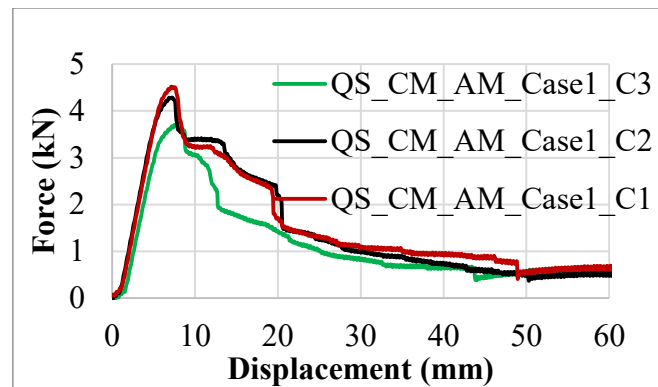


**Figure 5-3 The 3-point bending; component type is Compression Molding (CM); The test is conducted in the ambient temperature (AM); Boundary condition: case1**

According to the Figure 5-4, the representative results can be achieved from the components number 3 or 4 while the second test is out of range and can be omitted.

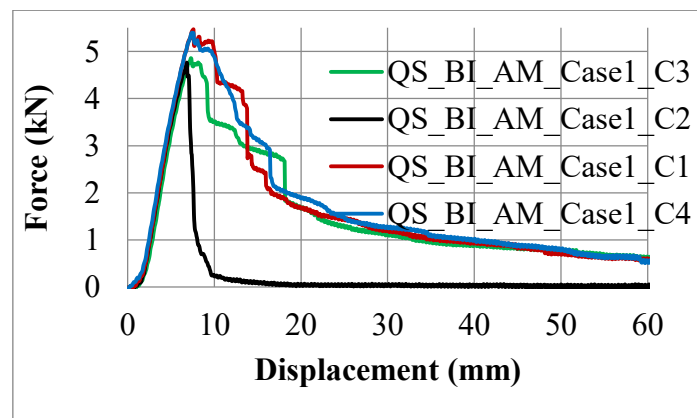


**Figure 5-4 The 3-point bending; component type is Back-Injected (BI); The test is conducted in the ambient temperature (AM); Boundary condition: case1**

The comparison between the results for the bending test for the components manufactured by compression molding and back-injected molding are presented in Figure 5-5.

It has been reported by [114], conducting simple tensile tests on the injected and compression molded samples, that the compression molded samples show higher strength than the injection molded samples. The conducted bending tests in the current research demonstrate the same result (see Figure 5-8) , not for the neat thermoplastics, but for the hybrid component which is reinforced by the short fiber reinforced thermoplastics. This is compatible with the result for Case2 which the internal part plays the more significant role than Case1. For the Case1 the internal part either made by injected or compression molding techniques is mainly under pressure due to the interaction between the outer shell and the internal part while for the Case2 the bending phenomenon might be considered alone; i.e., with minimum interactions between the outer shell and the internal part. However, due to the lack of information about the comparison between compression molded and injected molded specimens under compression and according to the later interpretation for the Cas1 as well as the results of comparison between two cases at Figure 5-5, it can be said that the compression molding made components show higher strength than injected molded ones under compression.

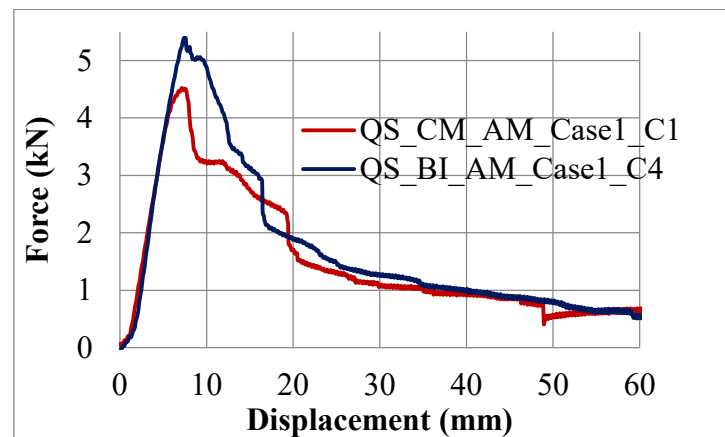


**Figure 5-5 Comparison between the responses of the hybrid components manufactured by the back-injected and compression molding; temperature: Ambient (AM); Case1**

According to the results in Figure 5-5, it might be concluded that the hybrid material manufactured by the compression molding procedure bears higher force than its counterpart (~5.4 kN. vs. ~4.4 kN ). In term of the elastic stiffness, both

products show the same level of the rigidity since the force versus displacement curves have coincided in the elastic zone (see Figure 5-5). Both components illustrate the negligible amount of nonlinearity before the occurrence of the main degradation. Hence it has been decided not to involve the plastic behavior of the material in the numerical solution. The material degradation which happens after the pick points are quasi similar.

Revolving the component about the main longitudinal axis provides the second case. In Figure 5-6 the experimental results of the bending tests for two components manufactured by injection process are illustrated. The tests again are conducted under the same situation for the case1. The elastic zone is quite distinguishable from the damaged area since the damage is not the progressive one and it happens quasi suddenly. Even though, there is a minor damage in both components before the occurrence of the main rupture.

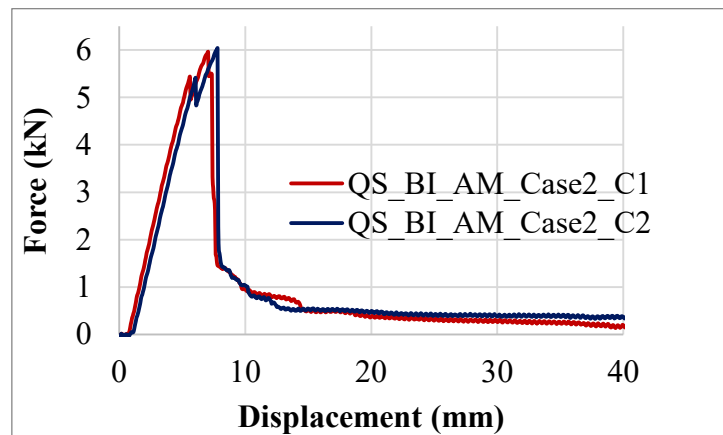


**Figure 5-6 The 3-point bending; component type is Back-Injected (BI); The test is conducted in the ambient temperature (AM); Boundary condition: case2**

The case2 test is also conducted for the material manufacture by the compression molding technology, and the experimental results are displayed in Figure 5-7. The results for three components were acceptable and are given here. In the main elastic zone, e.g., before the main failure, all components show couples of minor damages which result in the reduction of the rigidity. To compare the case2 results of compression molding and back-injected molding components the sample number one is chosen to be the representative of the set.

The comparison between two manufacturing technology, for the second case which is shown in Figure 5-8, reveals that the hybrid component manufactured by

the compression molding reach a higher level of the force and might dissipate more energy than the component manufactured by the back-injection molding. The comparison between two manufacturing technology, for the case2, reveals that the hybrid component manufactured by the compression molding reach the higher level of the force and might dissipate more energy than the component manufactured by the back-injection molding technique.

From the very beginning also it is clear that in this case, the BI component is more rigid than the CM component. The initiation of the crack observed in the CM component by the manifestation of the minor cracks, and since both types possess the same geometry, it might be concluded that the CM made a component is tougher than the BI. However, this conclusion must be proved by conducting the toughness related basic experiments to find the GI and GII. Even after the main failure, e.g., the pick points, the CM made component does not drop suddenly to the zero value and still can resist loading while on the contrary, the BI made component nearly collapses.

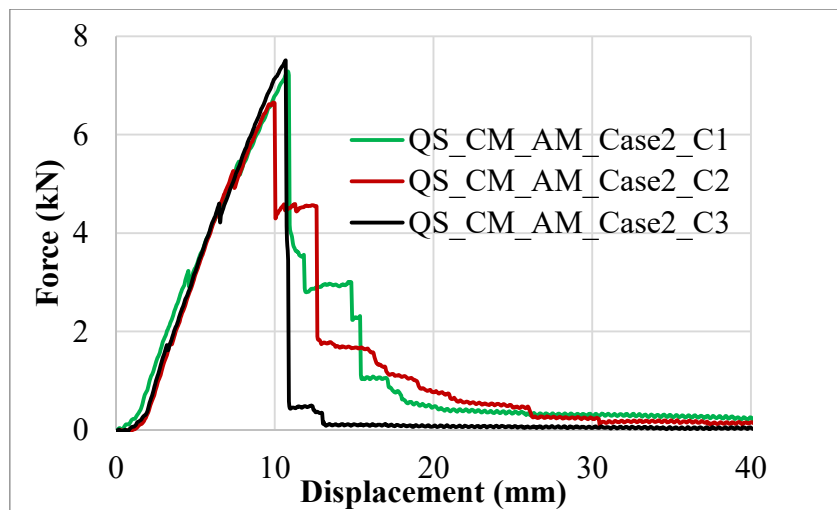


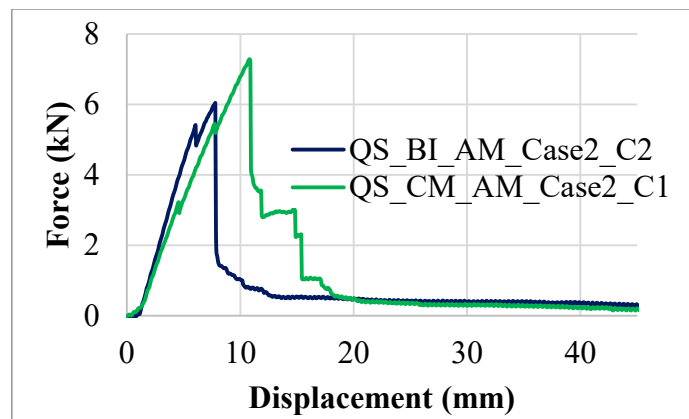
**Figure 5-7 The 3-point bending; component type is Compression Molding (CM); The test is conducted in the ambient temperature (AM); Boundary condition: case2**

According to our observation through the experiments, the collapse in both cases can be referenced to the initiation and progression of the damage in the central column of the internal constituent.

The quasi static 3-point bending tests are conducted at a different temperature than the ambient temperature. They are accomplished by preheating the samples

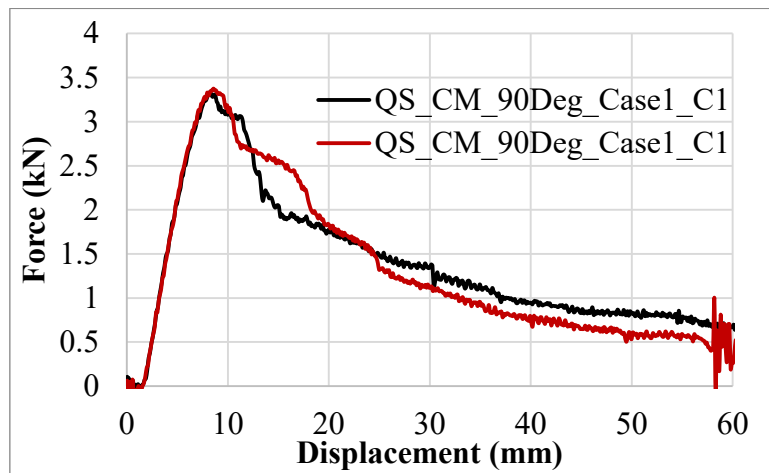
up to 90 degree Celsius then they are loaded such as the previously described experiments. The bending test for the preheated components are only carried out for the Case1.

Figure 5-9 shows the experimental results of the 3-point bending for the hybrid component manufactured by the compression molding procedure and preheated by 90 degree Celsius. In this case, unlike the test at the ambient condition, the components show a lower stiffness before the main failure occurs and the degradation phenomenon is quite gradual.



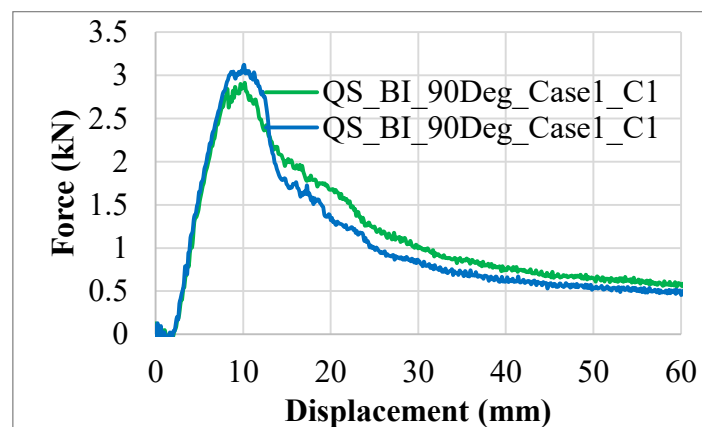
**Figure 5-8 Comparison between the responses of the hybrid components manufactured by the back-injected and compression molding; temperature: Ambient(AM); Case2**

Figure 5-10 demonstrates the conducted bending test on the hybrid components manufactured by the back-injection method while the boundary conditions are Case2 and the components are preheated by 90 degree Celsius. In fact, more than two components have been tested, but for a couple of reasons, e.g., the technical problems, most of them were out of reasonable ranges and had been omitted. Also, the nonlinearity degree before the failure point is not negligible and the degradation occurs quite gradually.



**Figure 5-9** The 3-point bending; component type is Compression Molding (CM); The test is conducted on the component preheated by 90 Degree Celsius (90Deg); Boundary condition: case1

In Figure 5-11 the comparison between the experimental results of quasi-static bending tests for the components made of the back-injection method and the compression molding technique, which both are preheated by 90 degree Celsius, are represented. As it can be seen, clearly, the CM made component shows higher resistance than the BI made one to the bending loading. This resistance includes



**Figure 5-10** The 3-point bending; component type is Back-Injected (BI); The test is conducted on the component preheated by 90 Degree Celsius (90Deg); Boundary condition: case1

having higher force pick point and the area under the force-displacement curve which demonstrates the amount of work has to be done to, in this case, bend the component until it completely collapses.

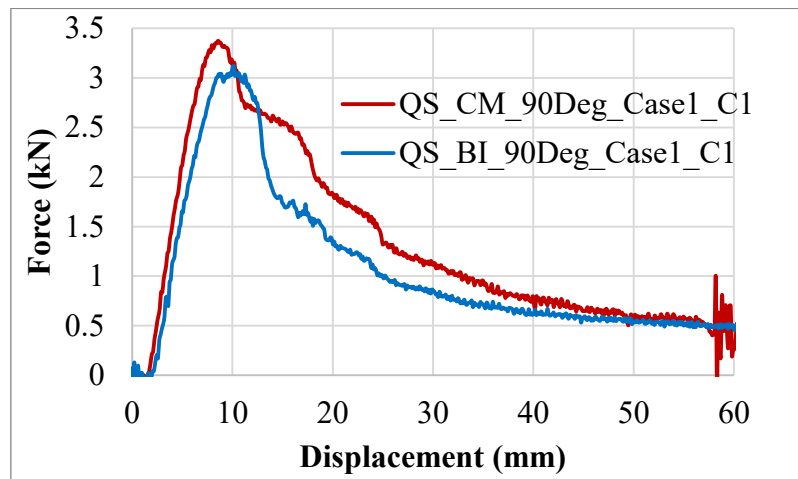


**Figure 5-11 Comparison between the responses of the hybrid components manufactured by the Back-Injected (BI) and Compression Molding (CM); temperature: 90 Degree Celsius (90Deg); Case1**

Unlike, the quasi-static bending tests performed for the Case1 at the ambient condition, see Figure 5-5, here the preheated components made of two different techniques show different stiffness (see Figure 5-11).

Here, various comparisons are presented between different quasi-static bending experimental results such as the bending results between Case1 and Case2 for BI manufactured components in Figure 5-13, and the CM made components in Figure 5-12. According to Figure 5-12, the stiffness differences are negligible between Case2 and Case1, as well as higher pick force ( $\sim 7\text{kN}$ ) versus ( $\sim 4\text{kN}$ ). Case2 In the real applications, we probably face the second case (Case2), since the exterior part of the components face the impacts or any kinds of loading. It might be claimed that the Case2 is a better choice than Case1 in terms of the higher stiffness, greater force tolerance and the bigger area under the force-displacement curve.

In contrast to the CM manufactured samples, the BI produced components show less difference of the force pick points between Case1 and 2 while their major differences appear after the main failure. In this case, on the contrary of Case2 which collapse after reaching the maximum force point, Case1 shows great resistance against damage and the damage is progressive.

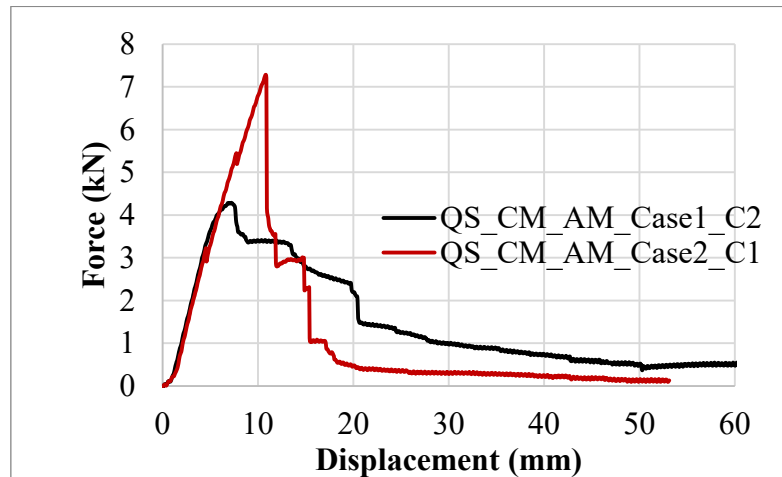


**Figure 5-12 Comparison between the responses of the hybrid components manufactured by the Compression Molding (CM); temperature: Ambient (AM); Case1& 2**

It seems for both manufacturing process the designer should not rely on the energy dissipation capacity of the hybrid components, unless the opposite side of the component; e.g., the open side, is reinforced by adding a piece of sheet. This might leads to having advantages of both cases.

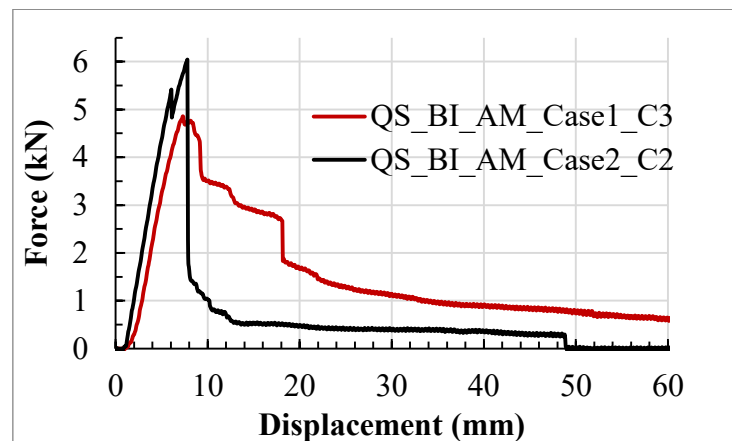


**Figure 5-13 Comparison between the responses of the hybrid components manufactured by the Back-Injected (BI); temperature: Ambient (AM); Case1& 2**

## 5.2 Simulation of the back-injected manufactured hybrid component under quasi-static bending at ambient conditions

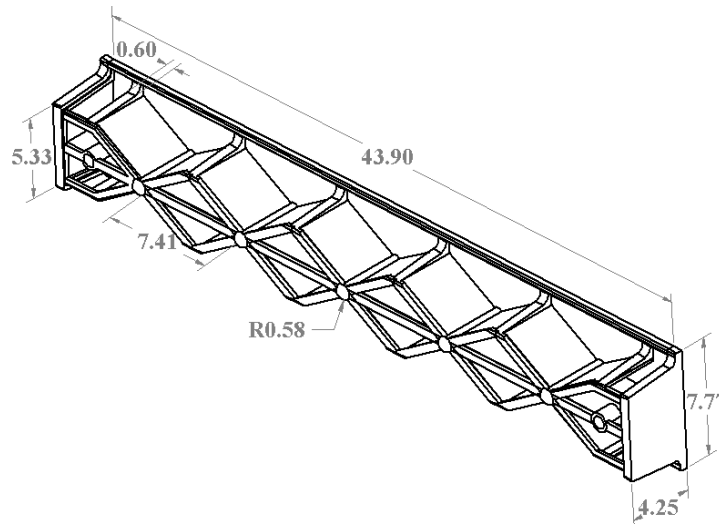
Here, We do not intend to simulate the compression molding manufactured components and the numerical simulation is concentrated on the quasi-static bending of the hybrid component manufactured by the injection over molded sheet. The simulation of the hybrid component is performed in the explicit fashion as described in section 4.5.2 considering the CDM model as discussed in section 4.4.1.1. the materials properties are given in Table 5-1 for the short fiber reinforced internal part and the outer shell.

Table 5-1 material properties of molded and injected constituents of the hybrid component; all modules of elasticity presented in GPa and strengths in MPa[6]

Property	$E_{11}$	$E_{22}$	$G_{12}$	$G_{23}$	$\nu_{12}$	$\nu_{23}$	$X_T$	$X_C$	$Y_T$	$Y_C$	$S_{12}$
Short fiber	8.5	6	2.1	2.3	0.29	0.3	125	200	125	200	50
Plane weave fabric	24.3	25.2	1.3	1.2	0.25	0.3	370	280	430	280	58

An isometric view of the hybrid component, without the outer shell and the details, is given in Figure 5-14. For the internal reinforcing part, it has been supposed that the material properties related to injected and compressed components have same values. The thickness assigned to the fabric shell is 1 mm while for the internal constituent varies from 2.2 to 5.4 mm at the route [6]. To perform the simulation at any stage; e.g., elastic, plastic or damage, the determination of the structural tensor and the material symmetries play significant roles.

We try to make the dedicated material symmetries and the structural tensor, for any type of the simulations, clear by assigning them some specific colors. Of course, due to the lack of knowledge about the exact distributions of the fibers in each point, this process cannot be accomplished without some sorts of the simplifications, but the care must be taken to not violate the basic principles of the structural tensors (see sections 2.1.1 and 1.3.2).



**Figure 5-14 Isometric view of the injected part of the hybrid component. The dimensions are in centimeters.**

According to Figure 1-6 and Figure 1-7, the preferred direction  $a$  which is introduced in section 2.5.2 for the injection gates, which are indicated by red color in Figure 5-15, as well as the segments are shown by the gray color might be  $a = [1,0,0]$ . For the ribs either in blue or green, the preferred direction can be defined as  $a = [0.5,0.5,0]$ .

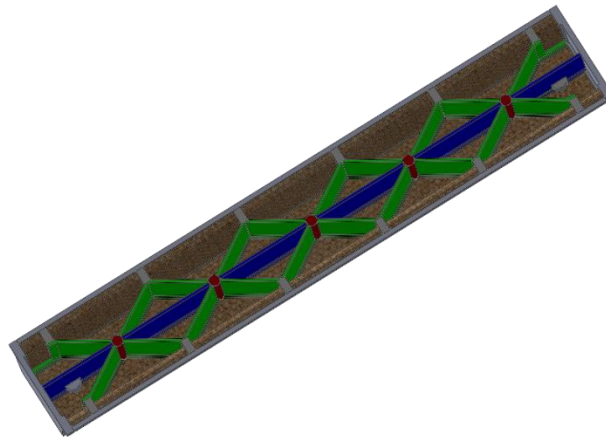


**Figure 5-15 The distinguished parts of the internal part in terms of the fiber distribution and determination of the structural tensors**

The numerical result for the case under quasi static bending is compared to the experimental results in Figure 5-16. Many simplifications have been applied,

such as ignoring the nonlinear response of the material, assigning bulk material symmetries according to the observations and not based on a flow simulation.

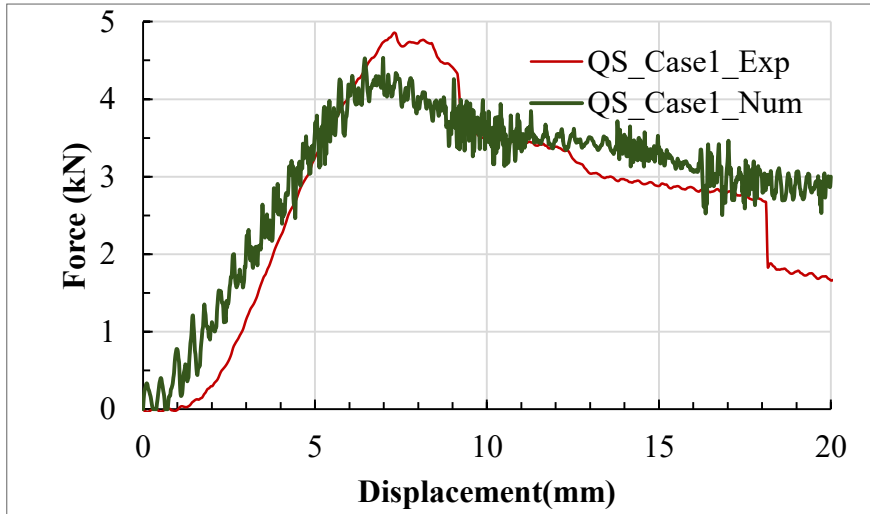


**Figure 5-16** Quasi static bending experimental and numerical results for Case1 and back-injection technology [6]

Considering the mentioned simplifications as well as the complex geometry of the case study and also the probability of the effect of the manufacturing process, including heating and cooling process, on the constituents properties, the numerical result shows a quite good agreement with the experimental one.

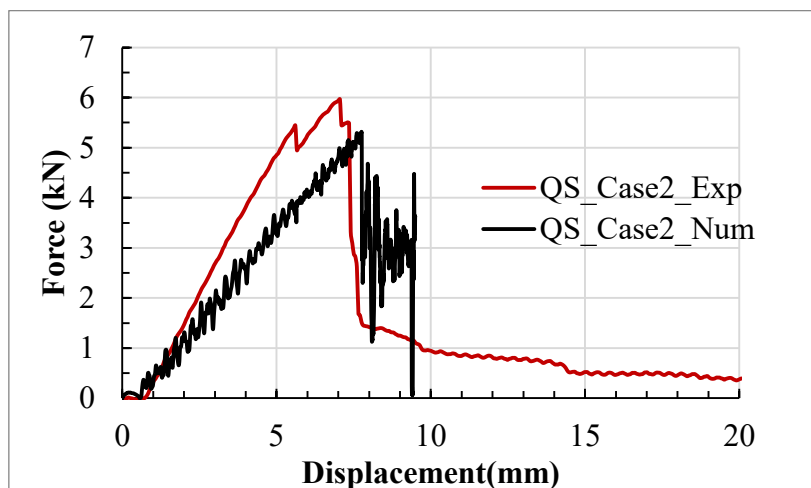


**Figure 5-17** Quasi static bending experimental and numerical results for Case2 and back-injection technology [6]

The numerical calculation has been for the Case2 as well, and the result is illustrated in Figure 5-17. The numerical calculation does not predict the total stiffness of the Case2, precisely, but in terms of the maximum deflection and the maximum force before the collapse, it provides acceptable results.

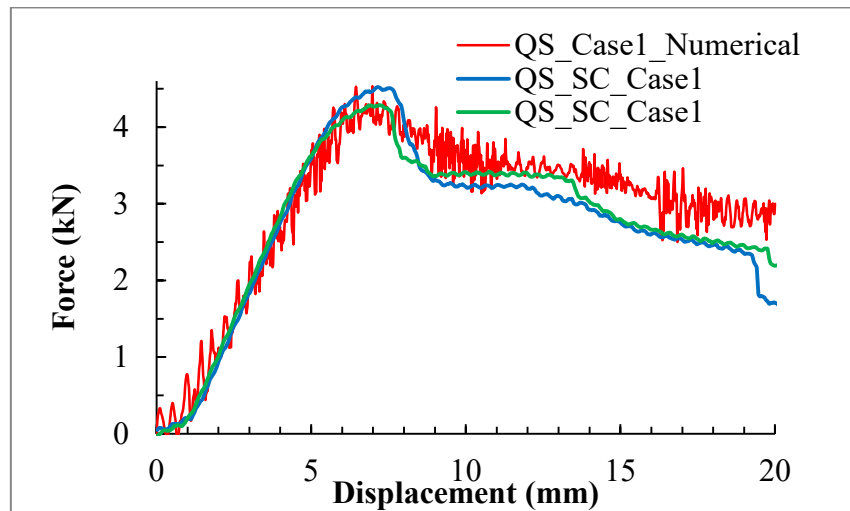


**Figure 5-18 Quasi static bending experimental and numerical results for Case1 with compression molding technology**

Comparing the numerical results obtained for the Case1 under quasi-static loading with the experimental results of the CM made a component in Figure 5-18 shows a good agreement between them. But it should be noted that the simulation is performed using the short fiber reinforced material constants, though, to have

### **5.3 Rate-dependent simulation of the back-injected manufactured hybrid**

This section is dedicated to the simulation of the hybrid component under bending test with the same conditions as explained in section 5.1 by changing the puncher's rate to 127 mm/sec. Even though the loading rate is not dramatically changed from the quasi-static one, but according to the experimental results, the response is changed, dramatically. The effect of a change in loading rate on the Case1 is illustrated in Figure 5-19 so that the force pick point is moved about one kN up. Accordingly, the damage mechanisms illustrate some changes, comparing to the quasi-static loading.

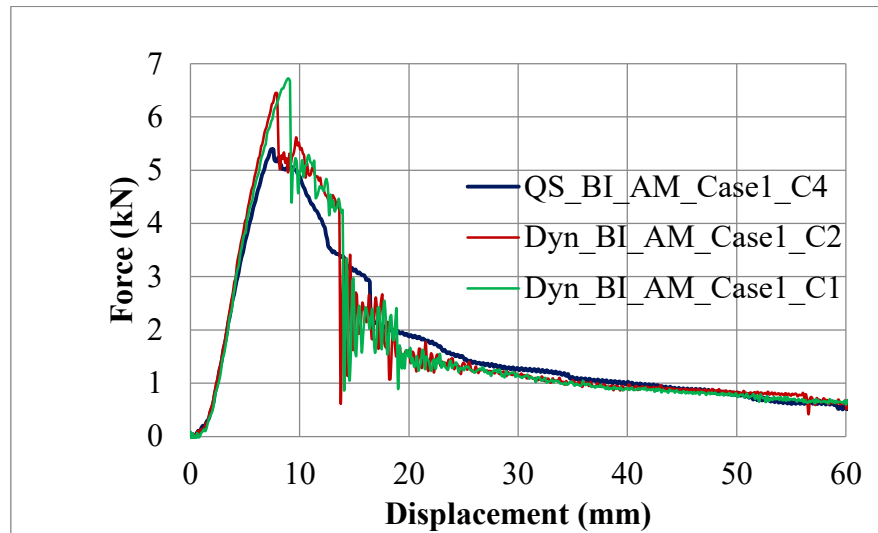


**Figure 5-19** The comparison between the Back-Injected component under loading condition Case1 at the ambient conditions subjected to the quasi-static and 127 mm/sec loading

On the contrary, as it is shown in Figure 5-20, the CM made component show less sensitivity to this rate of loading, and it remains quasi unchanged comparing to the quasi-static loading condition. In this case, the pick force is the same as a quasi-static condition while a small change can be observed in the response of the component in the degraded zone.

The simulation of the rate-dependency is accomplished based on the visco-elastic model is introduced in section 4.3 as well as the CDM damage model presented in section 4.4.1.1.

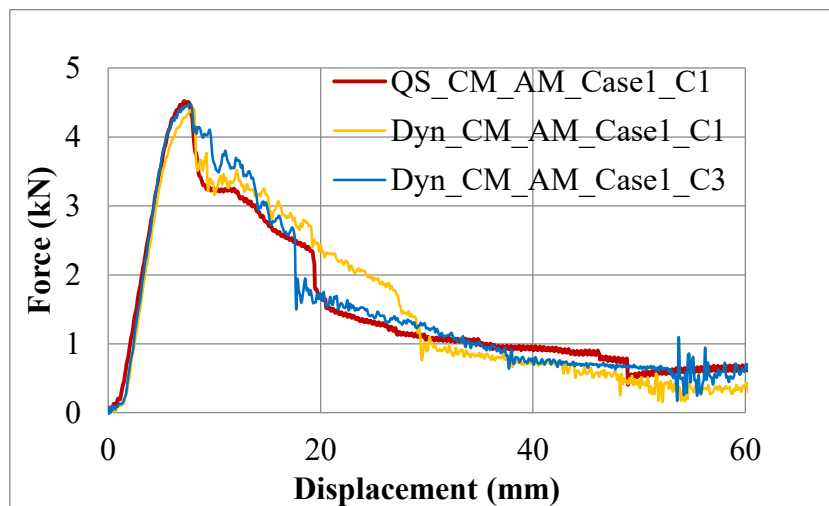


**Figure 5-20** The comparison between the Compression Molding (CM) made component under loading condition Case1 at the ambient conditions subjected to the quasi-static and 127 mm/sec loading

The numerical and experimental result for the BI made component under 3-point bending test with the 127 mm/sec velocity are presented in Figure 5-21.

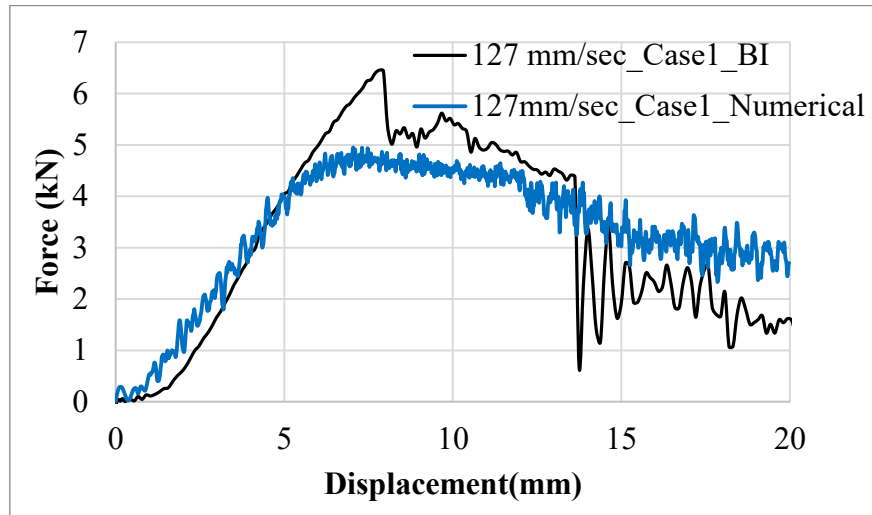


**Figure 5-21** The comparison between the numerical and experimental results for the BI made component under 3-point bending test with 127 mm/sec puncher velocity [6].

The rate-dependent model reaches to  $\sim 5$  kN while the experimental results show higher pick point ( $\sim 6.3$  kN) while for the degradation process the numerical and experimental results show more agreement. Since in this research we focus on the quasi-static cases and mostly on the nonlinear elasto-plasticity behavior of the short fiber reinforced thermoplastics in detail, then we do not intend to discuss more visco-plasticity or visco-elasticity concepts.

## 5.4 Elasto-plasticity results

In this section, the numerical results of the model for the elasto-plasticity damage which is mathematically presented in sections 4.2 and numerically in 4.5 are illustrated. Firstly, the model is applied to one 3D element using the implicit solver by incorporating the so-called UMAT subroutine which is given in 8.1.1. Then the model is applied to the fine elements, but the results do not show considerable differences with those obtained for the one element. We are also interested in the effect of the fiber distribution function, e.g., the structural tensor

which discussed in sections 2.1.1, on the stiffness matrix components (see the equations (2-56) and (2-66)). The numerical results for longitudinal tension with a different distribution of the fibers are presented. The element type is C3D8R, and the primary assumption for the preferred direction of the fibers is  $a = [1,0,0]$ . According to the equations (2-56) and (2-66) for the stiffness matrix, the variations of some of the stiffness matrix component are illustrated in . As it can be seen in Figure 5-22,  $C_{11}$  earns its maximum value when 100% of the fibers are aligned with the preferred direction 1, but its variation with respect to the fibers distribution is not linear. In other words, when the percentage of the aligned fibers in the direction 1 drops from 100 to 90, the value of  $C_{11}$  decreases about 22 percent. Since this variation are nonlinear and the major governing component of the stress in the direction 1 is  $C_{11}$ , then a minor change in the fiber distribution can affect the material behavior dramatically.  $C_{22}$  which governs the second principal stress component exhibits the same behavior in an opposite direction which is a small change in the direction of the fiber direction can affect the stiffness component value, drastically. On the other hand, for example, the component  $C_{44}$  which manages the in-plane shear response of the material is much more insensitive than those govern the principal component of the stress tensor. It might be interpreted the the effect of the shear governing component of the stiffness matrix is rather constant respect to the distribution of the fibers.

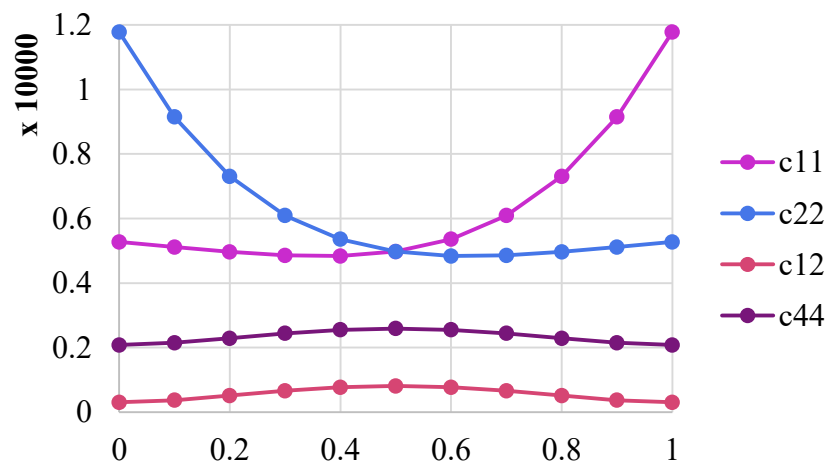


**Figure 5-22 the variation of the stiffness matrix components with respect to the fiber distribution function**

Having discussed the effect of the distribution function on the main component of the stiffness matrix, now we prefer to expand its effects on the basic

parameters of the introduced elasto-plasticity model in chapter 3. The core element of the elasto-plasticity model is the yield function which is introduced into the equation (3-14). The yield function itself includes two main arguments:

- Invariants ( $I_i$ )
- Hardening parameters ( $\alpha_i$ )

According to the invariants set ( see equation (3-13) ), all four invariants are related to stress tensors as well as the structural tensor A and their behaviors under different structural tensor might be predicted mathematically. But, the objective is to validate the segment of the subroutine UMAT (see Appendix1) which calculates the invariants. Comparing the expected mathematical results for the set of the invariants ,considering equation (3-13), to the numerical results presented in Figure 5-23 for the first invariant, Figure 5-24 for the second invariant, Figure 5-25 for the third invariant and Figure 5-26 for the last one, might prove the validity of the given subroutine in Appendix1 for the calculation of the invariants. The first invariant under longitudinal tension, i.e., first loading condition at Table 3-1, behaves exactly as expected from equation (3-13) which indicates no effect of the structural tensor having the following form:

$$A = \begin{bmatrix} 0 & 0 & 0 \\ 0 & 1 & 0 \\ 0 & 0 & 0 \end{bmatrix} \quad (5-1)$$

Which the first invariant under the first loading conditions becomes:

$$I_1 = \frac{1}{2} \sigma_{11}^2 \quad (5-2)$$

The result for that is shown by the black dashed line in Figure 5-23 which is completely compatible with the equation (5-2). Another simple check point might be introduced by the following structural tensor

$$A = \begin{bmatrix} 1 & 0 & 0 \\ 0 & 0 & 0 \\ 0 & 0 & 0 \end{bmatrix} \quad (5-3)$$

Which gives the first invariant as

$$I_1 = -\frac{1}{2} \sigma_{11}^2 \quad (5-4)$$

Where the result for this specific conditions, which is shown in Figure 5-23, is well-matched with equation (5-4).

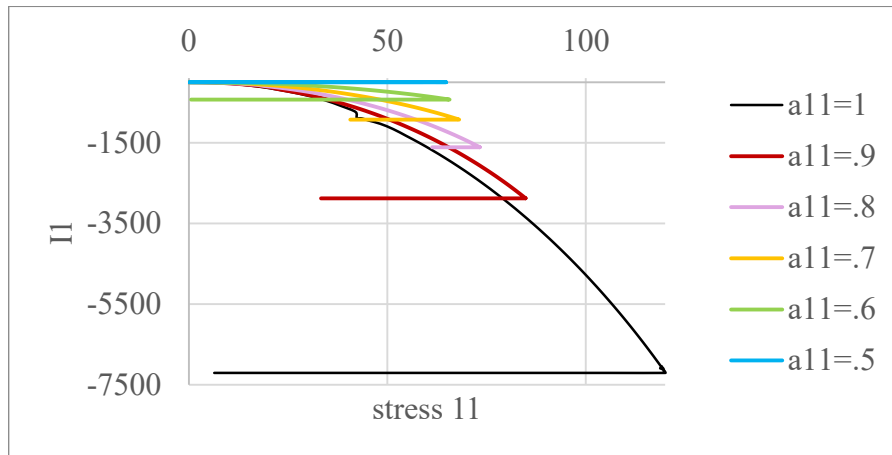


**Figure 5-23 variations of the invariant  $I_1$  versus  $\sigma_{11}$  under longitudinal tension**

Such examination, as it is accomplished before for the first invariant, is performed for the second one. Considering the structural tensor as introduced in equation (5-1) the second invariant obtain zero values which are fitted with the result in Figure 5-24. Inserting the introduced structural tensor in equation (5-3) into equation (3-13) gives:

$$I_2 = \sigma_{11}^2 \quad (5-5)$$

Which is completely fit with the numerical result. The result for both first and second invariant under a longitudinal simple tensile condition with any type of the structural tensor must be the quadratic type, and the numerical result shows the same fashion as they are shown in Figure 5-23 and Figure 5-24.

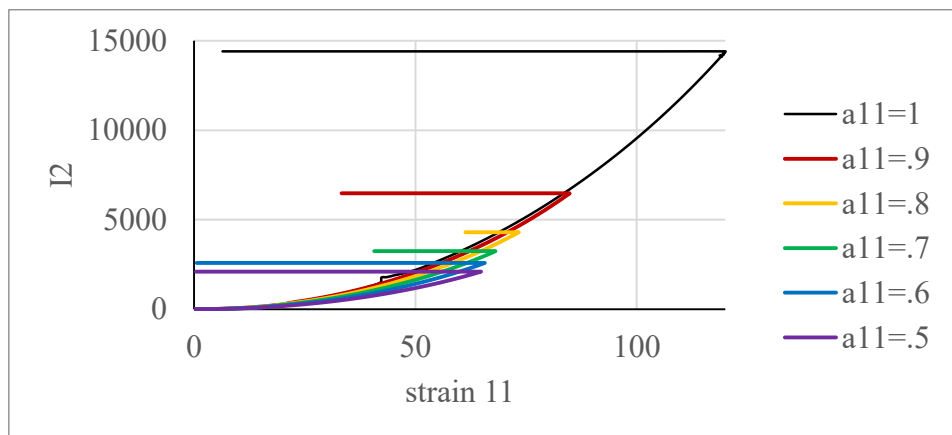


**Figure 5-24 variations of the invariant  $I_2$  versus  $\sigma_{11}$  under longitudinal tension**

According to equation (3-13), the third and fourth invariants are linear in combination with any structural tensor which can be proved by the numerical results in Figure 5-25 and Figure 5-26. According to the Table 3-4, the hardening parameters of the introduced yield function are rather complicated, thus, to avoid the corresponding computational errors, the respective subroutines within the UMAT or VUMAT must be checked, individually. Since two hardening parameters  $\alpha_1$  and  $\alpha_2$  are similar, then to avoid reiteration only one of the respective results is represented in Figure 5-27 which indicates two points:

- The numerical outcomes are as expected from the from the corresponding formula at Table 3-4 including the trends, which is more obvious, as well as point by point random check of the curves.
- The hardening parameter does not change dramatically with respect to the fiber distribution function and becomes less sensitive to the fiber distribution when their alignment with the tensile direction approach to 80 percent.

According to the relevant formula from Table 3-4, the hardening parameter  $\alpha_3$  must demonstrate the same trend as the hardening parameter  $\alpha_1$  which is displayed in Figure 5-28. The same approach has been considered to check the validity of the numerical results as for the hardening parameter  $\alpha_1$ .

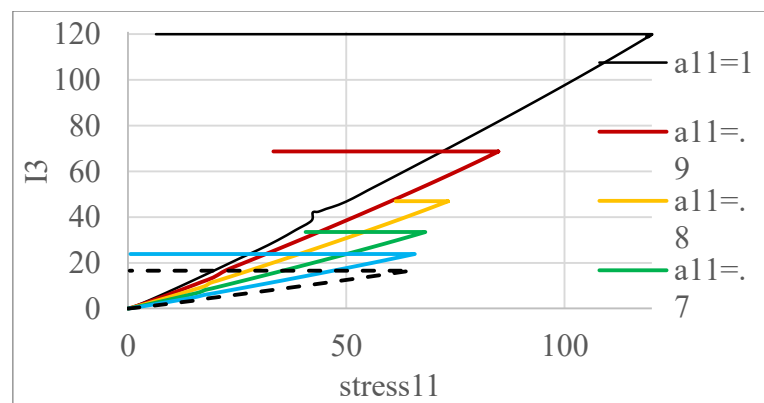


**Figure 5-25 variations of the invariant  $I_3$  versus  $\sigma_{11}$  under longitudinal tension**

It has to be taken into account that only the results indicate the nonlinear plasticity behavior of the material are relevant to the context while those results which belong to the linear elasticity and the damaged segments must be skipped since they are irrelevant.

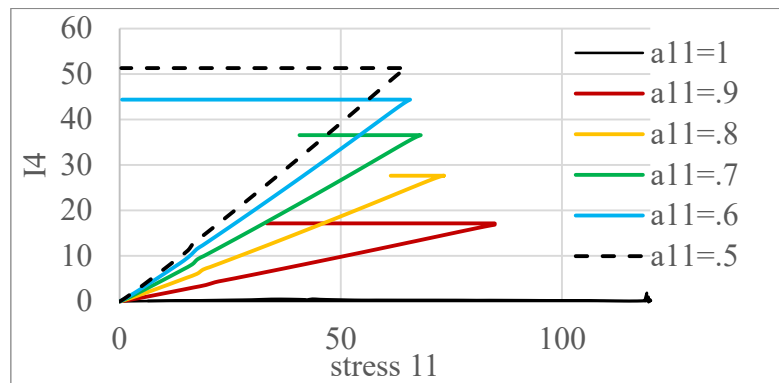


**Figure 5-26 variations of the invariant  $I_4$  versus  $\sigma_{11}$  under longitudinal tension**

Since there is a distinct relationship between  $\alpha_3$  and  $\alpha_{32}$  as well as the direct relation between  $\alpha_4$  and  $\alpha_{42}$ , therefore, to avoid irritation, only one of each pair is investigated. The variations of the hardening parameter  $\alpha_4$  versus  $\sigma_1$  are presented in Figure 5-29 under different distributions of the fibers vary from 100% alignment with the preferred direction a to 50%. Again, the dramatic changes are no observed in the range from 80% alignment of the fibers in the preferred direction a to 50% alignment.

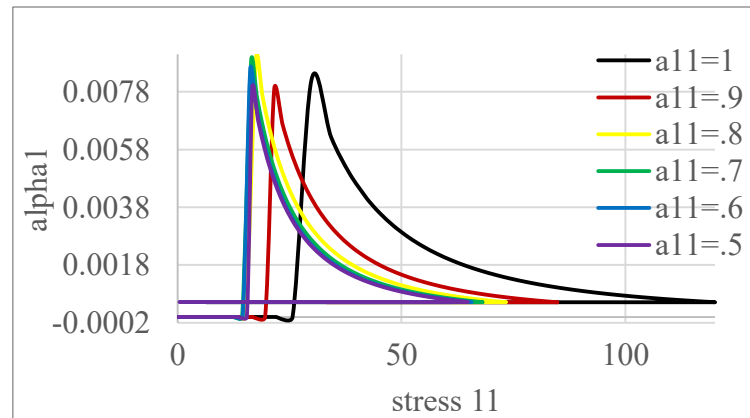


**Figure 5-27 hardening parameter  $\alpha_1$  vs  $\sigma_1$**

Having verified the core elements of the yield function, now we may turn to the entire model verification under different loading conditions. To verify the model which is numerically introduced in section 4.5.1 as well as the elastoplastic damage introduced in section 4.4.1.1, we begin with one 3-D element under different loading and different fiber distribution functions.

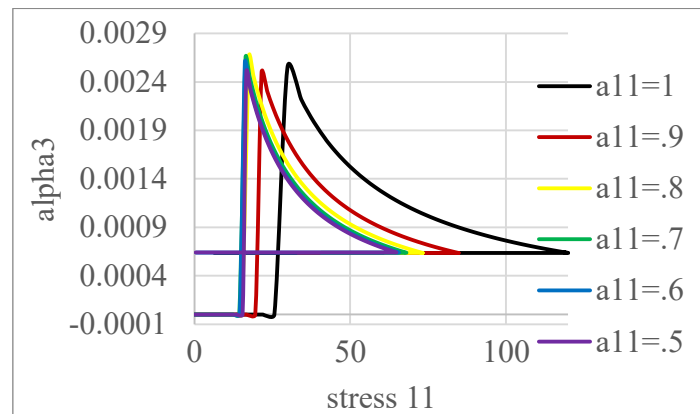


**Figure 5-28 hardening parameter  $\alpha_3$  vs  $\sigma_1$**

The element type is C3D8R, and the primary assumption for the preferred direction of the fibers is  $a=[1,0,0]$ . The experimental data are available just for the state that the entire fibers are aligned with the preferred direction. Thus the other numerical results for the different distribution of the fibers must be considered as the prediction of the model. Considering the major effect of the fibers distribution on  $C_{11}$  which is the dominant component of the stiffness matrix in the tensile loading of first direction (see Figure 5-22), of course when the major portion of the fibers are still inclined toward on the first direction, then, the minor change of the fiber distribution( from 100% to 90% ) cause a considerable change in the material response to the tensile loading.

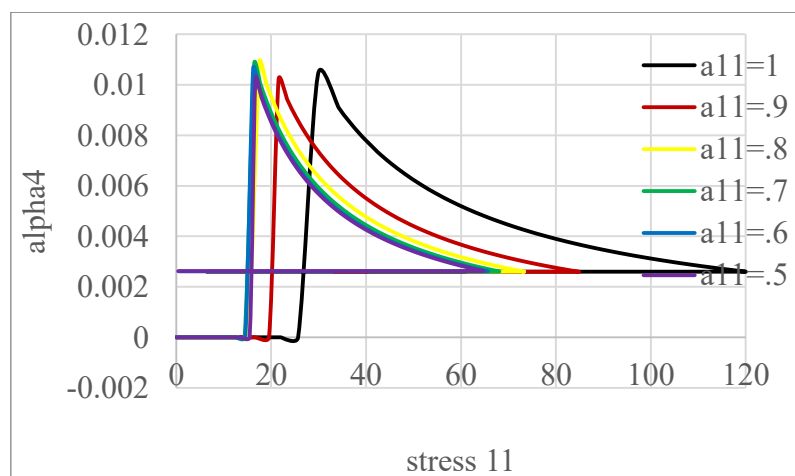


**Figure 5-29 hardening parameter  $\alpha_4$  vs  $\sigma_1$**

Since the possibility of misalignment of the fibers is extremely high, even under fully controlled laboratorial conditions, the design might be more reliable if the designer considers a minimum (here 10%) of misalignment for the material. The experimental data for the short fiber reinforced thermoplastic PA6GF60 which are used to validate the presented elasto-plasticity model are obtained from reference [1]. The results of an element under tensile in the longitudinal direction with a different distribution of the fibers for PA6GF60 are presented in Figure 5-30. The legend LT demonstrates the experimental results and the others show the simulation results which are performed under the same loading conditions but considering different structural tensor. Since the experimental results are just available for the specific case that 100% of the fibers are aligned with the tensile direction, then the other numerical results remain in the prediction level and cannot be validated. According to Figure 5-30, the saturation stress for the case with  $a_{11} = 1$  and  $a_{ij} = 0, ij \neq 11$  is about 120(Mpa) while by decreasing the value of  $a_{11}$ , the corresponding saturation stresses drop until  $a_{11}$  reaches the value of 0.5. Then a reverse trend begins so that by decreasing the value of  $a_{11}$ , the saturation stress grows, but always remain under the result of the case with  $a_{11} = 0.9$ . As it is in the graph, there is no available result for the response of the material after reaching the saturation point, and the numerical results for the damage are presented to show the functionality of the user-written subroutine in the damaged area.

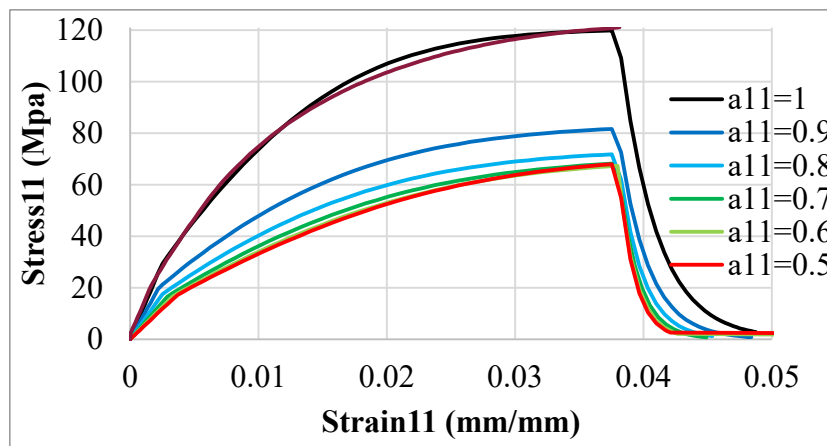


**Figure 5-30 one element analysis ( $\sigma_1$  vs  $\epsilon_1$ ) of a short fiber reinforced thermoplastic under loading condition 1 (see Table 3-1) with different fiber distribution ( $a_{11}$ )**

The numerical along with the experimental results for the compression in the longitudinal direction are illustrated in Figure 5-31. The saturation stress for the structural tensor with the components  $a_{11} = 1$  and  $a_{ij} = 0, ij \neq 11$  is rather higher than the tension with the same situation (see Figure 5-30). The variation of the  $a_{11}$  from 0.8 to zero affects the response of the PA6GF60 very slightly. Therefore, the mean value of 80 Mpa can be considered as a proper value for the maximum strength of PA6GF60 under compression.

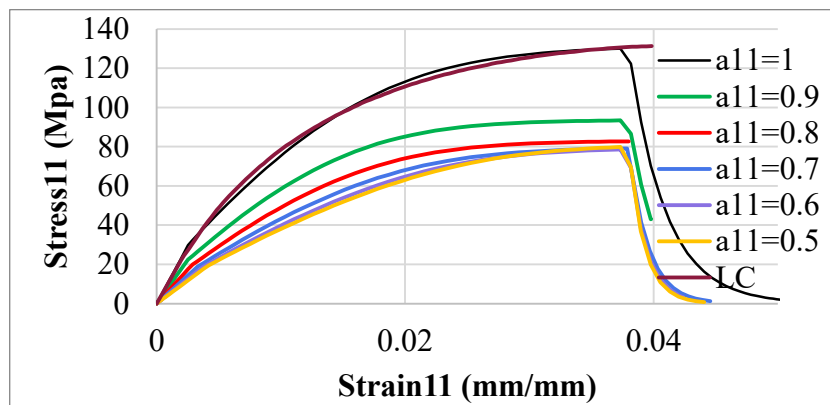


**Figure 5-31 one element analysis ( $\sigma_1$  vs  $\epsilon_1$ ) of a short fiber reinforced thermoplastic under loading condition 1 (see Table 3-1) with different fiber distribution ( $a_{11}$ )**

For the tension and compression loadings in the transverse direction the result is illustrated in Figure 5-32. Since the effect of the fiber orientation function have been already described and illustrated for the longitudinal tension and compression, we skip this discussion for the transverse direction. The experimental results for PA6GF60 under tension and compression are conducted by [115] and also reported by [1]. The tensile and compression tests are conducted based on ASTM D3039 and ASTM D695–10, respectively.

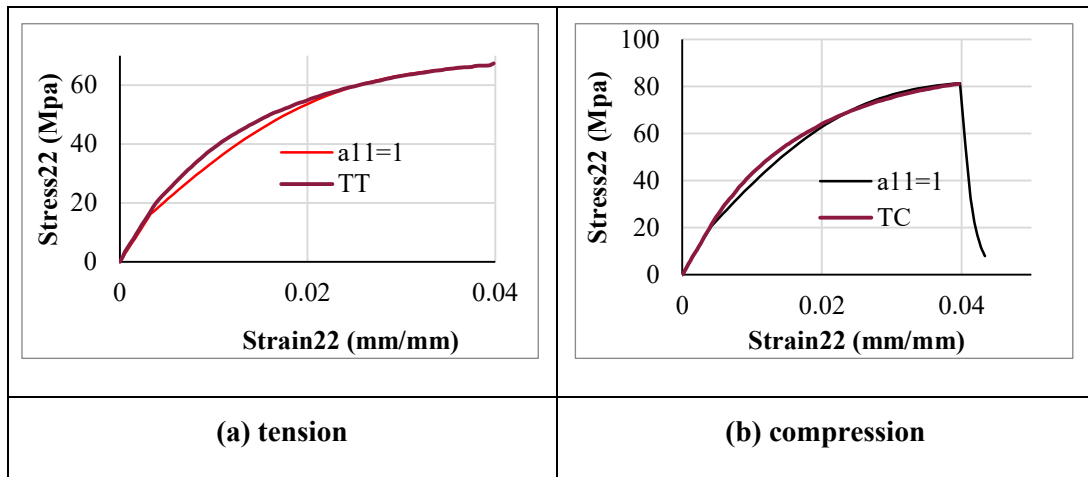


**Figure 5-32 one element analysis ( $\sigma_2$  vs  $\epsilon_2$ ) of a short fiber reinforced thermoplastic under loading condition 1 (see Table 3-1) with different fiber distribution ( $a_{11}$ )**

The associated tensile and compressive test geometries are available in Figure 5-34. To virtualize the tests by applying the introduced model in chapter 4, we have to define an appropriate structural tensor as well as the hardening curves. The hardening curves can be extracted from stress versus strain basic curves, i.e., the curves from Figure 5-30 to Figure 5-32, by skipping the elastic segments. The structural tensor is introduced by [115] by taking the specimens cross section into consideration and accomplishing CT scan of the PA6GF60 mold flow plate. According to [1] and as it can be observed from the sample's cross section in Figure 5-33, the typical fiber orientation distribution of the short fiber thermoplastic injected plate is divided into three layers including two skin layers and the core. According to [72], in the outer layers, nearly 80% of the fibers are inclined toward the flow direction while in the core layer the 20% of the fibers are aligned with the flow direction. Considering the CT scan results from the samples cross section which is shown in Figure 5-33, it seems the fibers orientation distribution in different layers are compatible with the statement of the reference [72]. Therefore, to virtualize both tension and compression tests the structural tensor can be considered such as follows for the skin layer:

$$A = \begin{bmatrix} 0.8 & 0 & 0 \\ 0 & 0.2 & 0 \\ 0 & 0 & 0 \end{bmatrix} \quad (5-6)$$

While for the core layer the nonzero values must be exchanged. As it can be seen in right side table in Figure 5-33, the component  $a_{12}$  is small enough

,comparing to  $a_{11}$  and  $a_{22}$  , to be neglected. Having defines the specimens' geometries, now we may introduce the model used in ABAQUS.

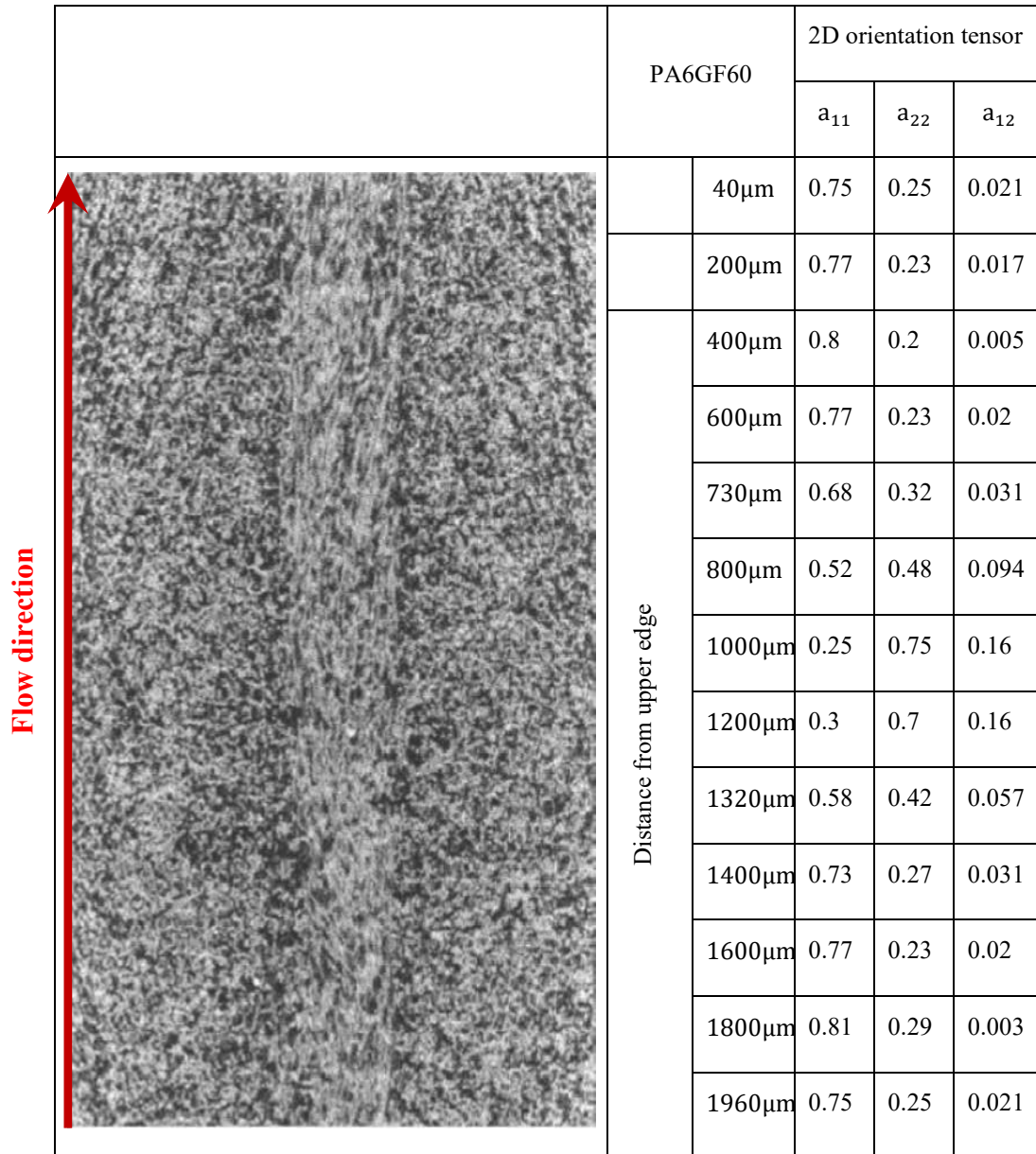


**Figure 5-33 2D-orientation tensor components according to the CT scan results taken from Ref [1]**

Since the specimens are symmetric with respect to three mutually perpendicular Cartesian planes, then to reduce the numerical costs, one eighth of the model is considered as the FEM model as it is illustrated in Figure 5-35 for the tensile test. The FEM analysis accomplished by applying the UMAT subroutines

such as presented in Appendix1. The UMAT subroutine in Appendix1 uses the introduced elasto-plasticity model in chapter 4 by taking the introduced EPCDM damage models (see section 4.4.1) into account. Since the non-local damage model is discussed in detail for the PA6GF60 in [1], then we here will focus on the damage model EPCDM. To obtain the material properties for the complete alignments of the fibers with flow direction, we assume the PA6GF60's mechanical properties belong to the material with the following structural tensor:

$$A = \begin{bmatrix} 0.65 & 0 & 0 \\ 0 & 0.35 & 0 \\ 0 & 0 & 0 \end{bmatrix} \quad (5-7)$$

The given values for  $a_{11}$  and  $a_{22}$  are the mean values of the respective numbers presented in right side table in Figure 5-33 and calculated by [1]. Besides, we assume that the material's mechanical properties vary with respect to the structural tensor as the components of the stiffness matrix are presented in Figure 5-22. Since the ratio of the variation

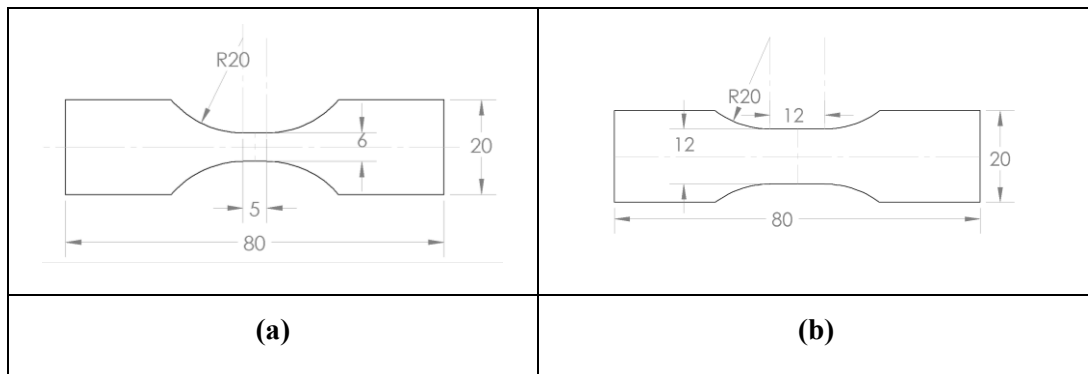


**Figure 5-34 tests specimens geometries (a) tension based on ASTM D3039; (b) compression based on ASTM D695 –10**

of the stiffness matrix's components with respect to the variation of  $a_{11}$  is not linear, then it is different than the linear inter-extrapolation method introduced by [1]. Applying the same ratio, the material properties for the PA6GF60 with 100% orientation of the fibers in the injection flow direction can be achieved.

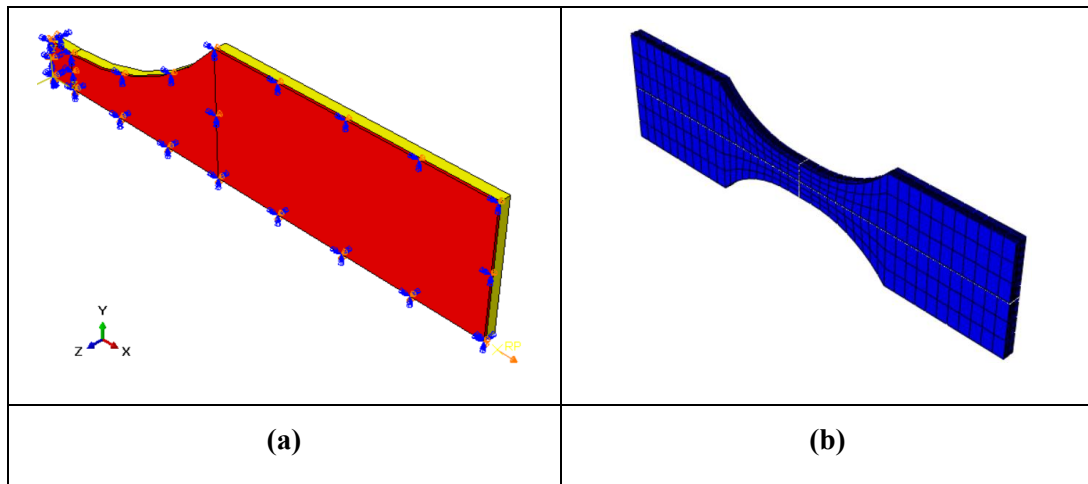


**Figure 5-35 FEM models for the tensile test; (a) one eighth of the real specimen with boundary conditions. The red and yellow parts represent the core and the skin, respectively. (b) the complete FEM model after applying the symmetries.**

The results are presented in Table 5-2 for the PA6GF60 with 100% and 65% alignments of the fibers in the flow direction. As it is stated and emphasized by [1], the method is not validated, and it is only an assumption in the lack of the required information for the mechanical properties of the short fiber reinforced thermoplastics with a different distribution of the fibers. The numerical and the experimental results, just for the longitudinal direction, are illustrated in Figure 5-36, in order to show the functionality of the method.

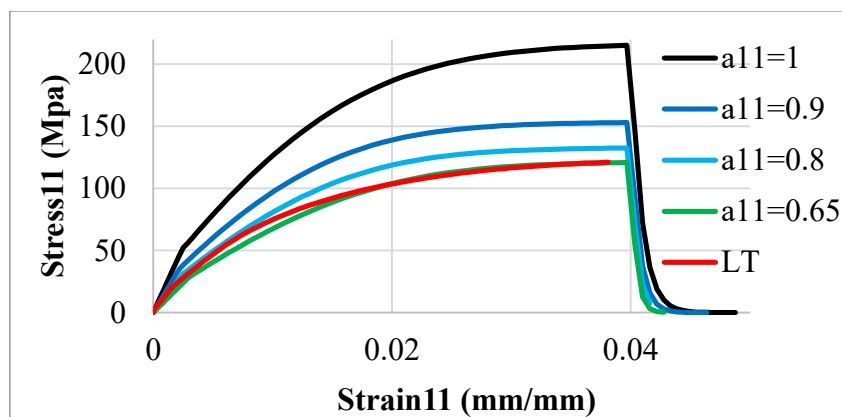


**Figure 5-36 one element analysis ( $\sigma_1$  vs  $\epsilon_1$ ) of PA6GF60 under loading condition 1 (see Table 3-1) using inter-extrapolation method**

Applying the extrapolation the maximum stress in the longitudinal direction for  $a_{11}$  increases by the level of 215 Mpa. A small decrease in the fibers orientation distributions in the longitudinal direction by causes a dramatic drop in the maximum stress. Since this behavior is not linear, then the maximum drop will happen in the first stage, i.e., when  $a_{11}$  changes from 1 to 0.9, while for the following steps the reductions decrease. The same approach is valid for the compression loading in the longitudinal direction with higher levels of the saturation stresses as it is seen in Figure 5-37.

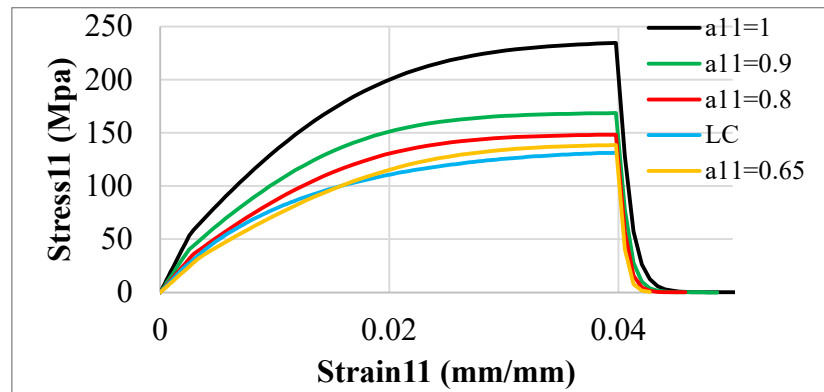


**Figure 5-37 one element analysis ( $\sigma_2$  vs  $\epsilon_2$ ) of PA6GF60 under loading condition 2 (see Table 3-1) using inter-extrapolation method**

The skin layers under the longitudinal tension are stiffer than the core layer. Therefore, they yield before the core. The phenomenon for the tensile test in the longitudinal direction is shown in Figure 5-38 which clearly shows that the plasticity begins from the outer sides of the layers of the skin and by increasing the load it progresses toward the core, then the core itself begins to yield, and the process continues until the entire zone yields. The numerical and experimental results for the component under tensile and compression loadings in the longitudinal direction are presented in Figure 5-39. The numerical results are not exactly fit the experimental results due to the fact that the distribution functions for each

Table 5-2 the mechanical properties of PA6GF60

Property	$E_{11}$	$E_{22}$	$G_{12}$	$G_{23}$	$\nu_{12}$	$\nu_{23}$
$a_{11} = 0.65$	11767	5019	2081	2083	0.0167	0.35
$a_{11} = 1$	21180.6	9034.2	3747.5	3749.5	0.0167	0.35

point is not determined and the mean value, as explained before, is applied to the model. It is impossible to determine the fiber distributions point by point, experimentally, for example using CT scan method. although an injection molding flow simulation software such as MOLDFLOW might be a numerical solution. Even in this case, i.e., having this kind of information, the entire procedure would be a grueling task, especially when a complicated geometry such as the hybrid component is introduced in section 1.2.

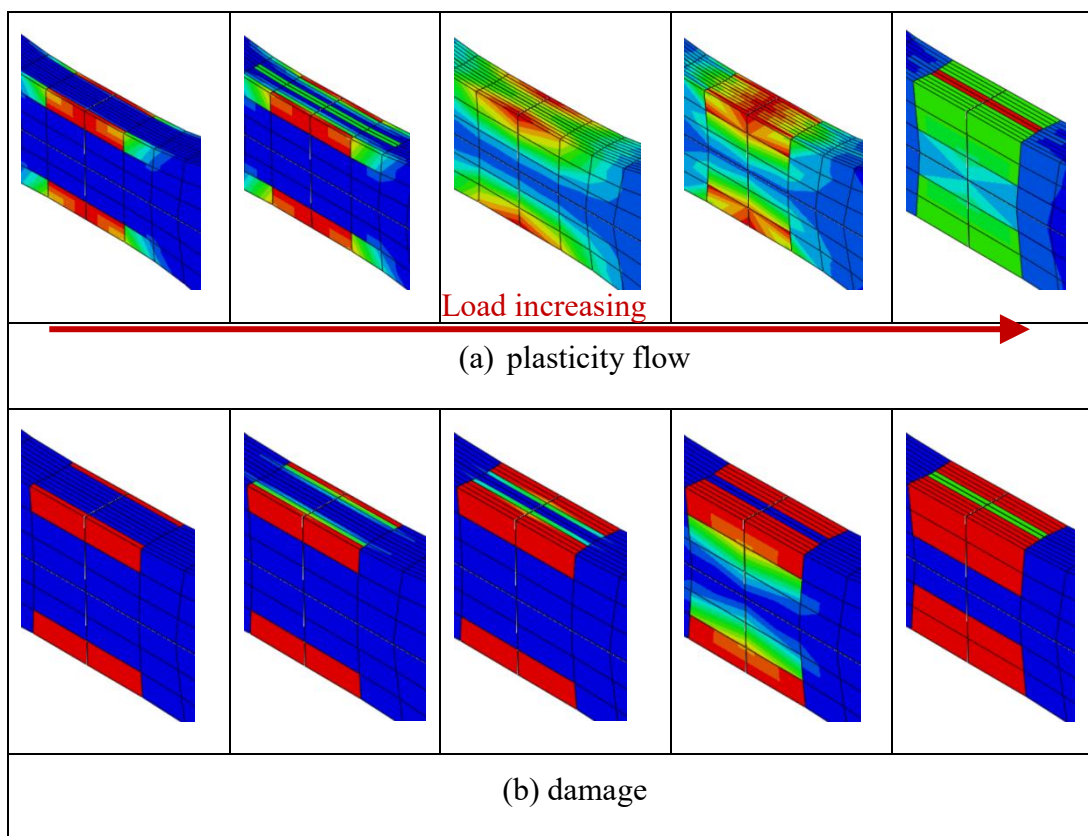


**Figure 5-38 plasticity and damage progression status**

The numerical and experimental results for both tensile and compression loadings under either tension or compression are presented in Figure 5-40. Since there are no available experimental results for damage phenomenon, then we skip the associated numerical results.

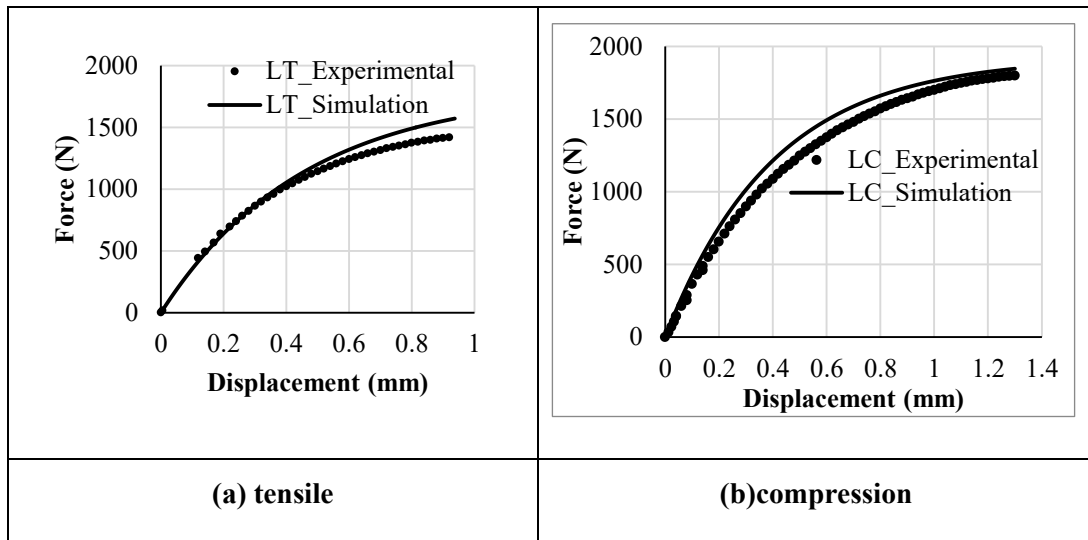


**Figure 5-39 displacement versus force; the experimental and the numerical results for the longitudinal direction**

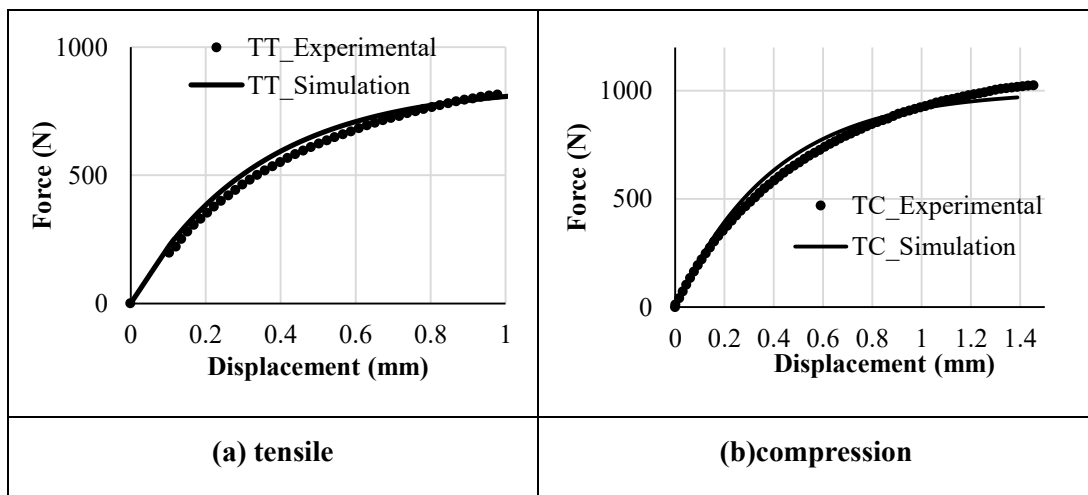


**Figure 5-40 displacement versus force; the experimental and the numerical results for the transverse direction**

## **5.5 Elasto-plastic simulation of the main component under torsion**

From the very beginning the aim to introduce the elasto-plasticity model, which is presented in sections 4.1 , theoretically, and 4.2 and numerically in section 4.5, was to simulate the nonlinear behavior of the main case study which

is introduced in section 1.2. Having some difficulties with the contacts, the explicit integration scheme, as explained in section 4.5.2, is chosen. The explicit integration scheme, which is called VUMAT, is introduced to ABAQUS in a 2D fashion and we use S4R shell element type for all the sections. The elasto-plasticity model is applied on the injected parts while for the outer shell the elastic continuum damage model, introduced in section 4.4.1.1, is applied.

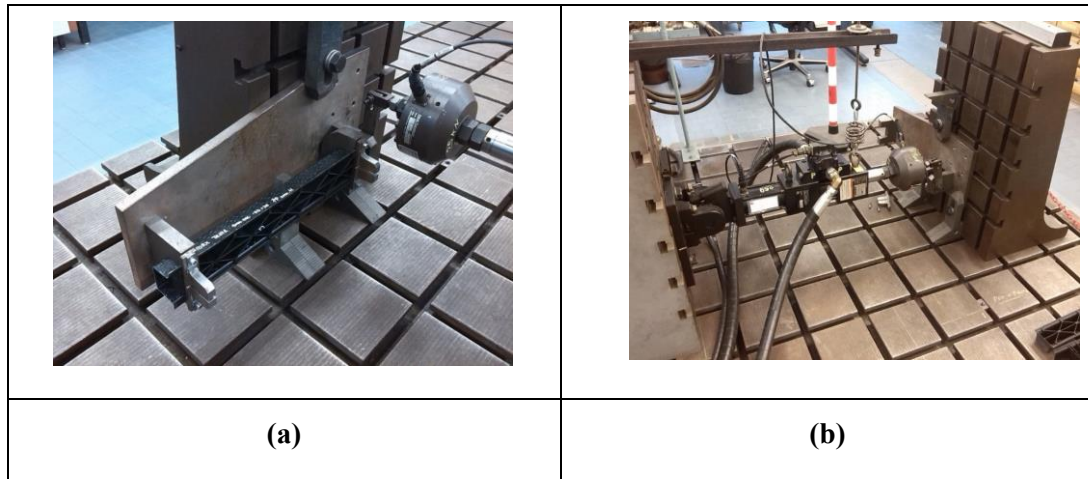


**Figure 5-41 torsion test configuration; (a) with component (b) without component**

The torsion experiment is conducted on the hybrid component with the same dimensions as illustrated in Figure 5-14 with the configuration which is presented in Figure 5-41. To apply the elasto-plasticity model, it is important to recognize a proper structural tensor for each segment which affects strongly the response of the component under torsion. According to Figure 1-6 and the given explanation in section 1.2.1 the fibers orientations distributions in the injected columns, which are illustrated by red color in Figure 5-15, can be considered as follows:

$$A = \begin{bmatrix} 1 & 0 & 0 \\ 0 & 0 & 0 \\ 0 & 0 & 0 \end{bmatrix} \quad (5-8)$$

Which means it is assumed that the 100% of the fibers are aligned in the flow direction, but for the ribs, which are demonstrated by green and blue colors in Figure 5-15, it is given as:

$$A = \begin{bmatrix} 0.5 & 0 & 0 \\ 0 & 0.5 & 0 \\ 0 & 0 & 0 \end{bmatrix} \quad (5-9)$$

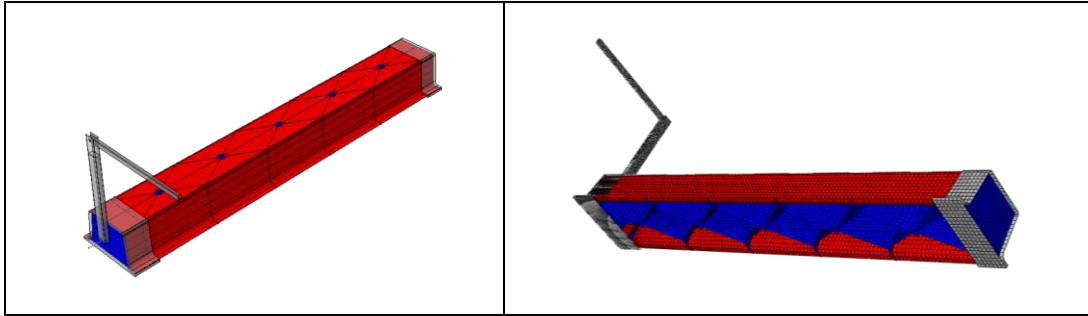


**Figure 5-42 main model in ABAQUS; blue area are injected, and the red one is made of the thermoplastic fabric shell**

The experimental results for the hybrid component are demonstrated in Figure 5-43 where shows a nonlinear behavior, and it is continued till the damage happens in the second column gate and leads the major drop in the component's load bearing. The numerical results show the same trend with a small amount of underestimation for either nonlinear and damage response of the component.

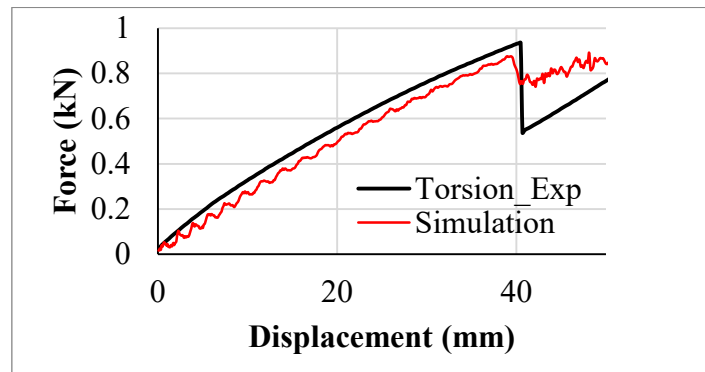


**Figure 5-43 numerical and experimental results for the component under torsion**

The different damage modes are demonstrated in Figure 5-44, and it is observed that the second injection gate fails suddenly while the ribs experience large deformation before damage.



**Figure 5-44 different damage modes under torsion**

## Chapter 7

# 6 Summery and future works

In this chapter, we present the conclusion of the current research and also discuss the possible direction for the future works on the short fiber-reinforced composites simulations.

### 6.1 Conclusion

This work is mainly dedicated to the short fiber reinforced thermoplastic composites, and according to some assumptions, they were considered as the transversely isotopic materials. The invariant and representation theories were employed to formulate and model the inelastic behavior of the fibrous thermoplastics. The elasto-plasticity model was able to capture the nonlinear behavior of the short fiber reinforced material for the simple components such as discussed in 5.4. In the proposed elasto-plasticity model, the structural tensor strongly affects the numerical results. It is a hard, sometimes impossible, task to determine the structural tensor for each point of complicated geometries such as the current work's case study (see section 1.2). Therefore, for the simulation of the hybrid component under torsion where its nonlinear response was observed, we used mean values for different part of the injected constituents. The decision about the mean values of the fiber orientation distribution for each section of the hybrid component was made based on the photos taken from the damaged zones of the internal part. The damaged areas were chosen due to the fact that these points are under maximum stress (critical) conditions and have the leading role in the mechanical responses. Two damage models were proposed for either of the brittle and ductile composites where they were used for the numerical simulation of the bending and torsion experiments of the hybrid component, respectively. Also, it was shown that the hybrid component manufactured by the compression molding process has higher load bearing capacity than the back-injected-manufactured one with the same geometry.

## **6.2 Future work**

The short fiber reinforced composites possess a complicated substructure which depends on many parameters such as the manufacturing techniques and conditions including the temperature, humidity and the flow direction and the velocity of the melted material. We proposed fully macromechanical constitutive equations which the environmental conditions are not regarded. Since any of these conditions have a huge impact on the mechanical behavior of the short fiber reinforced material, then the implementation of any of these parameters into the constitutive equations might be a further improvement of the proposed model. Also, the difference between the compression and injected molded short fiber reinforced materials are not investigated except for the simple tensile strength. Therefore, carrying out the basic experiments such as compression, shear and fatigue tests might be a new research activity.

## References

1. Vogler, M., Anisotropic Material Models for Fiber Reinforced Polymeres, in Der Fakultät für Bauingenieurwesen und Geodäsie der Leibniz Universität Hannover zur Erlangung des Grades. 2012: Unpublished.
2. Biron, M., Thermoplastics and thermoplastic composites. 2012: William Andrew.
3. Mallick, P.K., Fiber-reinforced composites: materials, manufacturing, and design. 2007: CRC press.
4. Clegg, D. and A. Collyer, Mechanical properties of reinforced thermoplastics. Vol. 326. 1986: Springer.
5. Mallick, P.K., FIBERREINFORCED COMPOSITES Materials, Manufacturing, and Design. 2007: Taylor & Francis Group, LLC.
6. Belingardi, G., et al., Progressive damage analysis of a rate-dependent hybrid composite beam. *Composite Structures*, 2016. **154**: p. 433-442.
7. Fu, S.-Y., B. Lauke, and Y.-W. Mai, Science and engineering of short fibre reinforced polymer composites. 2009: Elsevier.
8. Arroyo, M. and F. Avalos, Polypropylene/low density polyethylene blend matrices and short glass fibers based composites. I. mechanical degradation of fibers as a function of processing method. *Polymer composites*, 1989. **10**(2): p. 117-121.
9. Fu, S.-Y., X. Hu, and C.-Y. Yue, Effects of fiber length and orientation distributions on the mechanical properties of short-fiber-reinforced polymers. *材料*, 1999. **48**(6Appendix): p. 74-83.
10. Fu, S.-Y. and B. Lauke, The fibre pull-out energy of misaligned short fibre composites. *Journal of Materials Science*, 1997. **32**(8): p. 1985-1993.

11. Fu, S.-Y. and B. Lauke, An analytical characterization of the anisotropy of the elastic modulus of misaligned short-fiber-reinforced polymers. *Composites Science and Technology*, 1998. **58**(12): p. 1961-1972.
12. Bader, M. and J. Collins, The effect of fibre-interface and processing variables on the mechanical properties of glass-fibre filled nylon 6. *Fibre science and technology*, 1983. **18**(3): p. 217-231.
13. Bijsterbosch, H. and R. Gaymans, Polyamide 6—long glass fiber injection moldings. *Polymer composites*, 1995. **16**(5): p. 363-369.
14. Biolzi, L., L. Castellani, and I. Pitacco, On the mechanical response of short fibre reinforced polymer composites. *Journal of materials science*, 1994. **29**(9): p. 2507-2512.
15. Curtis, P., M. Bader, and J. Bailey, The stiffness and strength of a polyamide thermoplastic reinforced with glass and carbon fibres. *Journal of Materials Science*, 1978. **13**(2): p. 377-390.
16. Denault, J., T. Vu-Khanh, and B. Foster, Tensile properties of injection molded long fiber thermoplastic composites. *Polymer composites*, 1989. **10**(5): p. 313-321.
17. Doshi, S. and J.M. Charrier, A simple illustration of structure-properties relationships for short fiber-reinforced thermoplastics. *Polymer composites*, 1989. **10**(1): p. 28-38.
18. Fu, S.-Y., et al., Effects of PA6, 6/PP ratio on the mechanical properties of short glass fiber reinforced and rubber-toughened polyamide 6, 6/polypropylene blends. *Composites Part B: Engineering*, 2006. **37**(2): p. 182-190.
19. Bay, R.S. and C.L. Tucker, Fiber orientation in simple injection moldings. Part I: Theory and numerical methods. *Polymer composites*, 1992. **13**(4): p. 317-331.
20. Gupta, M. and K. Wang, Fiber orientation and mechanical properties of short-fiber-reinforced injection-molded composites: Simulated and experimental results. *Polymer Composites*, 1993. **14**(5): p. 367-382.

21. Silva, C.A., et al., Fiber orientation in divergent/convergent flows in expansion and compression injection molding. *Polymer composites*, 2006. **27**(5): p. 539-551.
22. Fu, S.-Y., et al., Correction of the measurement of fiber length of short fiber reinforced thermoplastics. *Composites Part A: Applied Science and Manufacturing*, 2002. **33**(11): p. 1549-1555.
23. Barbosa, S.E. and J.M. Kenny, Analysis of the relationship between processing conditions-fiber orientation-final properties in short fiber reinforced polypropylene. *Journal of reinforced plastics and composites*, 1999. **18**(5): p. 413-420.
24. Darlington, M. and P. McGinley, Fibre orientation distribution in short fibre reinforced plastics. *Journal of Materials Science*, 1975. **10**(5): p. 906-910.
25. Friedrich, K., Mesoscopic aspects of polymer composites: processing, structure and properties. *Journal of materials science*, 1998. **33**(23): p. 5535-5556.
26. Solomon, S., et al., Microstructure and fracture behavior of (co) injection-molded polyamide 6 composites with short glass/carbon fiber hybrid reinforcement. *Journal of applied polymer science*, 2005. **97**(3): p. 957-967.
27. Fu, S.-Y. and B. Lauke, Characterization of tensile behaviour of hybrid short glass fibre/calcite particle/ABS composites. *Composites Part A: Applied Science and Manufacturing*, 1998. **29**(5): p. 575-583.
28. Ramsteiner, F. and R. Theysohn, Tensile and impact strengths of unidirectional, short fibre-reinforced thermoplastics. *Composites*, 1979. **10**(2): p. 111-119.
29. Takahashi, K. and N.-S. Choi, Influence of fibre weight fraction on failure mechanisms of poly (ethylene terephthalate) reinforced by short-glass-fibres. *Journal of materials science*, 1991. **26**(17): p. 4648-4656.
30. Bernasconi, A., F. Cosmi, and D. Dreossi, Local anisotropy analysis of injection moulded fibre reinforced polymer composites. *Composites Science and Technology*, 2008. **68**(12): p. 2574-2581.

31. Clarke, A., N. Davidson, and G. Archenhold, Measurements of fibre direction in reinforced polymer composites. *Journal of Microscopy*, 1993. **171**(1): p. 69-79.
32. Kim, E., J. Park, and S. Jo, A study on fiber orientation during the injection molding of fiber-reinforced polymeric composites:(Comparison between image processing results and numerical simulation). *Journal of Materials Processing Technology*, 2001. **111**(1): p. 225-232.
33. Smith, G.F., *Constitutive equations for anisotropic and isotropic materials*. Vol. 3. 2012: Newnes.
34. Forghani, A., et al., An overview of continuum damage models used to simulate intralaminar failure mechanisms in advanced composite materials, in *Numerical Modelling of Failure in Advanced Composite Materials*. 2015, Elsevier. p. 151-173.
35. Bažant, Z.k.P., I.M. Daniel, and Z. Li, Size Effect and Fracture Characteristics of Composite Laminates. *Journal of Engineering Materials and Technology*, 1996. **118**(3): p. 317-324.
36. Bažant, Z.P. and B.H. Oh, Microplane model for progressive fracture of concrete and rock. *Journal of Engineering Mechanics*, 1985. **111**(4): p. 559-582.
37. Bažant, Z.P. and B.H. Oh, Crack band theory for fracture of concrete. *Matériaux et construction*, 1983. **16**(3): p. 155-177.
38. Matzenmiller, A., J. Lubliner, and R. Taylor, A constitutive model for anisotropic damage in fiber-composites. *Mechanics of materials*, 1995. **20**(2): p. 125-152.
39. Talreja, R. A continuum mechanics characterization of damage in composite materials. in *Proceedings of the Royal Society of London A: Mathematical, Physical and Engineering Sciences*. 1985. The Royal Society.
40. Talreja, R. and C.V. Singh, *Damage and failure of composite materials*. 2012: Cambridge University Press.

41. Hashin, Z. and A. Rotem, A fatigue failure criterion for fiber reinforced materials. *Journal of composite materials*, 1973. **7**(4): p. 448-464.
42. Puck, A. and H. Schürmann, Failure analysis of FRP laminates by means of physically based phenomenological models. *Composites Science and Technology*, 1998. **58**(7): p. 1045-1067.
43. Hinton, M.J., A.S. Kaddour, and P.D. Soden, Failure criteria in fibre reinforced polymer composites: the world-wide failure exercise. 2004: Elsevier.
44. Dávila, C.G. and P.P. Camanho, Failure criteria for FRP laminates in plane stress. *NASA TM*, 2003. **212663**(613).
45. Chang, F.-K. and K.-Y. Chang, A progressive damage model for laminated composites containing stress concentrations. *Journal of composite materials*, 1987. **21**(9): p. 834-855.
46. Hill, R., *The mathematical theory of plasticity*. Vol. 11. 1998: Oxford university press.
47. Lemaitre, J., R. Desmorat, and M. Sauzay, Anisotropic damage law of evolution. *European Journal of Mechanics-A/Solids*, 2000. **19**(2): p. 187-208.
48. Maimí, P., et al., A continuum damage model for composite laminates: Part II—Computational implementation and validation. *Mechanics of Materials*, 2007. **39**(10): p. 909-919.
49. Camanho, P.P. and C.G. Dávila, Mixed-mode decohesion finite elements for the simulation of delamination in composite materials. 2002.
50. Lapczyk, I. and J.A. Hurtado, Progressive damage modeling in fiber-reinforced materials. *Composites Part A: Applied Science and Manufacturing*, 2007. **38**(11): p. 2333-2341.
51. Duvant, G. and J.L. Lions, *Inequalities in mechanics and physics*. Vol. 219. 2012: Springer Science & Business Media.
52. Ryou, H., K. Chung, and W.-R. Yu, Constitutive modeling of woven composites considering asymmetric/anisotropic, rate dependent, and

- nonlinear behavior. *Composites Part A: Applied Science and Manufacturing*, 2007. **38**(12): p. 2500-2510.
53. Shokrieh, M.M. and M.J. Omid, Tension behavior of unidirectional glass/epoxy composites under different strain rates. *Composite Structures*, 2009. **88**(4): p. 595-601.
54. Shokrieh, M.M. and M.J. Omid, Investigating the transverse behavior of Glass–Epoxy composites under intermediate strain rates. *Composite Structures*, 2011. **93**(2): p. 690-696.
55. Naik, N., et al., High strain rate tensile behavior of woven fabric E-glass/epoxy composite. *Polymer Testing*, 2010. **29**(1): p. 14-22.
56. Foroutan, R., et al., Experimental investigation of high strain-rate behaviour of fabric composites. *Composite Structures*, 2013. **106**: p. 264-269.
57. Daniel, I.M., B.T. Werner, and J.S. Fenner, Strain-rate-dependent failure criteria for composites. *Composites Science and Technology*, 2011. **71**(3): p. 357-364.
58. Wei, X., et al., A new rate-dependent unidirectional composite model- Application to panels subjected to underwater blast. *Journal of the Mechanics and Physics of Solids*, 2013. **61**(6): p. 1305-1318.
59. Camanho, P.P. and S.R. Hallett, Numerical modelling of failure in advanced composite materials. 2015: Woodhead Publishing.
60. Dopker, B., et al. Damage tolerance analysis of composite transport fuselage structure. in 35th Structures, Structural Dynamics, and Materials Conference. 1994.
61. Ilcewicz, L., et al. Tension fracture of laminates for transport fuselage–part 4: damage tolerance analysis. in Fourth NASA Advanced Technology Conference. 1993.
62. Kongshavn, I. and A. Poursartip, Experimental investigation of a strain-softening approach to predicting failure in notched fibre-reinforced composite laminates. *Composites Science and Technology*, 1999. **59**(1): p. 29-40.

63. Williams, K.V. and R. Vaziri, Application of a damage mechanics model for predicting the impact response of composite materials. *Computers & Structures*, 2001. **79**(10): p. 997-1011.
64. Williams, K. and R. Vaziri. Finite element analysis of the impact response of CFRP composite plates. in *Tenth International Conference on Composite Materials. V. Structures*. 1995.
65. Boehler, J.-P., *Applications of tensor functions in solid mechanics*. Vol. 292. 1987: Springer.
66. Spencer, A.J.M., *Continuum theory of the mechanics of fibre-reinforced composites*. Vol. 282. 1984: Springer.
67. Spencer, A., Isotropic polynomial invariants and tensor functions, in *Applications of tensor functions in solid mechanics*. 1987, Springer. p. 141-169.
68. Dafalias, Y., Corotational rates for kinematic hardening at large plastic deformations. *J. appl. Mech*, 1983. **50**(3): p. 561.
69. Dafalias, Y. On the evolution of structure variables in anisotropic yield criteria at large plastic transformations. in *Colloque International du CNRS*. 1983.
70. Dafalias, Y. A missing link in the macroscopic constitutive formulation of large plastic deformation, plasticity today, modeling, methods and application. in *Proc. int. symp. on current trends and results in plasticity*, CISM, Udine, Italy. 1982.
71. Dafalias, Y.F., The plastic spin concept and a simple illustration of its role in finite plastic transformations. *Mechanics of Materials*, 1984. **3**(3): p. 223-233.
72. Advani, S.G. and C.L. Tucker III, The use of tensors to describe and predict fiber orientation in short fiber composites. *Journal of rheology*, 1987. **31**(8): p. 751-784.
73. Zeng, D., et al., Effect of Fiber Orientation on the Mechanical Properties of Long Glass Fiber Reinforced (LGFR) Composites. 2014, SAE Technical Paper.

74. Wineman, A.S. and A. Pipkin, Material symmetry restrictions on constitutive equations. *Archive for Rational Mechanics and Analysis*, 1964. **17**(3): p. 184-214.
75. Pipkin, A. and A. Wineman, Material symmetry restrictions on non-polynomial constitutive equations. *Archive for Rational Mechanics and Analysis*, 1963. **12**(1): p. 420-426.
76. Spencer, A., Part III. Theory of invariants. *Continuum physics*, 2017. **1**: p. 239-353.
77. Wang, C., A new representation theorem for isotropic functions. *Arch. Internat. Mech. Anal*, 1970. **36**.
78. Smith, G., On isotropic functions of symmetric tensors, skew-symmetric tensors and vectors. *International Journal of Engineering Science*, 1971. **9**(10): p. 899-916.
79. Smith, G., On isotropic integrity bases. *Archive for rational mechanics and analysis*, 1965. **18**(4): p. 282-292.
80. Mase, G.T., R.E. Smelser, and G.E. Mase, *Continuum mechanics for engineers*. 2009: CRC press.
81. Zheng, Q.-S. and A. Spencer, Tensors which characterize anisotropies. *International Journal of Engineering Science*, 1993. **31**(5): p. 679-693.
82. Boehler, J., Representations for isotropic and anisotropic non-polynomial tensor functions, in *Applications of tensor functions in solid mechanics*. 1987, Springer. p. 31-53.
83. Spencer, A., Kinematic constraints, constitutive equations and failure rules for anisotropic materials, in *Applications of Tensor Functions in Solid Mechanics*. 1987, Springer. p. 187-201.
84. Lempriere, B., Poisson's ratio in orthotropic materials. *AIAA J*, 1968. **6**(11): p. 2226-2227.
85. Jones, R.M., *Mechanics of composite materials*. Vol. 193. 1975: Scripta Book Company Washington, DC.

86. Bhatia, R., Positive definite matrices. 2009: Princeton university press.
87. Weisstein, E.W., Positive definite matrix. 2003.
88. Hyer, M.W., Stress analysis of fiber-reinforced composite materials. 2009: DEStech Publications, Inc.
89. Achenbach, J.D., A theory of elasticity with microstructure for directionally reinforced composites. Vol. 167. 2014: Springer.
90. Chakrabarty, J., Applied plasticity. 2010: Springer.
91. Launay, A., et al., Cyclic behaviour of short glass fibre reinforced polyamide: Experimental study and constitutive equations. *International Journal of Plasticity*, 2011. **27**(8): p. 1267-1293.
92. Launay, A., et al., Multiaxial fatigue models for short glass fiber reinforced polyamide–Part I: Nonlinear anisotropic constitutive behavior for cyclic response. *International Journal of Fatigue*, 2013. **47**: p. 382-389.
93. Mortazavian, S., Fatigue behavior and modeling of short fiber reinforced polymer composites. 2015.
94. Dunne, F. and N. Petrinic, Introduction to computational plasticity. 2005: Oxford University Press on Demand.
95. Krabbenhøft, K., Basic computational plasticity. Lecture Notes, 2002.
96. Daniel, I.M., et al., Interfiber/interlaminar failure of composites under multi-axial states of stress. *Composites Science and Technology*, 2009. **69**(6): p. 764-771.
97. Daniel, I., et al. Mechanical behaviour and failure criteria of composite materials under static and dynamic loading. in *Proceeding of 17th international conference on composite materials (ICCM17)*, Edinburgh, UK. 2009.
98. Ochola, R., et al., Mechanical behaviour of glass and carbon fibre reinforced composites at varying strain rates. *Composite Structures*, 2004. **63**(3): p. 455-467.

99. Daniel, I., B. Werner, and J. Fenner, Strain-rate-dependent failure criteria for composites. *Composites Science and Technology*, 2011. **71**(3): p. 357-364.
100. Iannucci, L. and M. Willows, An energy based damage mechanics approach to modelling impact onto woven composite materials—Part I: Numerical models. *Composites Part A: Applied Science and Manufacturing*, 2006. **37**(11): p. 2041-2056.
101. Donadon, M., et al., A progressive failure model for composite laminates subjected to low velocity impact damage. *Computers & Structures*, 2008. **86**(11): p. 1232-1252.
102. Maimí, P., et al., A thermodynamically consistent damage model for advanced composites. 2006.
103. Tijssens, M.G., B.L. Sluys, and E. van der Giessen, Numerical simulation of quasi-brittle fracture using damaging cohesive surfaces. *European Journal of Mechanics-A/Solids*, 2000. **19**(5): p. 761-779.
104. Andrade, F., et al. User-Defined Nonlocal Models in LS-DYNA. in 7th European LS-DYNA Users Conference. 2011.
105. Vogler, M., R. Rolfes, and P. Camanho, Modeling the inelastic deformation and fracture of polymer composites—Part I: plasticity model. *Mechanics of Materials*, 2013. **59**: p. 50-64.
106. Bažant, Z.P. and B.H. Oh, Crack band theory for fracture of concrete. *Materials and structures*, 1983. **16**(3): p. 155-177.
107. Linde, P., et al. Modelling and simulation of fibre metal laminates. in ABAQUS Users' conference. 2004.
108. Hagenbeek, M., et al., Static properties of fibre metal laminates. *Applied Composite Materials*, 2003. **10**(4): p. 207-222.
109. De Vries, T.J., Blunt and sharp notch behaviour of Glare laminates. 2001.
110. ABAQUS, V., 6.14, Online Documentation Help, Theory manual: Dassault Systms. 2016, Accessed on.

- 
111. Eidel, B., *Anisotropic Inelasticity: Modelling, Simulation, Validation*. 2004: Shaker.
  112. Doghri, I., Fully implicit integration and consistent tangent modulus in elasto-plasticity. *International Journal for Numerical Methods in Engineering*, 1993. **36**(22): p. 3915-3932.
  113. Smelser, R. and R. Becker. Abaqus user subroutines for material modeling. in *ABAQUS Users' Conference Proceedings*, Stresa, Italy, Hibbitt, Karlsson, and Sorenson, Inc. 1989.
  114. Škrobák, A., et al., Comparison of mechanical properties of injection molded and compression molded rubber samples. *International Journal of Mechanics*, 2013.
  115. Schöpfer, J., *Spritzgussbauteile aus kurzfaserverstärkten Kunststoffen: Methoden der Charakterisierung und Modellierung zur nichtlinearen Simulation von statischen und crashrelevanten Lastfällen*. 2011.

# Annex

## 8 Appendix

In the appendix, some of the subroutines which are developed based on the introduced elasto-plasticity model, in the UMAT format are given.

### 8.1 Appendix1

#### 8.1.1 Elasto-plasticity with damage UMAT subroutine

The proposed elasto-plasticity model has been coded in the FORTRAN for the implicit solver which is called UMAT in ABAQUS documentation. Writing a UMAT subroutine is well-documented in the ABAQUS documents, and it is not that much different than a written code in the FORTRAN. Some difficulties might be encountered during the coding process which using the following tips might be alleviated:

- 1- Try not to use the main updated variables, i.e., STRESS and DDSDD, with the original name in the internal subroutines arguments.
- 2- If you declare a variable in the main subroutine and the variable is used as a dummy argument in an internal subroutine, it has to be re-declared in the internal subroutine.
- 3- To debug the written code, use the command `write(*,*)` in UMAT and `write(6,*)` in VUAMT to receive the desired line information in .log format.
- 4- Before applying the written code on the main model, try to apply it on one element with different boundary conditions.
- 5- Begin writing a code with a simple elastic model and then develop it to the complicated models.

In the following, you can find one of the subroutine which is developed for the proposed elasto-plasticity model for transversely isotropic materials. The

VUMAT is not given here due to the fact that a UMAT subroutine is easily can be converted to a VUMAT type and vice versa. The given subroutines employ the isotropic hardening formula to generate the hardening curves with can be easily replaced by a look-up type procedure.

```

SUBROUTINE UMAT (STRESS, STATEV, DDSDD, SSE, SPD, SCD,
1 RPL, DDSDDT, DRPLDE, DRPLDT,
2 STRAN, DSTRAN, TIME, DTIME, TEMP, DTEMP, PREDEF, DPRED, CMNAME,
3 NDI, NSHR, NTENS, NSTATV, PROPS, NPROPS, COORDS, DROT, PNEWDT,
4 CELENT, DFGRD0, DFGRD1, NOEL, NPT, LAYER, KSPT, JSTEP, KINC)
C
INCLUDE 'ABA_PARAM.INC'
C
CHARACTER*80 CMNAME
DIMENSION STRESS (NTENS), STATEV (NSTATV),
1 DDSDD (NTENS, NTENS), DDSDDT (NTENS), DRPLDE (NTENS),
2 STRAN (NTENS), DSTRAN (NTENS), TIME (2), PREDEF (1), DPRED (1),
3 PROPS (NPROPS), COORDS (3), DROT (3, 3), DFGRD0 (3, 3), DFGRD1 (3, 3),
4 JSTEP (4)

DIMENSION STRAINPLAVECOLD (NTENS), STRAINPLAVECNEW (NTENS),
* STRAINTOTVECNEW (NTENS), STRAINTOTVECOLD (NTENS),
*
STRAIN_EFF (NTENS), CE_MAT_2D (3, 3), CE_MAT_3D (6, 6), CDFULL (6, 6),
* STRESSTRVECNEW (NTENS), STRESSTRVECOLD (NTENS),
CE4TH (3, 3, 3, 3),
* C_TAN (NTENS, NTENS), STRESS_OLD (NTENS), STRESS_TMP (NTENS),
*
DFCDEPS (NTENS), DFTDEPS (NTENS), DMTDEPS (NTENS), DMCDEPS (NTENS),
* STRESS_P_OLD (NTENS), STRESS_P (NTENS), STRAINTEMP (NTENS),
* DDSDDTEMP (NTENS, NTENS), STRESST (NTENS), A_DIR (3, 3),
* STRESSELASTIC (NTENS), STRESSELASTIC_OLD (NTENS),
* DDFDE (NTENS), DDMDE (NTENS), SIGMA (NTENS, NTENS),
STRAN_DIST (NTENS),
* EPS_PERT (NTENS), STRESS_DIST (NTENS),
DDSDD_OLD (NTENS, NTENS),
*
STRESSU (NTENS), STRESSU_OLD (NTENS), DSTRAIN (NTENS), DSTRAIN_OLD (NTENS
), TANG_OLD (NTENS, NTENS)
PARAMETER (ZERO = 0.D0, ONE = 1.D0, TWO = 2.D0, HALF = 0.5D0,
* THREE = 3.D0)
C GET THE MATERIAL PROPERTIES---ENGINEERING CONSTANTS
E_11 = PROPS (1) !YOUNG'S MODULUS IN DIRECTION 1
E_22 = PROPS (2) !YOUNG'S MODULUS IN DIRECTION 2
G_12 = PROPS (3) !SHEAR MODULUS IN 12 PLANE
XNU_12 = PROPS (4) !POISON'S RATIO
XNU_23 = PROPS (5) !POISON'S RATIO
G_23 = PROPS (6) !SHEAR MODULUS IN 23 PLANE
X_T = PROPS (7) !FAILURE STRESS IN 1 DIRECTION IN
TENSION
X_C = PROPS (8) !FAILURE STRESS IN 1 DIRECTION IN
COMPRES

```

```

      Y_T = PROPS (9)           !FAILURE STRESS IN 2 DIRECTION IN
TENSION
      Y_C = PROPS (10)          !FAILURE STRESS IN 2 DIRECTION IN
COMPRES
      S_12 = PROPS (11)         !FAILURE STRESS IN SHEAR IN 1-2
PLANE
      S_21 = PROPS (12)         !FAILURE STRESS IN SHEAR IN 1-2
PLANE
      S_23 = PROPS (13)
      ALPHA = PROPS (14)        ! HASHIN'S COEFFICIENT
      ETAFT = PROPS (15)        ! REGULARIZATION COEFFICIENT
      ET AFC = PROPS (16)       ! REGULARIZATION COEFFICIENT
      ET AMT = PROPS (17)       ! REGULARIZATION COEFFICIENT
      ET AMC = PROPS (18)       ! REGULARIZATION COEFFICIENT
      G_MT_C = PROPS (19)       ! MATRIX TAUGHNESS ENERGY IN TENSION
      G_MC_C = PROPS (20)       ! MATRIX TAUGHNESS ENERGY IN
COMPRESSION
      G_FC_C = PROPS (21)       ! FIBER TAUGHNESS ENERGY IN
COMPRESSION
      G_FT_C = PROPS (22)       ! FIBER TAUGHNESS ENERGY IN TENSION
      XMF_M = PROPS (23)        ! NOT USED
      XMF_S = PROPS (24)        ! NOT USED
      XMF_G = PROPS (25)        ! NOT USED
      EPS_QS = PROPS (26)       ! NOT USED
      EPS_F_X_T = PROPS (27)
      EPS_F_X_C = PROPS (28)
      EPS_F_Y_T = PROPS (29)
      EPS_F_Y_C = PROPS (30)
      EPS_SC = PROPS (31)
      PLAST_TOL = PROPS (32)
      Y_TR_0 = PROPS (33)
      Y_IP_0 = PROPS (34)
      Y2T_0 = PROPS (35)
      Y2C_0 = PROPS (36)
      Y1T_0 = PROPS (37)
      Y1C_0 = PROPS (38)
      A_ST_11 = PROPS (39)
      A_ST_22 = PROPS (40)
      A_ST_33 = PROPS (41) ! NOT USED
      CONST1 = PROPS (42)
      CONST2 = PROPS (43)
      NUMBREAKINP = PROPS (44)
      ZETHA = PROPS (45)

```

```

C      DEFINE STATE VARIABLES
      DO I = 1, NTENS
      STRAINTOTVECOLD (I) = STATEV (I)
      END DO
      DFTOLD = STATEV (NTENS+1)
      DFCOLD = STATEV (NTENS+2)
      DMTOLD = STATEV (NTENS+3)
      DMCOLD = STATEV (NTENS+4)
      DFVTOLD = STATEV (NTENS+5)
      DFVCOLD = STATEV (NTENS+6)

```

```

DMVTOLD = STATEV (NTENS+7)
DMVCOLD = STATEV (NTENS+8)
XFFTOLD = STATEV (NTENS+9)
XFFCOLD = STATEV (NTENS+10)
XMFTOLD = STATEV (NTENS+11)
XMFCOLD = STATEV (NTENS+12)
SIGMA_FT_EQ_0_OLD = STATEV (NTENS+13)
DEL_FT_EQ_0_OLD = STATEV (NTENS+14)
XFFTOLD = STATEV (NTENS+15)
DEL_FC_EQ_0_OLD = STATEV (NTENS+16)
XF_MC_SC_OLD = STATEV (NTENS+17)
SIGMA_FC_EQ_0_OLD = STATEV (NTENS+18)
SIGMA_MT_EQ_0_OLD = STATEV (NTENS+19)
DEL_MT_EQ_0_OLD = STATEV (NTENS+20)
SIGMA_MC_EQ_0_OLD = STATEV (NTENS+21)
DEL_MC_EQ_0_OLD = STATEV (NTENS+22)
DO I = NTENS+23, 2 * NTENS + 22
STRAINPLAVECOLD (I-NTENS-22) = STATEV (I)
END DO
EPSVAR_P_OLD = STATEV (2 * NTENS+24)
XF_YIELD_INI_OLD = STATEV (2 * NTENS+25)
DO I = 2 * NTENS+26, 3 * NTENS+25
STRESSTRVECOLD (I-2 * NTENS-25) = STATEV (I)
END DO
TOTALTIME_OLD = STATEV (3 * NTENS+27)
TIMEINCREMENT_OLD = STATEV (3 * NTENS+28)
DELTAGAMMAINTOLD = STATEV (3 * NTENS+29)
Y_TR_INI_OLD = STATEV (3 * NTENS+30)
Y_IP_INI_OLD = STATEV (3 * NTENS+31)
Y1T_INI_OLD = STATEV (3 * NTENS+32)
Y1C_INI_OLD = STATEV (3 * NTENS+33)
Y2C_INI_OLD = STATEV (3 * NTENS+34)
Y2T_INI_OLD = STATEV (3 * NTENS+35)
M_UXC_OLD = STATEV (3 * NTENS+36)
M_UXT_OLD = STATEV (3 * NTENS+37)
M_TUC_OLD = STATEV (3 * NTENS+38)
M_TUT_OLD = STATEV (3 * NTENS+39)
M_IP_OLD = STATEV (3 * NTENS+40)
M_TR_OLD = STATEV (3 * NTENS+41)
Y_1C_OD = STATEV (3 * NTENS+42)
Y_1T_OD = STATEV (3 * NTENS+43)
Y_2C_OD = STATEV (3 * NTENS+44)
Y_2T_OD = STATEV (3 * NTENS+45)
Y_IP_OD = STATEV (3 * NTENS+46)
Y_TR_OD = STATEV (3 * NTENS+47)
XINV_1_OLD = STATEV (3 * NTENS+48)
XINV_2_OLD = STATEV (3 * NTENS+49)
XINV_3_OLD = STATEV (3 * NTENS+50)
XINV_4_OLD = STATEV (3 * NTENS+51)
DO I = 3 * NTENS+52, 4 * NTENS+51
STRESS_P_OLD (I-3 * NTENS-51) = STATEV (I)
END DO
DO I = 4 * NTENS+52, 5 * NTENS+51
STRESSELASTIC_OLD (I-4 * NTENS-51) = STATEV (I)

```

```

END DO
DO I = 5 * NTENS+52, 6 * NTENS+51
STRESSU_OLD(I-5 * NTENS-51) = STATEV(I)
END DO
DO I = 6 * NTENS+52, 7 * NTENS+51
DSTRAIN_OLD(I-6 * NTENS-51) = STATEV(I)
END DO
XF_YIELD_CURRENT_OLD = STATEV(7 * NTENS+52)
ALPHA1_OLD = STATEV(7 * NTENS+53)
ALPHA2_OLD = STATEV(7 * NTENS+54)
ALPHA4_OLD = STATEV(7 * NTENS+55)
ALPHA42_OLD = STATEV(7 * NTENS+56)
ALPHA5_OLD = STATEV(7 * NTENS+57)
ALPHA52_OLD = STATEV(7 * NTENS+58)

      NALI = NDI
      STRAINTEMP = DSTRAN
      NTALI = NTENS
      NSHT = NSHR
      DTIMET = DTIME
      NTEMP = NDI
C   DEFINE OLD STRESS
      DO I = 1, NTENS
        STRESS_OLD(I) = STRESS(I)
      END DO
C   DEFINE THE NEW STRAIN
      DO I = 1, NTENS
C     STRAINTOTVECOLD(I) = STRAN(I)
        STRAINTOTVECNEW(I) = STRAN(I) + DSTRAN(I)
      END DO
C   TEST
      DO I=1, NTENS
        DSTRAIN(I) = DSTRAN(I)
      END DO
C   DEFINE THE STIFFNESS TENSOR
      CALL STIFF4TH_2D (CE4TH, XNU_12,E_11, E_22,XNU_23,
G_12,A_DIR,
*     NALI, NSHT,A_ST_11,A_ST_22, CE_MAT_2D,CE_MAT_3D)

      IF (NDI .EQ. 3) THEN
        DO I=1, NTENS
          DO J=1, NTENS
            DDSDE(I,J) = CE_MAT_3D(I,J)
          END DO
        END DO
      ELSE
        DO I=1, NTENS
          DO J=1, NTENS
            DDSDE(I,J) = CE_MAT_2D(I,J)
          END DO
        END DO
      END IF

C   CALCULATE ELASTIC STRESS

```

```

      CALL GETSTRESS3D(CE_MAT_3D, CE_MAT_2D, STRESSELASTIC,
*      STRAINTOTVECNEW, NTALI, NALI)

C TIME DEFINITIONS
      TOTALTIME_OLD = TIME(2)
      TOTALTIME_NEW = TOTALTIME_OLD + DTIME
      TIMEINCREMENT_NEW = DTIME
C CHECK THE FAILURE BASED ON OLD STRESS
      CALL CHECKFAILURE(X_C, X_T, Y_C, Y_T, S_12, STRESS_OLD,
DFTOLD, DMTOLD,
*      NALI, NSHT, CELENT, G_FT_C, G_MT_C, STRAINTOTVECNEW,
EPS_F_X_T,
*      EPS_F_X_C, EPS_F_Y_T, EPS_F_Y_C, EPS_SC, CE_MAT_3D, NTALI,
*      STRAINPLAVECOLD, TDFT, TDMT, NOEL, DDFDE, DDMDE)

C ! USE VISCOUS REGULARIZATION
      DFVT = ETAFT / (ETAFT + DTIME) * DFVTOLD + DTIME /
*      (ETAFT + DTIME) * TDFT
      DMVT = ETAMT / (ETAMT + DTIME) * DMVTOLD + DTIME /
*      (ETAMT + DTIME) * TDMT

C PLASTIC BEHAVIOUR MUST BE CHEKED IN THIS POINT TO DEFINE NEW
STRESSES BEFORE....
C .... DAMAGE INITIATION

      IF (DFVT .NE. ZERO .OR. DMVT.NE. ZERO ) GOTO 730
      CALL SHORTFIBERPLAST3D( STRAINPLAVECOLD, STRAINPLAVECNEW,
*      STRAINTOTVECNEW, STRESST, STRESS_OLD, EPSVAR_P_OLD,
*      NALI,
NSHT, CE_MAT_2D, CE_MAT_3D, XF_YIELD_INI_OLD, XF_YIELD_INI_NEW,
*      C_TAN, STRAINTOTVECOLD, STRESSTRVECNEW, STRESSTRVECOLD,
*      DTIMET, TOTALTIME_NEW, TOTALTIME_OLD, DELTAGAMMAINT,
*      Y_TR_INI_OLD, Y_TR_INI, Y_IP_INI_OLD, Y_IP_INI, Y1T_INI_OLD,
*      Y1T_INI, Y1C_INI_OLD, Y1C_INI, Y2C_INI_OLD,
Y2C_INI, Y2T_INI_OLD,
*      Y2T_INI, M_UXC, M_UXT, M_TUC, M_TUT, M_IP, M_TR,
Y_1CT, Y_1C_OD,
*      Y_1TT, Y_1T_OD, Y_2CT, Y_2C_OD, Y_2TT, Y_2T_OD, Y_IP_T, Y_IP_OD,
Y_TR_T,
*      Y_TR_OD, Y_TR_0, Y_IP_0, Y2T_0, Y2C_0, Y1T_0, Y1C_0, A_ST_11,
A_ST_22,
*      CONST1, CONST2, XINV_1, XINV_2, XINV_3,
XINV_4, NTALI, STRESS_P_OLD,
*      STRESS_P, NUMBREAKINP, DSTRAN, STRESSELASTIC, XF_YIELD_NEW,
DSTRAIN_OLD,
*      DELTAGAMMAINTOLD, ALPHA2, ALPHA4, ALPHA42, ALPHA5, ALPHA52)
      DO I=1, NTENS
          STRESS(I) = STRESST(I)
      END DO
      DO I=1, NTENS
          DO J=1, NTENS
              DDSDE(I, J) = C_TAN(I, J)
          END DO
      END DO

```

```

      END DO
C DEFINE MAXIMUM STRESS ( THE PICK POINT)
      DO I=1, NTENS
        STRESSU(I) = MAX(STRESS(I),STRESS_OLD(I))
      END DO
      GOTO 731
730 CONTINUE

C UPDATE THE STATE VARIABLES WHICH ARE NOT PASSING THROUGH THE
PLASTIC SUBROUTINE
      EPSVAR_P_NEW = EPSVAR_P_OLD
C UPDATE PLASTIC STRAINS
      DO I=1,NTENS
        STRAINPLAVECNEW(I) = STRAINPLAVECOLD(I)
        STRESSTRVECNEW(I) = STRESSTRVECOLD(I)
      END DO
      XF_YIELD_INI_NEW = XF_YIELD_INI_OLD
      DELTAGAMMAINT = DELTAGAMMAINTOLD
      Y_TR_INI = Y_TR_INI_OLD
      Y_IP_INI = Y_IP_INI_OLD
      Y1T_INI = Y1T_INI_OLD
      Y1C_INI = Y1C_INI_OLD
      Y2C_INI = Y2C_INI_OLD
      Y2T_INI = Y2T_INI_OLD
      M_UXC = M_UXC_OLD
      M_UXT = M_UXT_OLD
      M_TUC = M_TUC_OLD
      M_TUT = M_TUT_OLD
      M_IP = M_IP_OLD
      M_TR = M_TR_OLD
      Y_1CT = Y_1C_OD
      Y_1TT = Y_1T_OD
      Y_2CT = Y_2C_OD
      Y_2TT = Y_2T_OD
      Y_IPT = Y_IP_OD
      Y_TRT = Y_TR_OD
      XINV_1 = XINV_1_OLD
      XINV_2 = XINV_2_OLD
      XINV_3 = XINV_3_OLD
      XINV_4 = XINV_4_OLD
      DO I = 1, NTENS
        STRESS_P (I) = STRESS_P_OLD(I)
      END DO
      DO I=1, NTENS
        STRESSU(I) = STRESSU_OLD(I)
      END DO
      DO I =1, NTENS
        STRESSELASTIC(I) = STRESSELASTIC_OLD(I)
      END DO
      XF_YIELD_NEW = XF_YIELD_CURRENT_OLD
      ALPHA1 = ALPHA1_OLD
      ALPHA2 = ALPHA2_OLD
      ALPHA4 = ALPHA4_OLD
      ALPHA42 = ALPHA42_OLD

```

```

ALPHA5 = ALPHA5_OLD
ALPHA52 = ALPHA52_OLD

C DEFINE AN EFFECTIVE ELASTIC STRAIN
  DO I=1,NTENS
    STRAIN_EFF(I) = STRAINTOTVECNEW(I)
  END DO

  STRESS(1) = (ONE - DFVT) * STRESSU(1)
  STRESS(2) = (ONE - DMVT) * STRESSU(2)
  STRESS(3) = (ONE - DMVT) * STRESSU(3)
  STRESS(4) = (ONE - DFVT) * (ONE - DMVT) * STRESSU(4)
  STRESS(5) = (ONE - DFVT) * (ONE - DMVT) * STRESSU(5)
  STRESS(6) = (ONE - DFVT) * (ONE - DMVT) * STRESSU(6)

  IF (STRAINTOTVECNEW(1).GE.ZERO .AND. DFVT.NE.ZERO )
*   STRAIN_EFF(1) = STRESS(1)/CE_MAT_3D(1,1)
  IF (STRAINTOTVECNEW(2).GE.ZERO .AND. DMVT.NE.ZERO)
*   STRAIN_EFF(2) = STRESS(2)/CE_MAT_3D(2,2)

  DO I=1, NTENS
    STRAIN_EFF(I)=(ONE-DFVT)*(STRAINTOTVECNEW(I)-
    STRAINPLAVECNEW(I))
  END DO

C   CALL GETSTRESS3D_FULL(CE_MAT_3D,CE_MAT_2D,DFVT,DMVT,
C   *   STRAIN_EFF, NTALI,NALI,STRESST,CDFULL)

  CALL
GETCD_FULL(CE_MAT_3D,CE_MAT_2D,DFVT,DMVT,NTALI,NALI,CDFULL)

  STRESS(1) = (ONE - DFVT) * STRESSU(1)
  STRESS(2) = (ONE - DMVT) * STRESSU(2)
  STRESS(3) = (ONE - DMVT) * STRESSU(3)
  STRESS(4) = (ONE - DFVT) * (ONE - DMVT) * STRESSU(4)
  STRESS(5) = (ONE - DFVT) * (ONE - DMVT) * STRESSU(5)
  STRESS(6) = (ONE - DFVT) * (ONE - DMVT) * STRESSU(6)

C   GOTO 578
  CALL XJACOBIAN_CALC(CDFULL,CE_MAT_3D,DTIMET,NTALI,NALI,DMVT,
*   DFVT,STRAIN_EFF,ETAFT,DDSDETTEMP,DDFDE,DDMDE)
    DO I=1, NTENS
      DO J=1, NTENS
        DDSDE(I,J) = DDSDETTEMP(I,J)
      END DO
    END DO

C 578 CONTINUE
    DO I=1, NTENS
      DO J=1, NTENS
        DDSDE(I,J) = 0.1D0 * CE_MAT_3D(I,J)
      END DO
    END DO

```

```

731 CONTINUE
C   DEFINE THE NEWVARIABLES
      DO I = 1, NTENS
        STATEV(I) = STRAINTOTVECNEW(I)
      END DO
      STATEV(NTENS+1) = TDFT
      STATEV(NTENS+2) = TDFC
      STATEV(NTENS+3) = TDMT
      STATEV(NTENS+4) = TDMC
      STATEV(NTENS+5) = DFVT
      STATEV(NTENS+6) = DFVC
      STATEV(NTENS+7) = DMVT
      STATEV(NTENS+8) = DMVC
      STATEV(NTENS+9) = XFFT
      STATEV(NTENS+10) = XFFC
      STATEV(NTENS+11) = XMFT
      STATEV(NTENS+12) = XMFC
      STATEV(NTENS+13) = SIGMA_FT_EQ_0_NEW
      STATEV(NTENS+14) = DEL_FT_EQ_0_NEW
      STATEV(NTENS+15) = XFFT
      STATEV(NTENS+16) = DEL_FC_EQ_0_NEW
      STATEV(NTENS+17) = XF_MC_SC_NEW
      STATEV(NTENS+18) = SIGMA_FC_EQ_0
      STATEV(NTENS+19) = SIGMA_MT_EQ_0_NEW
      STATEV(NTENS+20) = DEL_MT_EQ_0_NEW
      STATEV(NTENS+21) = SIGMA_MC_EQ_0_NEW
      STATEV(NTENS+22) = DEL_MC_EQ_0_NEW
      DO I = NTENS+23, 2 * NTENS + 22
        STATEV(I) = STRAINPLAVECNEW(I-NTENS-22)
      END DO
      STATEV(2 * NTENS+24) = EPSVAR_P_NEW
      STATEV(2 * NTENS+25) = XF_YIELD_INI_NEW
      DO I = 2 * NTENS+26, 3 * NTENS+25
        STATEV(I) = STRESSTRVECNEW(I-2 * NTENS-25)
      END DO
      STATEV(3 * NTENS+27) = TOTALTIME_NEW
      STATEV(3 * NTENS+28) = TIMEINCREMENT_NEW
      STATEV(3 * NTENS+29) = DELTAGAMMAINT
      STATEV(3 * NTENS+30) = Y_TR_INI
      STATEV(3 * NTENS+31) = Y_IP_INI
      STATEV(3 * NTENS+32) = Y1T_INI
      STATEV(3 * NTENS+33) = Y1C_INI
      STATEV(3 * NTENS+34) = Y2C_INI
      STATEV(3 * NTENS+35) = Y2T_INI
      STATEV(3 * NTENS+36) = M_UXC
      STATEV(3 * NTENS+37) = M_UXT
      STATEV(3 * NTENS+38) = M_TUC
      STATEV(3 * NTENS+39) = M_TUT
      STATEV(3 * NTENS+40) = M_IP
      STATEV(3 * NTENS+41) = M_TR
      STATEV(3 * NTENS+42) = Y_1CT
      STATEV(3 * NTENS+43) = Y_1TT
      STATEV(3 * NTENS+44) = Y_2CT
      STATEV(3 * NTENS+45) = Y_2TT

```

```

STATEV(3 * NTENS+46) = Y_IPT
STATEV(3 * NTENS+47) = Y_TRT
STATEV(3 * NTENS+48) = XINV_1
STATEV(3 * NTENS+49) = XINV_2
STATEV(3 * NTENS+50) = XINV_3
STATEV(3 * NTENS+51) = XINV_4
DO I = 3 * NTENS+52, 4 * NTENS+51
STATEV(I) = STRESS_P(I-3 * NTENS-51)
END DO
DO I = 4 * NTENS+52, 5 * NTENS+51
STATEV(I) = STRESSELASTIC(I-4 * NTENS-51)
END DO
DO I = 5 * NTENS+52, 6 * NTENS+51
STATEV(I) = STRESSU(I-5 * NTENS-51)
END DO
DO I = 6 * NTENS+52, 7 * NTENS+51
STATEV(I) = DSTRAIN(I-6 * NTENS-51)
END DO
STATEV(7 * NTENS+52) = XF_YIELD_NEW
STATEV(7 * NTENS+53) = ALPHA1
STATEV(7 * NTENS+54) = ALPHA2
STATEV(7 * NTENS+55) = ALPHA4
STATEV(7 * NTENS+56) = ALPHA42
STATEV(7 * NTENS+57) = ALPHA5
STATEV(7 * NTENS+58) = ALPHA52

RETURN
END
C*****
*****
C PLASTICITY SUBROUTINE FOR SHORT FIBERS OF 2-D CASE
C*****
*****
SUBROUTINE SHORTFIBERPLAST3D( STRAINPLAVECOLD,
STRAINPLAVECNEW,
* STRAINTOTVECNEW, STRESS_NEW, STRESS_OLD, EPSVAR_P_OLD,
* EPSVAR_P_NEW, ND, NSH, CE_2D, CE_3D,
* XF_YIELD_INI_OLD, XF_YIELD_INI_NEW, C_TAN,
* STRAINTOTVECOLD, STRESSTRVECNEW, STRESSTRVECOLD,
PLAST_TOL,
* DT, TOTALTIME_NEW, TOTALTIME_OLD,
* DELTAGAMMAINT, Y_TR_INI_OLD, Y_TR_INI,
* Y_IP_INI_OLD, Y_IP_INI, Y1T_INI_OLD, Y1T_INI, Y1C_INI_OLD,
* Y1C_INI, Y2C_INI_OLD, Y2C_INI, Y2T_INI_OLD, Y2T_INI, M_UXC,
M_UXT,
* M_TUC, M_TUT, M_IP, M_TR,
Y_1C, Y_1C_OLD, Y_1T, Y_1T_OLD, Y_2C,
* Y_2C_OLD, Y_2T, Y_2T_OLD, Y_IP, Y_IP_OLD,
Y_TR, Y_TR_OLD, Y_TR_0,
* Y_IP_0, Y2T_0, Y2C_0, Y1T_0, Y1C_0, A_ST_11, A_ST_22, CONST1,
* CONST2, XI1_T, XI2_T, XI5_T, XI4_T, NTT, STRESS_P_OLD,
STRESS_P,
* NUMBREAK,
DSTRAIN, STRESSELAST, XF_YIELD_NEW, DSTRAIN_OLD, CE4TH,

```

```

*
DELTAGAMMAINTOLD,ALPHA1,ALPHA2,ALPHA4,ALPHA42,ALPHA5,ALPHA52)

  INCLUDE 'ABA_PARAM.INC'
  CHARACTER(LEN=:), ALLOCATABLE :: FILEPATH_IP, FILEPATH_TR,
* FILEPATH_TUC, FILEPATH_TUT, FILEPATH_UXC, FILEPATH_UXT
  DIMENSION STRAINTRVECNEW(NTT), STRAINTRVECOLD(NTT),
* STRAINPLAVECOLD(NTT), STRAINPLAVECNEW(NTT),
* STRAINTOTVECNEW(NTT), STRAINTOTVECOLD(NTT),
* X_N_F(NTT),DISTURB(NTT), STRESSELAST(NTT),
* STRESSTRVECNEW(NTT),STRESSTRVECOLD(NTT), CE_3D(6,6),
* DELTA(3,3), X_N_G(NTT), A_DIR(3,3), C_TAN(NTT,NTT),
* CE_2D(3,3), STRESS_NEW(NTT), STRESS_OLD(NTT),
* DI1DSIGMA(NTT), DI2DSIGMA(NTT),
DI4DSIGMA(NTT),DI5DSIGMA(NTT),
* DI3DSIGMA(NTT),STRESS_P_OLD(NTT),STRESS_P(NTT),
* DSTRESS_P(NTT),
DSTRAIN(NTT),STRAINPLAVECINT(NTT),TANG_OLD(NTT,NTT),
* SIGMA(NTT,NTT), STRAN_DIST(NTT),
EPS PERT(NTT),STRESS_DIST(NTT),
*
DSTRAIN_OLD(NTT),X_M_MAT(6,6),X_M_TEN(3,3,3,3), TENSOR1(3,3,3,3),
*
TENSOR2(3,3,3,3), TENSOR3(3,3),X_I_S(3,3,3,3),X_I(3,3,3,3),CE4TH(3,
3,3,3),
*
TENSOR5(3,3,3,3), TENSOR4(3,3),F_TEN(NTT,NTT),DSIGMADELTAGAMMA(NTT
),
* TERM3(NTT), A_DIR_VEC(3),
P_PIND(3,3,3,3),P_PIND_A(3,3,3,3), A_DEV(3,3),
*
TERM20(NTT,NTT),TERM21(NTT,NTT),TERM22(NTT,NTT),TERM23(NTT,NTT),
*
TERM24(NTT,NTT),TERM30(NTT),TERM31(NTT),TERM32(NTT),TERM25(NTT,NTT
)

  ALLOCATABLE XY_TRSHEAR(:,:),
* XY_IPSHEAR(:,:), XY_IPSHEAR_T(:,:), XY_TRBC(:,:),
XY_TRBC_T(:,:),
* XY_TRUC(:,:), XY_TRUC_T(:,:), XY_TRT(:,:), XY_TRT_T(:,:),
* XY_UXT_T(:,:), XY_TRSHEAR_T(:,:),XY_TRBT(:,:),
XY_TRBT_T(:,:),
* XY_UXC(:,:), XY_UXC_T(:,:), XY_UXT(:,:)
  PARAMETER (ZERO = 0.D0, ONE = 1.D0, TWO = 2.D0, HALF =
0.5D0,
1 THREE = 3.D0, FOUR = 4.D0, EPS_P = 0.5D0 )
  CALL FIBER_DIR(A_DIR,A_ST_11,A_ST_22)
  A_DIR_VEC(1) = A_DIR(1,1)
  A_DIR_VEC(2) = A_DIR(2,2)
  A_DIR_VEC(3) = A_DIR(3,3)
C  DEFINE KRONECKER DELTA
  DO I = 1, 3
  DO J = 1, 3
  IF ( I .EQ. J ) THEN

```

```

        DELTA(I,J) = ONE
        ELSE
        DELTA(I,J) = ZERO
        END IF
    END DO
END DO
C      DEFINE ELASTIC STRAIN
    DO I = 1 , NTT
    STRAINTRVECNEW(I) = STRAINTOTVECNEW(I) - STRAINPLAVECOLD(I)
C      STRAINTRVECNEW(I) = STRAINTOTVECNEW(I)
    END DO
    CALL GETSTRESS3D(CE_3D, CE_2D, STRESSTRVECNEW, STRAINTRVECNEW,
*      NTT, ND)
C      IMPORT PLASTICITY DATA FROM EXTERNAL FILE FOR DIFFERENT
EXPERIMENTS
    XF_CF_SH = ONE ! FOR SHORT FIBER REINFORCED
THERMOPLASTICS
    XF_CF_UNI = ONE ! FOR SHORT FIBER REINFORCED
THERMOPLASTICS

    Y_TR_INI = Y_TR_0 * ( 1.D0 - EXP(-CONST1 * CONST2) )
    Y_IP_INI = Y_IP_0 * ( 1.D0 - EXP(-CONST1 * CONST2) )
    Y2T_INI = Y2T_0 * ( 1.D0 - EXP(-CONST1 * CONST2) )
    Y2C_INI = Y2C_0 * ( 1.D0 - EXP(-CONST1 * CONST2) )
    Y1T_INI = Y1T_0 * ( 1.D0 - EXP(-CONST1 * CONST2) )
    Y1C_INI = Y1C_0 * ( 1.D0 - EXP(-CONST1 * CONST2) )
    Y_TR = ZERO
    Y_IP = ZERO
    Y2T = ZERO
    Y2C = ZERO
    Y1T = ZERO
    Y1C = ZERO
    IF (Y_TR_OLD.EQ.ZERO) Y_TR_OLD = Y_TR_INI
    IF (Y_IP_OLD.EQ.ZERO) Y_IP_OLD = Y_IP_INI
    IF (Y_2T_OLD.EQ.ZERO) Y_2T_OLD = Y2T_INI
    IF (Y_2C_OLD.EQ.ZERO) Y_2C_OLD = Y2C_INI
    IF (Y_1T_OLD.EQ.ZERO) Y_1T_OLD = Y1T_INI
    IF (Y_1C_OLD.EQ.ZERO) Y_1C_OLD = Y1C_INI
    CALL INVARIANTS(STRESS_OLD, ND, NSH, XI1_T,
*      XI2_T, XI5_T, XI4_T, NTT, A_ST_11, A_ST_22,
*      TRSIGMA, DI1DSIGMA, DI2DSIGMA, DI4DSIGMA, DI5DSIGMA)
C*****
C      DEFINE THE INVARIANTS FOR SHORT FIBER REINFORCED
THERMOPLASTICS
C*****
    CALL INVARIANTS(STRESSTRVECNEW, ND, NSH, XI1_INI,
*      XI2_INI, XI5_INI, XI4_INI, NTT, A_ST_11, A_ST_22,
*      TRSIGMA, DI1DSIGMA, DI2DSIGMA, DI4DSIGMA, DI5DSIGMA)

    CALL CALCALPHA(Y_TR_INI, Y_IP_INI, Y1T_INI, Y1C_INI,
*      Y2C_INI, Y2T_INI, ALPHA1_INI, ALPHA2_INI, ALPHA4_INI,
*      ALPHA42_INI, ALPHA5_INI, ALPHA52_INI )

C      DEFINE INITIA YIELD CRITERION

```

```

      XF_YIELD_INI_NEW = ALPHA1_INI * XI1_INI+ ALPHA2_INI *
XI2_INI +
      * ALPHA4_INI * XI4_INI + ALPHA42_INI * XI4_INI ** TWO +
      * ALPHA5_INI * XI5_INI + ALPHA52_INI * XI5_INI ** TWO

      CALL CALCBETA(Y_TR_INI,Y_IP_INI,Y1T_INI, Y1C_INI, Y2C_INI,
      * Y2T_INI, BETA1, BETA2, BETA32T,BETA32C, BETA42T, BETA42C )

C DEFINE TENSION OR COMPRESSION SITUATION
      IF (TRSIGMA >= ZERO) THEN
      BETA32 = BETA32T
      BETA42 = BETA42T
      ELSE
      BETA32 = BETA32C
      BETA42 = BETA42C
      END IF

C DEFINE POTENTIAL FUNCTION
      X_G_NEW = BETA1 * XI1_INI+ BETA2 * XI2_INI +
      * BETA32 * XI3_INI ** TWO + BETA42 * XI4_INI ** TWO - ONE

C ADDITIONAL DATA FOR NEWTON METHOD
      DO I = 1, 3
      DO J = 1, 3
      DO K = 1, 3
      DO L = 1, 3
      X_I(I,J,K,L) = 0.5D0 * DELTA(I,K) * DELTA(J,L)
      X_I_S(I,J,K,L) = X_I(I,J,K,L) - (1.D0/3.D0) * DELTA(I,J) *
DELTA(K,L)
      TENSOR5(I,J,K,L) = A_DIR(I,J) * A_DIR(K,L)
      END DO
      END DO
      END DO
      END DO

      DO I = 1, 3
      DO J = 1, 3
      DO K = 1, 3
      DO L = 1, 3
      TENSOR2(I,J,K,L) = ZERO      ! DECLARE THE TENSORS'
DIMENSIONS
      DO M = 1, 3
      TENSOR2(I,J,K,L) = TENSOR2(I,J,K,L) + (A_DIR(I,M) *
X_I(M,J,K,L)
      * + X_I(I,J,K,M) * A_DIR(M,L))
      END DO
      END DO
      END DO
      END DO
      END DO

      DO I = 1, 3
      DO J = 1, 3
      TENSOR3(I,J) = ZERO
      DO K = 1, 3
      DO L = 1, 3

```

```

    TENSOR3(I,J) = TENSOR3(I,J) + A_DIR(K,L) * X_I_S(K,L,I,J)

        END DO
    END DO
END DO

DO I = 1, 3
    DO J = 1, 3
        DO K = 1, 3
            DO L = 1, 3
                TENSOR1(I,J,K,L) = X_I(I,J,K,L) - TENSOR2(I,J,K,L)
            END DO
        END DO
    END DO
END DO

DO I = 1, 3
    DO J = 1, 3
        TENSOR4(I,J) = 3.D0 * A_DIR(I,J) - (A_DIR(1,1) + A_DIR(2,2) +
* A_DIR(3,3)) * DELTA(I,J)
    END DO
END DO

DO I = 1, 3
    DO J = 1, 3
        DO K = 1, 3
            DO L = 1, 3
                X_M_TEN(I,J,K,L) = BETA1 * TENSOR1(I,J,K,L) + BETA2 *
TENSOR2(I,J,K,L) +
* (3.D0 / 2.D0) * BETA32 * TENSOR3(I,J) * TENSOR4(K,L) +
2.D0 *
* BETA42 * TENSOR5(I,J,K,L)
            END DO
        END DO
    END DO
END DO

CALL TENSTOMATRIX6(X_M_TEN,X_M_MAT)
DO I = 1, 6
    DO J = 1, 6
        X_M_MAT(J,I) = X_M_MAT(I,J)
    END DO
END DO

C    IMPORT PLASTICITY DATA FROM EXTERNAL FILE FOR DIFFERENT
EXPERIMENTS
    DO I=1,NTT
        STRESS_P(I) = ZERO
    END DO

CALL GETSTRESS3D(CE_3D, CE_2D, STRESSELAST, DSTRAIN, NTT, ND)
C
IF ( EPSVAR_P_OLD .NE. ZERO ) GOTO 125
IF ( XF_YIELD_INI_NEW < ONE ) GOTO 600

```

```

125 CONTINUE
C          """"""ELASTIC PREDICTOR""""""
C
C   SET DELTAGAMMAINT INITIAL VALUE
      DELTAGAMMAINT = ZERO
C   SET EPSVAR_P
C   START THE ITERATION (LOOP) TO FIND PLASTIC MULTIPLIER
DELTAGAMMAINT AND UPDATING PLASTIC STRAINS
      NUMC = 0
C INITIALIZE NEW STRESS
      DO I = 1, NTT
C          STRESS_NEW(I) = STRESSELAST(I)+STRESS_OLD(I)
          STRESS_NEW(I) = STRESSTRVECNEW(I)
          END DO
C INITIALIZE THE EQUIVALENT PLASTIC STRAIN
      DO I = 1, NTT
          STRAINPLAVECINT(I) = STRAINPLAVECOLD(I)
          END DO
          EPSVAR_P_INT = EPSVAR_P_OLD
DO ! MAIN LOOP
      NUMC = NUMC + 1

C          CALL F_TEN_GENERATOR(F_TEN, X_M_MAT,DELTAGAMMAINT, CE_3D)
          CALL F_TEN_GENERATOR_TOT(F_TEN, X_M_TEN,DELTAGAMMAINT,
CE4TH)

C   CALCULATE STRESS TENSOR
      DO I = 1, NTT
          STRESS_NEW(I) = ZERO
          DO J = 1, NTT
              STRESS_NEW(I) = STRESS_NEW(I) + F_TEN(I,J)*
STRESSTRVECNEW(J)
          END DO
          END DO
C   IMPORT PLASTICITY DATA FROM EXTERNAL FILE FOR DIFFERENT
EXPERIMENTS

C*****
C 1. (TRANSVERSE SHEAR PLASTIC-STRAIN VS YIELD STRESS) Y_TR
C*****
      EPS_TRSHEAR_P = EPSVAR_P_INT * XF_CF_SH
      Y_TR = Y_TR_0 * (1.D0 - EXP(-CONST1 * (EPS_TRSHEAR_P +
CONST2) ) )
      D_Y_TR_D_EPSVAR_P = Y_TR_0 * CONST1 * EXP(-CONST1 *
(EPS_TRSHEAR_P + CONST2) )
C*****
C 2. (IN-PLANE SHEAR PLASTIC-STRAIN VS YIELD STRESS) Y_IP
C*****
      EPS_IPSHEAR_P = EPSVAR_P_INT * XF_CF_SH
      Y_IP = Y_IP_0 * (1.D0 - EXP(-CONST1 * (EPS_IPSHEAR_P +
CONST2) ) )
      D_Y_IP_D_EPSVAR_P = Y_IP_0 * CONST1 * EXP(-CONST1 *
(EPS_IPSHEAR_P + CONST2) )
C*****

```

```

C 3. (TRANSVERSE UNIAXIAL TENSION PLASTIC-STRAIN VS YIELD STRESS)
C*****
      EPS_TUT_P = EPSVAR_P_INT * XF_CF_UNI
      Y_2T = Y2T_0 * (1.D0 - EXP(-CONST1 * (EPS_TUT_P + CONST2) )
)
      D_Y_2T_D_EPSVAR_P = Y2T_0 * CONST1 * EXP(-CONST1 *
(EPS_TUT_P + CONST2) )
C*****
C 5. (TRANSVERSE UNIAXIAL COMPRESSION PLASTIC-STRAIN VS YIELD
STRESS) Y_UC
C*****
      EPS_TRUC_P = EPSVAR_P_INT * XF_CF_UNI
      Y_2C = Y2C_0 * (1.D0 - EXP(-CONST1 * (EPS_TRUC_P + CONST2) )
)
      D_Y_2C_D_EPSVAR_P = Y2C_0 * CONST1 * EXP(-CONST1 *
(EPS_TRUC_P + CONST2) )
C*****
C 7. (UNIAXIAL TENSION IN FIBER DIRECTION PLASTIC-STRAIN VS YIELD
STRESS) Y_1T
C*****
      EPS_UXT_P = EPSVAR_P_INT * XF_CF_UNI
      Y_1T = Y1T_0 * (1.D0 - EXP(-CONST1 * (EPS_UXT_P + CONST2) )
)
      D_Y_1T_D_EPSVAR_P = Y1T_0 * CONST1 * EXP(-CONST1 *
(EPS_UXT_P + CONST2) )
C
*****
C 8. (UNIAXIAL COMPRESSION IN FIBER DIRECTION PLASTIC-STRAIN VS
YIELD STRESS) Y_1C
C
*****
      EPS_UXC_P = EPSVAR_P_INT * XF_CF_UNI
      Y_1C = Y1C_0 * (1.D0 - EXP(-CONST1 * (EPS_UXC_P + CONST2) )
)
      D_Y_1C_D_EPSVAR_P = Y1C_0 * CONST1 * EXP(-CONST1 *
(EPS_UXC_P + CONST2) )
C*****
C      DEFINE THE INVARIANTS FOR SHORT FIBER REINFORCED
THERMOPLASTICS
C*****
      CALL INVARIANTS(STRESS_NEW, ND, NSH,XI1,XI2,XI5,XI4,NTT,
A_ST_11,
* A_ST_22,TRSIGMA,DI1DSIGMA,DI2DSIGMA,DI4DSIGMA,DI5DSIGMA)
C CALCULATE NEW ALPHA

      CALL CALCALPHA(Y_TR,Y_IP,Y_1T, Y_1C,Y_2C,Y_2T, ALPHA1,
ALPHA2,
* ALPHA4,ALPHA42, ALPHA5, ALPHA52 )
C DEFINE TENSION OR COMPRESSION SITUATION

C DEFINE INITIA YIELD CRITERION
      XF_YIELD_NEW = ALPHA1 * XI1+ ALPHA2 * XI2 +ALPHA4* XI4 +
* ALPHA42 * XI4** TWO + ALPHA5* XI5 + ALPHA52 * XI5 ** TWO -
ONE

```

```

C   CALCULATE THE GRADIENT OF THE YIELD FUNCTION
      DO I = 1, NTT
        X_N_F(I) = ALPHA1 * DI1DSIGMA(I) + ALPHA2 * DI2DSIGMA(I)
+
        * ALPHA4 * DI4DSIGMA(I) + TWO * ALPHA42 * XI4 *
DI4DSIGMA(I)+
        * ALPHA5 * DI5DSIGMA(I) + TWO * ALPHA52 * XI5 *
DI4DSIGMA(I)
      END DO
C   DETERMINE DALPHA/DEPS BASED ON VOGLERS FORMULA
      DALPHA1DEPSVAR_P = ( -2.D0 / Y_TR ** 3.D0 ) *
D_Y_TR_D_EPSVAR_P
      DALPHA2DEPSVAR_P = ( -2.D0 / Y_IP ** 3.D0 ) *
D_Y_IP_D_EPSVAR_P

      DEN = Y_1T + Y_1C
      XNUM = ONE/Y_1C + ONE/Y_1T + HALF * ALPHA1 * (Y_1C+Y_1T) -
ALPHA2 *
      * (Y_1C+Y_1T)
      DALPHA42DEPSVAR_P = ( (-ONE/Y_1T**TWO + HALF * ALPHA1 -
ALPHA2) *
      * DEN - XNUM ) * D_Y_1T_D_EPSVAR_P / DEN**2.D0 + ( (-
ONE/Y_1C**
      * TWO + HALF * ALPHA1-ALPHA2) *DEN - XNUM ) *
D_Y_1C_D_EPSVAR_P /
      * DEN**2.D0+ HALF * DALPHA1DEPSVAR_P - DALPHA2DEPSVAR_P
      DALPHA4DEPSVAR_P = (-ONE/Y_1T**TWO + HALF * ALPHA1 - ALPHA2
-
      * ALPHA42) * D_Y_1T_D_EPSVAR_P + HALF * Y_1T *
DALPHA1DEPSVAR_P -
      * Y_1T * DALPHA2DEPSVAR_P - Y_1T * DALPHA42DEPSVAR_P
      DEN = Y_2T + Y_2C
      XNUM = ONE/Y_2C + ONE/Y_2T - HALF * ALPHA1 * (Y_2C+Y_2T)
      DALPHA52DEPSVAR_P = ( (-ONE/Y_2T**TWO - HALF * ALPHA1) *DEN
-
      * XNUM ) * D_Y_2T_D_EPSVAR_P /DEN**2.D0 + ((-ONE/Y_2C**TWO -
HALF *
      * ALPHA1) *DEN - XNUM ) * D_Y_2C_D_EPSVAR_P /DEN**2.D0 -
HALF *
      * DALPHA1DEPSVAR_P
      DALPHA5DEPSVAR_P = -(ONE/Y_2T**TWO + HALF * ALPHA1 + ALPHA52
) *
      * D_Y_2T_D_EPSVAR_P - HALF * Y_2T * DALPHA1DEPSVAR_P - Y_2T *
      * DALPHA52DEPSVAR_P
C   END FOR D(ALPHA)/D(EQUIVALENT STRAIN)
      DO I = 1, NTT
        DSIGMADELTA GAMMA(I) = ZERO
      DO J = 1, NTT
        DO K = 1, NTT
          DO L = 1, NTT
            DSIGMADELTA GAMMA(I) = DSIGMADELTA GAMMA(I)+ F_TEN(I,J) *
      * CE_3D(J,K) * X_M_MAT(K,L) * STRESS_NEW(L)
          END DO
        END DO
      END DO

```

```

        END DO
        DSIGMADELTA_GAMMA(I) = - DSIGMADELTA_GAMMA(I)
    END DO

    DO I = 1, NTT
    X_N_G(I) = ZERO
        DO J = 1, NTT
        X_N_G(I) = X_N_G(I) + X_M_MAT(I,J) * STRESS_NEW(I)
        END DO
    END DO

C TEST CALCULATE THE NORM OF N?G
    X_NG_NORM = ZERO
    DO I = 1, NTT
    X_NG_NORM = X_NG_NORM + X_N_G(I)**TWO
    END DO

C
    X_NG_NORM = DSQRT(6.D0 * X_NG_NORM/2.D0)
    X_NG_NORM = DSQRT(5.D0 * X_NG_NORM/2.D0)

    DO I = 1, NTT
        TERM3(I) = ZERO
        DO J = 1, NTT
        TERM3(I) = TERM3(I) + X_M_MAT(I,J) * STRESS_NEW(J)
        END DO
    END DO

VALTERM3 = ZERO
    DO I = 1, NTT
    VALTERM3 = VALTERM3 + TERM3(I)** TWO
    END DO

    VALTERM3 = SQRT(HALF* VALTERM3)

C DEFINE THE VALUE OF STRESS TENSOR
    STRESSVAL = ZERO
    DO I = 1, NTT
    STRESSVAL = STRESSVAL + STRESS_NEW(I)** TWO
    END DO

    STRESSVAL = SQRT(HALF* STRESSVAL)

    DEPS_PDELTA_GAMMA = ZERO
    DO I = 1, NTT
        DO J = 1, NTT
        DEPS_PDELTA_GAMMA = DEPS_PDELTA_GAMMA +
* X_M_MAT(I,J) * STRESS_NEW(I) * DSIGMADELTA_GAMMA(J)
        END DO
    END DO

    DEPS_PDELTA_GAMMA = DELTA_GAMMA_INT * DEPS_PDELTA_GAMMA /
    STRESSVAL + VALTERM3

    DALPHA1DGAMA = DALPHA1DEPSVAR_P * DEPS_PDELTA_GAMMA
    DALPHA2DGAMA = DALPHA2DEPSVAR_P * DEPS_PDELTA_GAMMA
    DALPHA5DGAMA = DALPHA5DEPSVAR_P * DEPS_PDELTA_GAMMA
    DALPHA52DGAMA = DALPHA52DEPSVAR_P * DEPS_PDELTA_GAMMA
    DALPHA4DGAMA = DALPHA4DEPSVAR_P * DEPS_PDELTA_GAMMA
    DALPHA42DGAMA = DALPHA42DEPSVAR_P * DEPS_PDELTA_GAMMA

C CALCULATE DI/DGAMA

```

```

DI1DGAMA = ZERO
DI2DGAMA = ZERO
DI4DGAMA = ZERO
DI5DGAMA = ZERO
  DO I = 1, NTT
DI1DGAMA = DI1DGAMA + DI1DSIGMA(I) * DSIGMADELTA GAMMA(I)
DI2DGAMA = DI2DGAMA + DI2DSIGMA(I) * DSIGMADELTA GAMMA(I)
DI4DGAMA = DI4DGAMA + DI4DSIGMA(I) * DSIGMADELTA GAMMA(I)
DI5DGAMA = DI5DGAMA + DI5DSIGMA(I) * DSIGMADELTA GAMMA(I)
  END DO
DFDGAMA = (XI1 * DALPHA1DGAMA + XI2 * DALPHA2DGAMA + XI4 *
* DALPHA4DGAMA+ XI4**TWO * DALPHA42DGAMA+ XI5 *DALPHA5DGAMA+
XI5**
* TWO * DALPHA52DGAMA) + (ALPHA1 * DI1DGAMA + ALPHA2
*DI2DGAMA +
* ALPHA4 * DI4DGAMA + ALPHA5 *DI5DGAMA + TWO* ALPHA42 * XI4*
* DI4DGAMA + TWO*ALPHA52 * XI5* DI5DGAMA )
  DELTATO2_GAMMA = - XF_YIELD_NEW/DFDGAMA
C
  DELTAGAMMAINT = DELTAGAMMAINT + DELTATO2_GAMMA
C
EPSVAR_P_INT = EPSVAR_P_INT + DELTATO2_GAMMA * X_NG_NORM
C

  IF ( DABS(XF_YIELD_NEW) .LT. PLAST_TOL )
*   GOTO 400

  IF ( NUMC > NUMBREAK ) THEN
  WRITE(*,*) 'NUMC=', NUMC
  GOTO 402
  END IF
C
  END DO ! END FOR MAIN LOOP
C
400 CONTINUE
C 401 CONTINUE
402 CONTINUE
DO I = 1, NTT
STRAINPLAVECNEW(I) = STRAINPLAVECOLD(I) + DELTAGAMMAINT *
X_NG(I)
END DO
EPSVAR_P_NEW = EPSVAR_P_INT

DO I = 1, 6
  DO J = 1, 6
    TERM20(I,J) = ZERO
    DO K1 = 1, 6
      TERM20(I,J) = TERM20(I,J) + CE_3D(I,K1) * X_M_MAT(K1,J)
    END DO
  END DO
END DO
DO I = 1, 6
  DO J = 1, 6
    TERM21(I,J) = STRESS_NEW(I) * X_N_F(J)

```

```
        END DO
    END DO

    DO I = 1, 6
        DO J = 1, 6
            TERM22(I,J) = ZERO
            DO K1 = 1, 6
                TERM22(I,J) = TERM22(I,J) + TERM20(I,K1) * TERM21(K1,J)
            END DO
        END DO
    END DO

    DO I = 1, 6
        DO J = 1, 6
            TERM23(I,J) = ZERO
            DO K1 = 1, 6
                TERM23(I,J) = TERM23(I,J) + TERM22(I,K1) * F_TEN(K1,J)
            END DO
        END DO
    END DO

    DO I = 1, 6
        DO J = 1, 6
            TERM24(I,J) = ZERO
            DO K1 = 1, 6
                TERM24(I,J) = TERM24(I,J) + TERM23(I,K1) * CE_3D(K1,J)
            END DO
        END DO
    END DO

    DO I = 1, 6
        TERM30(I) = ZERO
        DO J = 1, 6
            TERM30(I) = TERM30(I) + X_N_F(I) * F_TEN(I,J)
        END DO
    END DO

    DO I = 1, 6
        TERM31(I) = ZERO
        DO J = 1, 6
            TERM31(I) = TERM31(I) + TERM30(I) * CE_3D(I,J)
        END DO
    END DO

    DO I = 1, 6
        TERM32(I) = ZERO
        DO J = 1, 6
            TERM32(I) = TERM32(I) + TERM31(I) * X_M_MAT(I,J)
        END DO
    END DO

    DENOM = ZERO
    DO I = 1, 6
        DENOM = DENOM + TERM32(I) * STRESS_NEW(I)
```

```

        END DO

        DENOM = DENOM + DABS (DFDGAMA)
C FOR COMPRESSION
C     DENOM = DENOM + DFDGAMA !JUST FOR TRANSVERSE DIRECTION
    DO I = 1, 6
        DO J = 1, 6
            TERM25 (I,J) = CE_3D (I,J) - TERM24 (I,J) / DENOM
        END DO
    END DO

    DO I = 1, 6
        DO J = 1, 6
            C_TAN (I,J) = ZERO
            DO K1 = 1, 6
                C_TAN (I,J) = C_TAN (I,J) + F_TEN (I,K1) * TERM25 (K1,J)
            END DO
        END DO
    END DO

        DO I=1, NTT
            DO J=1, NTT
                IF (C_TAN (I,J) .LT. ZERO) C_TAN (I,J) = ZERO
            END DO
        END DO
GOTO 300

600 CONTINUE ! IF THE PLASTICITY HAS NOT BEEN OCCURED
C GET ELASTIC STRESS
    CALL GETSTRESS3D (CE_3D, CE_2D , STRESS_NEW, STRAINTOTVECNEW,
*     NTT, ND)
C SET ZERO VALUES FOR STRAN PLASTIC VECTOR IN PLASTICITY NOT
HAPPENED
    DO I = 1, NTT
        STRAINPLAVECNEW (I) = ZERO
    END DO
C SET ELASTIC STIFFNESS MATRIX AS THE SECANT STIFFNESS MATRIX
        IF (ND .EQ. 3) THEN
    DO I = 1, 6
        DO J = 1, 6
            C_TAN (I,J) = CE_3D (I,J)
        END DO
    END DO
        ELSE
    DO I = 1, 3
        DO J = 1, 3
            C_TAN (I,J) = CE_2D (I,J)
        END DO
    END DO
        END IF
C UPDATE EQUIVALENT PLASTIC STRAIN
    EPSVAR_P_NEW = EPSVAR_P_OLD
300 CONTINUE

```

```

      RETURN
    END
C*****
*****
C   CONVERT A FOURTH ORDE TENSOR TO CORRESPONDING 3*3 SQUARE
MATRIX IN VOIGT FORM
C*****
*****
      SUBROUTINE TENSTOMATRIX3 (A,B)
      INCLUDE 'ABA_PARAM.INC'
      DIMENSION A(3,3,3,3) , B(3,3)

      DO I = 1 , 3
        DO J = 1,3
          B(I,J) = 0.D0
        END DO
      END DO

      B(1,1) = A(1,1,1,1)
      B(2,1) = A(2,2,1,1)
      B(2,2) = A(2,2,2,2)
      B(3,3) = A(1,2,1,2)
      DO I = 1 , 3
        DO J = 1,3
          B(J,I) = B(I,J)
        END DO
      END DO
C
      RETURN
    END
C*****
*****
C   CONVERT A SECOND ORDE TENSOR TO CORRESPONDING VECTOR IN
VOIGT FORM
C*****
*****
      SUBROUTINE TENS3TOVECTOR (A,B,ND1,NTT1)
      INCLUDE 'ABA_PARAM.INC'
      DIMENSION A(3,3) , B(NTT1)

      IF (ND1.EQ.3) THEN
      DO I = 1 , 3
        DO J = 1,3
          IF ( I .EQ. 1 .AND. J .EQ. 1) M = 1
          IF ( I .EQ. 2 .AND. J .EQ. 2) M = 2
          IF ( I .EQ. 3 .AND. J .EQ. 3) M = 3
          IF ( I .EQ. 1 .AND. J .EQ. 2) M = 4
          IF ( I .EQ. 1 .AND. J .EQ. 3) M = 5
          IF ( I .EQ. 2 .AND. J .EQ. 3) M = 6
          B(M) = A(I,J)
        END DO
      END DO
      ELSE
      DO I = 1 , 3
        DO J = 1,3
          IF ( I .EQ. 1 .AND. J .EQ. 1) M = 1

```

```

                IF ( I .EQ. 2 .AND. J .EQ. 2) M = 2
                IF ( I .EQ. 1 .AND. J .EQ. 2) M = 3
                B(M) = A(I,J)
            END DO
        END DO
    END IF
C
    RETURN
    END
C*****
C    CONVERT A FOURTH ORDE TENSOR TO CORRESPONDING 9*9 SQUARE
MATRIX IN VOIGT FORM
C*****
    SUBROUTINE TENSTOMATRIX(A,B)
    INCLUDE 'ABA_PARAM.INC'
    DIMENSION A(3,3,3,3), B(9,9)

    DO I = 1, 3
        DO J = 1,3
            DO K = 1,3
                DO L = 1,3
                    IF ( I .EQ. 1 .AND. J .EQ. 1) M = 1
                    IF ( K .EQ. 1 .AND. L .EQ. 1) N = 1
                    IF ( I .EQ. 2 .AND. J .EQ. 2) M = 2
                    IF ( K .EQ. 2 .AND. L .EQ. 2) N = 2
                    IF ( I .EQ. 3 .AND. J .EQ. 3) M = 3
                    IF ( K .EQ. 3 .AND. L .EQ. 3) N = 3
                    IF ( I .EQ. 2 .AND. J .EQ. 3) M = 4
                    IF ( K .EQ. 2 .AND. L .EQ. 3) N = 4
                    IF ( I .EQ. 1 .AND. J .EQ. 3) M = 5
                    IF ( K .EQ. 1 .AND. L .EQ. 3) N = 5
                    IF ( I .EQ. 1 .AND. J .EQ. 2) M = 6
                    IF ( K .EQ. 1 .AND. L .EQ. 2) N = 6
                    B(M,N) = A(I,J,K,L)
                END DO
            END DO
        END DO
    END DO

C TO FILL THE COULUMNS 7, 8 AND 9
    DO I = 1, 9
        DO J = 7,9
            B(I,J) = B(I, J-3)
        END DO
    END DO

C TO FILL THE ROWS 7, 8 AND 9
    DO I = 7, 9
        DO J = 1,9
            B(I,J) = B(I-3, J)
        END DO
    END DO

C
    RETURN
    END

```

```

C*****
C                                     DEFINE FOURTH ORDER STIFFNESS TENSOR CE
C*****
      SUBROUTINE STIFF4TH_2D(CE, XNU_12,E_11, E_22, XNU_23,
G_12,A_DIR,
*   ND, NSH,A_ST_11,A_ST_22, CE_2D,CE_3D)
      INCLUDE 'ABA_PARAM.INC'
      DIMENSION CE(3,3,3,3), DELTA(3,3),CE_2D(3,3),
*   A_DIR(3,3),X_I_A(3,3,3,3), CE_3D(6,6),
A_DIR_V(3),X_I(3,3,3,3)
      XNU_21 = E_11 * XNU_12 / E_22
      E_33 = E_22
      XNU_32 = E_22 * XNU_23 / E_33
      XNU_13 = XNU_12 ! CHECK IT AGAIN
      XNU_31 = E_11 * XNU_13 / E_33
      G_13 = G_12
      G_23 = E_22 / ( 2.D0 * ( 1.D0 + XNU_23) )
      DET = 1.D0 - XNU_32 ** 2.D0 - 2.D0 * XNU_13 * XNU_31 -
2.D0 *
*   XNU_32 * XNU_31 * XNU_13

      XNU12_LIMIT = SQRT(.5D0 * (1.D0 - XNU_23)* E_22 / E_11)
      XNU21_LIMIT = SQRT(.5D0 * (1.D0 - XNU_23)* E_11 / E_33)
      XNU23_LIMIT = 1.D0 - 2.D0 * (XNU_12 ** 2.D0) * E_11 /E_22

      IF ( DABS(XNU_12).GE.XNU12_LIMIT )THEN
WRITE(*,*) 'XNU12=LIMIT', XNU12_LIMIT
      WRITE(*,*) 'E_11=', E_11
      WRITE(*,*) 'E_22=', E_22
      WRITE(*,*) 'XNU_12=', XNU_12
      WRITE(*,*) 'XNU_21=', XNU_21
      WRITE(*,*) 'E_33=', E_33
      WRITE(*,*) 'G_13=', G_13
      WRITE(*,*) 'XNU_23=', XNU_23
WRITE(*,*) 'ERROR: THE GIVEN MAT PROPERTIES CAN NOT BE TRUE'
      CALL XIT
END IF
      IF ( DABS(XNU_21).GE.XNU21_LIMIT )THEN
WRITE(*,*) 'XNU21_LIMIT', XNU21_LIMIT
WRITE(*,*) 'ERROR: THE GIVEN MAT PROPERTIES CAN NOT BE TRUE'
      CALL XIT
END IF
      IF ( XNU_23.GE.XNU23_LIMIT .OR. XNU_23.LT. (-1.D0) )THEN
WRITE(*,*) 'XNU23_LIMIT=', XNU23_LIMIT
WRITE(*,*) 'ERROR: THE GIVEN MAT PROPERTIES CAN NOT BE TRUE'
      CALL XIT
END IF

      GOTO 234
      XLANDA = E_22 * (XNU_23 + XNU_31 * XNU_13) / DET
      ALPHA = E_22 * ( XNU_31 * ( 1.D0 + XNU_32 - XNU_13 ) -
XNU_32 ) /DET
      BETHA = E_11 * ( 1.D0 - XNU_32 * XNU_23 ) / DET - E_22 * (
1.D0 -

```

```

* XNU_21 * ( XNU_12 + 2.00 * ( 1.00 + XNU_23 ) ) ) / DET -
4.00 *
* G_12
234 CONTINUE
C
DELTA1 = 1.00 - XNU_12 * XNU_21 * (1.00 + XNU_23) -
XNU_23**2.00
XLANDA = (1.00 - XNU_12 * XNU_21) * E_22 / DELTA1 - 2.00 *
G_12
ALPHA = (XNU_21 + XNU_21 * XNU_23) * E_22 / DELTA1 - XLANDA
BETHA = (1.00 - XNU_23**2.00) * E_11 / DELTA1 - XLANDA - 2.00
*
* ALPHA - 4.00 * G_12 + 2.00 * G_23
C
C DEFINE KRONECKER DELTA
DO I = 1, 3
DO J = 1, 3
IF ( I .EQ. J ) THEN
DELTA(I,J) = 1.00
ELSE
DELTA(I,J) = 0.00
END IF
END DO
END DO
CALL FIBER_DIR(A_DIR,A_ST_11,A_ST_22)
A_DIR_V(1) = A_DIR(1,1)
A_DIR_V(2) = A_DIR(2,2)
A_DIR_V(3) = A_DIR(3,3)

DO I = 1, 3
DO J = 1, 3
DO K = 1, 3
DO L = 1, 3
X_I(I,J,K,L) = 0.500 * ( DELTA(I,K) * DELTA(J,L) +
DELTA(I,L) * DELTA(J,K) )
END DO
END DO
END DO
END DO

DO I = 1, 3
DO J = 1, 3
DO K = 1, 3
DO L = 1, 3
X_I_A(I,J,K,L) = 0.00
DO M = 1, 3
X_I_A(I,J,K,L) = X_I_A(I,J,K,L) + A_DIR_V(I) * X_I(J,M,K,L)
*
* A_DIR_V(M) + A_DIR_V(M) * X_I(M,I,K,L) * A_DIR_V(J)
END DO
END DO
END DO
END DO
END DO

```

```

      DO I = 1, 3
        DO J = 1, 3
          DO K = 1, 3
            DO L = 1, 3
              X_I_A(I,J,K,L) = 0.D0
              DO M = 1, 3
                X_I_A(I,J,K,L) = X_I_A(I,J,K,L) + A_DIR(I,M)* 0.5D0 *
* ( DELTA(J,K)* DELTA(M,L) + DELTA(J,L)* DELTA(M,K) ) +
* A_DIR(J,M) * 0.5D0 * ( DELTA(M,K)* DELTA(I,L) + DELTA(M,L)*
* DELTA(I,K) )
              END DO
            END DO
          END DO
        END DO
      END DO

      DO I = 1, 3
        DO J = 1, 3
          DO K = 1, 3
            DO L = 1, 3
              CE(I,J,K,L) = XLANDA *DELTA(I,J)* DELTA(K,L) +2.D0 * G_23 *
0.5D0*
* ( DELTA(I,K)* DELTA(J,L) + DELTA(I,L)* DELTA(J,K) ) +
ALPHA *
* ( A_DIR(I,J) * DELTA(K,L) + DELTA(I,J) * A_DIR(K,L)) +
BETHA *
* A_DIR_V(I) * A_DIR_V(J) *A_DIR_V(K) * A_DIR_V(L) + 2.D0 *
* (G_12 - G_23 ) * X_I_A(I,J,K,L)
            END DO
          END DO
        END DO
      END DO

      CALL TENSTOMATRIX6(CE,CE_3D)
      CALL TENSTOMATRIX3(CE,CE_2D)
      GOTO 326
      DO I = 1, 6
        DO J = 1, 6
          CE_3D(I,J) = 0.D0
        END DO
      END DO
      CE_3D(1,1) = (1.D0 - XNU_32 * XNU_23) * E_11 / DET
      CE_3D(1,2) = (XNU_21 + XNU_31 * XNU_23) * E_22 / DET
      CE_3D(1,3) = (XNU_31 + XNU_21 * XNU_32) * E_33 / DET
      CE_3D(2,2) = (1.D0 - XNU_31 * XNU_13) * E_22 / DET
      CE_3D(2,3) = (XNU_32 + XNU_31 * XNU_12) * E_33 / DET
      CE_3D(3,3) = (1.D0 - XNU_21 * XNU_12) * E_33 / DET
      CE_3D(4,4) = G_12
      CE_3D(5,5) = G_13
      CE_3D(6,6) = G_23
      DO I = 1, 6
        DO J = 1, 6
          CE_3D(J,I) = CE_3D(I,J)
        END DO
      END DO

```

```

                END DO
            END DO
326 CONTINUE

RETURN
END
C*****
C   CALCULATE INITIAL ALPHA VALUES FOR SHORT FIBER REINFORCED
THERMOPLASTICS
C*****
    SUBROUTINE CALCALPHA(Y_TR,Y_IP,Y1T, Y1C, Y2C,Y2T, ALPHA1,
*       ALPHA2,ALPHA4,ALPHA42, ALPHA5, ALPHA52 )
    INCLUDE 'ABA_PARAM.INC'
    PARAMETER (ZERO = 0.D0, ONE = 1.D0, TWO = 2.D0, HALF =
0.5D0,
1       THREE = 3.D0, FOUR = 4.D0 )
C   DETERMINATION OF ALPHA VALUES FOR INITIAL PLASTICITY OF SHORT
FIBERS
    ALPHA1 = ONE / Y_TR ** TWO      ! TR = TRANSVERSE SHEAR
    ALPHA2 = ONE / Y_IP ** TWO      ! IP = IN-PLANE SHEAR
C
    ALPHA42 = (ONE/Y1C +ONE/Y1T + HALF * ALPHA1 * (Y1C+Y1T) -
ALPHA2 * (Y1C+Y1T) )/(Y1C+Y1T)
    ALPHA4 = ONE/Y1T + HALF * Y1T *ALPHA1 - Y1T * ALPHA2 -
ALPHA42 * Y1T
    ALPHA52 =(ONE/Y2C +ONE/Y2T - HALF * ALPHA1 * (Y2C+Y2T)
)/ (Y2C+Y2T)
    ALPHA5 = ONE/Y2T - HALF * Y2T * ALPHA1 - ALPHA52 * Y2T

RETURN
END
C*****
C   CALCULATE INITIAL BETA VALUES FOR SHORT FIBER REINFORCED
THERMOPLASTICS
C*****
    SUBROUTINE CALCBETA(Y_TR,Y_IP,Y1T, Y1C, Y2C,Y2T, BETA1,
*       BETA2,BETA32T,BETA32C, BETA42T, BETA42C )
    INCLUDE 'ABA_PARAM.INC'
    PARAMETER (ZERO = 0.D0, ONE = 1.D0, TWO = 2.D0, HALF =
0.5D0,
1       THREE = 3.D0, FOUR = 4.D0 )
C   DETERMINATION OF ALPHA VALUES FOR INITIAL PLASTICITY OF SHORT
FIBERS
    BETA1 = 1.D0 / Y_TR ** 2.D0      ! TR = TRANSVERSE SHEAR
    BETA2 = 1.D0 / Y_IP ** 2.D0      ! IP = IN-PLANE SHEAR
C
    BETA32T = FOUR/(Y2T ** TWO )- TWO * BETA1
    BETA42T = ONE / Y1T ** TWO - BETA32T - BETA2 + HALF * BETA1
C
    BETA32C= FOUR / (Y2C ** TWO )- BETA1
    BETA42C = ONE / (Y1C ** TWO ) + BETA1 / TWO - BETA2 - BETA32C
C

RETURN

```

```

END
C*****
C                                     CONVERT VECTOR TO TENSOR (SYMMETRIC ONE)
C*****
SUBROUTINE CONVVECTORTO2RANKTENS_2D(VECTOR,TENSOR, ND, NSH)
INCLUDE 'ABA_PARAM.INC'
DIMENSION TENSOR(3,3), VECTOR(ND+NSH)
DO I = 1, 3
  DO J = 1, 3
    TENSOR(I,J) = 0.D0
  END DO
END DO
IF (ND.EQ.3) THEN
  TENSOR(1,1) = VECTOR(1)
  TENSOR(2,2) = VECTOR(2)
  TENSOR(3,3) = VECTOR(3)
  TENSOR(1,2) = VECTOR(4)
  TENSOR(1,3) = VECTOR(5)
  TENSOR(2,3) = VECTOR(6)
ELSE
  TENSOR(1,1) = VECTOR(1)
  TENSOR(2,2) = VECTOR(2)
  TENSOR(3,3) = 0.D0
  TENSOR(1,2) = VECTOR(3)
  TENSOR(1,3) = 0.D0
  TENSOR(2,3) = 0.D0
END IF

DO I = 1, 3
  DO J = 1, 3
    TENSOR(J,I) = TENSOR(I,J)  ! FOR SYMMETRIC TENSORS
  END DO
END DO
C
RETURN
END
C*****
C  LINEAR INTERPOLATION FUNCTION
C*****
FUNCTION YIINTP(XA ,YA ,XB , YB, X)
INCLUDE 'ABA_PARAM.INC'
  YIINTP = YA + (YB - YA) * (X-XA) / (XB-XA)
RETURN
END
C*****
C  TRACE FUNCTION
C*****
FUNCTION TR(A11 ,A22 , A33)
INCLUDE 'ABA_PARAM.INC'
  TR = A11 + A22 + A33

RETURN
END
C*****

```

```

C  CALCULATE THE SQUARE OF THE 2-D T TENSOR AND ITS TRACE
C*****
      SUBROUTINE INVARIANTS(T_3D, NDT,
NSHT,XI1_T,XI2_T,XI5_T,XI4_T, NTTT,A_11_T,
      * A_22_T , TRT,DI1DSIGMAV,DI2DSIGMAV,DI4DSIGMAV,DI5DSIGMAV)
      INCLUDE 'ABA_PARAM.INC'
      DIMENSION T_3D(NDT+NSHT) , T_2D(3,3) , TTO2(3,3) ,
STRT(3,3) ,
      * AT(3,3) , UNI(3,3) , SIG_P(3,3) , T_DEV(3,3) , TA(3,3) ,
      * A_DIR(3,3) , ADEVT(3,3) , DELTA(3,3) ,ATTO2(3,3) , DEVT(3,3) ,
      * DI1DSIGMA(3,3) , DI2DSIGMA(3,3) ,DI4DSIGMA(3,3) ,
DI3DSIGMA(3,3) ,
      * DI1DSIGMAV(NTTT) , DI2DSIGMAV(NTTT) ,DI4DSIGMAV(NTTT) ,
      * DI3DSIGMAV(NTTT) ,DI5DSIGMA(3,3) ,DI5DSIGMAV(NTTT) ,A_DIR_V(3)
      PARAMETER (ZERO = 0.D0, ONE = 1.D0, TWO = 2.D0, HALF =
0.5D0,
      1          THREE = 3.D0)

C      DEFINE KRONECKER DELTA
      DO I = 1, 3
        DO J = 1, 3
          IF ( I .EQ. J ) THEN
            DELTA(I,J) = ONE
          ELSE
            DELTA(I,J) = ZERO
          END IF
        END DO
      END DO

C      CONVERT VECTOR TO TENSOR; IN THIS CASE T = STRESS OR STRAIN
      CALL CONVVECTORTO2RANKTENS_2D(T_3D,T_2D, NDT, NSHT)
C      DEFINE MATERIAL DIRECTION VECTOR A(A1,A2,A3)
      CALL FIBER_DIR(A_DIR,A_11_T,A_22_T)
      A_DIR_V(1)=A_DIR(1,1)
      A_DIR_V(2)=A_DIR(2,2)
      A_DIR_V(3)=A_DIR(3,3)
C      DETERMINE TRACE STRESS TENSOR
      TRT = ZERO
      DO I = 1, 3
        DO J = 1, 3
          TRT = TRT + T_2D(I,J) * DELTA(I,J)
        END DO
      END DO

C      DEFINE DEVIATORIC STRESS ?^'= ?-1/3 TR(?)?
      DO I = 1, 3
        DO J = 1, 3
          DEVT(I,J) = T_2D(I,J) - (ONE / THREE) * TRT * DELTA(I,J)
        END DO
      END DO

C      DETERMINE THE TERM A?^'
      DO I = 1, 3
        DO J = 1, 3
          ADEVT(I,J) = ZERO
          DO M = 1, 3
            ADEVT(I,J) = ADEVT(I,J) + A_DIR(I,M) * DEVT(M,J)
          END DO
        END DO
      END DO

```

```

        END DO
    END DO
END DO
C   DETERMINE THE TRACE A?^'
    TRADEVT = ZERO
    DO I = 1, 3
        DO J = 1, 3
            TRADEVT = TRADEVT + ADEVT(I,J) * DELTA(J,I)
        END DO
    END DO
C   DETERMINE THE TRACE A
    TRA = ZERO
    DO I = 1, 3
        DO J = 1, 3
            TRA = TRA + ADEVT(I,J) * DELTA(I,J)
        END DO
    END DO
C   DETERMINE THE TERM A?
    DO I = 1, 3
        DO J = 1, 3
            AT(I,J) = ZERO
            TA(I,J) = ZERO
            DO M = 1, 3
C           AT(I,J) = AT(I,J) + A_DIR(I,M) * T_2D(M,J)
                AT(I,J) = AT(I,J) + A_DIR_V(I) * T_2D(J,M) * A_DIR_V(M)
                TA(I,J) = TA(I,J) + A_DIR_V(M) * T_2D(M,I) * A_DIR_V(J)
            END DO
        END DO
    END DO
C   DETERMINE THE TRACE A?^'
    TRAT = ZERO
    TRTA = ZERO
    DO I = 1, 3
        DO J = 1, 3
            TRAT = TRAT + AT(I,J) * DELTA(I,J)
            TRTA = TRTA + TA(I,J) * DELTA(I,J)
        END DO
    END DO
C   DETERMINE THE TERM SIG^2
    DO I = 1, 3
        DO J = 1, 3
            TTO2(I,J) = ZERO
            DO M = 1, 3
                TTO2(I,J) = TTO2(I,J) + T_2D(I,M) * T_2D(M,J)
            END DO
        END DO
    END DO
C   CALCULATE TRACE SIG^2
    TRTTO2 = ZERO
    DO I = 1, 3
        DO J = 1, 3
            TRTTO2 = TRTTO2 + TTO2(I,J) * DELTA(I,J)
        END DO
    END DO

```

```

C   DETERMINE THE TERM A*SIG^2
      DO I = 1, 3
        DO J = 1, 3
          ATTO2(I,J) = ZERO
            DO M = 1, 3
              ATTO2(I,J) = ATTO2(I,J) + A_DIR(I,M) * TTO2(M,J)
            END DO
          END DO
        END DO
      END DO

C   CALCULATE TRACE A*SIG^2
      TRATTO2 = ZERO
      DO I = 1, 3
        DO J = 1, 3
          TRATTO2 = TRATTO2 + ATTO2(I,J) * DELTA(I,J)
        END DO
      END DO

C   DETERMINE FIRST INVARIANT I_1=1/2 TR[?^2 ]-TR[A?^2 ]
      XI1_T = HALF * TRTTO2 - TRATTO2

C   DETERMINE THE SECOND INVARIANT I_2=TR[A?^2 ]
      XI2_T = TRATTO2

C   DETERMINE THIRD INVARIANT I3 = 3/2 TR[A?^' ]
      XI3_T = (THREE / TWO) * TRADEVT

C   DETERMINE I4 =TR[A?]
      XI4_T = TRAT
      XI5_T = TRT-TRAT

C   DEFINE INITIAL YIELD CRITERION
C   DEFINE DEVIATORIC STRESS ?^' = ?-1/3 TR(??)
      DO I = 1, 3
        DO J = 1, 3
          DI1DSIGMA(I,J) = T_2D(I,J) - ( AT(I,J) + TA(I,J) )
          DI2DSIGMA(I,J) = AT(I,J) + TA(I,J)
          DI3DSIGMA(I,J) = HALF * ( THREE * A_DIR(I,J) -TRA
*DELTA(I,J) )
          DI4DSIGMA(I,J) = A_DIR(I,J)
          DI5DSIGMA(I,J) = DELTA(I,J) - A_DIR(I,J)
        END DO
      END DO

C   CONVERT TO VECTORS
      CALL TENS3TOVECTOR(DI1DSIGMA,DI1DSIGMAV,NDT,NTTT)
      CALL TENS3TOVECTOR(DI2DSIGMA,DI2DSIGMAV,NDT,NTTT)
      CALL TENS3TOVECTOR(DI3DSIGMA,DI3DSIGMAV,NDT,NTTT)
      CALL TENS3TOVECTOR(DI4DSIGMA,DI4DSIGMAV,NDT,NTTT)
      CALL TENS3TOVECTOR(DI5DSIGMA,DI5DSIGMAV,NDT,NTTT)
      RETURN
      END

C*****
C   DETERMINE THE STRUCTRUL TENSOR A WHICH SHOWS THE DIRECTIONS OF
THE FIBERS
C*****
      SUBROUTINE FIBER_DIR(A_DIR_TEN,A_ST_11,A_ST_22)
      INCLUDE 'ABA_PARAM.INC'
      DIMENSION A_DIR_TEN(3,3)
      A_DIR_TEN(1,1) = A_ST_11
      A_DIR_TEN(1,2) = 0.D0

```

```

A_DIR_TEN(1,3) = 0.D0
A_DIR_TEN(2,1) = 0.D0
A_DIR_TEN(2,2) = A_ST_22
A_DIR_TEN(2,3) = 0.D0
A_DIR_TEN(3,1) = 0.D0
A_DIR_TEN(3,2) = 0.D0
A_DIR_TEN(3,3) = 1.D0 - A_ST_22 - A_ST_11
RETURN
END
C*****
C  MATRIX N BY N INVERSE SUBROUTINE
C*****
SUBROUTINE INVERSE (A,C,N)
INCLUDE 'ABA_PARAM.INC'
!-----
! INVERSE MATRIX
! METHOD: BASED ON DOOLITTLE LU FACTORIZATION FOR AX=B
! ALEX G. DECEMBER 2009
!-----
! INPUT ...
! A(N,N) - ARRAY OF COEFFICIENTS FOR MATRIX A
! N      - DIMENSION
! OUTPUT ...
! C(N,N) - INVERSE MATRIX OF A
! COMMENTS ...
! THE ORIGINAL MATRIX A(N,N) WILL BE DESTROYED
! DURING THE CALCULATION
!-----

DIMENSION A(N,N) , C(N,N) , PTEM(N,N) , U(N,N) , B(N) , D(N) ,
X(N)

! STEP 0: INITIALIZATION FOR MATRICES L AND U AND B
! FORTRAN 90/95 ALOOWS SUCH OPERATIONS ON MATRICES
PTEM=0.D0
U=0.D0
B=0.D0
! STEP 1: FORWARD ELIMINATION
DO K=1, N-1
DO I=K+1,N
COEFF=A(I,K)/A(K,K)
PTEM(I,K) = COEFF
DO J=K+1,N
A(I,J) = A(I,J) - COEFF*A(K,J)
END DO
END DO
END DO

! STEP 2: PREPARE L AND U MATRICES
! L MATRIX IS A MATRIX OF THE ELIMINATION COEFFICIENT
! + THE DIAGONAL ELEMENTS ARE 1.0
DO I=1,N
PTEM(I,I) = 1.D0

```

```

      END DO
! U MATRIX IS THE UPPER TRIANGULAR PART OF A
      DO J=1,N
      DO I=1,J
        U(I,J) = A(I,J)
      END DO
    END DO

! STEP 3: COMPUTE COLUMNS OF THE INVERSE MATRIX C
      DO K=1,N
        B(K)=1.D0
        D(1) = B(1)
! STEP 3A: SOLVE LD=B USING THE FORWARD SUBSTITUTION
        DO I=2,N
          D(I)=B(I)
          DO J=1,I-1
            D(I) = D(I) - PTEM(I,J)*D(J)
          END DO
        END DO
! STEP 3B: SOLVE UX=D USING THE BACK SUBSTITUTION
        X(N)=D(N)/U(N,N)
        DO I = N-1,1,-1
          X(I) = D(I)
          DO J=N,I+1,-1
            X(I)=X(I)-U(I,J)*X(J)
          END DO
          X(I) = X(I)/U(I,I)
        END DO
! STEP 3C: FILL THE SOLUTIONS X(N) INTO COLUMN K OF C
        DO I=1,N
          C(I,K) = X(I)
        END DO
        B(K)=0.D0
      END DO

      RETURN
    END

C*****
C CALCULATE THE STRESS BASED ON THE DAMAGE
VARIABLES*****
C*****
      SUBROUTINE GETSTRESS3D(CFULL,CDTHREE,
STRESS_T,STRANT,NTT,ND)
      INCLUDE 'ABA_PARAM.INC'
      DIMENSION CFULL(6,6),STRESS_T(NTT),STRANT(NTT),
* CDTHREE(3,3)
      PARAMETER (ZERO = 0.D0, ONE = 1.D0, TWO = 2.D0, HALF =
0.5D0,
* THREE = 3.D0)

C UPDATE THE STRESS STATE IF 3D CASE
C

```

```

      IF (ND .EQ. 3) THEN
        DO I = 1, NTT
          STRESS_T(I)=ZERO
          DO J = 1, NTT
            STRESS_T(I)=STRESS_T(I)+CFULL(I,J) * STRANT(J)
          END DO
        END DO
      C
      C      INITIALIZE THE 3X3 CONDENSED STIFFNESS MATRIX IF PLANE
      C      STRESS CASE
      C
      ELSE IF ( ND .EQ. 2) THEN
      C      UPDATE THE STRESS
        DO I = 1, NTT
          STRESS_T(I)=ZERO
          DO J = 1, NTT
            STRESS_T(I)=STRESS_T(I)+CDTHREE(I,J) * STRANT(J)
          END DO
        END DO

      END IF
      C
      RETURN
      END
      C*****
      C CALCULATE THE STRESS IN PLASTIC REGION
      C*****
      SUBROUTINE GETSTRESS3D_FULL(CFULL,CDTHREE ,DFT,
*      DMT,STRANT,NT,ND, STR,CFDT)
      INCLUDE 'ABA_PARAM.INC'
      DIMENSION CFULL(6,6),CFDT(6,6),STR(NT),STRANT(NT),
*      CDTHREE(3,3)
      PARAMETER (ZERO = 0.D0, ONE = 1.D0, TWO = 2.D0, HALF =
0.5D0,
*      THREE = 3.D0)
      C      CDTHREE.....DAMAGED CONDENSED-ELASTICITY MATRIX FOR PLANE
      C      STRESS PROBLEM
        DO I = 1, NT
          DO J = 1, NT
            CFDT(I,J) = CFULL(I,J)
          END DO
        END DO

      IF ( (DFT .NE. ZERO) .OR. (DMT .NE. ZERO) ) THEN
        CFDT(1,1) = (ONE - DFT)* CFULL(1,1)
        CFDT(1,2) = (ONE - DFT) * (ONE - DMT) * CFULL(1,2)
        CFDT(2,1) = CFDT(1,2)
        CFDT(2,2) = (ONE - DMT) * CFULL(2,2)
        CFDT(1,3) = (ONE - DFT) * CFULL(1,3)
        CFDT(3,1) = CFDT(1,3)
        CFDT(2,3) = (ONE - DMT) * CFULL(2,3)
        CFDT(3,2) = CFDT(2,3)
        CFDT(4,4) = (ONE - DMT) * (ONE - DFT) * CFULL(4,4)
      END IF

```

```

C
  IF (ND .EQ. 3) THEN
    DO I = 1, NT
      STR(I)=ZERO
      DO J = 1, NT
        STR(I)=STR(I)+CFDT(I,J) * STRANT(J)
      END DO
    END DO
  C   INITIALIZE THE 3X3 CONDENSED STIFFNESS MATRIX IF PLANE
  STRESS CASE
  ELSE IF ( ND .EQ. 2) THEN
  C   UPDATE THE STRESS
    DO I = 1, NT
      STR(I)=ZERO
      DO J = 1, NT
        STR(I)=STR(I)+CDTHREE(I,J) * STRANT(J)
      END DO
    END DO
  END IF
  RETURN
  END
C*****
C   CONVERT A FOURTH ORDE TENSOR TO CORRESPONDING 6*6 SQUARE
  MATRIX IN VOIGT FORM
C*****
  SUBROUTINE TENSTOMATRIX6(A,B)
  INCLUDE 'ABA_PARAM.INC'
  DIMENSION A(3,3,3,3), B(6,6)

    DO I = 1,6
      DO J = 1,6
        B(J,I) = 0.D0
      END DO
    END DO

  DO I = 1, 3
    DO J = 1,3
      DO K = 1,3
        DO L = 1,3
          IF ( I .EQ. 1 .AND. J .EQ. 1) M = 1
          IF ( K .EQ. 1 .AND. L .EQ. 1) N = 1
          IF ( I .EQ. 2 .AND. J .EQ. 2) M = 2
          IF ( K .EQ. 2 .AND. L .EQ. 2) N = 2
          IF ( I .EQ. 3 .AND. J .EQ. 3) M = 3
          IF ( K .EQ. 3 .AND. L .EQ. 3) N = 3
          IF ( I .EQ. 1 .AND. J .EQ. 2) M = 4
          IF ( K .EQ. 1 .AND. L .EQ. 2) N = 4
          IF ( I .EQ. 1 .AND. J .EQ. 3) M = 5
          IF ( K .EQ. 1 .AND. L .EQ. 3) N = 5
          IF ( I .EQ. 2 .AND. J .EQ. 3) M = 6
          IF ( K .EQ. 2 .AND. L .EQ. 3) N = 6
          B(M,N) = A(I,J,K,L)
        END DO
      END DO
    END DO
  END DO

```

```

        END DO
    END DO
C     APPLY SYMMETRY
        DO I = 1,6
            DO J = 1,6
                B(J,I) = B(J,I)
            END DO
        END DO

    RETURN
END

C*****
C     SUBROUTINE JACOBIAN
C*****
    SUBROUTINE XJACOBIAN_CALC (CFDT, CFULL,DT, NTT,ND,DMT,
*   DFT ,STRANT,ETA, XJACOBI,DDFDE,DDMDE)
    INCLUDE 'ABA_PARAM.INC'
    DIMENSION CFDT(6,6), DCDDMT(6,6),DCDDMC(6,6),DCDDFT(6,6),
1   DCDDFC(6,6),DFCDE(NTT), DFTDE(NTT), DMTDE(NTT),
2   XJACOBI(NTT,NTT), TDDSDDE(6,6), ATEMP1(NTT),ATEMP2(NTT),
3   ATEMP3(NTT),ATEMP4(NTT),DMCDE(NTT), TSTRANT(4),
4   STRANT(NTT),
CFULL(6,6),DDFDE(NTT),DDMDE(NTT),DCDDM(NTT,NTT),
5   DCDDF(NTT,NTT)
    PARAMETER (ZERO = 0.00, ONE = 1.00, HALF = 0.500)

C     CALCULATE THE DERIVATIVE MATRIX DC/DDM, DC/DDF OF THE
DAMAGED MATRIX
C
    CALL ELASTICDERIVATIVE_TEST(CFULL,DMT,DFT, DCDDM,DCDDF)
C     UPDATE THE JACOBIAN
C
C     FULL 3D CASE
    IF (ND .EQ. 3) THEN
        DO I = 1, NTT
            ATEMP1(I) = ZERO
            DO J = 1, NTT
                ATEMP1(I) = ATEMP1(I) + DCDDM(I,J) * STRANT(J)
            END DO
        END DO
        DO I = 1, NTT
            ATEMP2(I) = ZERO
            DO J = 1, NTT
                ATEMP2(I) = ATEMP2(I) + DCDDF(I,J) * STRANT(J)
            END DO
        END DO
        DO I = 1, NTT
            DO J = 1, NTT
                XJACOBI(I,J)=CFDT(I,J) + ( ATEMP1(I) * DDMDE(J)
1             + ATEMP2(I) * DDFDE(J) ) * DT / (DT + ETA)
            END DO
        END DO
C     ! PLANE STRESS CASE

```

```

C
  ELSE IF (ND .EQ.2) THEN
    TSTRANT(1) = STRANT(1)
    TSTRANT(2) = STRANT(2)
    TSTRANT(3) = -CFDT(1,3) / CFDT(3,3) * STRANT(1)
1      - CFDT(2,3) / CFDT(3,3) * STRANT(2)
    TSTRANT(4) = STRANT(3)
    DO I = 1, 4
      ATEMP1(I) = ZERO
      DO J = 1, 4
        ATEMP1(I) = ATEMP1(I) + DCDDM(I,J) * TSTRANT(J)
      END DO
    END DO

    DO I = 1, 4
      ATEMP2(I) = ZERO
      DO J = 1, 4
        ATEMP2(I) = ATEMP2(I) + DCDDF(I,J) * TSTRANT(J)
      END DO
    END DO

    DO I = 1,6
      DO J = 1,6
        TDDSDDE(I,J) = ZERO
      END DO
    END DO
C
C TO GET THE UNCONDENSED JACOBIAN FOR PLANE STRESS CASE
  DO I = 1, NTT
    DO J = 1, NTT
      XJACOBI(I,J) = ZERO
    END DO
  END DO
  DO I = 1, 4
    DO J = 1, 4
1      TDDSDDE(I,J) = CFDT(I,J) + ( ATEMP1(I) * DDMDE(J)
      + ATEMP2(I) * DDFDE(J) ) * DT / (DT + ETA)
    END DO
  END DO
C
C CONDENSE THE JACOBIAN MATRIX FOR PLANE STRESS PROBLEM
C
  CALL MATRIXCONDENSE(TDDSDDE,XJACOBI)
END IF

RETURN
END
C*****
C
C SUBROUTINE : DERIVDELTA
C*****
SUBROUTINE DERIVDELTA(DDDDELTA0,DDDDELTAEQ, DEL_EQ, DEL_F,
* DELTA_PLA, DEL_EQ_0)
  INCLUDE 'ABA_PARAM.INC'
  DDDDELTA0 = (DEL_EQ - DEL_F) / ((DEL_EQ - DELTA_PLA) *
* (DEL_F - DEL_EQ_0) ** 2.D0)
  DDDDELTAEQ = (DEL_F - DELTA_PLA) * (DEL_EQ - DEL_F )

```

```

* / ( (DEL_EQ - DELTA_PLA) ** 2.D0 * (DEL_F - DEL_EQ_0))
RETURN
END
C*****
C SUBROUTINE TO CONDENSE THE 4X4 MATRIX INTO 3X3 MATRIX*
C*****
SUBROUTINE MATRIXCONDENSE (CFULL,CTHREE)
INCLUDE 'ABA_PARAM.INC'
DIMENSION CFULL (6,6),CTHREE (3,3)
C
CTHREE (1,1) = CFULL (1,1) - CFULL (1,3) * CFULL (3,1) /
CFULL (3,3)
CTHREE (1,2) = CFULL (1,2) - CFULL (1,3) * CFULL (3,2) /
CFULL (3,3)
CTHREE (2,1) = CFULL (2,1) - CFULL (2,3) * CFULL (3,1) /
CFULL (3,3)
CTHREE (2,2) = CFULL (2,2) - CFULL (2,3) * CFULL (3,2) /
CFULL (3,3)
CTHREE (3,3) = CFULL (4,4)
RETURN
END
C*****
C TO CHECK THE FAILURE INITIATION AND THE CORRESPONDING
DERIVATIVE
C*****
SUBROUTINE CHECKFAILURE (X_C,X_T,Y_C,Y_T,S_12,STRESST,
DFTOLDT,
* DMTOLDT,NDI, NSH, XLC,G_FT_C,G_MT_C,STRAIN,EPS_F_X_T,
EPS_F_X_C,
* EPS_F_Y_T, EPS_F_Y_C, EPS_SC, CFULL, NTT, STRAINPLA,DFT,
* DMT, NOEL,DDFDET, DDMDET)
INCLUDE 'ABA_PARAM.INC'
DIMENSION STRESST (NTT), STRAIN (NTT),CFULL (6,6),
* STRAINPLA (NTT),DFMNDE (NTT), STRAINPLAVECNEW (NTT),
* DDMDET (NTT),DFFNDE (NTT),DDFDET (NTT)
PARAMETER (ZERO = 0.D0, ONE = 1.D0, TWO = 2.D0, HALF =
0.5D0,
1 THREE = 3.D0, FOUR = 4.D0)
C CALCULATE THE FAILURE STRAIN BY FAILURE STRESS
EPITL = X_T / CFULL (1,1) !FAILURE STRAIN 1 DIRECTION IN
TENSION
EPICL = X_C / CFULL (1,1) !FAILURE STRAIN 1 DIRECTION IN
COMPRESSION
EPITT = Y_T / CFULL (2,2) !TENSILE FAILURE STRAIN 2 DIRECTION
EPICT = Y_C / CFULL (2,2) !COMPRESSIVE FAILURE STRAIN 2
DIRECTION
EPISLT = S_12/ CFULL (4,4) ! FAILURE SHEAR STRAIN
...ENGINEERING STRAIN
IF ( EPS_F_X_T .EQ. ZERO ) THEN
EPS_F_X_T = X_T / CFULL (1,1)
END IF
IF ( EPS_F_X_C .EQ. ZERO ) THEN

```

```

EPS_F_X_C = X_C / CFULL(1,1)
END IF
IF (EPS_F_Y_T .EQ. ZERO) THEN
EPS_F_Y_T = Y_T / CFULL(2,2)
END IF
IF ( EPS_F_Y_C .EQ. ZERO ) THEN
EPS_F_Y_C = Y_C / CFULL(2,2)
END IF
IF ( EPS_SC .EQ. ZERO ) THEN
EPS_SC = S_12 / CFULL(4,4)
ENDIF

DMT = ZERO
DFT = ZERO
STRAINFAIL_XT = EPS_F_X_T
STRAINFAIL_XC = EPS_F_X_C
STRAINFAIL_YT = EPS_F_Y_T
STRAINFAIL_YC = EPS_F_Y_C

TERM1 = STRAIN(2)**TWO / EPIC1T / EPITT
TERM2 = (EPIC1T - EPITT) / EPIC1T / EPITT * STRAIN(2)
IF (NDI .EQ. 3) THEN
TERM3 = (STRAIN(4))**TWO / EPISLT**TWO
ELSE IF (NDI .EQ. 2) THEN
TERM3 = (STRAIN(3))**TWO / EPISLT**TWO
END IF
TERM = TERM1 + TERM2 + TERM3
IF (TERM .GT. ZERO) THEN
XFMN = SQRT(TERM)
ELSE
XFMN = ZERO
END IF
C
IF (STRAIN(2) .GE. ZERO) XFMN = DABS(STRAIN(2)) /
STRAINFAIL_YT
IF (STRAIN(2) .LT. ZERO) XFMN = DABS(STRAIN(2)) /
STRAINFAIL_YC
C INITIALIZE THE ARRAY AND VARIABLE
C
DDMDFMN = ZERO
DO I = 1, 6
DFMNDE(I) = ZERO
DDMDET(I) = ZERO
END DO
IF (XFMN .GT. ONE ) THEN !.AND. DFTOLDDT.EQ.ZERO
C CALCULATE DM, DDMDFMN
CALL DAMAGEEVALUATION( CFULL(2,2), XFMN, G_MT_C, XLC,
* EPITT, DMT, DDMDFMN)
C CALCULATE DFMNDE
IF (DMT .GT. DMTOLDDT) THEN
DFMNDE(2) = HALF / XFMN * (TWO * STRAIN(2) + EPIC1T -
EPITT)
* / EPIC1T / EPITT
IF (NDI .EQ. 3) THEN

```

```

          DFMNDE(4) = ONE / XFMN * STRAIN(4) / EPISLT**TWO
    ELSE IF (NDI .EQ. 2) THEN
          DFMNDE(4) = ONE / XFMN * STRAIN(3) / EPISLT**TWO
    END IF
    DO I = 1, 6
          DDMDDET(I) = DFMNDE(I) * DDMDFMN
    END DO
    END IF
  END IF
  DMT = MAX (DMT, DMTOLDT)

  IF (STRAIN(1) .GE. ZERO) XFFN = MAX(DABS(STRAIN(1)) /
STRAINFAIL_XT, XFFNOLD)
  IF (STRAIN(1) .LT. ZERO) XFFN = DABS(STRAIN(1)) /
STRAINFAIL_XC

  DDFDFFN = ZERO
  DO I = 1, 6
          DFFNDE(I) = ZERO
          DDFDET(I) = ZERO
  END DO

  IF (XFFN .GT. ONE ) THEN ! .AND. DMTOLDT.EQ.ZERO
C   CALCULATE DFT, DDFDFFN
    CALL DAMAGEEVALUATION( CFULL(1,1), XFFN, G_FT_C, XLC,
*   EPITL, DFT, DDFDFFN)
C   CALCULATE DFFNDE
    IF (DFT .GT. DFTOLDT) THEN
      DFFNDE(1) = HALF / XFFN * (TWO * STRAIN(1) + EPICL -
EPITL)
*   / EPICL / EPITL
      DDFDET(1) = DFFNDE(1) * DDFDFFN
    END IF
  END IF

  DFT = MAX (DFT, DFTOLDT)

  RETURN
  END
C*****
C   SUBROUTINE TO EVALUATE THE DAMAGE AND THE
C   DERIVATIVE*
C*****
  SUBROUTINE DAMAGEEVALUATION(STIFF, FN, GF, XLC, EPIT, D,
1   DDDFN)
C   CALCULATE DAMAGE VARIABLE
  INCLUDE 'ABA_PARAM.INC'
  PARAMETER (ONE = 1.D0, TOL=1D-3, ZERO = 0.D0)
  TERM1 = STIFF * EPIT**2 * XLC / GF
  TERM2 = (ONE - FN) * TERM1
  D = ONE - EXP(TERM2) / FN

```

```

C      CALCULATE THE DERIVATIVE OF DAMAGE VARIABLE WITH RESPECT TO
FAILURE
C      RITERION
      DDDFN = (ONE / FN + TERM1) * (ONE - D)
      RETURN
      END
C*****
C SUBROUTINE TO GET THE DERIVATIVE MATRIX OF CONDENSE DAMAGED
MATRIX OVER
C**** THE DAMAGE VARIABLE
C*****
      SUBROUTINE ELASTICDERIVATIVE_TEST (CFULL,DMV,DFV,
DCDDM,DCDDF)
      INCLUDE 'ABA_PARAM.INC'
      DIMENSION CFULL(6,6), DCDDM(6,6),
1      DCDDF(6,6)
      PARAMETER (ZERO = 0.00, ONE = 1.00, HALF = 0.500)
C      INITIALIZE THE DATA TO ZERO
      DO I = 1, 6
          DO J = 1, 6
              DCDDM(I,J) = ZERO
              DCDDF(I,J) = ZERO
          END DO
      END DO
C      CALCULATE DC/DDF
      DCDDF(1,1) = - CFULL(1,1)
      DCDDF(1,2) = - (ONE - DMV) * CFULL(1,2)
      DCDDF(2,1) = DCDDF(1,2)
      DCDDF(1,3) = -CFULL(1,3)
      DCDDF(3,1) = DCDDF(1,3)
      DCDDF(4,4) = -(ONE - DMV) * CFULL(4,4)
C      CALCULATE DC/DDM
      DCDDM(1,2) = - (ONE - DFV) * CFULL(1,2)
      DCDDM(2,1) = DCDDM(1,2)
      DCDDM(2,2) = -CFULL(2,2)
      DCDDM(2,3) = -CFULL(2,3)
      DCDDM(3,2) = DCDDM(2,3)
      DCDDM(4,4) = -(ONE - DFV) * CFULL(4,4)
      RETURN
      END
C*****
C      DEFINE FOURTH ORDER F(I,J,K,L) TENSOR
C*****
      SUBROUTINE F_TEN_GENERATOR_TOT (F_MAT, X_M_TEN,GAMA, CE)
      INCLUDE 'ABA_PARAM.INC'
      DIMENSION CE(3,3,3,3), X_M_TEN(3,3,3,3),
DELTA(3,3),TEMP(3,3,3,3),
      * F_TEN_INV(3,3,3,3), F_TEN(3,3,3,3), F_MAT(6,6),
F_MAT_INV(6,6)
C      DEFINE DELTA KRONEKER
          DO I = 1, 3
              DO J = 1, 3
                  IF (I .EQ. J) DELTA(I,J) = 1.00
                  IF (I .NE. J) DELTA(I,J) = 0.00
              END DO
          END DO

```

```

        END DO
    END DO

    DO I = 1, 3
        DO J = 1, 3
            DO K = 1, 3
                DO L = 1, 3
                    TEMP(I,J,K,L) = ZERO
                    DO M = 1, 3
                        DO N = 1, 3
                            TEMP(I,J,K,L) = TEMP(I,J,K,L) + CE(I,J,M,N) *
X_M_TEN(M,N,K,L)
                        END DO
                    END DO
                END DO
            END DO
        END DO
    END DO

    DO I = 1, 3
        DO J = 1, 3
            DO K = 1, 3
                DO L = 1, 3
                    TEMP(I,J,K,L) = GAMA * TEMP(I,J,K,L)
                END DO
            END DO
        END DO
    END DO

    DO I = 1, 3
        DO J = 1, 3
            DO K = 1, 3
                DO L = 1, 3
                    F_TEN_INV(I,J,K,L) = DELTA(I,K) * DELTA(J,L) +
TEMP(I,J,K,L)
                END DO
            END DO
        END DO
    END DO

    C CONVERT F_INVERSE(I,J,K,L) TO F_INVERSE(I,J) , I=1,9 AND J=1,9
    CALL TENSTOMATRIX6(F_TEN_INV,F_MAT_INV)
    DO I = 1, 6
        DO J = 1, 6
            F_MAT_INV(J,I) = F_MAT_INV(I,J)
        END DO
    END DO

    C CALCULATE INVERSE OF F_MAT_INV AND GET F_MAT
    CALL INVERSE(F_MAT_INV,F_MAT,6)

    RETURN
    END

C*****
C CALCULATE THE STRESS IN PLASTIC REGION
C*****

```

```

      SUBROUTINE GETCD_FULL(CFULL,CDTHREE ,DFT, DMT,NT,ND,CFDT)
      INCLUDE 'ABA_PARAM.INC'
      DIMENSION CFULL(6,6),CFDT(6,6),STR(NT),STRANT(NT),
*      CDTHREE(3,3)
      PARAMETER (ZERO = 0.D0, ONE = 1.D0, TWO = 2.D0, HALF =
0.5D0,
*      THREE = 3.D0)
C      CDTHREE.....DAMAGED CONDENSED-ELASTICITY MATRIX FOR PLANE
STRESS PROBLEM
      DO I = 1, NT
        DO J = 1, NT
          CFDT(I,J) = CFULL(I,J)
        END DO
      END DO

      IF ( (DFT .NE. ZERO) .OR. (DMT .NE. ZERO) ) THEN
        CFDT(1,1) = (ONE - DFT)* CFULL(1,1)
        CFDT(1,2) = (ONE - DFT) * (ONE - DMT) * CFULL(1,2)
        CFDT(2,1) = CFDT(1,2)
        CFDT(2,2) = (ONE - DMT) * CFULL(2,2)
        CFDT(1,3) = (ONE - DFT) * CFULL(1,3)
        CFDT(3,1) = CFDT(1,3)
        CFDT(2,3) = (ONE - DMT) * CFULL(2,3)
        CFDT(3,2) = CFDT(2,3)
        CFDT(4,4) = (ONE - DMT) * (ONE - DFT) * CFULL(4,4)
      END IF

      RETURN
      END

```

## 8.2 Appendix.2

In this appendix a plasticity internal subroutine is given which uses the perturbation method to calculate the numerical tangent.

```

C*****
C   PLASTICITY SUBROUTINE FOR SHORT FIBERS OF 3-D CASE
C*****
      SUBROUTINE SHORTFIBERPLAST3D( STRAINPLAVECOLD,
STRAINPLAVECNEW,
      * STRAINTOTVECNEW, STRESS_NEW, STRESS_OLD, EPSVAR_P_OLD,
      * EPSVAR_P_NEW, ND, NSH, CE_2D, CE_3D,
      * XF_YIELD_INI_OLD, XF_YIELD_INI_NEW, C_TAN,
      * STRAINTOTVECOLD, STRESSTRVECNEW, STRESSTRVECOLD,
PLAST_TOL,
      * DT ,TOTALTIME_NEW, TOTALTIME_OLD,
      * DELTAGAMMAINT, Y_TR_INI_OLD, Y_TR_INI,
      * Y_IP_INI_OLD, Y_IP_INI, Y1T_INI_OLD, Y1T_INI, Y1C_INI_OLD,
      * Y1C_INI, Y2C_INI_OLD, Y2C_INI, Y2T_INI_OLD, Y2T_INI, M_UXC,
M_UXT,
      * M_TUC, M_TUT, M_IP, M_TR,
Y_1C, Y_1C_OLD, Y_1T, Y_1T_OLD, Y_2C,
      * Y_2C_OLD, Y_2T, Y_2T_OLD, Y_IP, Y_IP_OLD,
Y_TR, Y_TR_OLD, Y_TR_0,
      * Y_IP_0, Y2T_0, Y2C_0, Y1T_0, Y1C_0, A_ST_11, A_ST_22, CONST1,
      * CONST2, XI1_INI, XI2_INI, XI3_INI,
XI4_INI, NTT, STRESS_P_OLD,
      * STRESS_P, NUMBREAK, DSTRAIN, STRESSELAST, XF_YIELD_NEW,
      * DSTRAIN_OLD, CE4TH, DELTAGAMMAINTOLD)
      INCLUDE 'ABA_PARAM.INC'
      CHARACTER(LEN=:), ALLOCATABLE :: FILEPATH_IP, FILEPATH_TR,
      * FILEPATH_TUC, FILEPATH_TUT, FILEPATH_UXC, FILEPATH_UXT
      DIMENSION STRAINTRVECNEW(NTT), STRAINTRVECOLD(NTT),
      * STRAINPLAVECOLD(NTT), STRAINPLAVECNEW(NTT),
      * STRAINTOTVECNEW(NTT), STRAINTOTVECOLD(NTT),
      * X_N_F(NTT), DISTURB(NTT), STRESSELAST(NTT),
      * STRESSTRVECNEW(NTT), STRESSTRVECOLD(NTT), CE_3D(6,6),
      * DELTA(3,3), X_N_G(NTT), A_DIR(3,3), C_TAN(NTT,NTT),
      * CE_2D(3,3), STRESS_NEW(NTT), STRESS_OLD(NTT),
      * DI1DSIGMA(NTT), DI2DSIGMA(NTT),
DI4DSIGMA(NTT), DI5DSIGMA(NTT),
      * DI3DSIGMA(NTT), STRESS_P_OLD(NTT), STRESS_P(NTT),
      * DSTRESS_P(NTT),
DSTRAIN(NTT), STRAINPLAVECINT(NTT), TANG_OLD(NTT,NTT),
      * SIGMA(NTT,NTT), STRAN_DIST(NTT),
EPS PERT(NTT), STRESS_DIST(NTT),
      *
DSTRAIN_OLD(NTT), X_M_MAT(6,6), X_M_TEN(3,3,3,3), TENSOR1(3,3,3,3),
      *
TENSOR2(3,3,3,3), TENSOR3(3,3), X_I_S(3,3,3,3), X_I(3,3,3,3), CE4TH(3,
3,3,3),

```

```

*
TENSOR5(3,3,3,3), TENSOR4(3,3), F_TEN(NTT,NTT), DSIGMADDELTA GAMMA(NTT
),
* TERM3(NTT), A_DIR_VEC(3),
P_PIND(3,3,3,3), P_PIND_A(3,3,3,3), A_DEV(3,3),
*
TERM20(NTT,NTT), TERM21(NTT,NTT), TERM22(NTT,NTT), TERM23(NTT,NTT),
*
TERM24(NTT,NTT), TERM30(NTT), TERM31(NTT), TERM32(NTT), TERM25(NTT,NTT
)
C      DOUBLEPRECISION, ALLOCATABLE, DIMENSION(:, :)::
XY_TRSHEAR,
C      * XY_IPSHEAR, XY_IPSHEAR_T, XY_TRBC, XY_TRBC_T, XY_TRBT,
XY_TRBT_T,
C      * XY_TRUC, XY_TRUC_T, XY_TRT, XY_TRT_T, XY_UXC, XY_UXC_T,
XY_UXT,
C      * XY_UXT_T, XY_TRSHEAR_T
      ALLOCATABLE XY_TRSHEAR(:, :),
      * XY_IPSHEAR(:, :), XY_IPSHEAR_T(:, :), XY_TRBC(:, :),
XY_TRBC_T(:, :),
      * XY_TRUC(:, :), XY_TRUC_T(:, :), XY_TRT(:, :), XY_TRT_T(:, :),
      * XY_UXT_T(:, :), XY_TRSHEAR_T(:, :), XY_TRBT(:, :),
XY_TRBT_T(:, :),
      * XY_UXC(:, :), XY_UXC_T(:, :), XY_UXT(:, :),
      PARAMETER (ZERO = 0.0D0, ONE = 1.0D0, TWO = 2.0D0, HALF =
0.5D0,
      1      THREE = 3.0D0, FOUR = 4.0D0, EPS_P = 0.5D0 )
      CALL FIBER_DIR(A_DIR, A_ST_11, A_ST_22)
      A_DIR_VEC(1) = A_DIR(1,1)
      A_DIR_VEC(2) = A_DIR(2,2)
      A_DIR_VEC(3) = A_DIR(3,3)
C      DEFINE KRONECKER DELTA
      DO I = 1, 3
      DO J = 1, 3
      IF ( I .EQ. J ) THEN
      DELTA(I,J) = ONE
      ELSE
      DELTA(I,J) = ZERO
      END IF
      END DO
      END DO
C      DEFINE ELASTIC STRAIN
      DO I = 1, NTT
      STRAINTRVECNEW(I) = STRAINTOTVECNEW(I) - STRAINPLAVECOLD(I)
C      STRAINTRVECNEW(I) = STRAINTOTVECNEW(I)
      END DO
      CALL GETSTRESS3D(CE_3D, CE_2D, STRESSTRVECNEW, STRAINTRVECNEW,
*      NTT, ND)
C      IMPORT PLASTICITY DATA FROM EXTERNAL FILE FOR DIFFERENT
EXPERIMENTS
      XF_CF_SH = 1.414D0 ! FOR SHORT FIBER REINFORCED
THERMOPLASTICS
      XF_CF_UNI = ONE ! FOR SHORT FIBER REINFORCED
THERMOPLASTICS

```

```

Y_TR_INI = Y_TR_0 * ( 1.D0 - EXP(-CONST1 * CONST2) )
Y_IP_INI = Y_IP_0 * ( 1.D0 - EXP(-CONST1 * CONST2) )
Y2T_INI = Y2T_0 * ( 1.D0 - EXP(-CONST1 * CONST2) )
Y2C_INI = Y2C_0 * ( 1.D0 - EXP(-CONST1 * CONST2) )
Y1T_INI = Y1T_0 * ( 1.D0 - EXP(-CONST1 * CONST2) )
Y1C_INI = Y1C_0 * ( 1.D0 - EXP(-CONST1 * CONST2) )
Y_TR = ZERO
Y_IP = ZERO
Y2T = ZERO
Y2C = ZERO
Y1T = ZERO
Y1C = ZERO
IF (Y_TR_OLD.EQ.ZERO) Y_TR_OLD = Y_TR_INI
IF (Y_IP_OLD.EQ.ZERO) Y_IP_OLD = Y_IP_INI
IF (Y_2T_OLD.EQ.ZERO) Y_2T_OLD = Y2T_INI
IF (Y_2C_OLD.EQ.ZERO) Y_2C_OLD = Y2C_INI
IF (Y_1T_OLD.EQ.ZERO) Y_1T_OLD = Y1T_INI
IF (Y_1C_OLD.EQ.ZERO) Y_1C_OLD = Y1C_INI
C*****
*****
C      DEFINE THE INVARIANTS FOR SHORT FIBER REINFORCED
THERMOPLASTICS
C*****
*****
      CALL INVARIANTS(STRESSTRVECNEW, ND, NSH,XI1_INI,
*   XI2_INI,XI5_INI,XI4_INI,NTT, A_ST_11,A_ST_22,
*   TRSIGMA,DI1DSIGMA,DI2DSIGMA,DI4DSIGMA,DI5DSIGMA)
      CALL CALCALPHA(Y_TR_INI,Y_IP_INI,Y1T_INI, Y1C_INI,
*   Y2C_INI,Y2T_INI, ALPHA1_INI, ALPHA2_INI,ALPHA4_INI,
*   ALPHA42_INI, ALPHA5_INI, ALPHA52_INI )
C DEFINE TENSION OR COMPRESSION SITUATION
C   DEFINE INITIA YIELD CRITERION
      XF_YIELD_INI_NEW = ALPHA1_INI * XI1_INI+ ALPHA2_INI *
X12_INI +
* ALPHA4_INI * XI4_INI + ALPHA42_INI * XI4_INI ** TWO +
* ALPHA5_INI * XI5_INI + ALPHA52_INI * XI5_INI ** TWO
      CALL CALCBETA(Y_TR_INI,Y_IP_INI,Y1T_INI, Y1C_INI, Y2C_INI,
*   Y2T_INI, BETA1, BETA2, BETA32T,BETA32C, BETA42T, BETA42C )
C DEFINE TENSION OR COMPRESSION SITUATION
      BETA32 = BETA32T
      BETA42 = BETA42T
C   DEFINE P_PIND [P^PIND= $\partial_{\Sigma} \Sigma^{PIND} = I - 1/2 (1 \otimes 1) + 1/2 (A \otimes 1 + 1 \otimes A) -$ 
3/2 (A $\otimes$ A)]
      DO I = 1, 3
        DO J = 1, 3
          DO K = 1, 3
            DO L = 1, 3
              P_PIND(I,J,K,L) = DELTA(I,L) * DELTA(J,K) - (1.D0 /
2.D0) *
* DELTA(I,J) * DELTA(K,L) + (1.D0 / 2.D0) * ( A_DIR(I,J) *
! NOTE: P_PIND IS INDEPENDENT OF ITERATION PROCESS
* DELTA(K,L) + DELTA(I,J) * A_DIR(K,L) ) - (3.D0/2.D0) *
* ( A_DIR(I,J) * A_DIR(K,L) )

```

```

        END DO
        END DO
        END DO
        END DO

C   P_PND IS SYMMETRIC
      DO I = 1, 3
        DO J = 1, 3
          DO K = 1, 3
            DO L = 1, 3
              P_PIND(I,J,L,K) = P_PIND(I,J,K,L)
              P_PIND(J,I,K,L) = P_PIND(I,J,K,L)
              P_PIND(K,L,I,J) = P_PIND(I,J,K,L)
            END DO
          END DO
        END DO
      END DO

C   DEFINE P_PIND_A [P_A^PIND=A_IM P_MJKL^PIND+A_MJ P_IMKL^PIND]
      DO I = 1, 3
        DO J = 1, 3
          DO K = 1, 3
            DO L = 1, 3
              SUM1 = 0.D0
              DO M = 1, 3
                SUM1 = SUM1 + A_DIR(I,M) * P_PIND(M,J,K,L) + A_DIR(M,J) * !
NOTE: P_PIND_A IS INDEPENDENT OF ITERATION PROCESS
* P_PIND(I,M,K,L)
              END DO
              P_PIND_A(I,J,K,L) = SUM1
            END DO
          END DO
        END DO
      END DO

      DO I = 1, 3
        DO J = 1, 3
          DO K = 1, 3
            DO L = 1, 3
              P_PIND_A(I,J,L,K) = P_PIND_A(I,J,K,L)
              P_PIND_A(J,I,K,L) = P_PIND_A(I,J,K,L)
              P_PIND_A(K,L,I,J) = P_PIND_A(I,J,K,L)
            END DO
          END DO
        END DO
      END DO

C   DEFINE DEVIATORIC PART OF A TENSOR A-----> A_DEV
      DO I = 1, 3
        DO J = 1, 3
          SUM2 = 0.D0
          DO K = 1, 3
            SUM2 = SUM2 + A_DIR(I,J) - (1.D0/3.D0)* A_DIR(K,K) *
DELTA(I,J) ! NOTE: A_DEV IS INDEPENDENT OF ITERATION PROCESS
          END DO
          A_DEV(I,J) = SUM2
        END DO
      END DO

```

```

        END DO
    END DO
C DEFINE TENSION OR COMPRESSION SITUATION
C     DEFINE M
        DO I = 1, 3
            DO J = 1, 3
                DO K = 1, 3
                    DO L = 1, 3
                        X_M_TEN(I,J,K,L) = BETA1 * P_PIND(I,J,K,L) + (BETA2 -
* BETA1) * P_PIND_A(I,J,K,L) + 2.D0 * BETA32 * (DELTA(I,J) -
* A_DIR(I,J) ) * ( DELTA(J,K) - A_DIR(J,K) ) + (9.D0 / 2.D0) *
* BETA42 * A_DEV(I,J) * A_DEV(K,L)
                    END DO
                END DO
            END DO
        END DO

        CALL TENSTOMATRIX6(X_M_TEN,X_M_MAT)
        DO I = 1, 6
            DO J = 1, 6
                X_M_MAT(J,I) = X_M_MAT(I,J)
            END DO
        END DO

C             """"PLASTIC CORRECTOR""""
C     IMPORT PLASTICITY DATA FROM EXTERNAL FILE FOR DIFFERENT
EXPERIMENTS
        DO I=1,NTT
            STRESS_P(I) = ZERO
        END DO

        CALL GETSTRESS3D(CE_3D, CE_2D,STRESSELAST,DSTRAIN, NTT,ND)
        IF ( EPSVAR_P_OLD .NE. ZERO ) GOTO 125
        IF ( XF_YIELD_INI_NEW < ONE ) GOTO 600
125 CONTINUE
C             """"""ELASTIC PREDICTOR""""""
C     SET DELTAGAMMAINT INITIAL VALUE
        DELTAGAMMAINT = ZERO
C     SET EPSVAR_P
C     START THE ITERATION (LOOP) TO FIND PLASTIC MULTIPLIER
DELTAGAMMAINT AND UPDATING PLASTIC STRAINS
        NUMC = 0
C INITIALIZE NEW STRESS
        DO I = 1, NTT
            STRESS_NEW(I) = STRESSTRVECNEW(I)
        END DO
C INITIALIZE THE EQUIVALENT PLASTIC STRAIN
        DO I = 1, NTT
            STRAINPLAVECINT(I) = STRAINPLAVECOLD(I)
        END DO
        EPSVAR_P_INT = EPSVAR_P_OLD
    DO ! MAIN LOOP

```

```

      NUMC = NUMC + 1
      CALL F_TEN_GENERATOR_TOT(F_TEN, X_M_TEN, DELTAGAMMAINT,
CE4TH)
C   CALCULATE STRESS TENSOR
      DO I = 1, NTT
          STRESS_NEW(I) = ZERO
          DO J = 1, NTT
              STRESS_NEW(I) = STRESS_NEW(I) + F_TEN(I,J)*
STRESSTRVECNEW(J)
          END DO
      END DO

C   IMPORT PLASTICITY DATA FROM EXTERNAL FILE FOR DIFFERENT
EXPERIMENTS
C*****
C   1. (TRANSVERSE SHEAR PLASTIC-STRAIN VS YIELD STRESS) Y_TR
C*****
      EPS_TRSHEAR_P = EPSVAR_P_INT * XF_CF_SH
      Y_TR = Y_TR_0 * (1.D0 - EXP(-CONST1 * (EPS_TRSHEAR_P +
CONST2) ) )
      D_Y_TR_D_EPSVAR_P = Y_TR_0 * CONST1 * EXP(-CONST1 *
(EPS_TRSHEAR_P + CONST2) )
C*****
C   2. (IN-PLANE SHEAR PLASTIC-STRAIN VS YIELD STRESS) Y_IP
C*****
      EPS_IPSHEAR_P = EPSVAR_P_INT * XF_CF_SH
      Y_IP = Y_IP_0 * (1.D0 - EXP(-CONST1 * (EPS_IPSHEAR_P +
CONST2) ) )
      D_Y_IP_D_EPSVAR_P = Y_IP_0 * CONST1 * EXP(-CONST1 *
(EPS_IPSHEAR_P + CONST2) )
C*****
C   3. (TRANSVERSE UNIAXIAL TENSION PLASTIC-STRAIN VS YIELD STRESS)
Y_UT
C*****
      EPS_TUT_P = EPSVAR_P_INT * XF_CF_UNI
      Y_2T = Y2T_0 * (1.D0 - EXP(-CONST1 * (EPS_TUT_P + CONST2) )
)
      D_Y_2T_D_EPSVAR_P = Y2T_0 * CONST1 * EXP(-CONST1 *
(EPS_TUT_P + CONST2) )
C*****
C   5. (TRANSVERSE UNIAXIAL COMPRESSION PLASTIC-STRAIN VS YIELD
STRESS) Y_UC
C*****
      EPS_TRUC_P = EPSVAR_P_INT * XF_CF_UNI
      Y_2C = Y2C_0 * (1.D0 - EXP(-CONST1 * (EPS_TRUC_P + CONST2) )
)
      D_Y_2C_D_EPSVAR_P = Y2C_0 * CONST1 * EXP(-CONST1 *
(EPS_TRUC_P + CONST2) )
C*****
C   7. (UNIAXIAL TENSION IN FIBER DIRECTION PLASTIC-STRAIN VS YIELD
STRESS) Y_1T
C*****
      EPS_UXT_P = EPSVAR_P_INT * XF_CF_UNI

```

```

      Y_1T = Y1T_0 * (1.D0 - EXP(-CONST1 * (EPS_UXT_P + CONST2) )
)
      D_Y_1T_D_EPSVAR_P = Y1T_0 * CONST1 * EXP(-CONST1 *
(EPS_UXT_P + CONST2) )
C
*****
C 8. (UNIAXIAL COMPRESSION IN FIBER DIRECTION PLASTIC-STRAIN VS
YIELD STRESS) Y_1C
C
*****
      EPS_UXC_P = EPSVAR_P_INT * XF_CF_UNI
      Y_1C = Y1C_0 * (1.D0 - EXP(-CONST1 * (EPS_UXC_P + CONST2) )
)
      D_Y_1C_D_EPSVAR_P = Y1C_0 * CONST1 * EXP(-CONST1 *
(EPS_UXC_P + CONST2) )
C*****
C DEFINE THE INVARIANTS FOR SHORT FIBER REINFORCED
THERMOPLASTICS
C*****
      CALL INVARIANTS(STRESS_NEW, ND, NSH,XI1,XI2,XI5,XI4,NTT,
A_ST_11,
      * A_ST_22,TRSIGMA,DI1DSIGMA,DI2DSIGMA,DI4DSIGMA,DI5DSIGMA)
C CALCULATE NEW ALPHA
      CALL CALCALPHA(Y_TR,Y_IP,Y_1T, Y_1C,Y_2C,Y_2T, ALPHA1,
ALPHA2,
      * ALPHA4,ALPHA42, ALPHA5, ALPHA52 )
C DEFINE INITIA YIELD CRITERION
      XF_YIELD_NEW = ALPHA1 * XI1+ ALPHA2 * XI2 +ALPHA4* XI4 +
      * ALPHA42 * XI4** TWO + ALPHA5* XI5 + ALPHA52 * XI5 ** TWO -
ONE
C CALCULATE THE GRADIENT OF THE YIELD FUNCTION
      DO I = 1, NTT
      X_N_F(I) = ALPHA1 * DI1DSIGMA(I) + ALPHA2 * DI2DSIGMA(I)
+
      * ALPHA4 * DI4DSIGMA(I) + TWO * ALPHA42 * XI4 *
DI4DSIGMA(I)+
      * ALPHA5 * DI5DSIGMA(I) + TWO * ALPHA52 * XI5 *
DI4DSIGMA(I)
      END DO
C DETERMINE DALPHA/DEPS BASED ON VOGLERS FORMULA
      DALPHA1DEPSVAR_P = ( -2.D0 / Y_TR ** 3.D0 ) *
D_Y_TR_D_EPSVAR_P
      DALPHA2DEPSVAR_P = ( -2.D0 / Y_IP ** 3.D0 ) *
D_Y_IP_D_EPSVAR_P

      DEN = Y_1T + Y_1C
      XNUM = ONE/Y_1C +ONE/Y_1T + HALF * ALPHA1 * (Y_1C+Y_1T) -
ALPHA2 *
      * (Y_1C+Y_1T)
      DALPHA42DEPSVAR_P = ( (-ONE/Y_1T**TWO +HALF * ALPHA1 -
ALPHA2) *
      * DEN - XNUM ) * D_Y_1T_D_EPSVAR_P / DEN**2.D0 + ( (-
ONE/Y_1C**

```

```

      * TWO + HALF * ALPHA1-ALPHA2) *DEN - XNUM ) *
D_Y_1C_D_EPSVAR_P /
      * DEN**2.D0+ HALF * DALPHA1DEPSVAR_P - DALPHA2DEPSVAR_P
      DALPHA4DEPSVAR_P = (-ONE/Y_1T**TWO + HALF * ALPHA1 - ALPHA2
-
      * ALPHA42) * D_Y_1T_D_EPSVAR_P + HALF * Y_1T *
DALPHA1DEPSVAR_P -
      * Y_1T * DALPHA2DEPSVAR_P - Y_1T * DALPHA42DEPSVAR_P
      DEN = Y_2T + Y_2C
      XNUM = ONE/Y_2C +ONE/Y_2T - HALF * ALPHA1 * (Y_2C+Y_2T)
      DALPHA52DEPSVAR_P = ( (-ONE/Y_2T**TWO - HALF * ALPHA1) *DEN
-
      * XNUM ) * D_Y_2T_D_EPSVAR_P /DEN**2.D0 + ((-ONE/Y_2C**TWO -
HALF *
      * ALPHA1) *DEN - XNUM ) * D_Y_2C_D_EPSVAR_P /DEN**2.D0 -
HALF *
      * DALPHA1DEPSVAR_P
      DALPHA5DEPSVAR_P = -(ONE/Y_2T**TWO + HALF * ALPHA1 + ALPHA52
) *
      * D_Y_2T_D_EPSVAR_P - HALF * Y_2T * DALPHA1DEPSVAR_P - Y_2T *
      * DALPHA52DEPSVAR_P
C      END FOR D(ALPHA)/D(EQUIVALENT STRAIN)
      DO I = 1, NTT
        DSIGMADELTA GAMMA(I) = ZERO
        DO J = 1, NTT
          DO K = 1, NTT
            DO L = 1, NTT
              DSIGMADELTA GAMMA(I) = DSIGMADELTA GAMMA(I)+ F_TEN(I,J) *
      * CE_3D(J,K) * X_M_MAT(K,L) * STRESS_NEW(L)
              END DO
            END DO
          END DO
        DSIGMADELTA GAMMA(I) = - DSIGMADELTA GAMMA(I)
      END DO
C CALCULATE DEPS_PDELTA GAMMA
      DO I = 1, NTT
        X_N_G(I) =ZERO
        DO J = 1, NTT
          X_N_G(I) = X_N_G(I) + X_M_MAT(I,J) * STRESS_NEW(I)
        END DO
      END DO
C TEST CALCULATE THE NORM OF N?G
      X_NG_NORM = ZERO
      DO I = 1, NTT
        X_NG_NORM = X_NG_NORM + DSQRT(HALF * X_N_G(I)**TWO)
      END DO

C RECALCULATE NG
      GOTO 621
      DO I = 1, NTT
        X_N_G(I) = X_N_G(I)/X_NG_NORM
      END DO

C TEST CALCULATE THE NORM OF NG

```

```

        X_NG_NORM = ZERO
        DO I = 1, NTT
        X_NG_NORM = X_NG_NORM + X_N_G(I)**TWO
        END DO
        X_NG_NORM = SQRT(HALF* X_NG_NORM)
621 CONTINUE
C      DEPS_PDELDTAGAMMA = DSQRT(HALF) * X_NG_NORM
        DO I = 1, NTT
            TERM3(I) = ZERO
            DO J = 1, NTT
                TERM3(I) = TERM3(I) + X_M_MAT(I,J) * STRESS_NEW(J)
            END DO
        END DO
        VALTERM3 = ZERO
        DO I = 1, NTT
        VALTERM3 = VALTERM3 + TERM3(I)** TWO
        END DO
        VALTERM3 = SQRT(HALF* VALTERM3)
C      DEFINE THE VALUE OF STRESS TENSOR
        STRESSVAL = ZERO
        DO I = 1, NTT
        STRESSVAL = STRESSVAL + STRESS_NEW(I)** TWO
        END DO
        STRESSVAL = SQRT(HALF* STRESSVAL)

        DEPS_PDELDTAGAMMA = ZERO
        DO I = 1, NTT
            DO J = 1, NTT
                DEPS_PDELDTAGAMMA = DEPS_PDELDTAGAMMA +
* X_M_MAT(I,J) * STRESS_NEW(I) * DSIGMADELDTAGAMMA(J)
            END DO
        END DO

        DEPS_PDELDTAGAMMA = DELTAGAMMAINT * DEPS_PDELDTAGAMMA /
        STRESSVAL + VALTERM3
        DALPHA1DGAMA = DALPHA1DEPSVAR_P * DEPS_PDELDTAGAMMA
        DALPHA2DGAMA = DALPHA2DEPSVAR_P * DEPS_PDELDTAGAMMA
        DALPHA5DGAMA = DALPHA5DEPSVAR_P * DEPS_PDELDTAGAMMA
        DALPHA52DGAMA = DALPHA52DEPSVAR_P * DEPS_PDELDTAGAMMA
        DALPHA4DGAMA = DALPHA4DEPSVAR_P * DEPS_PDELDTAGAMMA
        DALPHA42DGAMA = DALPHA42DEPSVAR_P * DEPS_PDELDTAGAMMA
C      CALCULATE DI/DGAMA
        DI1DGAMA = ZERO
        DI2DGAMA = ZERO
        DI4DGAMA = ZERO
        DI5DGAMA = ZERO
        DO I = 1, NTT
            DI1DGAMA = DI1DGAMA + DI1DSIGMA(I) * DSIGMADELDTAGAMMA(I)
            DI2DGAMA = DI2DGAMA + DI2DSIGMA(I) * DSIGMADELDTAGAMMA(I)
            DI4DGAMA = DI4DGAMA + DI4DSIGMA(I) * DSIGMADELDTAGAMMA(I)
            DI5DGAMA = DI5DGAMA + DI5DSIGMA(I) * DSIGMADELDTAGAMMA(I)
        END DO
        DFDGAMA = (XI1 * DALPHA1DGAMA + XI2 * DALPHA2DGAMA + XI4 *

```

```

* DALPHA4DGAMA+ XI4**TWO * DALPHA42DGAMA+ XI5 *DALPHA5DGAMA+
XI5**
* TWO * DALPHA52DGAMA) + (ALPHA1 * DI1DGAMA + ALPHA2
*DI2DGAMA +
* ALPHA4 * DI4DGAMA + ALPHA5 *DI5DGAMA + TWO* ALPHA42 * XI4*
* DI4DGAMA + TWO*ALPHA52 * XI5* DI5DGAMA )

DELTATO2_GAMMA = - XF_YIELD_NEW/DFDGAMA
C
DELTAGAMMAINT = DELTAGAMMAINT + DELTATO2_GAMMA
EPSVAR_P_INT = EPSVAR_P_INT + DELTATO2_GAMMA* X_NG_NORM
IF ( DABS(XF_YIELD_NEW) .LT. PLAST_TOL )
* GOTO 400

IF ( NUMC > NUMBREAK ) THEN
WRITE(*,*) 'NUMC=', NUMC
C CALL EXIT
GOTO 402
END IF

C
END DO ! END FOR MAIN LOOP
C
400 CONTINUE
C 401 CONTINUE
402 CONTINUE
DO I = 1, NTT
STRAINPLAVECNEW (I) = STRAINPLAVECOLD (I) + DELTAGAMMAINT *
* X_N_G(I)
END DO
EPSVAR_P_NEW = EPSVAR_P_INT
C *****
C DEFINE THE PURTURBATED STRAIN AND ADD IT TO THE CURRENT STRAIN
TENSOR ONE BY ONE

DO K = 1,NTT
STRAN_DIST(K) = STRAINTOTVECNEW(K)
EPS_PERT(K) = MAX(1D-8* STRAINTOTVECNEW(K) , 1D-8)
END DO

DO K = 1,NTT
STRAN_DIST(K) = STRAINTOTVECNEW(K) + EPS_PERT(K)

C
C """"PLASTIC CORRECTOR""""
C IMPORT PLASTICITY DATA FROM EXTERNAL FILE FOR DIFFERENT
EXPERIMENTS

DO I=1,NTT
STRESS_P(I) = ZERO
END DO
C DEFINE ELASTIC STRAIN
DO I = 1 , NTT
STRAINRVECNEW(I) = STRAN_DIST(I) - STRAINPLAVECOLD(I)
C STRAINRVECNEW(I) = STRAN_DIST(I)
END DO

```

```

      CALL GETSTRESS3D(CE_3D, CE_2D, STRESSTRVECNEW, STRAINTRVECNEW,
*      NTT, ND)
      CALL GETSTRESS3D(CE_3D, CE_2D, STRESSELAST, DSTRAIN, NTT, ND)

C      """"""ELASTIC PREDICTOR""""""

C      SET DELTAGAMMAINT INITIAL VALUE
C      SET EPSVAR_P
C      START THE ITERATION (LOOP) TO FIND PLASTIC MULTIPLIER
DELTAGAMMAINT AND UPDATING PLASTIC STRAINS
      NUMC1 = 0
C INITIALIZE NEW STRESS
      DO I = 1, NTT
        STRESS_DIST(I) = STRESSTRVECNEW(I) ! STRESS IN POINT A
      END DO
C INITIALIZE THE EQUIVALENT PLASTIC STRAIN
      DO I = 1, NTT
        STRAINPLAVECINT(I) = STRAINPLAVECOLD(I)
      END DO
      EPSVAR_P_INT_DIST = EPSVAR_P_OLD
      DELTAGAMADIST = ZERO
      DO ! MAIN LOOP FOR THE PERTURBATION METHOD
        NUMC1 = NUMC1 + 1
        CALL F_TEN_GENERATOR_TOT(F_TEN, X_M_TEN, DELTAGAMADIST,
CE4TH)
        DO I = 1, NTT
          STRESS_DIST(I) = 0.D0
          DO J = 1, NTT
            STRESS_DIST(I) = STRESS_DIST(I) + F_TEN(I, J) *
STRESSTRVECNEW(J)
          END DO
        END DO
C DEFINE OLD PARAMETERS
C*****
C*****
C 1. (TRANSVERSE SHEAR PLASTIC-STRAIN VS YIELD STRESS) Y_TR
C*****
C*****
      EPS_TRSHEAR_P = EPSVAR_P_INT_DIST * XF_CF_SH
      Y_TR = Y_TR_0 * (1.D0 - EXP(-CONST1 * (EPS_TRSHEAR_P +
CONST2) ) )
      D_Y_TR_D_EPSVAR_P = Y_TR_0 * CONST1 * EXP(-CONST1 *
(EPS_TRSHEAR_P + CONST2) )
C*****
C*****
C 2. (IN-PLANE SHEAR PLASTIC-STRAIN VS YIELD STRESS) Y_IP
C*****
C*****
      EPS_IPSHEAR_P = EPSVAR_P_INT_DIST * XF_CF_SH
      Y_IP = Y_IP_0 * (1.D0 - EXP(-CONST1 * (EPS_IPSHEAR_P +
CONST2) ) )
      D_Y_IP_D_EPSVAR_P = Y_IP_0 * CONST1 * EXP(-CONST1 *
(EPS_IPSHEAR_P + CONST2) )

```

```

C*****
*****
C 3. (TRANSVERSE UNIAXIAL TENSION PLASTIC-STRAIN VS YIELD STRESS)
Y_UT [ ?_UNI^P=F_UNI^(C.F.) ? ?_P ]
C*****
*****
      EPS_TUT_P = EPSVAR_P_INT_DIST * XF_CF_UNI
      Y_2T = Y2T_0 * (1.D0 - EXP(-CONST1 * (EPS_TUT_P + CONST2) )
)
      D_Y_2T_D_EPSVAR_P = Y2T_0 * CONST1 * EXP(-CONST1 *
(EPS_TUT_P + CONST2) )
C*****
*****
C 5. (TRANSVERSE UNIAXIAL COMPRESSION PLASTIC-STRAIN VS YIELD
STRESS) Y_UC
C*****
*****
      EPS_TRUC_P = EPSVAR_P_INT_DIST * XF_CF_UNI
      Y_2C = Y2C_0 * (1.D0 - EXP(-CONST1 * (EPS_TRUC_P + CONST2) )
)
      D_Y_2C_D_EPSVAR_P = Y2C_0 * CONST1 * EXP(-CONST1 *
(EPS_TRUC_P + CONST2) )
C*****
*****
C 7. (UNIAXIAL TENSION IN FIBER DIRECTION PLASTIC-STRAIN VS YIELD
STRESS) Y_1T
C*****
*****
      EPS_UXT_P = EPSVAR_P_INT_DIST * XF_CF_UNI
      Y_1T = Y1T_0 * (1.D0 - EXP(-CONST1 * (EPS_UXT_P + CONST2) )
)
      D_Y_1T_D_EPSVAR_P = Y1T_0 * CONST1 * EXP(-CONST1 *
(EPS_UXT_P + CONST2) )
C
*****
*****
C 8. (UNIAXIAL COMPRESSION IN FIBER DIRECTION PLASTIC-STRAIN VS
YIELD STRESS) Y_1C
C
*****
*****
      EPS_UXC_P = EPSVAR_P_INT_DIST * XF_CF_UNI
      Y_1C = Y1C_0 * (1.D0 - EXP(-CONST1 * (EPS_UXC_P + CONST2) )
)
      D_Y_1C_D_EPSVAR_P = Y1C_0 * CONST1 * EXP(-CONST1 *
(EPS_UXC_P + CONST2) )
C*****
*****
C      DEFINE THE INVARIANTS FOR SHORT FIBER REINFORCED
THERMOPLASTICS
C*****
*****
      CALL INVARIANTS(STRESS_DIST, ND, NSH,XI1,XI2,XI5,XI4,NTT,
A_ST_11,

```

```

      * A_ST_22, TRSIGMA, DI1DSIGMA, DI2DSIGMA, DI4DSIGMA, DI5DSIGMA)
      CALL CALCALPHA(Y_TR, Y_IP, Y_1T, Y_1C, Y_2C, Y_2T, ALPHA1,
ALPHA2,
      * ALPHA4, ALPHA42, ALPHA5, ALPHA52 )
C   DEFINE INITIA YIELD CRITERION
      XF_YIELD_NEW_PERT = ALPHA1 * XI1 + ALPHA2 * XI2 + ALPHA4 * XI4
+
      * ALPHA42 * XI4** TWO + ALPHA5 * XI5 + ALPHA52 * XI5 ** TWO -
ONE
C   CALCULATE THE GRADIENT OF THE YIELD FUNCTION
      DALPHA1DEPSVAR_P = ( -2.D0 / Y_TR ** 3.D0 ) *
D_Y_TR_D_EPSVAR_P
      DALPHA2DEPSVAR_P = ( -2.D0 / Y_IP ** 3.D0 ) *
D_Y_IP_D_EPSVAR_P
      DEN = Y_1T + Y_1C
      XNUM = ONE/Y_1C + ONE/Y_1T + HALF * ALPHA1 * (Y_1C + Y_1T) -
ALPHA2
      * (Y_1C + Y_1T)
      DALPHA42DEPSVAR_P = ( (-ONE/Y_1T**TWO + HALF * ALPHA1 -
ALPHA2) *
      * DEN - XNUM ) * D_Y_1T_D_EPSVAR_P / DEN**2.D0 + ( (-
ONE/Y_1C**
      * TWO + HALF * ALPHA1 - ALPHA2) * DEN - XNUM ) *
D_Y_1C_D_EPSVAR_P /
      * DEN**2.D0 + HALF * DALPHA1DEPSVAR_P - DALPHA2DEPSVAR_P
      DALPHA4DEPSVAR_P = (-ONE/Y_1T**TWO + HALF * ALPHA1 - ALPHA2
-
      * ALPHA42) * D_Y_1T_D_EPSVAR_P + HALF * Y_1T *
DALPHA1DEPSVAR_P -
      * Y_1T * DALPHA2DEPSVAR_P - Y_1T * DALPHA42DEPSVAR_P
      DEN = Y_2T + Y_2C
      XNUM = ONE/Y_2C + ONE/Y_2T - HALF * ALPHA1 * (Y_2C + Y_2T)
      DALPHA52DEPSVAR_P = ( (-ONE/Y_2T**TWO - HALF * ALPHA1) * DEN
-
      * XNUM ) * D_Y_2T_D_EPSVAR_P / DEN**2.D0 + ( (-ONE/Y_2C**TWO -
HALF *
      * ALPHA1) * DEN - XNUM ) * D_Y_2C_D_EPSVAR_P / DEN**2.D0 -
HALF *
      * DALPHA1DEPSVAR_P
      DALPHA5DEPSVAR_P = -(ONE/Y_2T**TWO + HALF * ALPHA1 + ALPHA52
) *
      * D_Y_2T_D_EPSVAR_P - HALF * Y_2T * DALPHA1DEPSVAR_P - Y_2T *
      * DALPHA52DEPSVAR_P
      DO I = 1, NTT
          DSIGMADELTA GAMMA(I) = ZERO
          DO J = 1, NTT
              DO K1 = 1, NTT
                  DO L = 1, NTT
                      DSIGMADELTA GAMMA(I) = DSIGMADELTA GAMMA(I) + F_TEN(I, J) *
      * CE_3D(J, K1) * X_M_MAT(K1, L) * STRESS_DIST(L)
                      END DO
                  END DO
              END DO
          END DO
          DSIGMADELTA GAMMA(I) = - DSIGMADELTA GAMMA(I)

```

```

        END DO
C   CALCULATE DEPS_PDELTA GAMMA
        DO I = 1, NTT
          X_N_G(I) = ZERO
          DO J = 1, NTT
            X_N_G(I) = X_N_G(I) + X_M_MAT(I,J) * STRESS_DIST(I)
          END DO
        END DO
C   TEST CALCULATE THE NORM OF NG
        X_NG_NORM = ZERO
        DO I = 1, NTT
          X_NG_NORM = X_NG_NORM + DSQRT(HALF * X_N_G(I)**TWO)
        END DO

C   RECALCULATE NG
        GOTO 622
        DO I = 1, NTT
          X_N_G(I) = X_N_G(I)/X_NG_NORM
        END DO
        X_NG_NORM = ZERO
        DO I = 1, NTT
          X_NG_NORM = X_NG_NORM + DSQRT(HALF * X_N_G(I)**TWO)
        END DO
622   CONTINUE

        DO I = 1, NTT
          TERM3(I) = ZERO
          DO J = 1, NTT
            TERM3(I) = TERM3(I) + X_M_MAT(I,J) * STRESS_DIST(J)
          END DO
        END DO
        VALTERM3 = ZERO
        DO I = 1, NTT
          VALTERM3 = VALTERM3 + TERM3(I)** TWO
        END DO
        VALTERM3 = SQRT(HALF* VALTERM3)
C   DEFINE THE VALUE OF STRESS TENSOR
        STRESSVAL = ZERO
        DO I = 1, NTT
          STRESSVAL = STRESSVAL + STRESS_DIST(I)** TWO
        END DO
        STRESSVAL = SQRT(HALF* STRESSVAL)
        DO I = 1, NTT
          DO J = 1, NTT
            DEPS_PDELTA GAMMA = DEPS_PDELTA GAMMA +
* X_M_MAT(I,J) * STRESS_DIST(I) * DSIGMADDELTA GAMMA (J)
          END DO
        END DO
        DEPS_PDELTA GAMMA = DELTA GAMMA DIST * DEPS_PDELTA GAMMA /
        STRESSVAL + VALTERM3
        DALPHA1DGAMA = DALPHA1DEPSVAR_P * DEPS_PDELTA GAMMA
        DALPHA2DGAMA = DALPHA2DEPSVAR_P * DEPS_PDELTA GAMMA
        DALPHA5DGAMA = DALPHA5DEPSVAR_P * DEPS_PDELTA GAMMA
        DALPHA52DGAMA = DALPHA52DEPSVAR_P * DEPS_PDELTA GAMMA

```

```

DALPHA4DGAMA = DALPHA4DEPSVAR_P * DEPS_PDELDTAGAMMA
DALPHA42DGAMA = DALPHA42DEPSVAR_P * DEPS_PDELDTAGAMMA
C CALCULATE DI/DGAMA
  DI1DGAMA = ZERO
  DI2DGAMA = ZERO
  DI4DGAMA = ZERO
  DI5DGAMA = ZERO
  DO I = 1, NTT
    DI1DGAMA = DI1DGAMA + DI1DSIGMA(I) * DSIGMADELDTAGAMMA(I)
    DI2DGAMA = DI2DGAMA + DI2DSIGMA(I) * DSIGMADELDTAGAMMA(I)
    DI4DGAMA = DI4DGAMA + DI4DSIGMA(I) * DSIGMADELDTAGAMMA(I)
    DI5DGAMA = DI5DGAMA + DI5DSIGMA(I) * DSIGMADELDTAGAMMA(I)
  END DO

DFDGAMA = (XI1 * DALPHA1DGAMA + XI2 * DALPHA2DGAMA + XI4 *
* DALPHA4DGAMA+ XI4**TWO * DALPHA42DGAMA+ XI5 *DALPHA5DGAMA+
XI5**
* TWO * DALPHA52DGAMA) + (ALPHA1 * DI1DGAMA + ALPHA2
*DI2DGAMA +
* ALPHA4 * DI4DGAMA + ALPHA5 *DI5DGAMA + TWO* ALPHA42 * XI4*
* DI4DGAMA + TWO*ALPHA52 * XI5* DI5DGAMA )

DELTATO2_GAMMA = - XF_YIELD_NEW_PERT/DFDGAMA

DELTAGAMADIST = DELTAGAMADIST + DELTATO2_GAMMA
C UPDATE EQUIVALENT PLASTIC STRAIN
  EPSVAR_P_INT_DIST = EPSVAR_P_INT_DIST + DELTATO2_GAMMA *
X_NG_NORM
  IF ( DABS(XF_YIELD_NEW_PERT) .LT. PLAST_TOL )
    * GOTO 800
    IF ( NUMC1 > NUMBREAK ) THEN
C      WRITE(*,*) 'NUMC=', NUMC1
      GOTO 802
    END IF
C
C      END DO ! END FOR MAIN LOOP
C
C 800 CONTINUE
C 401 CONTINUE
C 802 CONTINUE
  DO M = 1, NTT
C CALCULATE THE DISTURBED STRESS MATRIX
    SIGMA(M,K) = STRESS_DIST(M)
  END DO
  STRAN_DIST(K) = STRAINTOTVECNEW(K)
  END DO
C END APPROXIMATE JACOBEAN MATRIX
  DO I=1, NTT
    DO J=1, NTT
C_TAN(I,J) = (SIGMA(I,J) - STRESS_NEW(I) )/ EPS_PERT(J)
    END DO
  END DO

GOTO 300

```

```

600 CONTINUE ! IF THE PLASTICITY HAS NOT BEEN OCCURED
C GET ELASTIC STRESS
    CALL GETSTRESS3D(CE_3D,CE_2D ,STRESS_NEW,STRAINTOTVECNEW,
*      NTT,ND)
C SET ZERO VALUES FOR STRAN PLASTIC VECTOR IN PLASTICITY NOT
HAPPENED
    DO I = 1, NTT
    STRAINPLAVECNEW (I) = ZERO
    END DO
C SET ELASTIC STIFFNESS MATRIX AS THE SECANT STIFFNESS MATRIX
    IF (ND .EQ. 3) THEN
    DO I = 1, 6
    DO J = 1, 6
    C_TAN(I,J) = CE_3D(I,J)
    END DO
    END DO
    ELSE
    DO I = 1, 3
    DO J = 1, 3
    C_TAN(I,J) = CE_2D(I,J)
    END DO
    END DO
    END IF
C UPDATE EQUIVALENT PLASTIC STRAIN
EPSVAR_P_NEW = EPSVAR_P_OLD
300 CONTINUE

    RETURN
    END

```

### 8.3 Appendix.3

A VUMAT subroutine must be started with the following piece of code to accomplish the initial calculations and checks. In the data check phase of the analysis Abaqus/Explicit calls user subroutine VUMAT with a set of fictitious strains and a totalTime and stepTime both equal to 0.0.

```

    IF ( STEPTIME .EQ. ZERO ) THEN

        DO KM = 1, NBLOCK
C     HERE JUST DEFINE THE ELASTIC RESPONSE OF THE MATERIAL
        END DO

    ELSE

        DO KM = 1, NBLOCK
C     USER MAIN CODE
        END DO

```

```
ENDIF
```

## 8.4 Appendix.4

In this study the case study, i.e. the hybrid component, is made of two materials which governed by two different material models. To implement more than one material model in the subroutine the following piece of code can be used[110]:

```
if (cmname(1:4) .eq. 'MAT1') then
call VUMAT_MAT1(argument_list)
else if (cmname(1:4) .eq. 'MAT2') then
call VUMAT_MAT2(argument_list)
end if
```

It must be taken into account that the materials name; e.g. 'MAT1', must be introduced in the capital letters.